Aus dem Institut für Pflanzenernährung und Bodenkunde

Mohamed Abd El-Rehim Abd El-Aziz Hassan

Environmental studies on coastal zone soils of the North Sinai peninsula (Egypt) using remote sensing techniques

Manuskript, zu finden in www.fal.de

Published as: Landbauforschung Völkenrode Sonderheft 238

Braunschweig
Bundesforschungsanstalt für Landwirtschaft (FAL)
2002

Sonderheft 238
Special Issue

Landbauforschung
Völkenrode
FAL Agricultural Research

Environmental studies on coastal zone soils of the north Sinai peninsula (Egypt) using remote sensing techniques

Mohamed Abd El-Rehim Abd El-Aziz Hassan

Table of content

List of Tables

List of Figures

List of Figures and Tables in Appendix

List of Abbreviation and Symbols

HEA	**Horizontal Extension Agriculture**
km	**kilometer**
°C	**degree of temperatures (Celsius)**
RS	**Remote Sensing**
ha	**hectare**
GIS	**Geographic Information System**
TM	**Thematic Mapper**
MSS	**Multi Spectral Scanner**
NASA	**National Aeronautics and Space Administration**
ERST	**Earth Resources Technology Satellites**
kg	**kilogram**
mg	**milligram**
g	**gram**
mg kg^{-1}	**milligram per kilogram**
µm	**micrometer**
mm	**millimeter**
cm	**centimeter**
l	**liter**
m	**meter**
IR	**infrared**
USGS	**U.S. Geological Survey**
mm y^{-1}	**millimeter per year (precipitation)**
mm d^{-1}	**millimeter per day (precipitation)**
m s^{-1}	**meter per second**
CAL	**Calcium Ammonium Lactate**
g cm^{-3}	**gram per cubic centimeter (Bulk density)**
cm hr^{-1}	**centimeter per hour (saturation hydraulic conductivity)**
CI	**Land Capability Index**
GC	**Geometric Correction**

UTM	**Universal Transverse Mercator system**
GCP	**Ground Control Point system**
PCA	**Principal Component Analysis**
a. s. l.	**above sea level**
OM	**Organic Matter**
$CaCO_3$	**Calcium Carbonate**
pH	**soil reaction**
EC	**Electrical Conductivity (ds m^{-1})**
CEC	**Cation Exchange Capacity (meq $100g^{-1}$)**
ESP	**Exchangeable Sodium Percent**
EMSDC	**Egyptian Military Survey Department Cairo**
OIF	**Optimum Index Factor**

1 Introduction

Deficiency in food production and a successive increase in population are the major important problems facing developing countries. Also Egypt suffers from these problems. The “Horizontal Extension Agriculture” (HEA) is the best proposed method to solve these problems. HEA means increasing of the cultivating areas for agriculture land by using scientific methods with good environmental management. This approach or philosophy is based on human aims which incorporates land stewardship with agricultural activities (NOWERS and SCHREUDER 1981, MPWWR 1994). The HEA method attempts to achieve the following objectives to:

1- Increase the food stuff resources and production.
2- Redistribute the population density.
3- Create more employment.
4- Build new agriculture areas.

The Egyptian government tries to incorporate HEA strategies especially in developing desert areas and solving the problems resulting from the progressive increase of population.

One of the most strategic project extension applied is the setup of the El-Salam Canal. This canal supplies about 168.000 hectares in the northern part of the Sinai region with mixed water from the Nile and agricultural drainage water to reclaim and cultivate the soils of the northern part of the Sinai. The total cost of the project is approximately 1.3 billion dollars, in addition to 0.3 billion dollars for establishment of 55 villages throughout the project (SIS 1999).

The extension of agriculture in the northern part of the Sinai needs more specific scientific investigations in order to evaluate, classify and to determine the fertility profile of these soils. Indeed, the obtained information will be a good tool for classifying and evaluating the different soil for agricultural, industrial and constructional use. This can lead not only to more development of the north Sinai but also more connection between the Sinai peninsula and the rest of Egypt.

Soil and vegetation resources in particular are very important economical and environmental parameters in the northern part of the Sinai. The Sinai peninsula has best conditions for the application of remote sensing techniques for soils because it represents an area with no

vegetation, furthermore it is characterized by a nearly cloud and pollution-free atmosphere. The pedological study in this area and the evaluation of soil fertility are important pre-requisites for an efficient management of the north Sinai natural resources. Extending agriculture to the Sinai may solve part of the food problem of the country. One way to optimize agriculture in a virgin area would be to allocate the farms on the most suitable soils for cropping. These are optimal conditions for the application of remote sensing. This study will indirectly contribute to words solving the over-population problem, by resettling in the Sinai more than 3 million people which in torn will create new urban-soil integrated communities, and realize a population balance involving moving out of the Nile valley to new horizons.

The El-Salam Canal project has been planned to cover about 168.000 hectares in the northern part of the Sinai peninsula from the South El-Kantara Shark to El-Arish. Figure (1-1) shows the planning image map of the El-Salam Canal project in the northern part of the Sinai peninsula. The total length of the El-Salam Canal is 242 km. The big part of the El-Salam Canal occupies about 155 km in the northern part of Sinai at the eastern bank of the Suez Canal and small part (87 km) in western bank of the Suez Canal. The water of the El-Salam Canal is mixed water, consisting of Nile water (about 2.11 billion m^3 $year^{-1}$) from Damietta branch and agricultural drainage water from the Hadous drain (about 1.91 billion m^3 $year^{-1}$) and the El-Serw drain (0.44 billion m^3 $year^{-1}$). This mixed water is transported by the tunnel underneath the Suez Canal (figure 1-2), which delivers about 14 million m^3 of mixing water per day (BALBA 1997 and SHATA 1998). The water of the El-Salam Canal is transported in pipes under pressure from the Bair El-Abd to the El-Manarah and lifted to the El-Arish area (El-Sir and El-Quarir) in order to avoid the sand dunes in this area. The water discharge now on the El-Salam Canal section in the northern part of the Sinai is shown in figure.(1-3).

Sinai is a triangular peninsula which makes up the north-eastern part of the Egyptian territory. The Sinai peninsula occupies a unique location in the Middle Eastern region and it is also the Asian part of African Egypt. Its total area is about 61.000 km^2; i.e. about 6.1 % of the total area of Egypt (ABDEL-RAHMAN et al. 1995). The top of this triangle is "Ras Mohammed" in the south and the base is the coastal line from Port Said to Rafah along the Mediterranean Sea all about 320 km long. Most of the area of Sinai is situated between latitudes 28° and 31° N and longitudes 32° 30' and 34° 30' E. The whole peninsula is surrounded by water from the Mediterranean sea from the north, by the Egypt-Palestine boundaries and the Gulf of Aqaba

from the east (about 150 km) and by the Suez Canal and the Gulf of Suez from the west (about 400 km). The total length of the Sinai peninsula coastlines is about 870 km, which is 30 % of Egypt coastlines (2400 km) as shown in figure (1-4).

The geology of the Suez Canal region was previously discussed by many researchers (EL-SHAZLY et al. 1974 and SAID 1990). The northern part of the Sinai peninsula comprises three geological structure units which are:

a) The Bitter lake to Rafah on the Mediterranean coast.
b) Mitlla pass to Arif El-Naga on the eastern border.
c) The north Sinai fractured area.

The study area of this work are situated in the first geological structure unit. The rock exposures are covered with young unconsolidated deposits of varying modes of formation including fluviatile, lagoonal and aeolian deposits. These deposits form most of the soil parent materials in the Suez Canal region. The deposits are mainly derived from the Halocene age.

Figure (1-5) shows that the Sinai peninsula is divided into five geomorphological units. These are: (I) the Afro-Arabian shield, (II) the Central plateau, (III) the Northern slope, (IV) the Mediterranean coastal plain and (V) the Gulf of Suez eastern coast (ABDALLAH and ABOU-KHADRAH 1977). The study areas are situated in the (IV) and (V) geomorphological units.

The climate of the Sinai peninsula is characterized by a hot dry summer with a temperature average of 32.5° C in August to 10° C in January (in winter). Rainfall varies in the Sinai, from scarce rainfall at Port Said of about 75 mm, and more than 130 mm in El-Arish and about 244 mm in Rafah. The temperature regimes have been defined as torric and thermic, (EL-SHAZLY and ABDEL-GAPHOUR 1990).

The current population of Egypt is about 57 million, mostly concentrated in the narrow Nile river valley (upper Egypt), the Nile delta in the North (lower Egypt) and the shore of the Suez Canal and the Sinai in the East. These are some of the most densely populated areas in the world. The population is expected to reach more than 85 million by the year 2010 (ABD EL-FATTAH 1993).

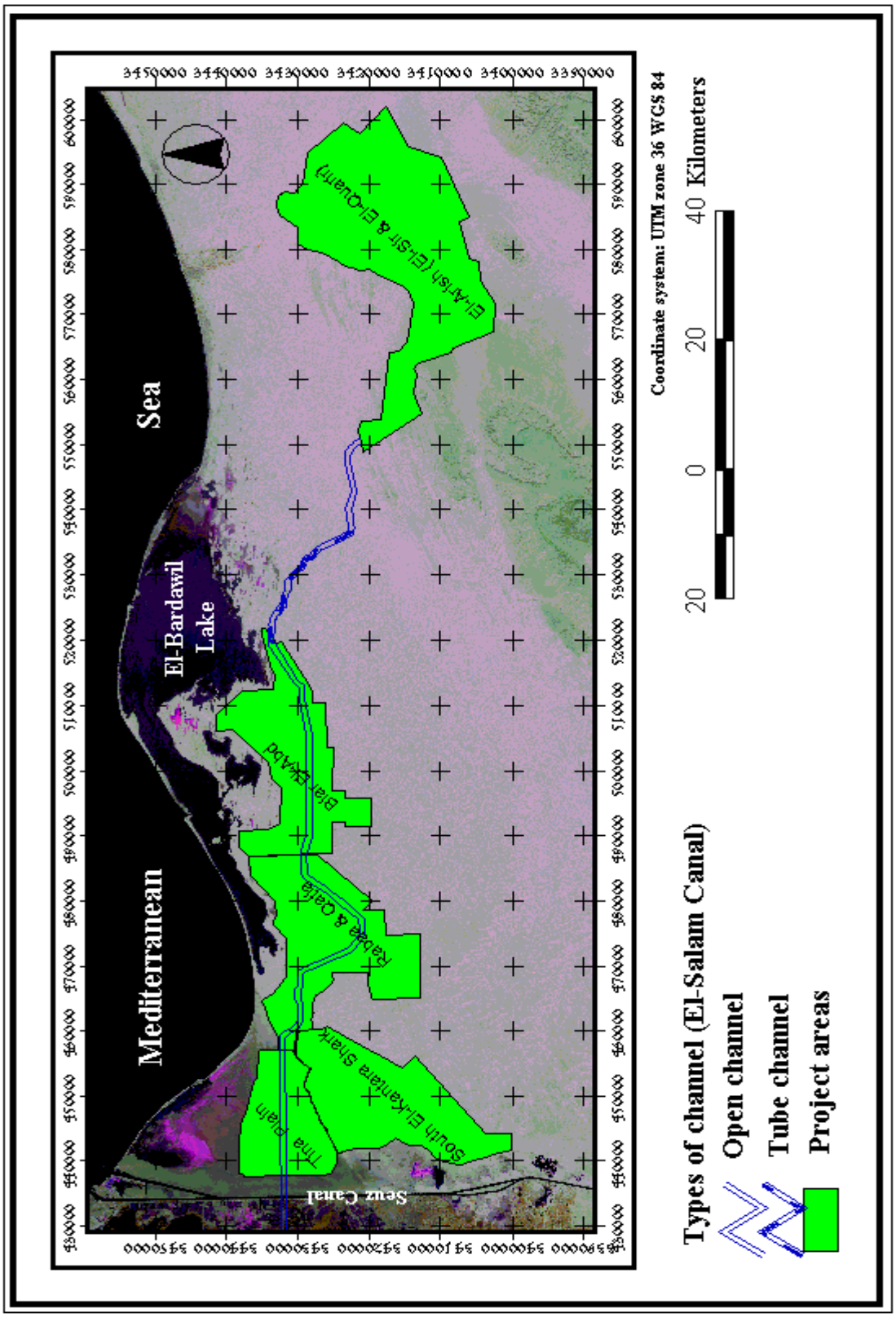

Fig. 1-1: Planing image map of the El-Salam Canal project area in the north part of the Sinai peninsula.

Fig. 1-2: El-Salam Canal passes underneath the Suez Canal to the north Sinai by 4 big tubes.

Fig. 1-3: Discharge of water to the north Sinai by the El-Salam Canal at the first pump station.

Fig. 1-4: Map of the Sinai peninsula.

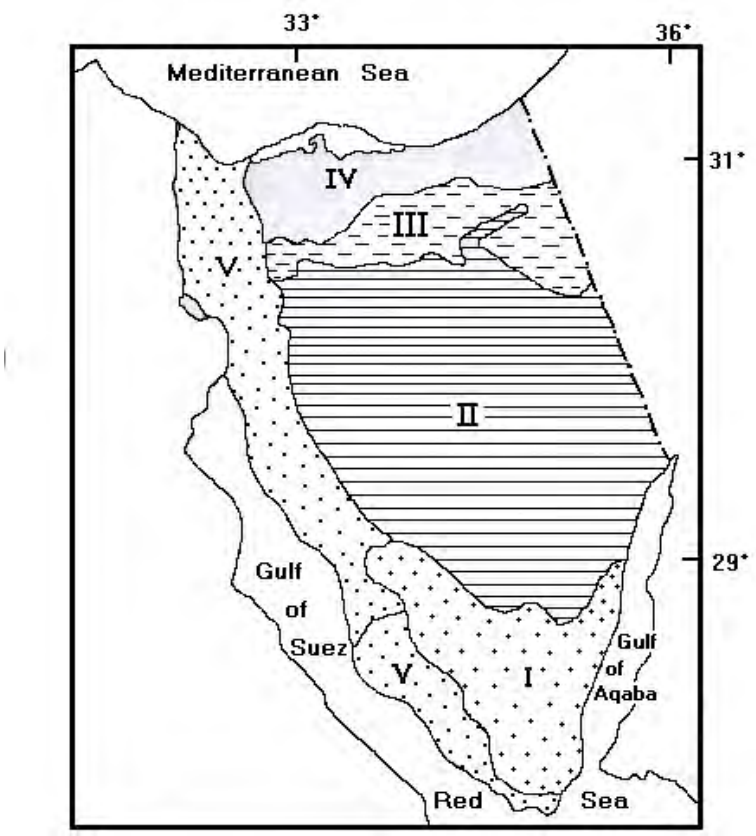

Fig. 1-5: Map of geomorphological units for the Sinai peninsula (ABDALLAH and ABOU-KHADRAH 1977).

The current population in the study area is a mix of Bedouin tribes, non Bedouins and foreign peoples. In early 1994 the population in the Sinai was about 270.000 distributed as follows:

a) about 213.000 in the governorate of Northern Sinai.

b) about 34.000 in the governorate of Southern Sinai.

c) about 23.000 in El-Kantara Shark in Ismailia governorate and in El-Shatt in the governorate of Suez, (SIS 2000).

Egypt consists of an area of about 1 million square kilometres (ABD EL-FATTAH 1993). The total areas under cultivation in Egypt are about 3.3 million hectares (ESA 1991). The government of Egypt plans to reclaim and cultivate about 168.000 hectares concentrated in the northern part of the Sinai peninsula. The Sinai peninsula bears suitable land for supporting Egypt's growing population with sufficient agricultural products of high quality, therefore it represents a promising and strategic region for land reclamation, development, settlement of

population and projects. The northern part of the Sinai peninsula is a new cultivation area added to the old cultivation areas in the wadi and delta soils around the River Nile.

Based on the present situation in Egypt in terms of potential available land, water and the growing population the main objectives of the research presented in this thesis are formula in order:

- to undertake an environmental study of the natural soil resources of the regions in the northern coastal part of the Sinai peninsula along the El-Salam Canal area.
- to investigate the possibilities of supervised classification of remote sensing images for classification of soils in the El-Salam Canal area in the northern part of the Sinai peninsula.
- to investigate relationships between remote sensing information and morphological units, physical and chemical soil characteristics in the northern part of the Sinai peninsula along the El-Salam Canal area.
- to evaluate the suitability of soils in the northern part of the Sinai peninsula along the El-Salam Canal area for agricultural use based on remote sensing and ground truth information.
- to establish maps for the investigated area in the northern part of the Sinai peninsula along the El-Salam Canal soil area by using remote sensing techniques. These maps are generated from the results of the data obtained by the Landsat TM-5 analysis, field survey work and laboratory analysis. (e.g. salinity maps, suitability maps and soil characteristic maps).

2 Principles of remote sensing

2.1 General concept of remote sensing

In recent literature remote sensing is defined as “a means to gather information about an object, area or phenomenon by which the analysis of data is obtained by a device, which is not in physical contact with the studied matter”. Although no touch contact exists between remote sensor and target, some physical emanation from the target must be found to investigate its properties and behavior. BARRET and CURTIS (1992) indicated that the most important physical links between objects and remote sensing devices involve electromagnetic energy, acoustic waves and force fields associated with gravity and magnetism. Figure (2-1) illustrates the generalized processes and elements involved in electromagnetic remote sensing of earth resources. The two basic processes, mentioned by LILLESAND and KIEFER (1994) in remote sensing, are:

1- Data acquisition, which comprises:

a. Energy sources.

b. Propagation of energy through the atmosphere.

c. Energy interaction with earth surface features.

d. Airborne and/or space borne sensors.

e. Resulting in the generation of sensor data in pictorial and/or numerical form.

2- Data analysis:

f. The data analysis and interpretation processes with different techniques.

g. The data presented in the form of maps, tables and reports.

h. The form of hard copy maps and tables or as computer files that can be merged with other „layers“ of information in a Geographic Information System (GIS).

i. Applying the final results for the decision-making process.

2.2 Physical background of remote sensing

All objects at a temperature above the absolute zero (0°K, or-273°C) continuously emit electromagnetic radiation. The sun as a body at a temperature of about 6000°K, emits

electromagnetic radiation in the same manner. The sun is the most important source of radiation for remote sensing. The visible and infrared regions of the electromagnetic spectrum (0.4-2.7µm) have been the most commonly used in remote sensing of planetary surfaces, specially in the Landsat TM-5 image data.

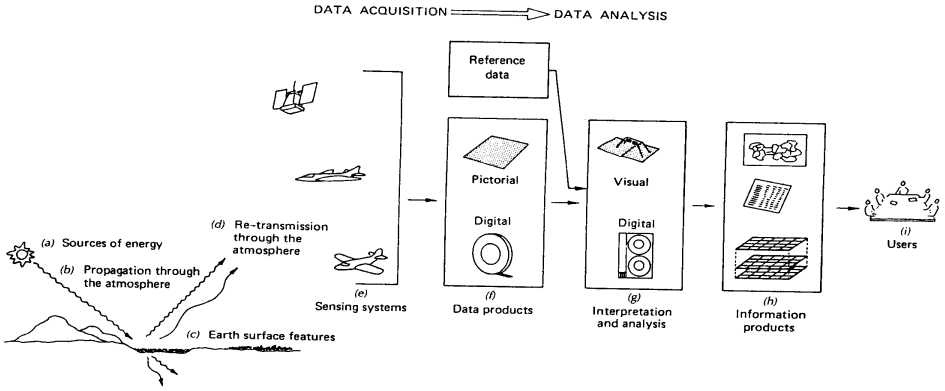

Fig. 2-1: Electromagnetic remote sensing of earth resources (LILLESAND and KIEFER 1994).

An important part of the electromagnetic spectrum is attenuated by the earth's atmosphere before the energy strikes the ground surface. Particles of haze, smoke, dust, water vapor, water droplets and various scatter gases cause the absorption and reflection of the major portions of the sun's energy. Spectral windows exist where the atmosphere has little or no attenuation effect figure (2-2). However, even in the windows atmospheric effects are significant, remote sensing data acquisition is limited to atmospheric spectral windows (WAY 1978, LILLSAND and KIEFER 1994). The spectral sensitivity range of the eye (visible light range) coincides both with an atmospheric window and the peak level energy of the sun.

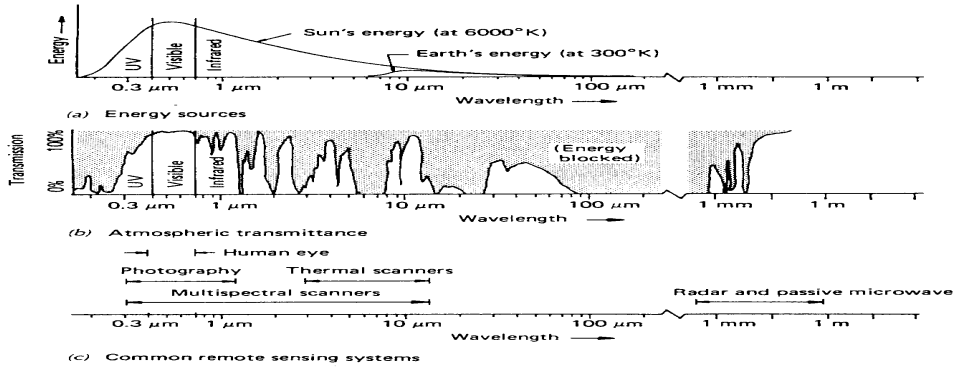

Fig. 2-2: Spectral characteristic of (a) energy sources, (b) atmospheric effect, and (c) remote sensing systems (Note that wavelength scale is logarithmic) (LILLESAND and KIEFER 1994).

The spectrum is divided into six main sections on practical grounds, influenced strongly by the absorption of large sections of the spectrum by water vapor in the earth's atmosphere. The usable portions cover so-called "atmospheric windows" wavelengths at which the atmosphere is essentially transparent.

Visible light is one of the largest atmospheric windows. The Visible wavelength used in remote sensing is essential for studies of water quality, pollution and coastal bathymetry. Near infrared is commonly used for structural studies and is very important in vegetation studies and discrimination of water area (hydrological studies). Mid-Infrared is important for geological and vegetation studies (LEGG 1994).

The visible and infrared range of the reflected energy measured by a sensor depends upon properties of objects such as the pigmentation, moisture content and cellular structure of vegetation, the mineral and moisture content of soils and the level of sedimentation of water (RICHARDS 1994).

A remote sensor which can detect such variations in reflectance between objects is dependent upon four interrelated factors. These factors are the radiometric resolution of the sensor (the Landsat TM can detect 256 levels of radiance and MSS 64 levels), the amount of atmospheric scatter (increases the amount of radiance received by the sensor for each object), the surface roughness of objects (majority of the Earth's surface appears rough at visible and near infrared wavelengths) and finally the spatial variability of reflectance within the scene (the radiance recorded from an area of ground also contains radiance from the surrounding areas) (CURRAN 1985). The main idea in acquiring data by airborne and space borne remote sensors, is that the different earth surface features emit and reflect the electromagnetic energy, which is recorded and analyzed to provide information about these features.

2.3 Reflectance characteristic

The object, exposed to the sun radiation reflects, absorbs or emits different proportions of each wavelength received. The unique conditions and physical properties of an object influence the reflection, absorption and emission of different portions of the electromagnetic spectrum. The

wavelengths of the electromagnetic spectrum that have proved to be of particular value in environmental remote sensing will be stressed and these are:

(i) Reflected radiation in visible, near and middle infrared wavebands.
(ii) Emitted radiation in middle and thermal infrared wavebands.
(iii) Reflected radiation in microwave wavebands.

The interaction of the electromagnetic spectrum with the four objects main components of a remotely sensed scene is different between vegetation, soils, water and urban areas. Figure (2-3) demonstrates the spectra signature of the three different materials in a limited portion of the spectra reflectance in the visible and infrared wavelengths. The spectral of three curves are for healthy vegetation, bare soil and water and the position of the Thematic Mapper (TM) spectral bands according to LILLSAND and KIEFER (1994).

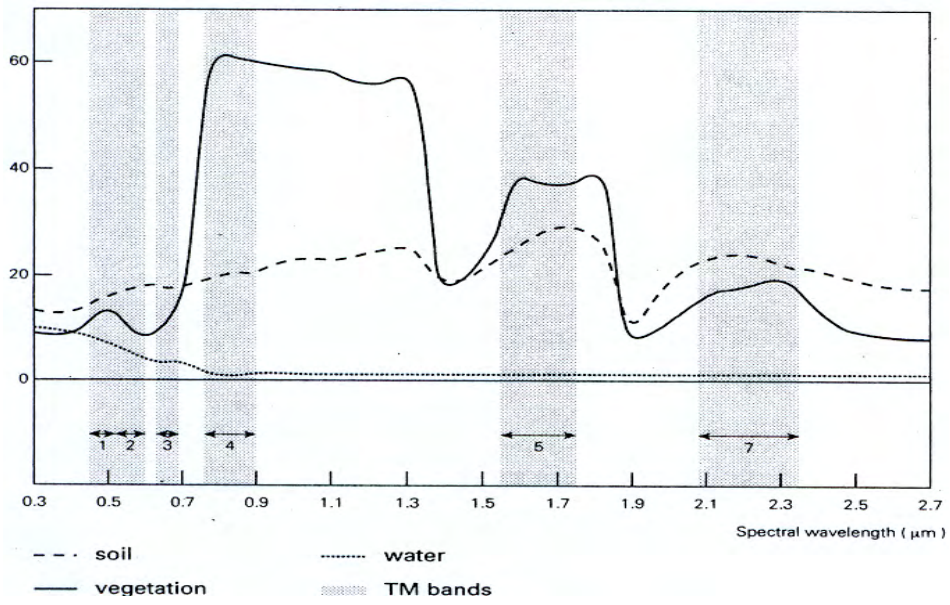

Fig. 2-3: Spectral curves for vegetation, bare soil and water and the position of (TM) spectral bands (LILLESAND and KIEFER 1994).

2.3.1 Spectral reflectance characteristic of vegetation

Remote sensing offers the feasibility of monitoring agricultural areas for rapid and continuous assessment of plant, soil and water resources and interrelated problems. The spectral reflectance of green vegetation is distinctive and quite variable with wavelength. The reflection of the vegetation is a function of the biological structure of the plant, the plant maturation, the

pigments, internal structure arrangements, leaf damages, leaf hairiness and leaf water content (REEVES 1975). Excellent review and discussion of the spectral reflectance characteristics of vegetation, soils, water, snow and clouds can be found in HOFFER (1978) and the optical properties of vegetation are described by BARET (1994), WESSMAN (1994), GUYOT et al. (1992), COHEN (1991), ELVIDGE (1990) and GOEL (1989). In general the reflectance of vegetation in the range of visible wavelengths (0.4-0.7 µm) is small and reflection in near infrared (0.7-1.1 µm) is league. Four features of leaves have an important effect on the reflectance properties of leaves (GOEL 1989, and CURRAN 1986) pigmentation, physiological structure, water content and vegetation indices.

2.3.1.1 Pigmentation

Pigmentation dominates the spectral response of plants in the visible wavelengths. Pigments (chlorophyll a and b) absorb radiation of the visible wavelength region. Chlorophyll a and b, which are the more important pigments, absorb portions of blue and red light; chlorophyll a absorbs at wavelengths of 0.43 µm and 0.66 µm and chlorophyll b at wavelengths of 0.45 µm and 0.65 µm. Other pigments of interest include the carotenes and xanthophylls (both yellow pigments) and the anthocyanins (red pigments). They are frequently in the green leaves but have an absorption band only in the blue portion of the spectrum (~ 0.45 µm) (figure 2-4).

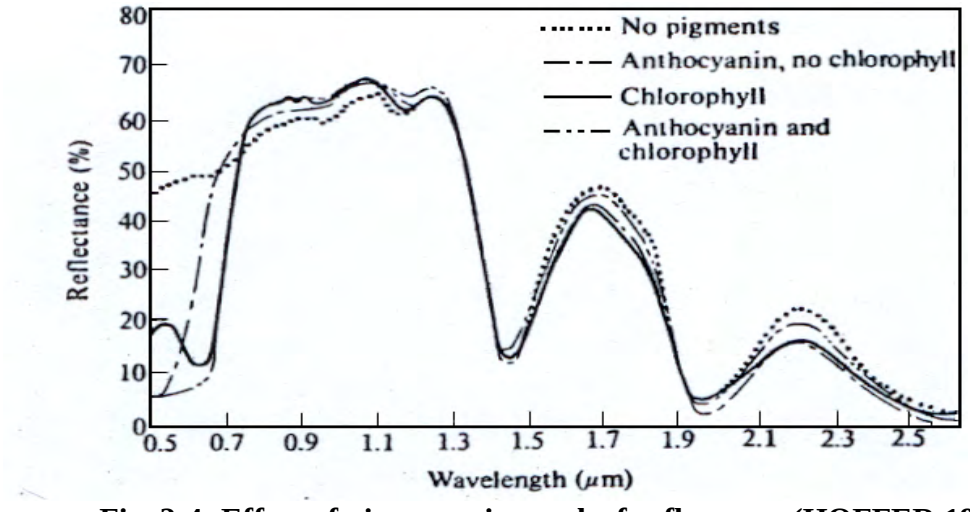

Fig. 2-4: Effect of pigmentation on leaf reflectance (HOFFER 1978)

Plant leaves reflect, absorb, and transmit incident radiation. Most types of vegetation, have approximately 45 to 50 percent reflectance, 45 to 50 percent transmittance, and less than 5 percent absorbency in the near-infrared wavelengths (HOFFER 1978).

The combined effect of pigments and physiological structure of healthy vegetation give typical reflectance properties: low reflectance of red and blue light, medium reflectance of green light and high reflectance of near infrared radiation. The major differences in leaf reflectance between species are dependent upon leaf thickness which affects both pigment content and physiological structure (CURRAN 1980a).

2.3.1.2 Water content

Water content of the leaves, and water in the atmosphere, reduce overall leaf reflectance and causes some narrow absorption features (water absorption bands). The moisture content of leaves decreases, reflectance in the middle infrared wavelength region increases markedly. Figure (2-5) shows the effect of moisture content in the reflectance of leaves of *Zea mays* L. Three major water absorption bands are located near 1.4, 1.9 and 2.7 µm. The absorption bands at 1.9 and 1.4 µm are dominate the spectral reflectance of leaves in the middle-infrared spectrum region, while very minor water-absorption bands occur near 0.96 and 1.1 µm, yet have a significant impact on reflectance, particularly for multiple layers of leaves (IRONS et al. 1989 and CURRAN 1986).

The majority of sensors are limited to three atmospheric windows that are free of water absorption at wavelengths of 0.3 to 1.3 µm; 1.5 to 1.8 µm and 2.0 to 2.6 µm. Fortunately within these wavebands, electromagnetic radiation is still sensitive to leaf moisture content (HOFFER 1978).

The degree to which incident solar energy in the middle-infrared portion of the spectrum is absorbed by vegetation is a function of the total amount of water present in the leaf, and that, in turn, is a function of both the percentage of moisture content of the leaf and the leaf thickness.

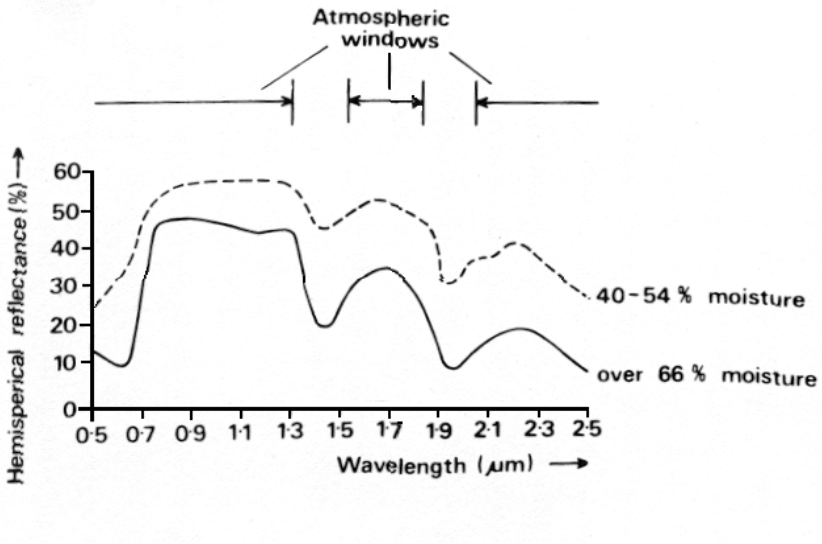

Fig. 2-5: The effect of moisture content on the reflectance of corn (*Zea mays* L.) leaves (CURRAN 1985).

2.3.1.3 Vegetation index

All spectral indices are based upon the fact that a green leaf's chlorophyll pigment strongly reflects sun radiation at wavelength between 0.5 and 0.7 µm and the reflectance factor is normally below 0.1 µm. In the near infrared region 0.75-1.35 µm, multiple scattering occurs due to the leaf's internal mesophyll structure and reflectance tends to be in the range of 0.4 to 0.6 µm (HILL 1993). The species specific structure causes discontinuities in the reflective indices within a leaf, which determine near infrared reflectance. Combinations of the visible and near infrared spectral bands enables discrimination between bare soil surfaces or water bodies from vegetation. These arithmetical band combinations can be referred to as „spectral vegetation indices" (LILLSAND and KIEFER 1994, MALTHUS et al. 1993, SABINS, 1987, HUETE and JACKSON 1987).

All vegetation indices only use a small part of the spectral information that is provided by the Thematic Mapper (TM) sensor (two or at maximum three out of totally six spectral channels) and the reduction to one single parameter for each date usually implies too significant information losses to be further used for covering class mapping (HILL 1993).

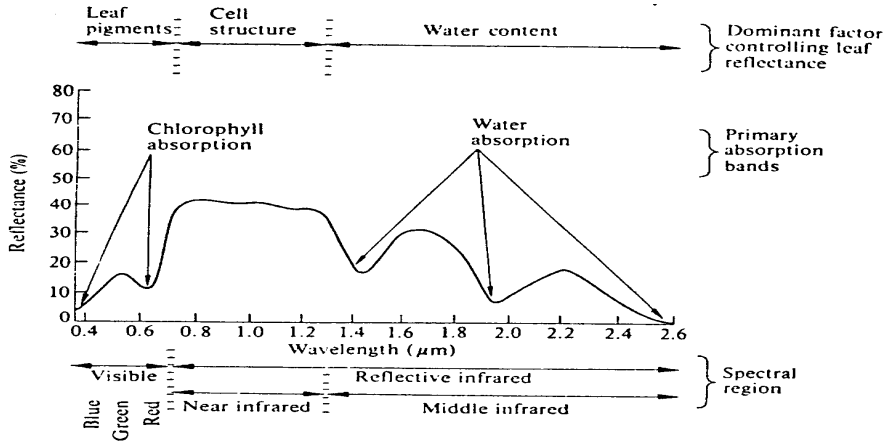

Fig. 2-6: Significant spectral response characteristics of green vegetation (HOFFER 1978).

Figure (2-6) shows a typical spectral reflectance curve for green vegetation and identifies the spectral response regions of major significance.

2.3.2 Spectral reflectance characteristics of soil

The reflectance spectra of soil are different from the ones of the vegetation. The characteristics of a soil that determine its reflectance properties have been described in several studies (LILLSAND and KIEFER 1994, COLEMAN et al. 1991, IRONS et al. 1989, MULDERS 1987 and HOFFER 1978). The most important soil properties regarding optical reflection are moisture content, organic matter content, texture, structure, iron content, mineral composition, type of clay minerals and surface conditions of the soil.

2.3.2.1 Moisture content

Reflectance spectra of moist soils include prominent absorption bands centered at 1.4 and 1.9 µm figure (2-7). These bands, along with weaker absorption bands at 0.97. 1.20, and 1.77 µm, are attributable to overtones and combinations of the fundamental vibration frequencies of water molecules in the soil. The bands at 1.4 and 1.9 µm are typically broad, indicating an unordered arrangement of water molecules at various sites in the soil (BAUMGARDNER et al. 1985).

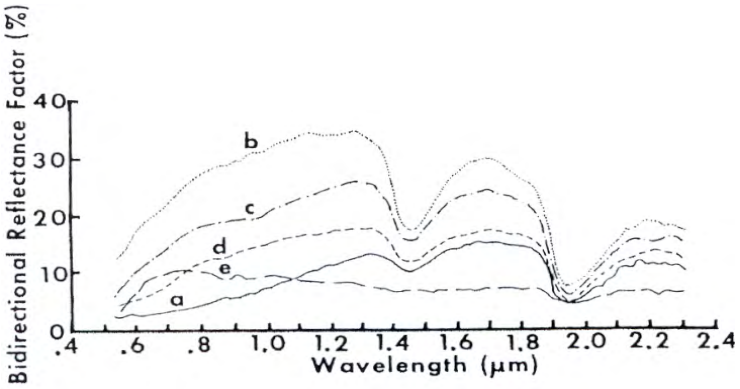

Fig. 2-7: Representative reflectance spectra of surface samples of 5 mineral soils: Curve A soils having high (>2%) organic-dominated (high organic content, fine texture). Curve B soils having low (<2%) organic matter content and low (<1%) iron-oxide content. Curve C soils having low (<2%) organic matter content and medium (1 to 4%) iron-oxide content. Curve D soils having high organic matter content (> 2%), low iron-oxide content (<1%), and moderately coarse texture. Curve E soils having high iron-oxide content (>4%) and fine texture (STONER and BAUMGARDNER 1981).

BOWERS and HANKS (1965) are frequently cited to demonstrate decreasing spectral reflectance as a function of increasing moisture content for a silt loam soil figure (2-8). In addition to the absorption bands, increasing moisture content generally decreases soil reflectance across the entire short-wave spectrum. In fact, wet soils usually appear darker to the eye than dry soils for this reason.

In addition to figure (2-8), the curve for air-dried silt can also decrease levels of reflectance in the water absorption bands. This is because the small size of silt particles, as compared to sand, which enables a significant amount of water to adhere to the soil particles even when the soil is in an air-dried condition (HOFFER 1979).

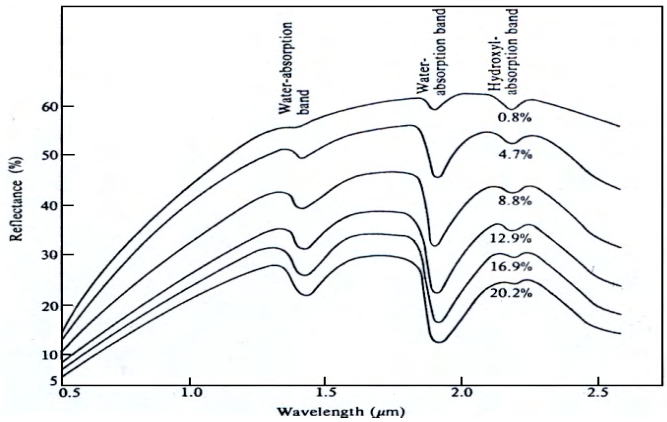

Fig. 2-8: Spectral reflectance curves for silt loam soil at various moisture content (BOWERS and HANKS 1965).

The reflectance spectra of moist soils include prominent absorption bands for water and hydroxyl at 1.9 and 1.4 µm and some weaker absorption bands at 0.97, 1.2 and 1.77 µm (IRONS et al. 1989).

2.3.2.2 Organic matter content

The organic matter content is another soil property that significantly influences the reflectance characteristics of a soil. The organic matter content of soils is extremely important to agriculturists since beside others it determines the amount and form of nitrogen in a soil. The level of organic matter found in most temperate-zone soils ranges only about 0.5 to 5 %, a soil with 5 percent organic matter will usually appear quite dark brown or black in color, lower amounts of organic matter content will result in lighter brown or gray tones in the soil. A very similar curvilinear relationship was also obtained for reflectance in the 0.62 to 0.66 µm wavelength band (BAUMGARDNER et al. 1970)

Organic matter has a strong influence on soil reflectance. Spectral reflectance generally decreases over the entire short-wave region as organic matter content increases (STONER and BAUMGARDNER 1980). At organic matter contents greater than 2 %, the decrease due to organic matter may mask other absorption features in soil spectra (BAUMGARDNER et al. 1970).

The spectra of soils with organic matter contents greater than 5 % often have a concave shape between 0.5 and 1.3 µm (figure 2-7, curve A) as compared to the convex shape of spectra for soils with lower organic matter content (STONER and BAUMGARDNER 1981).

The reflectance spectra of organic soils (i.e., organic matter content greater than 20 %) depend on the decomposition of the organic material. Spectra of fully decomposed (sapric) materials resemble curve A of figure (2-7), whereas spectra of partially decomposed (hemic) materials resemble curve D of figure (2-7) (STONER and BAUMGARDNER 1981). The spectral reflectance of minimally decomposed (fibric) organic matter is high in the near infrared and is similar to the spectral reflectance of senescent leaves (STONER and BAUMGARDNER 1981).

An increase of the organic matter content of a soil generally causes a decrease of reflectance over the entire spectrum that is similar to moisture. A high organic matter content and hence, a strong decrease of overall reflectance, might even mask other absorption features in soil spectra (IRONS et al. 1989).

This effect is minimal for soils having organic matter content below 2.0 to 2.5 % (BAUMGARDNER et. al. 1985). The soils with less than 1.5 % organic matter, the iron content of the soil showed a significant influence on the level of reflectance (MONTGOMERY 1976).

Figure (2-9) illustrates the relationship between organic matter content and hemispherical reflectance in visible wavelengths (PAGE 1974).

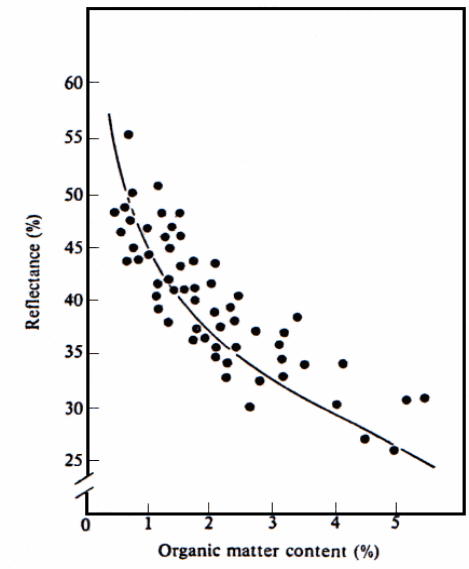

Fig. 2-9: Relationship between organic matter content and reflectance in visible wavelengths (PAGE 1974).

2.3.2.3 Iron and iron-oxide content

Iron and Iron oxide can also have a significant influence on the spectral reflectance characteristics of soil. The red colors of many soils are generally related to unhydrated iron oxides, although partially hydrated iron oxides and manganese dioxides can also cause this red coloration. Iron also commonly occurs as a principal constituent of some soil minerals. Many of the absorption features in soil reflectance spectra are due to the presence of iron in some

forms. Iron ions can also easily substitute into octahedral sites and less into tetrahedral sites and are thus retained in soils (HUNT 1980 and WEISMILLER et al. 1985).

The steep decrease in reflectance toward the blue and ultraviolet wavelengths is a characteristic of almost all soil reflectance spectra figure (2-7). The absorption bands often occur near 0.7 and 0.87 µm and iron can cause strong absorption bands near 1.0 µm show it in figure (2-7) curves C and E (STONER and BAUMGARDNER 1980).

Several weaker absorption bands between 0.4 and 0.55 µm can be found in some spectra due to iron ions (Mulders 1987).

Curve E in figure (2-7) represents the spectra of soils with high iron-oxide content (greater than 4 %), such as the tropical soils (oxisols) observed by STONER and BAUMGARDNER (1980). Iron absorption in the middle infrared by these soils can be strong enough to obliterate the water-absorption band at 1.4 µm (STONER and BAUMGARDNER 1981).

The increase in iron oxide can cause a significant decrease in reflectance, at least in the visible wavelengths. Figure (2-10) illustrates that removal of the iron oxide from a soil will cause a marked increase in reflectance throughout the 0.5 to 1.1 µm wavelength region, but the reflectance above 1.1 µm is not particularly affected. This Figure also shows that the removal of the organic matter from a soil will cause a similar marked increase in reflectance over about the same range of wavelengths (MATTHEWS 1972).

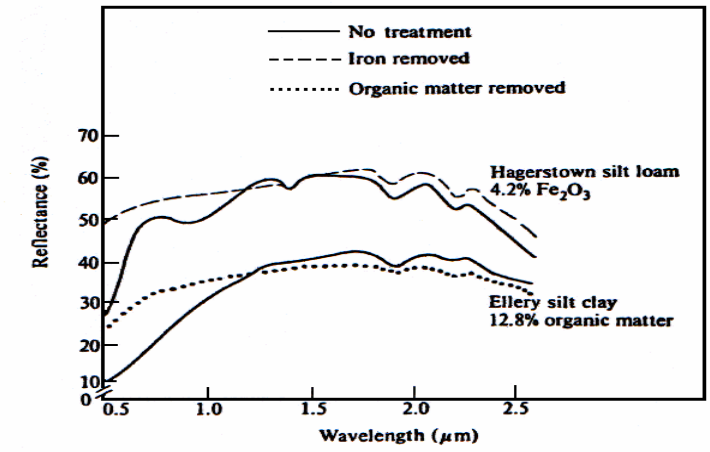

Fig. 2-10: Spectral reflectance curves illustrating the effect of removal of iron and organic matter from the soil (MATTHEWS 1972).

2.3.2.4 Texture and structure

The texture and structure of soil affects the reflectance of the soil both because of its influence on the moisture holding capacity and the fact that the size of soil particles strongly influences the reflectance. Soil particle size influences a number of soil properties such as moisture content and soil structure. Thus it is very difficult to measure the exact effect of increasing soil particle size on reflectance. Apart from the reflectance differences which can be accounted for by differences in particle size and soil structure, size and shape of soil aggregates appear to influence the soil reflectance in varying manners (BAUMGARDNER et al. 1985). Bi-directional reflectance of particulate soil minerals generally increase and the contrasts of absorption features decrease as particle size decreases (BOWERS and HANKS 1965, HUNT 1980, STONER and BAUMGARDNER 1980). In contrast, the bi-directional reflectance of opaque materials decrease as particle size decreases (HUNT 1980).

Theoretically, a decrease of the particle size would result in an increase of reflectance. This increase is caused by heavier light scattering and lower extinction of light, passing through the particles. Also, the area covered by micro-shadows occurring between particles under oblique illumination becomes smaller (NASA 1987).

Clayey soils often appear darker to the eye than sandy soils even though primary clay particles are much smaller than sand grains. The difference may be explained in part by the different mineralogy of clay and sand particles, but may also be due to the tendency of clay particles to aggregate. That aggregation into agglomerates and clods larger than sand grains can contribute to the darker appearance clayey soils (ASRAR 1989). A clay soil tends to have a strong structure which leads to a rough surface on ploughing, clay soils also tend to have a high moisture content and as a result have a fairly low diffuse reflectance. In contrast a sandy soil tends to have a weak structure which leads to a fairly smooth surface on ploughing, sandy soils also tend to have a low moisture content and as a result have fairly high and often spectral reflectance properties (BOWERS and HANKS 1965).

MONTGOMERY (1976) found that the amount of silt present was the major factor in explaining the level of reflectance in both the visible and reflective infrared portions of the spectrum for the soils. Since silt particles are of a relatively small size, the relationship was

directly proportional (i.e., an increase in the amount of silt present caused an increase in the level of reflectance). Figure (2-11) shows typical spectral curves for three different texture types of a soil in air-dried condition. The dry soils show generally increasing level of reflectance with increasing wavelength, particularly in the visible and near infrared portions of the spectrum.

As previously noted, the good relationships between texture, structure and soil moisture content can best be described by compressing two contrasting soil texture types (clay and silt loam). In figure (2-12) the spectral reflectance curves for wet and dry silt loam and wet and a dry clay soil textures are shown. Figure (2-13) shows the spectral reflectance curves for sand soil texture in three moisture content groupings.

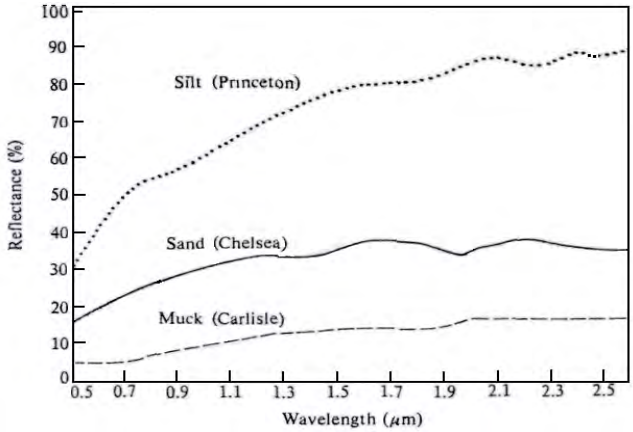

Fig. 2-11: Spectral reflectance curves for three soil texture types at low moisture contents (HOFFER 1976).

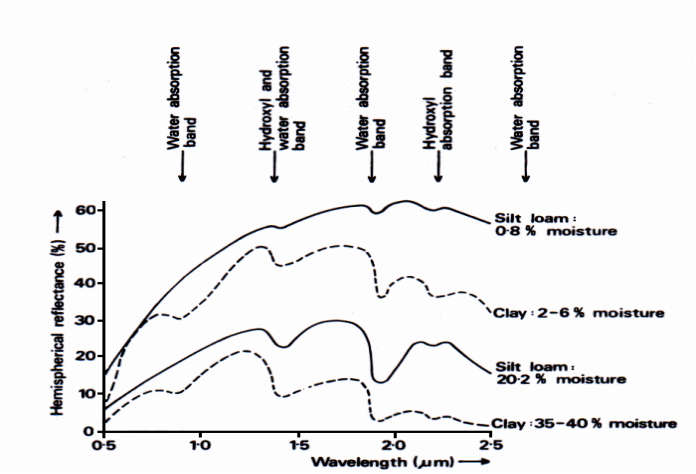

Fig. 2-12: Spectral reflectance curves for silt loam and clay soil textures (Modified from BOWERS and HANKS 1965, HOFFER and JOHANNSEN 1969).

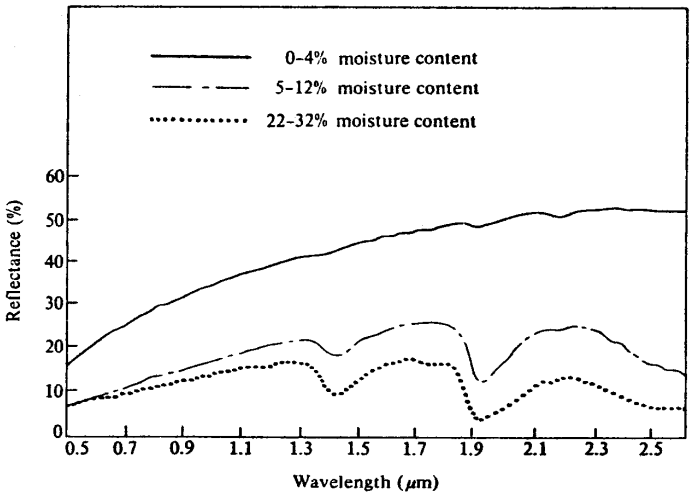

Fig. 2-13: Spectral reflectance curves for sand soil texture in three moisture content groupings (HOFFER and JOHANNSEN 1969).

2.3.2.5 Mineralogy

Most soils are predominantly composed of minerals. The principal atomic constituents of soil minerals, however, are silicon, aluminum, and oxygen, which do not possess energy levels having permissible transitions within the visible and near-infrared portions of the spectrum. Therefore, soil minerals primarily affect short-wave spectra in an indirect manner. They impose their crystal structures on the energy levels of ions (e.g., ferrous iron and hydroxyls) bound to the structures (HUNT 1980).

The most comprehensive collection of mineral spectra from particulate samples was acquired and published by HUNT et al. (1970, 1971 and 1973). Briefly, quartz has high reflectance throughout the short-wave region, and short-wave quartz spectra do not contain absorption features unless impurities are present. Other primary minerals are less reflective and have spectra containing absorption features due to electronic iron transitions (e.g., amphiboles display an absorption feature near 1.0 µm) or due to the vibrations of hydroxyl ions (e.g., muscovite displays absorption bands at 1.4 µm and between 2.2 and 2.6 µm). Spectra of the secondary layer silicates also display absorption features due to electronic iron transitions and hydroxyl ion vibrations. Hydroxyl bands near 1.4 and 2.2 µm are characteristic of layer silicates.

STONER and BAUMGARDNER (1980) found the 2.2 µm hydroxyl band difficult to identify in most of their soil spectra, but the band was apparent in the spectra of a few soils having clay contents greater than 20%. The hydroxyl band at 1.4 µm could not be distinguished due to the strong water band also at 1.4 µm.

The spectra of other secondary minerals also contain characteristic features. Calcite spectra display absorption bands between 1.8 and 2.5 µm due to carbonate. Gypsum spectra exhibit absorption bands at 1.8 and 2.3 µm due to overtones and combinations of water-molecule vibration frequencies (MULDERS 1985).

STONER and BAUMGARDNER (1980) found that the Montmorillonitic soils had the lowest average spectral reflectance between 0.52 and 1.0 µm. Kaolinitic soils generally displayed a wide absorption band near 0.9 µm due to the common presence of free iron oxides. The basic component of soil minerals are silicon, aluminum and oxygen. None of these soil constituents have diagnostic absorption features (IRONS et al. 1989).

NASA (1987) issued the reflectance of various minerals for the granulomertric class < 0.001mm in selected spectral intervals. The data in table (2-1) showed that the quartz is the brightest, and the biotite is the darkest.

Table 2-1: Reflectance of various mineral for the granulometric class <0.01mm in selected spectral intervals (NASA 1987).

Mineral Spectral region	Reflectance in %			
	blue	green	red	visible
wavelength (µm)	430-490	510-590	610-670	430-670
Quartz	92.9	93.0	93.0	93.1
Biotite	7.4	7.4	7.4	7.4
Muscovite	59.3	60.3	60.2	60.0
Microcline	61.4	71.7	80.7	71.3
Garnet	11.0	18.3	30.3	19.7
Epidote	18.6	34.7	36.5	30.3

The spectral resolution has been improved by the introduction of relatively narrow bands. Besides the statements made by the U.S. Geological Survey (1982) about the information of the TM bands for vegetation, rocks and soil moisture, additions can be made with regard to soil mineralogy (table 2-2).

Table 2-2: Spectral properties of the TM bands.

TM band No.	Wavelength in µm	Information on vegetation, rock and soil moisture (US. Geol. Survey 1982)	Information on soil mineralogy by absorption (Mulder & Epema 1986)
1-	0.45-0.52	differentiation of soil from vegetation and deciduous from coniferous flora.	Iron oxides
2-	0.52-0.60	green reflectance of vegetation.	Iron oxides
3-	0.63-0.69	chlorophyll absorption .	Iron oxides
4-	0.76-0.90	determination biomass content, delineation of moist areas.	Iron oxides
5-	1.55-1.75	vegetation and soil moisture content	gypsum
6-	10.40-12.50	vegetation stress, soil moisture	
7-	2.08-2.35	discrimination of rock type hydrothermal mapping.	calcite, gypsum and layer silicates

2.3.2.6 Surface conditions

Changes in bare-soil surface conditions complicate the remote sensing of soils. Conditions such as roughness, moisture content, and the presence of plant residue are easily and frequently altered by weather and tillage, and affect the spectral reflectance of soils.

LATZ et al. (1984) studied the effects of erosion on Alfisols. Reflectance from the A horizons were found to be low and reflectance spectra had the concave curve shape between 0.5 and 0.8 µm, typical of soils having high organic matter contents. Surface roughness and the formation of dry surface crusts have also been observed to affect spectral reflectance. Recently tilled soils are generally rougher, with larger clods and higher surface moisture contents, than soil left to the effects of weather (ASRAR 1989).

COULSON and REYNOLDS (1971) found that the hemispherical reflectance from dry smooth soil is about 50% higher than reflectance from soil after disking. CIPRA et al. (1971) observed higher spectral reflectance values between 0.43 and 0.73 µm from a crusted soil relative to the same soil with the crust broken.

2.3.3 Spectral and radiometric signatures in surface studies

This signature is used to separate surface units and to classify them into general categories. In some cases, identification can be achieved, such as in the use of color photography to separate vegetated areas from water and sand soils.

The spectral signature corresponds to high resolution (spectrally) radiometric measurements cover a fairly broad region of the spectrum. In this case, surface units can be separated, classified, and identified based upon some unique characteristics in their reflectivity spectrum, such as a diagnostic absorption band or combination of absorption bands, a diagnostic reflectivity change at a certain wavelength, or ratio of reflectivity in two separate spectral regions. The spectral signature is the most diagnostic tool in remotely identifying the composition of a surface unit (ELACHI 1987).

The analysis of radiometric and spectral signatures in surface studies can be divided into three general steps of increasing complexity:

1) detection and delineation,
2) classification and
3) identification.

2.3.3.1 Detection and delineation

The first step in the analysis of surface polychromatic or multispectral images is to recognize and delineate areas with different reflectivity characteristics. This can be done manually or with computers by simply delineating areas with image brightness within a certain range of values. In general, change in brightness is associated with changes in surface chemical composition, biological cover, or physical properties (roughness, slope, etc.). Change in brightness can also result from changes in the illumination geometry or atmospheric conditions.

In the case of multispectral images, the delineation process should take into consideration albedo variation in any one of the spectral channels. In many situations, accurate delineation of surface units is better done by using ratios of reflectivity in two different spectral bands. Delineation of units can also be based on a number of other criteria, such as presence or absence of a certain spectral feature (e.g., absorption line, reflectivity step, combination of lines, spectral slope at a certain wavelength). The selection of a specific delineation criterion is usually based on experience and on an understanding of the spectral behavior of the objects, surfaces, or covers being studied (ELACHI 1987).

2.3.3.2 Classification

The next step after delineation is to classify units based on a set of criteria. Classifications extend not only to individual images, but also to a number of images taken at different times of the same area or of different areas. The classification criteria range from the most simple, such as all areas with identical reflectivity in a certain spectral band being put into the same class, to more sophisticated criteria, such as equality of the coefficient of polynomial type expansion of the spectral signature as a function of wavelength over a wide spectral range. Some intermediate criteria include albedo (simple and composite), specific spectral absorption bands, spectral response slope in specific spectral regions, or the presence of specific spectral features (ELACHI 1987).

2.3.3.3 Identification

The last step in the spectral analysis of imaging data is the unique identification of the classified elements. This requires a detailed knowledge of the spectral signatures of the materials being sought, as well as of all the other materials at the site, and the development of a spectral signature library of all expected natural materials (ELACHI 1987).

In the ideal case, if a certain material, or family of materials, is the only one which has a certain spectral feature, such as an absorption line at a certain wavelength, the identification becomes simple. The identification feature could be a single absorption line or an association of lines.

2.4 Landsat satellites

2.4.1 General

Since 1972, the U.S. National Aeronautics and Space Administration (NASA) has started a series of Earth Resources Technology Satellites (ERTS). Seven Landsat spacecraft have been launched until now, sensing the earth's surface and transmitting to the ground receiving station.

The first Landsat was launched on July 23rd, 1972 and many other were launched and retired after that. Table (2-3) illustrates all of the Landsat satellites that were launched and their orbit characteristics (NASA 1998).

Table 2-3: The Landsat satellites launched date and characteristics (NASA 1998)

System		Launch (End of service)	I(s)	Resolution (meters)	Communications	Alt Km	D Days	R Mbps
Landsat	1	7/23/72 (1/6/78)	RBV MSS	80 80	Direct downlink with recorders	917	18	15
Landsat	2	1/22/75 (2/25/82)	RBY MSS	80 80	Direct downlink with recorders	917	18	15
Landsat	3	3/5/78 (3/31/83)	RBV MSS	30 80	Direct downlink with recorders	917	18	15
Landsat	4*	7/16/82	MSS TM	80 30	Direct downlink TDRSS	705	16	85
Landsat	5	3/1/84	MSS TM	50 30	Direct downlink TDRSS**	705	16	85
Landsat	6	10/5/93 (10/5/93)	ETM	15 (pan) 30 (ms)	Direct downlink with recorders	705	16	85
Landsat	7	12/98(est.)	ETM+	15 (pan) 30 (ma)	Direct downlink with recorders (solid state)	705	16	150

I(s) = Instruments (sensors) **R = Revisit interval** **D = Data rate**

*** TM data transmission failed in August, 1993.**

**** Current data transmission by direct downlink only. No recording capability.**

2.4.2 Description of the Landsat-TM5 and orbit characteristics

The satellite has a weight of about 815 Kg, is 3 m in height, 1.5 m in diameter and has a solar panel extending to 4 m width (figure 2-14). The satellite orbits the earth in a near-polar orbit which traverses any point on the ground every 18 days. The orbit is at 946 km and the satellite is sun synchronous, so that the repeated coverage is always at approximately the same time of day. The orbit time is 103 minutes, giving 14 orbits per day. The imaging swath of the sensors is 185 km wide.

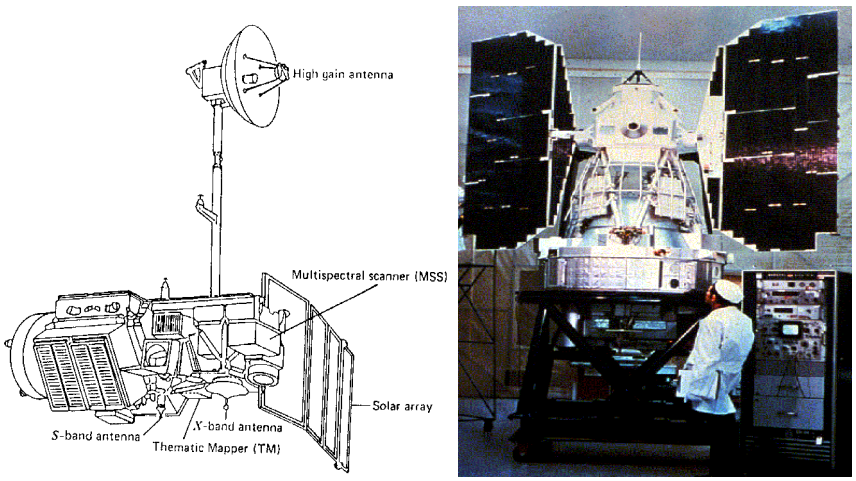

Fig. 2-14: Sketch and photo of the Landsat-TM 4 and 5 satellites.

Figures (2-15) and (2-16) shown the Orbit parameters and swathing pattern of the Landsat TM system and construction and operation principles of the Landsat TM sensor and the Landsat TM instrument images a swath of approximately 185 km. At the equator, adjacent orbits have a distance of 172 km, which leads to an overlap of 7 percent. Towards higher latitudes this side-lap increases to a maximum of 84 % (table 2-4) which in many cases compensates for the more frequent cloud coverage in these regions (KONTOES and STAKENBORG 1990).

Table 2-4: Sidelap of adjacent the Landsat TM 4 and 5 coverage swaths (EURIMAGE product information).

Latitude	**0°**	**10°**	**20°**	**30°**	**40°**	**50°**	**60°**	**70°**	**80°**
Sidelap %	**7.3**	**8.7**	**12.9**	**19.7**	**29.0**	**40.4**	**53.6**	**68.3**	**83.9**

2.4.3 Sensors on board of the Landsat-4 and 5

The Landsat-4 and 5 are carrying a sensor system, called Thematic Mapper (TM). The TM provides a spatial resolution of approximately 30 m for bands 1 through 5 and band 7. The band six is a thermal band and providing a 120 m resolution.

The bands 1, 2 and 3 are in the visible portion of the spectrum and are useful in detecting cultural features such as roads. These bands also show detail in water. Bands 4, 5 and 7 are in the reflective infrared portion of the spectrum and can be used in land/water discrimination. Band 6 is in the thermal portion of the spectrum and is used for thermal mapping (JENSEN 1996).

2.4.4 Thematic Mapper system (TM)

The second generation, Earth sensing satellite called the Thematic Mapper (TM) was launched in July 1982. It has sensor system with improved spatial resolution (30 m), spectral separation (seven narrow bands), geometric fidelity, and radiometric accuracy. The selection of the bands for TM are such that four bands (0.45-0.52, 0.52-0.60, 0.63-0.69, and 0.76-0.90 µm) are similar to the Landsat multispectral scanner (MSS) bands (0.5-0.6, 0.6-0.7, 0.7-0.8, and 0.8-1.1 µm). Two bands in the middle infrared (mid-IR) region (1.55-1.75 and 2.08-2.35 µm) and one in the thermal region (10.4-12.5 µm) were intended to provide new information for vegetation and

soil monitoring. The improved spatial resolution (over that of the MSS) is also an important attribute of the TM. A pixel (picture element) size or resolution element of 30 m (ground resolution) in all but band 6 will allow classification of areas as small as 2.5 to 4 ha.

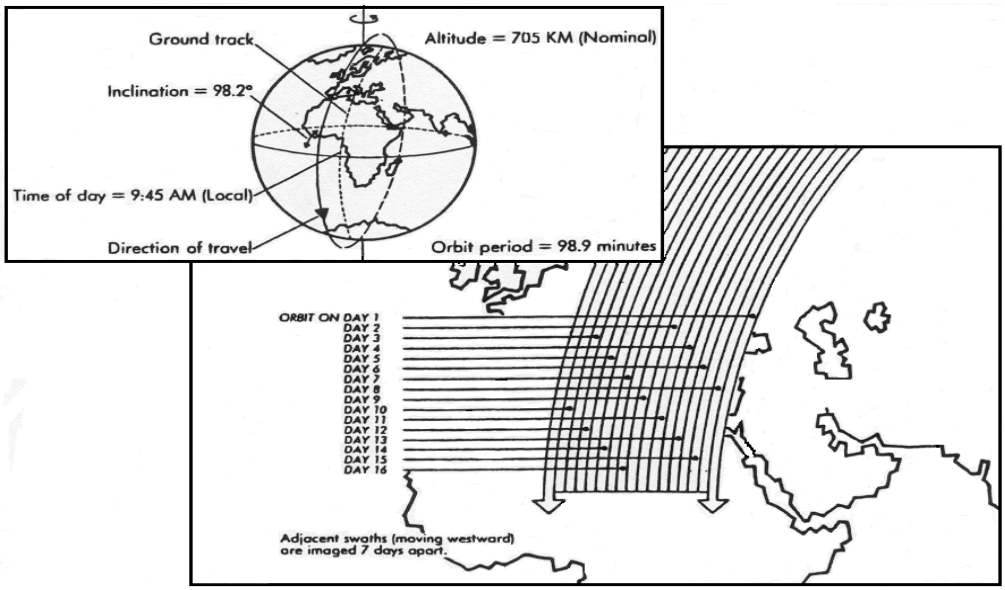

Fig. 2-15: Orbit parameters and swathing pattern of the Landsat TM system (from EURIMAGE product information).

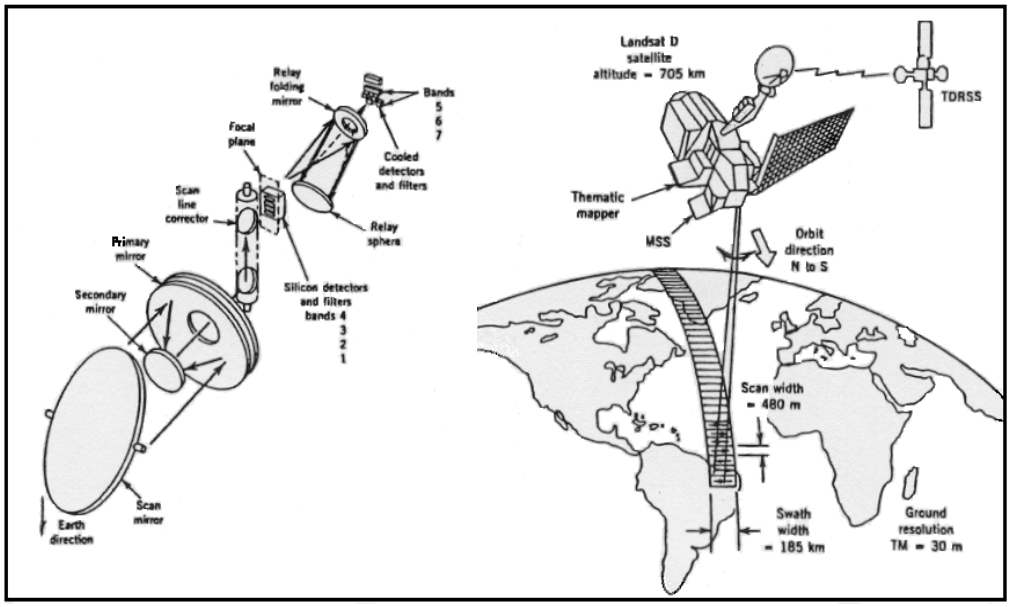

Fig. 2-16: Construction and operation principles of the Landsat TM 4 and 5 sensor (BLANCHARD and WEINSTEIN 1980).

3 Materials and Methods

In this chapter materials and available data, methods of soil sample analysis and image data analysis by remote sensing techniques used for the soil coastal zone environment studies in the northern part of the Sinai Peninsula are presented.

3.1 Survey area

The investigated area was the El-Salam Canal region in the northern coastal part of the Sinai peninsula. A detailed description of the El-Salam Canal project is already given in introduction to this thesis.

Four sources of materials and data were collected from the northern coastal part of the Sinai peninsula for this study:

Landsat TM image digital data

This digital image data were provided by the U.S. Department of the Interior, U.S. Geological Survey (USGS). Four of the Landsat TM scenes were selected to cover the entire region of the north Sinai peninsula. Figures (3-1) and (3-2) shown the four scenes which were selected in employing the DESCW 4.15 program new version (EURIMAGE 2000) according to suitable conditions for pick and record scenes. These scenes are:

1-	Track 175	Frame 38	Date 5 / 8 /1987.
2-	Track 175	Frame 39	Date 5 / 8 /1987.
3-	Track 176	Frame 38	Date 21 / 7 /1987.
4-	Track 176	Frame 39	Date 21 / 7 /1987.

This scenes were selected because on the Landsat TM-5 images. Most of the soils were not covered by vegetation and the images were free of interfering atmospheric distortions (i.e. clouds, haze and dust). In addition, Thamatic mapper images data (the Landsat TM-5) have proved high performance land cover classification (MIKIHIRO and MASATO 1986), also in lithological discrimination (GREENBAUM 1987).

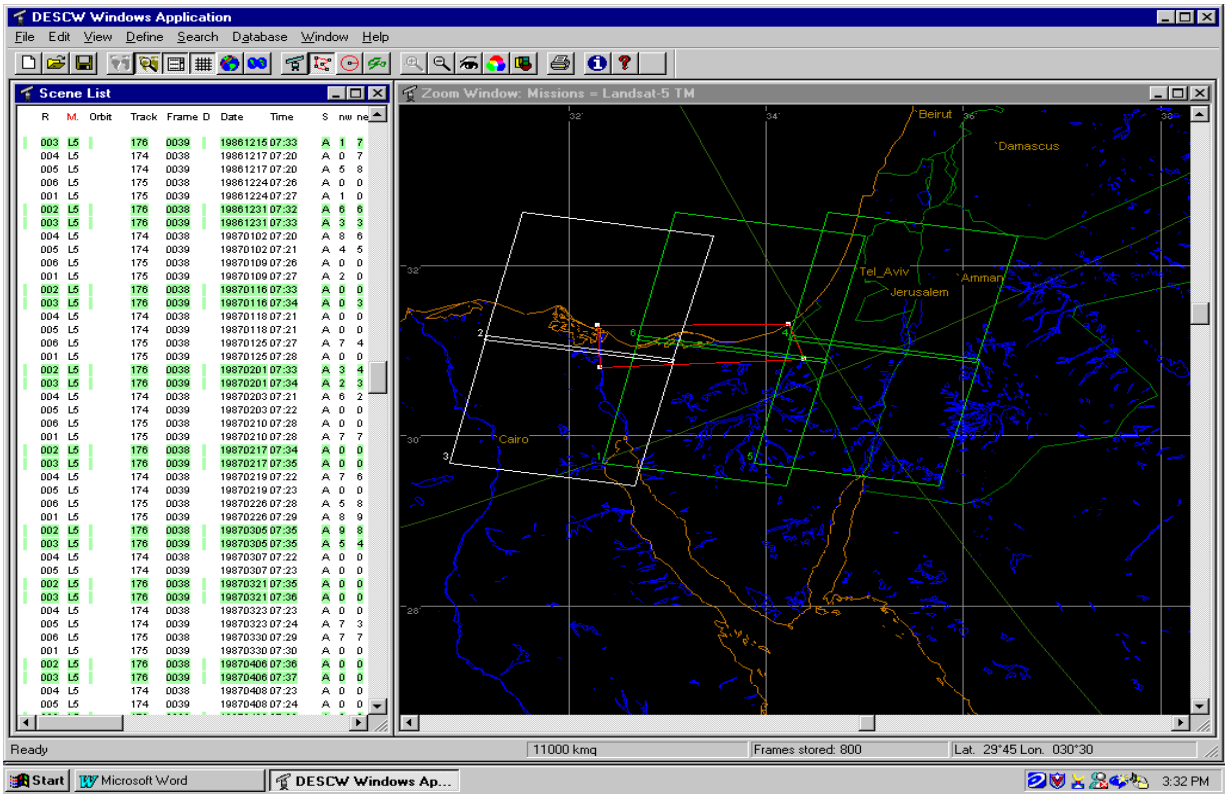

Fig. 3-1: The first and second scenes cover part of the north Sinai peninsula (DESCW 4.15 EURIMAGE 2000).

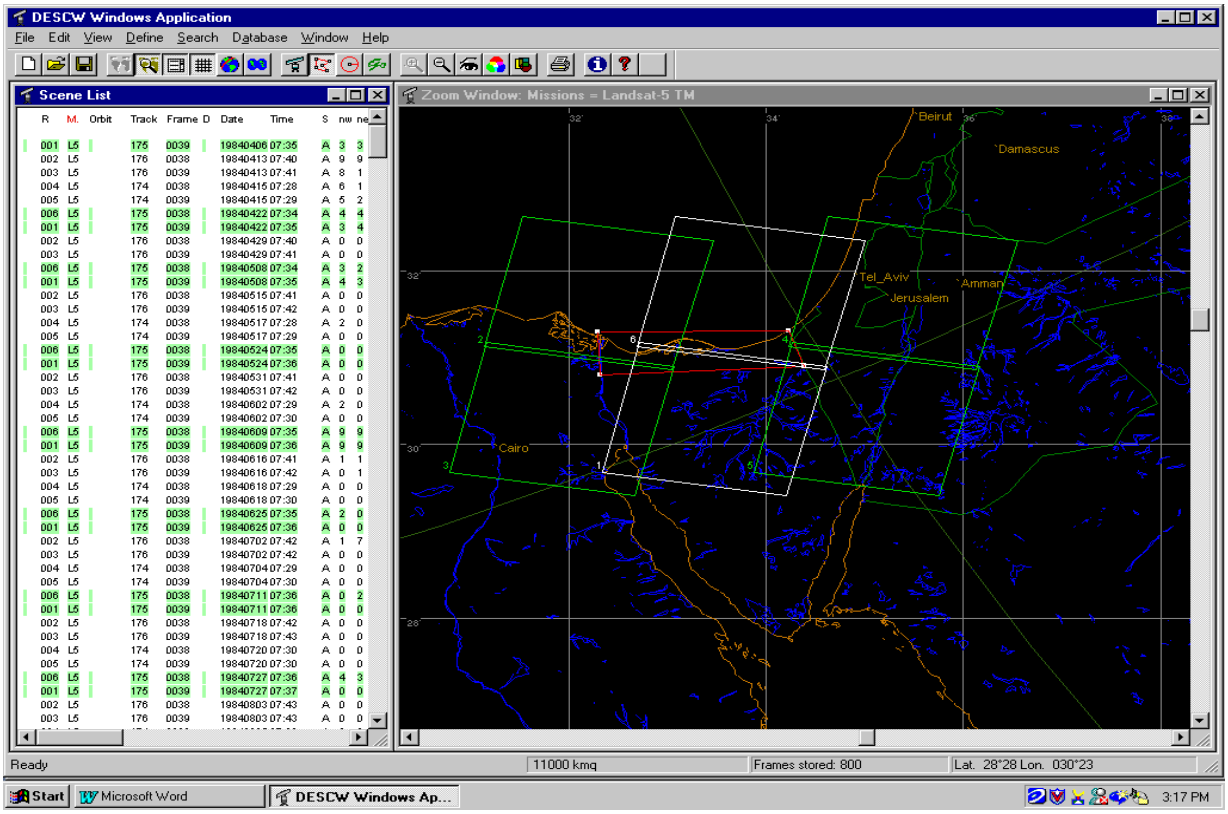

Fig. 3-2: The third and fourth scenes completely cover the northern part of the Sinai peninsula (DESCW 4.15 EURIMAGE 2000).

Topographic maps

The study area in the north Sinai peninsula was covered by 13 Topographic color maps scale 1:50.000. Figure (3-3) shows the indices of this maps. The maps were used together with satellite images to describe topographical features along the coast of the Mediterranean sea from Port Said to El-Arish. The maps were published in 1988 and 1987 according to new system released by the Egyptian Military Survey Department Cairo (EMSDC). The project areas of the El-Salam Canal in the northern part of the Sinai peninsula were digitized from this maps.

Field work

The field survey was accomplished by pedological studies on soil profiles and surface samples, in order to verify the primary results of the satellite images classification (the Landsat TM-5).

Eleven representative soil profiles (35 samples) were collected from the five locations of the study areas (along the El-Salam Canal soil project). These profiles are, more or less, representative for the five soil locations under consideration. Two soil profiles were taken from the soil of the South El-Kantara Shark, the El-Tina Plain, the Rabaa, and three from the Bair El-Abd and two from the El-Arish areas.

The location image map of these soil profiles and surface samples in the northern part of the Sinai peninsula along the El-Salam Canal project were shown in figures 3-4, 3-5, 3-6, 3-7 and 3-8. These profiles were morphologically described according to the guidelines of soil description by FAO (1970) and the SOIL SURVEY MANUAL (1951). The complete description of this profiles are given in the appendix (I). Soil classification was carried out according to SOIL TAXONOMY (1975).

Thirty six surface samples were collected from different locations in the same areas. These surface samples were taken from between 0-70 cm depth. In total, seventy one soil samples were collected from the different morphological unites in the investigation area.

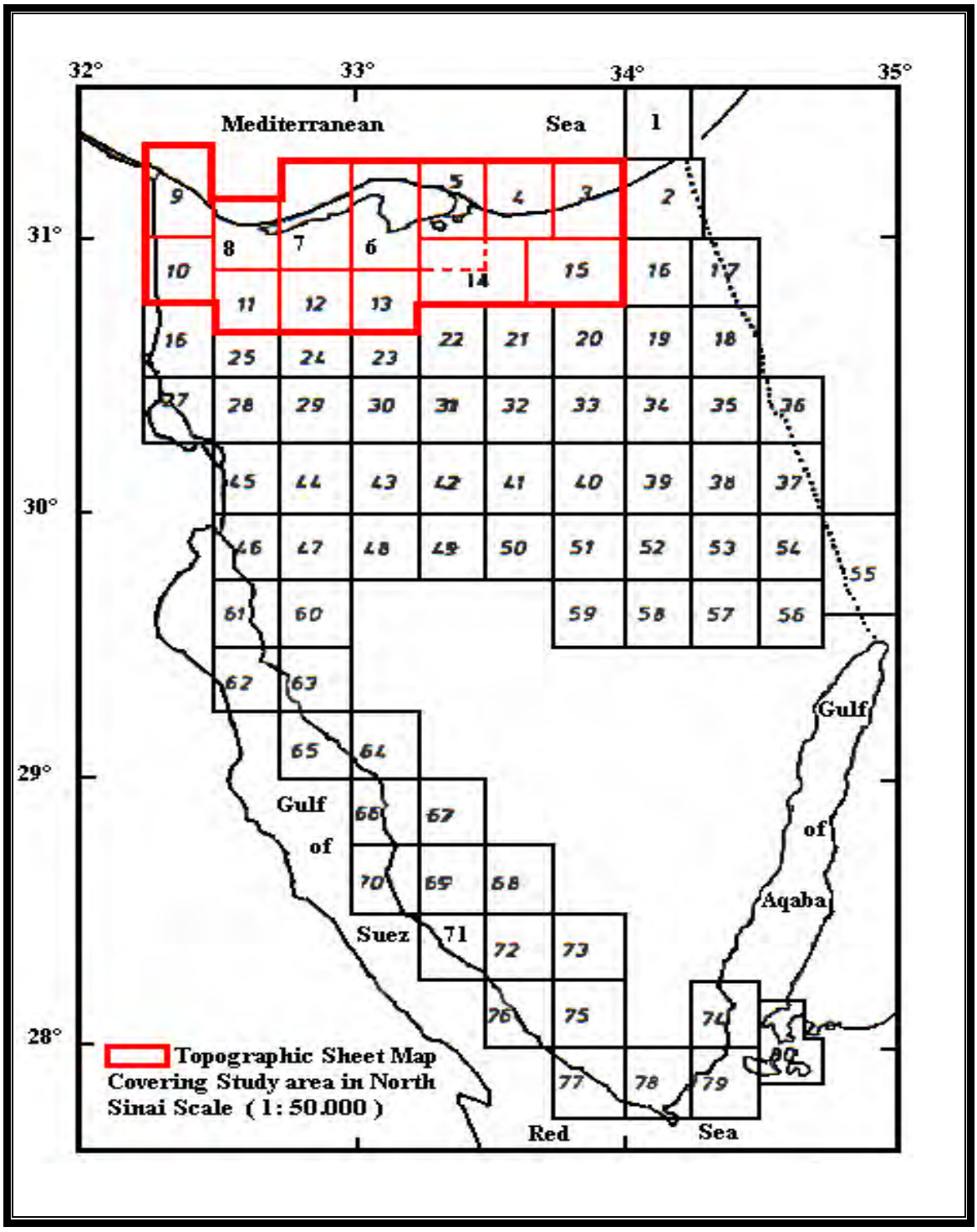

Fig. 3-3: Index map of topographic sheets, scale 1:50.000 covering the Sinai peninsula.

In addition to profile and surface samples, two samples were collected to describe a typical salt crust and a typical hard pan shown in figures (3-9 and 3-10), respectively. The location of the different investigation areas are gives in table (3-1).

Table 3-1: The boundary coordinates of the study area by hectares.

Study area	Boundary coordinates		Area by (Hectare)
	N	E	
1- South El-Kantara Shark	30° 50`and 30° 59`	32° 15` and 32° 35`	31.500
2- El-Tina Plain	30° 59`and 31° 05`	32° 10`and 32° 33`	21.000
3- Rabaa and Qatia	30° 51`and 31° 04`	32° 33`and 32° 52`	29.400
4- Bair El-Abd	30° 57`and 31° 07`	32° 52`and 33° 10`	29.400
5- Wadi El-Arish	30° 42`and 31° 02`	33° 35`and 34° 15`	56.700

The collected soil samples were prepared for analysis by air drying, gently disaggregating in an agate mortar and finally sieving through a 2 mm sieve.

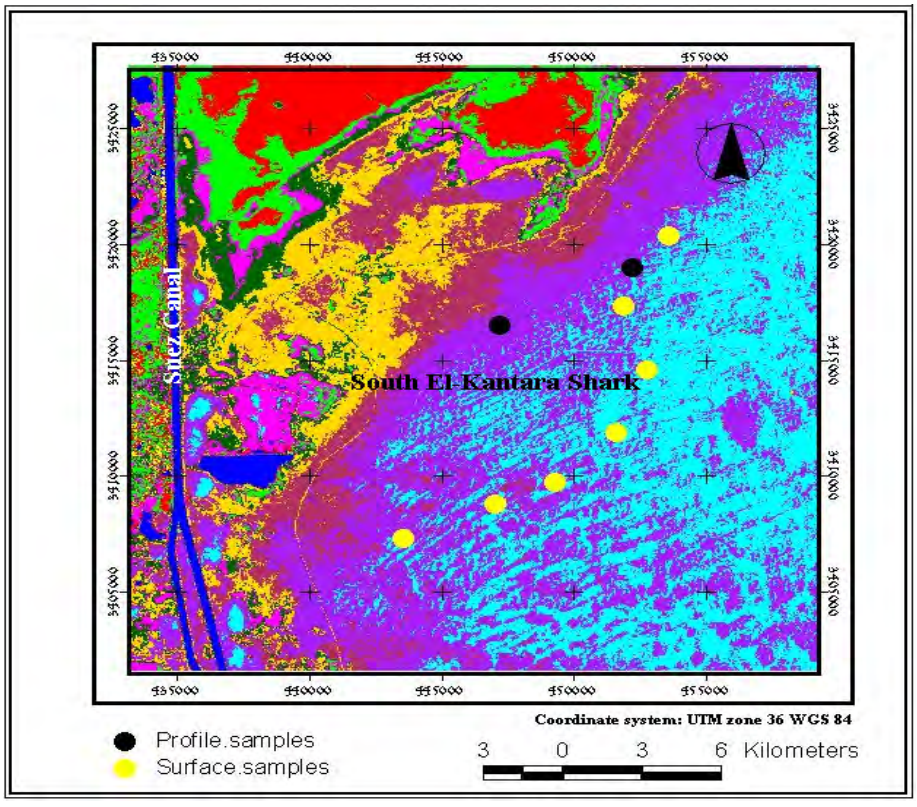

Fig. 3-4: Image map of the surface and profile samples of the South El-Kantara Shark area in the north Sinai peninsula. (based on the Landsat TM-5 images acquired from USGS).

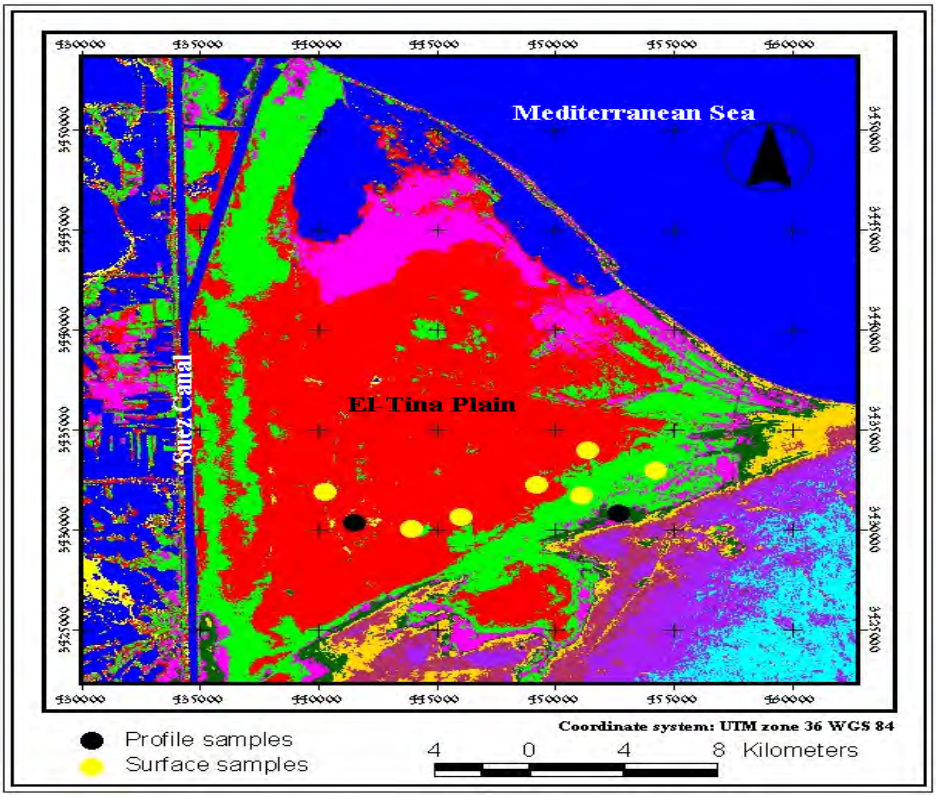

Fig. 3-5: Image map of the surface and profile samples of the Tina Plain area in the north Sinai peninsula. (based on the Landsat TM-5 images acquired from USGS).

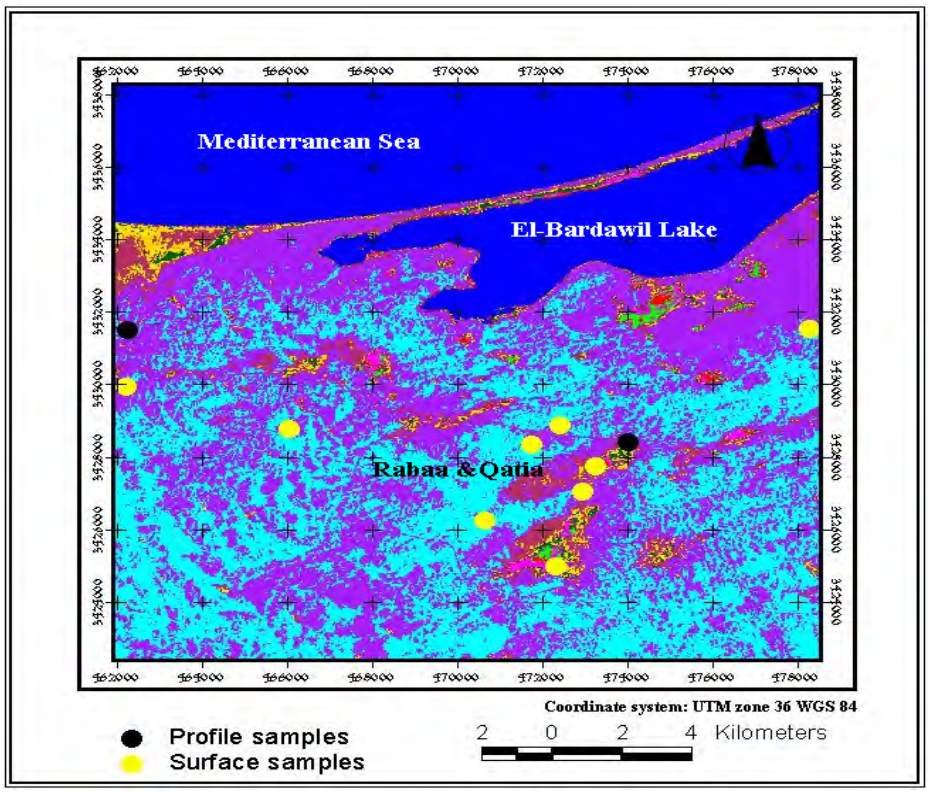

Fig. 3-6: Image map of the surface and profile samples of the Rabaa and Qatia areas in the north Sinai peninsula. (based on the Landsat TM-5 images acquired from USGS).

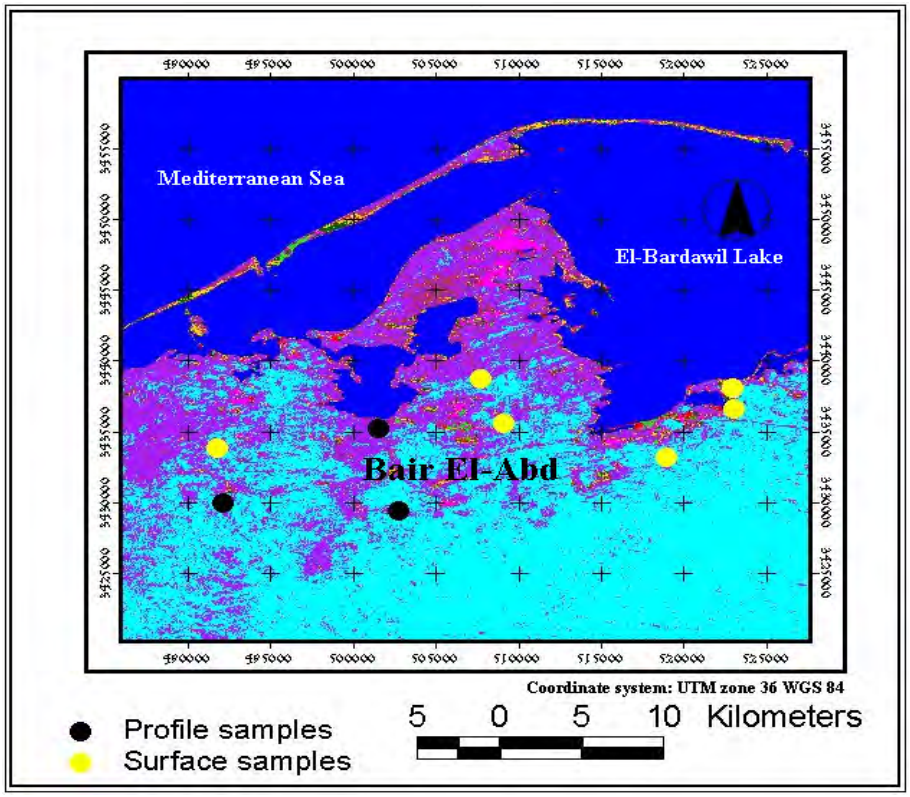

Fig. 3-7: Image map of the surface and profile samples of the Bair El-Abd area in the north Sinai peninsula. (based on the Landsat TM-5 images acquired from USGS).

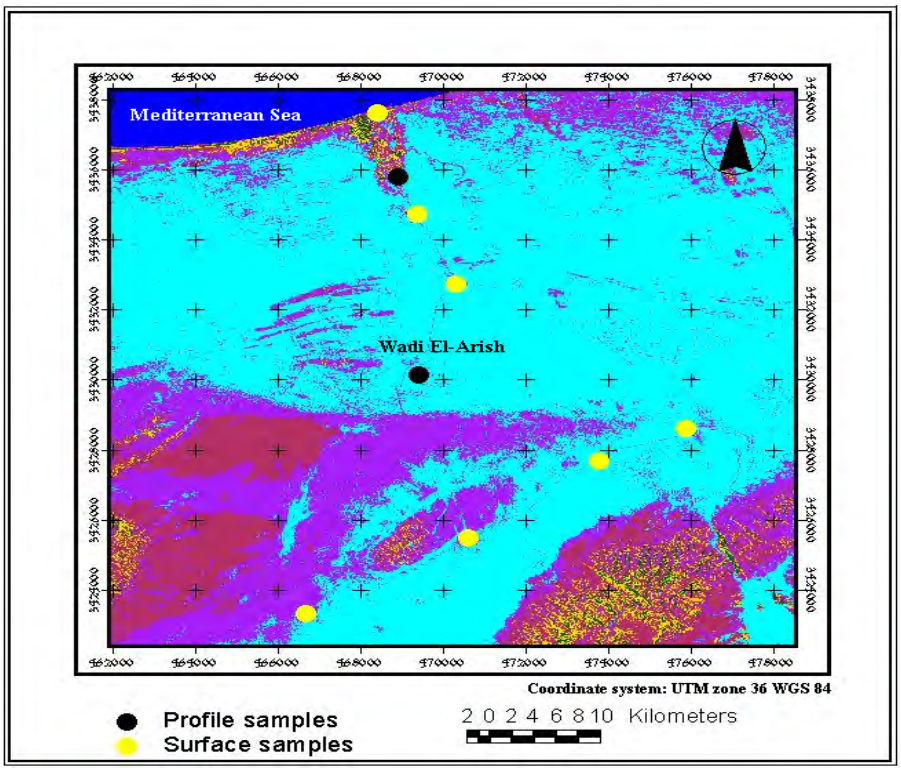

Fig. 3-8: Image map of the surface and profile samples of the El-Arish area in the north Sinai peninsula. (based on the Landsat TM-5 images acquired from USGS).

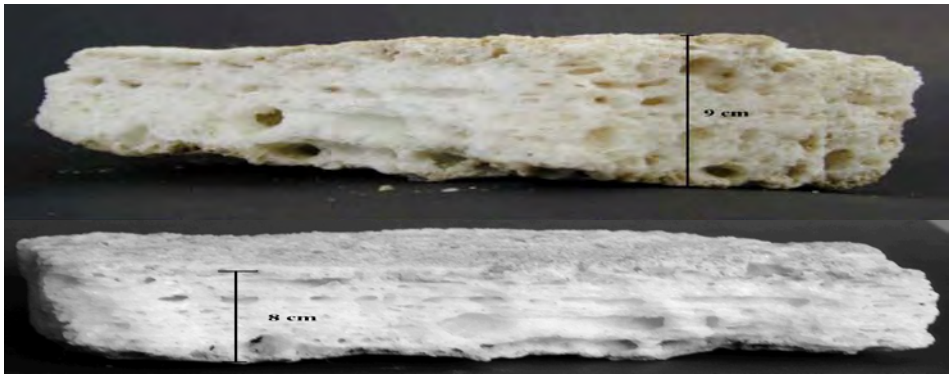

Fig. 3-9: Surface salt crust sample from the El-Tina Plain area in profile No. (1) surface samples.

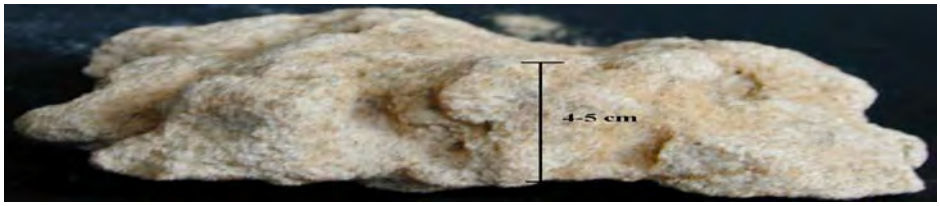

Fig. 3-10: Silica hard pans sample from the South El-Kantara Shark area in profile No. (2) layer (4).

3.2 Climatic data

The climatological conditions of the northern part of Sinai play an important role in shaping the study area and in controlling the ecology of the area. These conditions include extreme aridity, long hot rainless summer periods and mild winters in which storms rarely occur. The northern part of Sinai is also characterized by a so called El-Khamasin storms or sandstorms. These are violent winds which blow intermittently over a period of 50 days during February and March (DAMES and MOOR 1983).

Generally, the prevailing climatic conditions in the north Sinai include low rainfall, high temperatures, strong wind, high evaporation and low relative humidity. The data were collected from six meteorological stations an a monthly basis during 1989-1999.

Rainfall

The maximum rainfall in the north Sinai occurs in January and February along the coastal area. The rainfall increases to the east and rapidly decreases to the south except in the Saint Catherine area in the south Sinai (high altitude). The maximum and minimum monthly data of

rainfall during 1989-1999 are given in table (3-1) and the processed data are given in figure (3-11). The mean average of rainfall ranges from 25 to 118 mm y^{-1}. Rainfall increases in eastern direction reading 244 mm y^{-1} in the Rafah. ATTIA (1994) reported that the annual rainfall is 73 mm at Port Said and increases up to 105 mm at El-Arish.

Temperature

The temperatures in the north Sinai differ from one location to another according to its position from the Mediterranean Sea and the direction of winds. In winter, the monthly mean maximum and minimum temperature values are 20°C and 11°C, respectively. In summer, the maximum mean monthly temperature is 32.5°C and the lowest mean monthly 18.7°C, except during the El-Khamasin period were the temperature can reach 40°C. The mean maximum and minimum monthly temperatures during the 12 months from different stations in the north Sinai are show in table (3-2) and figure (3-11). Figure (3-11) shows the area under consideration lies in an arid zone. Figure (3-12) shows the map of annual mean temperature in the Sinai peninsula.

Evaporation

Evaporation in the arid zones is the most affecting factor in the hydrological cycle. The evaporation data for the north Sinai are presented in table (3-1) as recorded from different meteorological stations. Figure (3-13) shows map of mean evaporation in the Sinai.

From the mean evaporation values it can be concluded that the monthly evaporation ranges from 1.5 to 10.3 mm d^{-1}. The monthly evaporation decreases during winter to 1.5 mm d^{-1} especially in December and increases to 10.3 mm d^{-1} in July. Generally, the evaporation rates decrease eastward.

Wind

The northern part of the Sinai is mainly affected by northwestern winds coming from the Mediterranean Sea. However, during El-Khamasin storms (which are warm storms carry out the fine sand and dust from location to another depend on direction of the wind with generally high temperature in atmosphere) the direction of the wind changes from south to southwest.

Table 3-1: Meteorological data form different clime stations in the northern part of the Sinai peninsula (mean monthly data).

Stations	Parameter	Jan.	Feb.	Mar	Apr.	May	June	July	Aug.	Sep.	Oct.	Nov.	Dec.	Mean
Port Said	Temp.°C	14.4	14.6	16.3	19.5	21.9	25.1	26.8	27.3	24.5	24.2	20.1	16	
	Rain mm	25.03	17.13	16.84	3.66	2.49	0	0	0	0.4	1.84	6.73	12.1	86.22
	Evap.mm.d^{-1}	2.8	2.8	2.9	3.4	3.1	3.1	3	3.1	3.3	4.5	2.8	2.3	
Rafah	Temp.°C	12.4	12.3	15	18.7	20.4	23.5	25.6	25.7	24.6	23.5	15.5	14	
	Rain mm	70.63	61.7	30.83	0.5	3.34	0.2	0	0	0	1.7	29.44	45.14	243.47
	Evap.mm.d^{-1}	3.9	4.6	5.1	7.5	8.2	9.9	10.3	9.4	8.4	6.9	4.8	3.9	
El-Arish	Temp.°C	13	13.4	15.3	18.9	21.1	24.1	26	26.2	24.8	22.6	18.4	14.4	
	Rain mm	30.88	1835	20.17	10.33	0.92	0	0	0	0	2.96	11.75	22.2	117.74
	Evap.mm.d^{-1}	1.8	1.8	1.9	2.6	2.2	2.4	2.3	1.9	1.9	2	1.9	1.5	
Ismailia	Temp.°C	13.5	14.5	17	21.4	24.2	27.2	28.7	28.6	26.6	23.8	19.2	14.9	
	Rain mm	9.01	6.23	7.05	4.03	2.11	0	0	0	0.03	0.79	5.05	8.65	42.95
	Evap.mm.d^{-1}	3.4	3.8	4.8	6.4	7	6.7	6.4	5.6	4.8	4.3	3.4	2.8	
El-Malease	Temp.°C	11	11.9	14.5	19.3	22.1	24.7	26.2	26.3	24.1	21.3	16.3	12.3	
	Rain mm	6.4	9.91	8.05	1.06	1.62	0	0	0	0	1.31	5.51	7.46	41.32
	Evap.mm.d^{-1}	3.3	3.6	4.3	6.3	6.9	7.4	6.6	5.9	4.9	3.6	3	2.5	
Faid	Temp.°C	13.9	15	17.3	21.5	24.7	27.9	29.2	29.2	27.1	24.3	19.3	15.1	
	Rain mm	6.4	3.2	4.98	2.71	0.78	0.03	0	0	0.04	0.32	1.86	4.79	25.25
	Evap.mm.d^{-1}	6.7	4.9	5.4	6.9	7	7	6.8	6.1	5.1	4.5	3.8	3.5	

Jan.= January **Fab.= February** **Mar.= March** **Apr.= April**

Aug.= August **Sep.= September** **Oct.= October** **Nov.= November**

Dec.= December

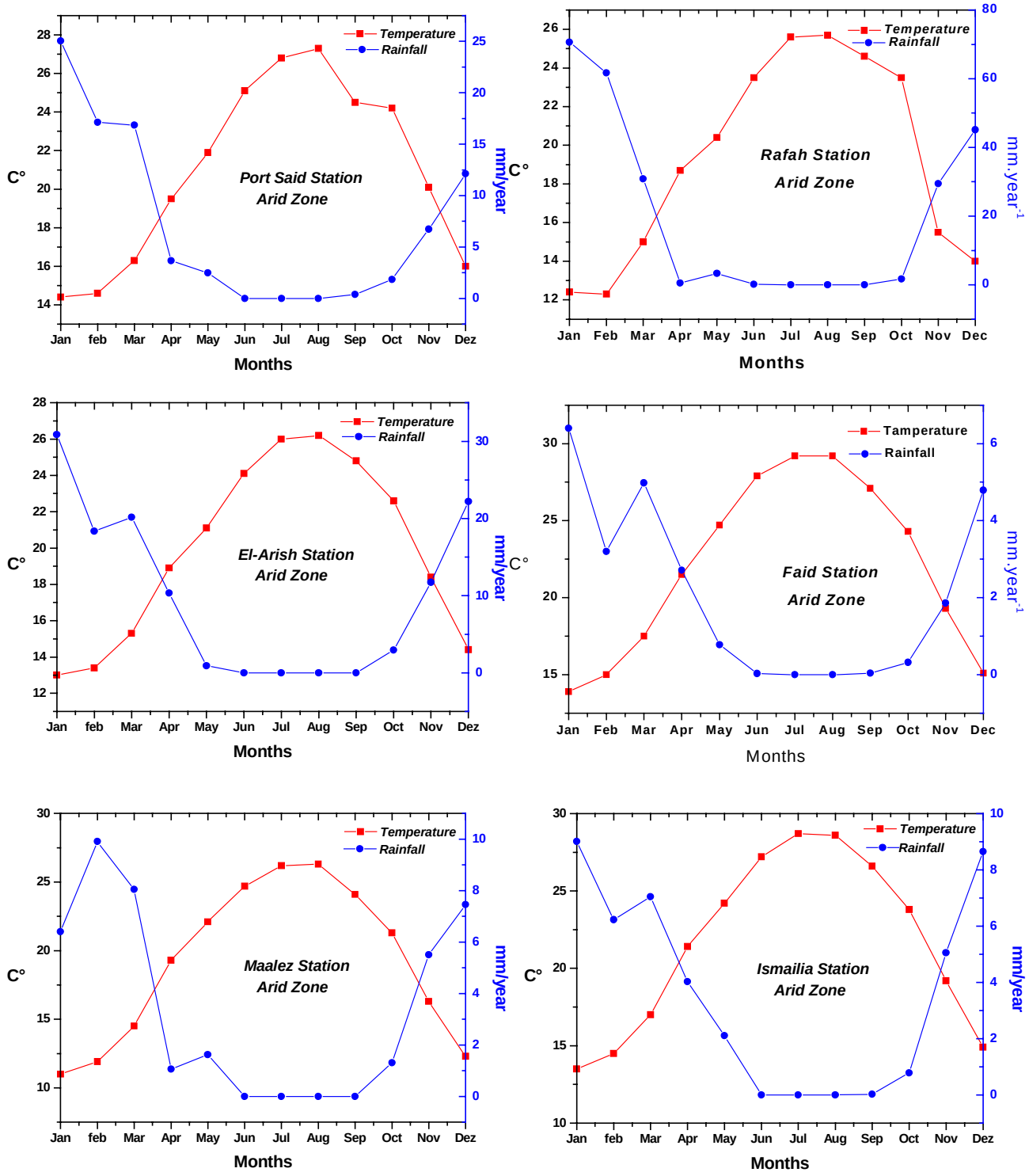

Fig. 3-11: Xerothermic diagram data from different climate stations in the northern part of the Sinai peninsula.

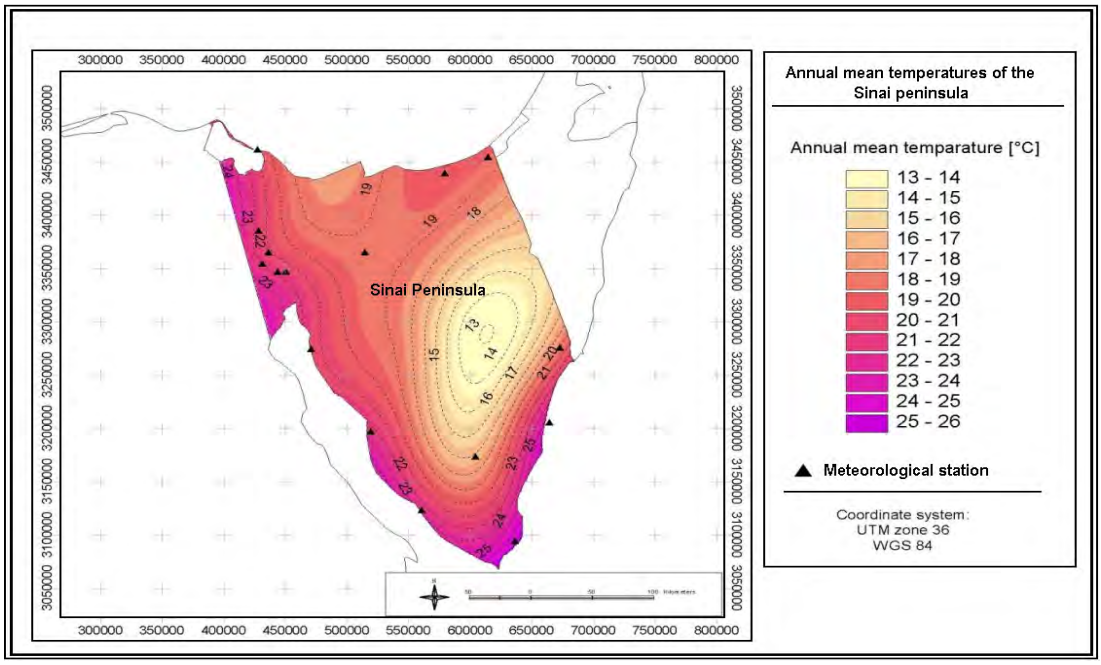

Fig. 3-12: Map of annual mean temperatures on the Sinai peninsula from different meteorological stations.

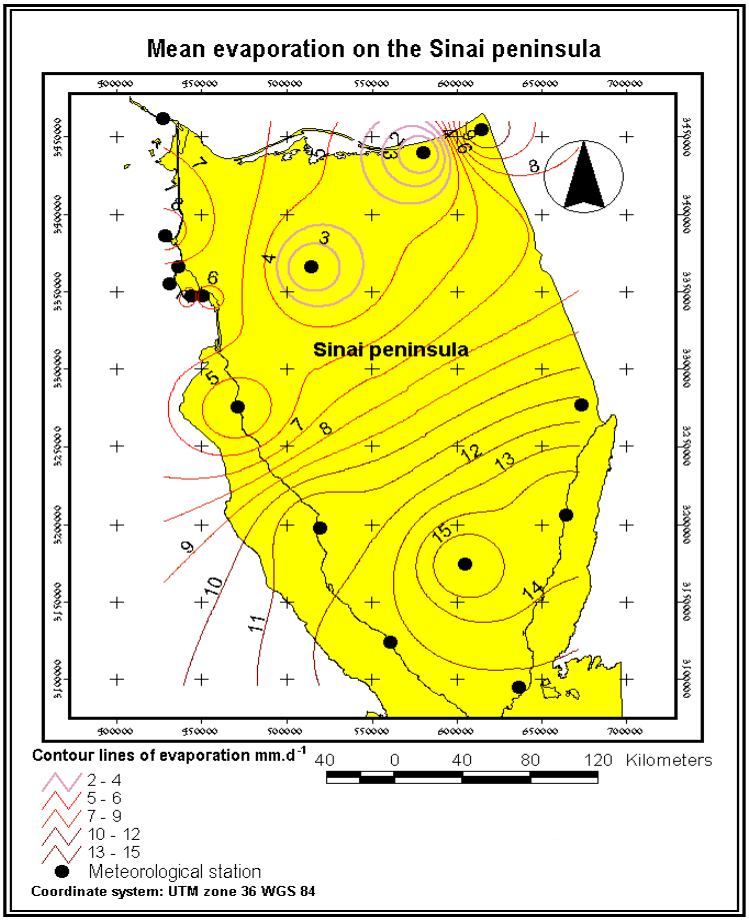

Fig. 3-13: Contour lines map of mean evaporation on the Sinai peninsula from different meteorological stations.

The monthly wind speed in some meteorological stations ranges from 2.6 to 11.3 m s^{-1}. The wind denudes the summits and translocates the fine materials. The monthly wind speed for some of the stations at Port Said, El-Arish and Ismailia are shown in table (3-3):

Table 3-3: Main monthly wind speed in the north Sinai (m s^{-1}) from some meteorological stations.

Stations	Jan.	Feb.	Mar.	April	May	June	July	Aug.	Sep.	Oct.	Nov.	Dec.
Port Said	**9.3**	**10.0**	**11.3**	**10.4**	**9.4**	**9.0**	**8.4**	**7.4**	**7.4**	**8.0**	**8.3**	**8.4**
El-Arish	**7.0**	**7.6**	**8.8**	**8.2**	**7.6**	**7.6**	**7.6**	**6.4**	**6.4**	**5.8**	**5.8**	**5.8**
Ismailia	**3.5**	**4.0**	**4.7**	**4.1**	**3.8**	**3.2**	**3.8**	**3.5**	**3.0**	**3.2**	**2.6**	**3.2**

Relative humidity

The average relative humidity in the north Sinai reaches 73% at El-Arish during July and August. In winter, it reaches 75% in El-Arish decreasing to 68% in April and May. In summer it reaches 78%. During the El-Khamasin storms it drops to 10%. The highest values recorded in August are found between 71% and 75% in the Port Said and the El-Arish, respectively.

3.3 Remote sensing data analysis

The Landsat TM-5 images data were used to study the coastal zone soils in the northern part of the Sinai peninsula along the El-Salam Canal area and separated the different soils units. Data processing was performed by two steps using the ERDAS Imagine program (version 8.3.1) for image processing and the Arc View program (version 3.2a) for visualization. Individual steps of the procedure were:

1- Pre-processing (Geocooding).
2- Image interpretation (Image processing).

3.3.1 Pre-processing

Generally, there are three types of data corrections needed: radiometric, atmospheric and geometric (Geocooding).

Radiometric and atmospheric correction

The radiometric and atmospheric correction were delivered with the satellite data preformed by the program AtCProc version 2 (see HILL 1993 for details). This program calculates the different atmospheric conditions affecting the image data. In order to convert the data to 8 bit, a scaling factor was used. This factor was 283.33 for the image data covering the study area. The atmospheric correction processing is recorded in appendix (II).

Geometric correction

There are two techniques that can be used to correct the various types of geometric distortion present in digital image data. The first is to model the nature and magnitude of the sources of distortion and use these models to establish correction formulae. This technique is effective when the types of distortion are well characterized, such as that caused by earth rotation. The second approach depends upon establishing mathematical relationships between the addresses of pixels in an image and the corresponding coordinates of those points on the ground (via a map or corrected image). These relationships can be used to correct the image geometry irrespective of the analyst's knowledge of the source and type of distortion. This procedure is the most commonly used and, as a technique, is independent of the platform used for data acquisition and each band of image data has to be corrected (RICHARDS 1994).

In order to analyze the satellite imagery it has to be transformed to a common coordinate system. This process is known as geocooding.

In many cases the image must also be oriented so that the north direction corresponds to the top of the image. In the rectification process the grid of the raw data has to be projected onto a new grid. Resembling is the process of extrapolating data values for the pixels on the new grid from the values of' the source pixels (LILLESAND and KIEFER 1997).

In the present study, the digital Landsat TM data were corrected geometrically for the four complete scenes covering the north part of the Sinai. Geometric Correction (GC) is applied to raw images data to transform them to map projections. The rectified imagery was projected

according to the Universal Transverse Mercator System (UTM) in appendix (II). This GC used in image-to-image registration and uses the Ground Control Point (GCP) system. The GCP of four raw scenes are in appendix (II).

By using the Landsat TM georefernced or geocooded image was rectified the Landsat TM raw scenes (images) covering the study areas in the north Sinai. The georefernced image was collected from the website in the internet (http://edcwww.cr.usgs.gov/gallery/dsatellite.html). This image covered only a very small area compared to the total area of study (four scenes). The georeferenced image was rectified using the state plane map projection.

Rectifying image data

The rectification of data involves, rearranging the pixels of the image onto a new grid, which conforms to a plane in the new image projection and coordinate system.

Ground control points (GCP)

Ground control points are specific pixels in the image data for which the output image coordinates. GCP consist of two sets of coordinates:

* **Source coordinates**, which are usually data file coordinates in the image.
* **Reference coordinates**, the coordinates of the image to which the source image is being registered.

The rectified coordinates of the image are extrapolated from the ground control points. The rectified coordinates for the ground control points are exactly equal to the reference coordinates, since there is often some error tolerance in the rectification.

The GCP were selected throughout the four scenes of the El-Salam Canal area. The dispersed of the GCP include the intersection point of two roads (Ismailia - El-Arish), airport runways (El-Arish Airport), cities (Port Said, El-Arish, Bair El-Abd, Rafah and El-Kantara), geological features (Gabal El-Magharah, Gabal Libina and streams and terraces of the Wadi El-Arish,) and edges point of lake and water bodies (the El-Bardawil lake, Suez Canal and the

Mediterranean sea) for more accuracy in transformation. The distribution of numbers of the GCP in the study images are 51, 105, 50, 50 GCP injected in the scenes from 1 to 4, respectively (see also values of GCP in appendix II).

Transformation

Polynomial equations were used to convert source coordinates to rectified coordinates. A transformation matrix was computed from the GCP. The size of the matrix depends upon the order of transformation. The goal, in calculating the coefficients of the transformation matrix is to derive the polynomial equations in which there is a least possible amount of error when they are used to transform source coordinates of the GCP into the reference coordinates.

The first order of transformation is a linear transformation. A linear transformation can change the location in X and Y scale in X and Y skew in X and Y and rotation. This order of transformation consist of six coefficients with three for each coordinate (X and Y), as shows in figure (3-14). The position of the coefficients in the matrix, and assignment of the coefficients in the polynomial follows the ERDAS convention (ERDAS 1997).

The output

In this study the nearest neighbor resembling method was used to determine pixels. The rectified coordinates (X0. Y0) of the pixel are retransform back to the source coordinate system using the inverse of the transformation matrix. The pixel that is closest to the retransform coordinates (Xi. Yi) is the nearest neighbor. The data file values for that pixel become the data file values of the pixel in the output image.

This method was more preferable then other methods because here the resembling process transforms original data values without averaging them. By this, the extremes and subtleties of the data values are not lost figure (3-15).

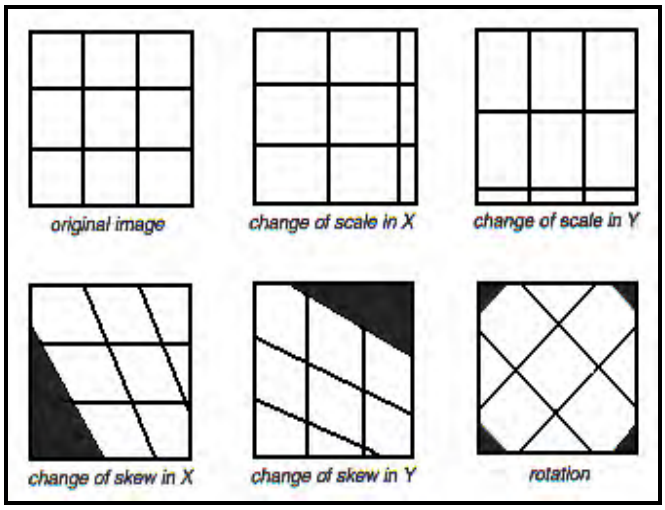

Fig. 3-14: Linear transformation (after ERDAS 1997).

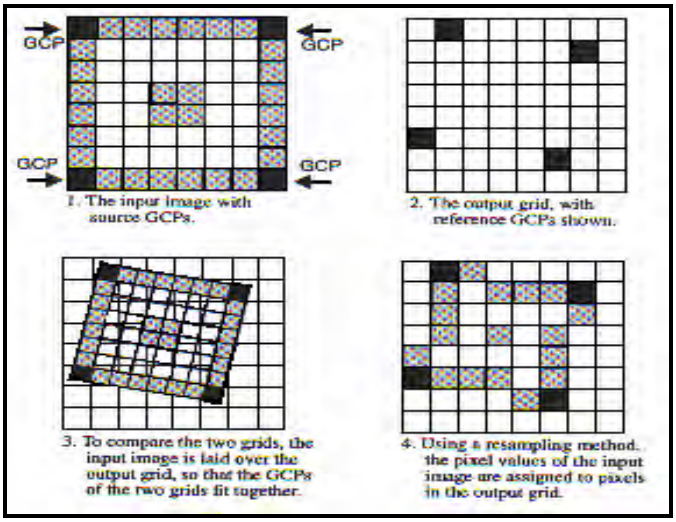

Fig. 3-15: Resembling (after ERDAS 1997).

3.3.2 Image processing

The Landsat TM-5 images data were applied to different methods of enhancement (Image processing).

Principal component analysis (PCA)

PCA allows redundant data to be compacted into fewer bands. The bands of PCA data are non-correlated and independent and are often more interpretable than the source data (JENSEN 1986, FAUST 1989). According, to CANAS and BARNET (1985) in terms of formal mathematical operation, PCA can be characterized by the following stages:

- Calculate the variance-covariance matrix for the image data set.
- Compute the eigenvalues and eigenvectors of variance covariance matrix (The eigenvectors define the PC direction and the eigenvalues measure the variances of the feature space distribution along these new PC axes).
- Implement the PCA by forming a weighted sum of the raw images using the eigenvector components as the weighting factors.

Image classification

Multispectral classification is the process of sorting pixels into a finite number of individual classes or categories of data, based on their data file values. If a pixel satisfies a certain set of criteria, the pixel is assigned to the class that corresponds to those criteria (ERDAS 1997). The computer system must be trained to recognize spatial patterns in the data. Defining, the criteria by which these patterns are recognized is called training (HORD, 1982). Training can be preformed with either a supervised or an unsupervised classification.

Supervised training (classification) is closely controlled by the analyst who chooses a group of pixels in the image to represent the criteria of each class.

Unsupervised training may also be unsupervised classification when the analysis is controlled by the computer program.

The training process uses the computer to calculate a specific spectral signature on which the classification process will be based. Each signature is supposed to correspond to a class. Using a specific equation (classification algorithm) tests every pixel on the image and 0 assigns it to a specific class.

In unsupervised training the analysts input to the computer are some parameters that will be used to uncover statistical patterns inherent in the data. These patterns do not necessarily correspond to real classes on the ground or any other features in the area represented by the image. They are simply determined mathematically. Some of the produced classes may need to be merged together, while others may need to be deleted.

Best three-band combination

Two methods have been used in this study to select the optimum three-band combination:

1- The first method was given by SHEFFIELD (1985). It depends on the use of the variance covariance matrix for a scene.
2- The second method was given by CHAVEZ et al. (1984). Chavez developed an optimum index factor (OIF) that ranks the 20 three-band combinations that may be made from six bands of the TM data (not including the thermal band). This technique is based on the amount of total variance and correlation within and between various band combinations.

3.4 Analytical methods

3.4.1 Chemical and physical methods

*** Total calcium carbonate content** was volumetrically determined using Scheibler's Calcimeter (BLACK et al. 1982).

*** Gypsum content** was quantitatively determined by conductometry using the acetone and water method (SAYEGH et al. 1978).

*** Organic matter** was determined using the LECO Carbon determinator (EC-12 Model 752–100) dry combustion method (ANONYMOUS 1982).

*** Soil reaction (pH)** was measured electrically in suspensions prepared with water and $CaCl_2$ after two hours by means of glass electrode (SILLANPÄÄ 1990)

*** Electrical conductivity (EC)** was measured in the supernatant of a soil : water (1 : 2.5) suspension after letting the suspension settle overnight (SILLANPÄÄ, 1990).

*** Sodium, Potassium, Calcium and Magnesium** were extracted from soil with (1N) CH_3COONH_4, pH 7.0, (soil : extract = 1 : 10) CAHOON (1974). **Sodium and Potassium** were

measured by emission spectroscopy using flame photometer (ELEX 6361). **Calcium and Magnesium** were determined by Atomic Absorption Spectroscopy (UNICAM 929).

*** Carbonate and Bicarbonate** were determined by titration using phenolphthalein as an indicator for the former and methyl orange for the latter (JACKSON 1973).

*** Chloride and Sulphates** were determined in descent extract soil extract according to FRENEY (1958). Chloride and sulphates were analyzed by Ionenchromatographie (Metrohm 761).

*** Cation Exchange Capacity (CEC)** was carried out using the $BaCl_2$ Triethanolamin extraction method by MEHLICH (1938).

*** Total Nitrogen** was determined using micro Kjeldahl method as described by BLUME (1966).

*** Soluble Phosphorus and Potassium** were determined in an Calcium Ammonium Lactate (CAL) extract. Phosphorus was analyzed colormetically while potassium by means of flame photometry SCHÜLLER (1969).

*** Plant available Zinc, Iron, Manganese and Copper** were determined the micronutrient by (DTPA-Extract) employment Atomic Absorption Spectroscopy (UNICAM 929), LINDSAY and NORVELL (1978).

*** Particle size distribution** was determined according to the method reported by (DE LEENHEER et al., 1954).

3.4.2 Hydraulic soil properties

The soil moisture properties were estimated according to SAXTON et al. (1986). The different hydraulic parameters of the soil were calculated from soil-water potential equations and “Soil texture triangle hydraulic properties calculator” program. This program calculates the soil moisture behavior depending on percent of the sand and clay to obtain the hydraulic soil properties.

The hydraulic and physical soil properties were achieved by calculating Wilting point (cm^3 water cm^{-3}soil), Field capacity (cm^3 water cm^{-3}soil), Saturation (cm^3 water cm^{-3}soil), Saturation hydraulic conductivity (cm hr^{-1}), Available water (cm^3 water cm^{-3}soil and in water/foot soil) and Bulk density (g cm^{-3}).

3.4.3 Land evaluation

The land capability classification method according to STORIE (1964) and SYS (1991) was used to evaluate the soil samples from the study area. The main soil parameters used in this assessment are: clime, soil depth, texture, gravel percent, $CaCO_3$ percent, gypsum percent, salinity (EC), alkalinity (ESP), slope pattern and drainage conditions. Land capability indices were calculated (SYS 1991) for each soil profile and consequently the land was allocated to a certain capability class. The land capability index (CI) was calculated as follows:

CI = A/100 x B/100 x C/100 x D/100 x E/100 x F/100 x G/100 x H/100 x I/100 x J/100 x 100

Where: A= availability and quality of irrigation water, B= texture class, C= soil profile depth, D= gypsum content %, E= slope %, F= wetness (drainage conditions), G= salinity level, H= sodicity (ESP), I= calcium carbonate content % and J= erosion.

Table (3-4) shows the rating of soil according to the system given by STORIE (1964) and MANSOUR (1979):

Table 3-4: The rating of soil quality evaluation after STORIE (1964) and MANSOUR (1979).

Grades	Quality	Rating
I	Excellent soils	100 – 80
II	Good soils	79 – 60
III	Fair soils	59 – 40
IV	Poor soils	39 – 20
V	Very poor soils	19 – 10
VI	Non agriculture soils	< 10

Table (3-5) illustrates the soil properties, rating and factors for different water and soil characteristics. The main characteristics in the assessment scheme according to STORIE (1964) and MANSSOUR (1979) are considered as limiting factors for irrigation and land use.

Table 3-5: Soil properties rating according to STORIE (1964) and MANSSOUR (1979).

Factor	Soil properties				Rating
A)	**Availability and quality of irrigation water:**				
	Nile water				100
	Mixed Nile and Drains water 1000 mg kg^{-1}				90
	Mixed Nile and Drains water < 2000 mg kg^{-1}				80
	Mixed Nile and Drains water 2000-4000 mg kg^{-1}				60
	Mixed Nile and Drains water 4000-5000 mg kg^{-1}				40
	Mixed Nile and Drains water > 5000 mg kg^{-1}				20
B)	**Texture:**				
	L, SiL, SCL, SI, SICL, CL				100
	Si				95-90
	LS, SC				85-80
	FS, MS, SiC, C				75-60
	Cs				55-40
	Texture	*SIGr.	*Gr.	*VGr .%	
	L, SiL, CL	80	70	60	
	SL	70	60	50	
	LS	60	50	40	
	S	50	40	30	
C)	**Soil Profile depth (cm):**				
	> 120				100
	120-90				100-90
	90-60				90-70
	60-30				70-40
	<30				<40
D)	**$CaSO_4$ Content %:**				
	<3				95
	3–10				100
	10-15				95
	15-25				75
E)	**Slope %**				
	Flat or Almost flat	(0-2 %)			100
	Undulating	(2-8 %)			95-90
	Rolling	(8-16 %)			90-85
	Hilly	(16-30 %)			85-70
	Steep	(30-45 %)			70-35
	Very steep	(> 45 %)			< 35

*SIGr: Slighlty gravelly, Gr :Gravelly, VGr: Very gravelly

Factor	Soil properties	Rating
F)	**wetness (drainage Conditions):**	
	Well drained	100
	Moderately drained	95-85
	Imperfectly drained	85-75
	Poorly drained	75-45
	Very poorly drained	45-25
G)	**Salinity level:**	
	< 4	100
	4-8	95-5
	8-16	85-45
	> 16	<45
H)	**Sodicity (ESP):**	
	< 10	100
	10-15	95-85
	15-30	85-75
	30-50	75-55
	> 50	<55
I)	**$CaCO_3$ Content %:**	
	< 5	100
	5-10	95-90
	10-20	90-75
	20-50	75-40
	> 50	<40
J)	**Erosion:**	
	1-Wind erosion	
	Non erosion	100
	Slightly erosion	95-90
	Moderately erosion	90-75
	Severe erosion	75-60
	2-Water erosion	
	Non-erosion	100
	Slightly erosion	95-100
	Moderately erosion	90-75
	Severe erosion	75-40
	Very Severe erosion	40-20

3.4.4 Statistical analysis

The methods for statistical analysis (correlation and regression) employed in this thesis are supplied by the SPSS (version 10.0) and the SAS (version 8.0) statistical program packages.

4 Results

4.1 Soil morphology and classification in the study area

The morphological characteristic, landforms and soils classification are explained here through the Landsat TM images description analysis of the different physiographic features, soil profiles and environment conditions (pedon) in the El-Salam Canal area. From these description analysis and field observations the following morphological units and landforms in the northern part of the Sinai peninsula along the El-Salam Canal soil project area under study could be recognized:

- Coastal plain sand sheet and sand dunes (active and passive).
- Individual Sabakha, marsh and swamp areas.
- Foreshore sand terrain, ridges and hummocks.
- Wadi El-Arish.

The parent materials of the studied soils in the northern part of the Sinai along the El-Salam Canal area were recognized according to the filed description into four groups. These groups are emphasized on the field as following:

- Nile alluvium, and lacustrine sand deposits of the El-Tina Plain area.
- Lacustrine sand deposits of the area surrounding the El-Bardawil lake in the Bair El-Abd and the El-Telol areas.
- Aeolian sand deposits of the active dunes and sand sheet deposits in the South El-Kantara Shark, the Rabaa and Qatia areas.
- Calcareous and sand deposits in the Wadi El-Arish area.

The studied soil profiles of the parent material are described in detail in the appendix (I).

The soil classification have been identified in two orders, Aridisols and Entisols in the El-Salam Canal area according to the USDA/SSS system of the soil classification (1975). The soils of the region in the northern part of Sinai under investigation were classified under three categories (suborders) *Typic Torripsamments, Calciorthids* and *Typic Salorthids*. The detail of the orders and suborders description of soil classification for the studied soil profiles are described in the appendix (I).

4.1.1 Morphology of the El-Tina Plain and the South El-Kantara Shark soils

El-Tina Plain occupies the northwestern corner of the Sinai, as an integral part of the ancient Nile Delta. It has a triangular shape, bordered to the east by the Suez Canal, to the north by the Mediterranean shoreline trending NW-SE, and to the south by a sharp straight contact with northern Sinai sand sheet (figure 4-1). It is an extensive mud flat, reaching nearly 3 to 5.5 m above sea level and is covered by a salt crust of thickness reaching nearly 2.5 to 9.5 cm (see photo of profile No.1 the El-Tina Plain, figure 4-2).

El-Tina Plain can be divided into two distinct zones, namely; a northern strand plain and a southern delta plain. The strand plain varies in width from 1 km in the east to 12.5 km in the west where it is covered by the El-Malaha lake. It consists of bundles of very low accretions beach ridges, a few ten centimeters higher than the surroundings.

The Mallaha lake occupies the northwestern corner of the El-Tina Plain (figure 4-1), where it covers an area of about 5 hectares. It is connected to the Mediterranean Sea by a small entrance near the Port Fouad. It is very shallow, with a depth between 0.15 and 0.50 m and its salinity is higher than that of the Mediterranean sea.

The southern delta plain is composed of muddy delta sediments and lies 1 to 2 m above sea level. The sandy plain sheet unit occupies a narrow zone to the east and southeast of the wetland zone. It is formed of flat to gently undulating sand sheet. The contact between the fringing wetlands and the sandy plain is marked with a very well developed belt of *Nitraria retusa* Nebkas. These are phytogenic accumulations of drifted sands associated with the halophyte *Nitraria retusa* (figure 4-3).

The sand sheet deposits are exposed for about a few kilometers in the east of South El-Kantara Shark area. It is an undulating area, having sand hummocks reaching sometimes 5-8 m high and few low inland dunes (figure 4-4).

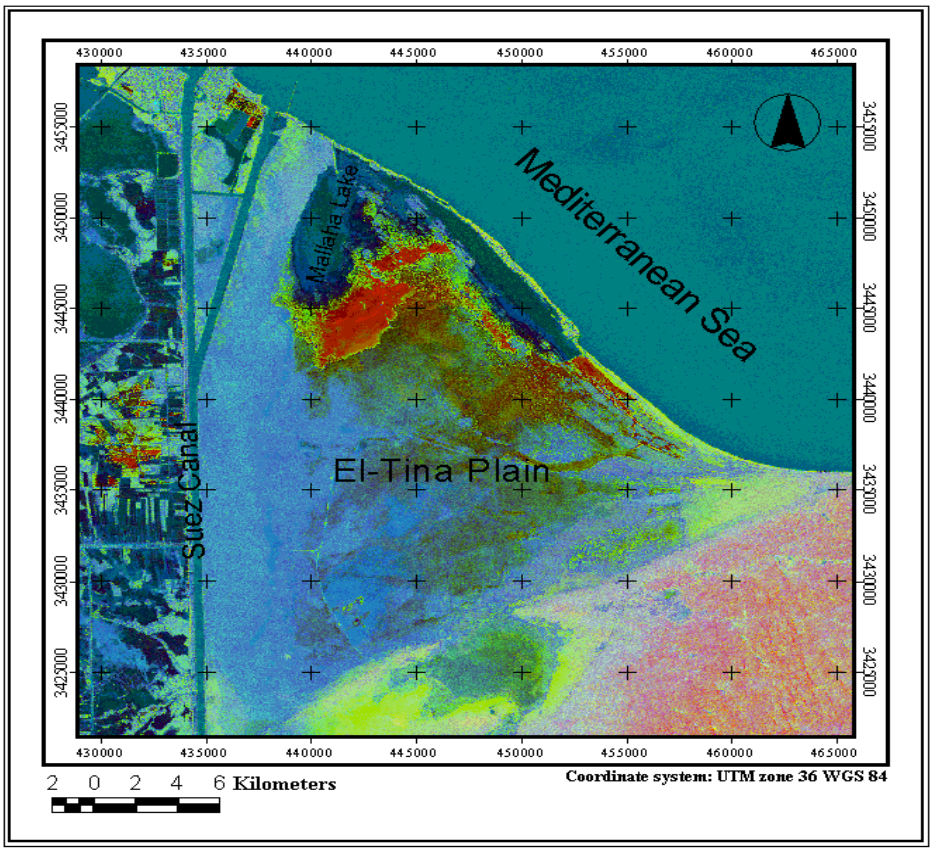

Fig. 4-1: Morphological image map of the El-Tina Plain area from the Landsat TM image bands (1, 3 and 2).

Fig. 4-2: Salt crust in the surface sample in profile No.1 the El-Tina Plain-Sabkha.

Fig. 4-3: Wetland soils between sand dune and sand sheet with many shrubs (*Nitraria retusa*) growing on water table.

Fig. 4-4: Undulating area, sand hummocks reaching 5-8m high and low inland dunes in the South El-Kantara Shark area.

The ground water in the South El-Kantara Shark area is deep and the drainage is excessive in many location in these soils. In the some of studied area the fresh water source is that stored from rainfall within the sand sheet in these area.

The South El-Kantara Shark area as shown in some locations have hard pans in some soil profile layers (profile No. 2, see the description in appendix I figure A-4). These type of hard pans are the calci and silica of chemical composition, with depth ranging between 50 and 168 cm from the surface soil and clear wavy boundary.

4.1.2 Morphology of the El-Bardawil, the Bair El-Abd and the Rabaa soils

These areas of study having many morphological features are recognized and observed from the field description, the Landsat TM image analysis and previous works as following:

Individual Sabkhas, Marshes and Swamps

The largest Sabkha in the study areas lies in the El-Tina Plain and the second important one is Sabkhas and Marshes El-Amia which lies between the El-Nigila and Rabaa (figures 4-5 and 4-6). In addition to, there are many Sabkhas around the El-Bardawil lake. The Bardawil Sabkhas can be described by flat Sabkha and dune Sabkha. The first is restricted to the sandy flats that fringe the lake at the extreme eastern and western ends. The dune Sabkha occupies most of the lake's southern shores, where the longitudinal sand ridges intersect the lake water. The evaporation wavy surface of flat Sabkhas was identified at many location in the Bair El-Abd and Rabaa area (figure 4-7).

Fig. 4-5: Morphological feature of Sabkhas, Marshes and Swamps near the coastal plain of the El-Telol and the Bair El-Abd areas.

Fig. 4-6: The Sabkhas (playas) and Marshes El-Amia lies between the El-Nigila and the Rabaa villages.

Fig. 4-7: Surface salt pan flat Sabkhas (2-5cm thickness) around the El-Bardawil lake.

The El-Bardawil lake extends along the northern coast of the Sinai for about 80 km and has a total area of about 70.000 hectares, this description from the Landsat TM image (figure 4-8). Its maximum width is about 8 km with a maximum depth of about 3 m. The lake is separated from the Mediterranean Sea by a long curving sand barrier.

Sand sheet and sand dunes (active and passive)

The study soil areas lie totally within coastal plain region of the Mediterranean sea at the northern part of the Sinai peninsula. The sand sheet is more or less flat and its wavy surface is sprinkled with small and large scale ripples and large scale coarse and fine sand dunes. These ripples and sand dunes have a wavelength of 5 to 200 cm and 3 to 30 m (figures 4-9 and 4-10).

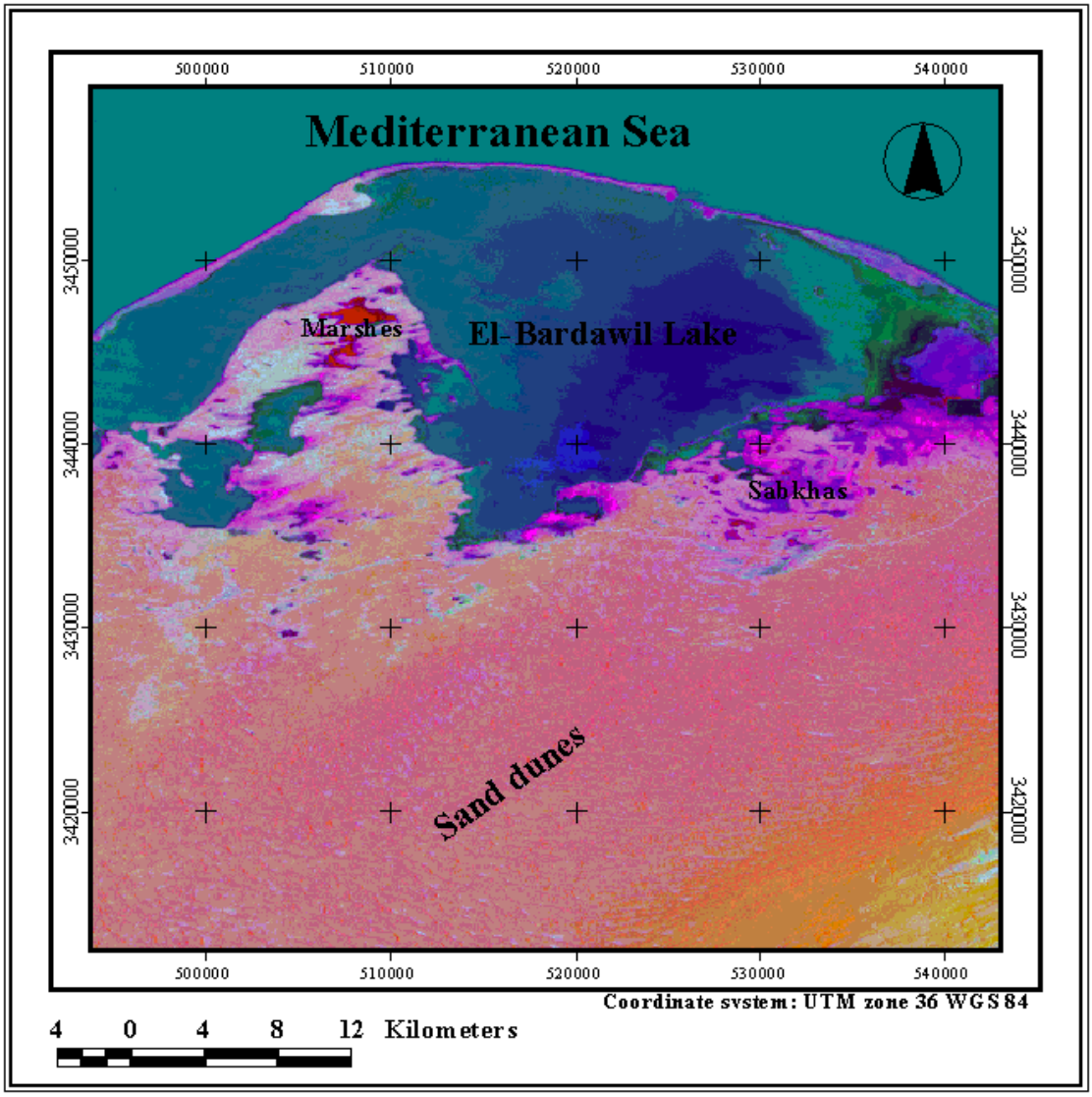

Fig. 4-8: Morphological image map of the El-Bardawil lake and the Bair El-Abd areas from the Landsat TM image bands (1, 3 and 2).

Fig.4-9: Small scale of ripples and small sand dunes (5 to 200cm).

Fig. 4-10: Large scales of ripples and large sand dunes (3 to 30m).

The surface is nearly flat with ripples and small sand dunes in the northwestern part of the study areas, while the central and northeastern part of study area are occupied by fine texture surface with sand sheets and mounds that form conical hammocks rising 1 to 2m (figures 4-11 and 4-12). The sand sheets are characterized by gently undulating and moderately vegetated surfaces covered with varying densities of vegetation. The study area of the Rabaa have large one of sand sheet area. From the field observation and the Landsat TM images the fine sand

texture and sand sheet areas, that are associated with Sabkhas could be discriminated and recognized.

Mobile sand dunes in the study area were described from the Landsat TM-5 image. Generally the active sand dunes are located along the southern boundary of study areas of the El-Salam Canal project, east Suez Canal (figure 4-13). Mobile sand dunes occupy a considerable area especially at the northwestern and southeastern of the Bair El-Abd area. They are generally arranged parallel to each other or sub-parallel to the resultant direction of the effective winds, where they follow a NW-SE direction and curve southward to follow an E-W direction. Their length ranges from a few hundred meters to more than 4 kilometers, however their average length in the northwestern study areas is about 3 kilometers, with an average width of about 150 and 750 m in wavelength. The field survey descriptions and observations (see appendix I) revealed that some of the active sand dunes were subjected to aeolian processes. These processes destroyed the natural vegetation life, highways and the buildings (e.g. some of palm trees covered by sand, sand partially covered the road and small special farms were damaged or disappeared) as show in the figures (4-14, 4-15, 4-16 and 4-17). By using the Landsat TM-5 data was preformed mapping of source zones of wind-deposited in western Erg (ABD EL-HADY et al. 1992), also suggested using the TM1, TM5 and TM7 bands to provide maximum information about the source zones of the wind-deposited soils.

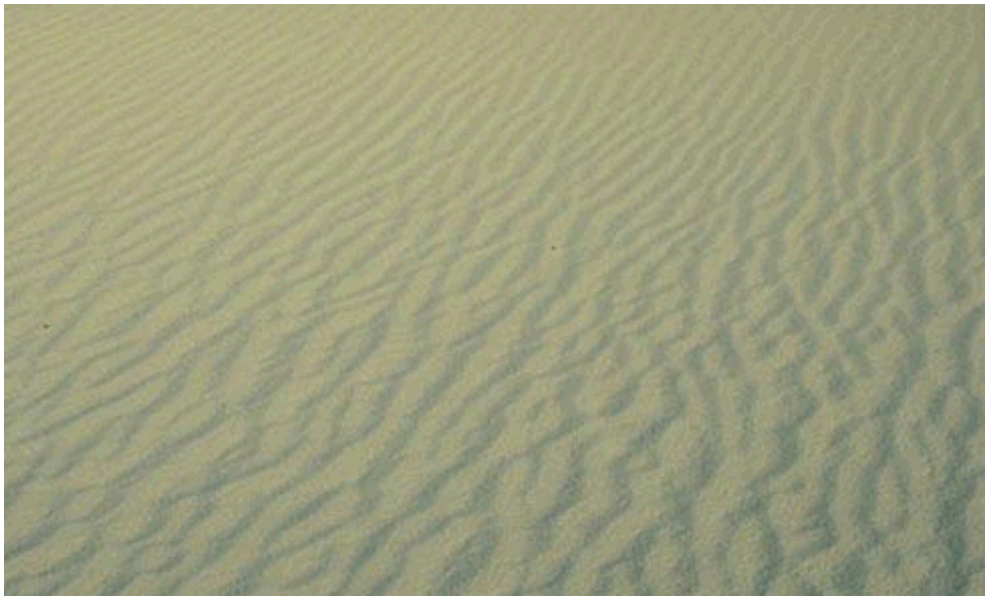

Fig. 4-11: Coarse sand sheet textured and their wavy surface with coarse sand in the northwestern of the study area in the north Sinai.

Fig. 4-12: Fine sand sheet textured and their wavy surface are sprinkled with coarse sand in the northeastern of the study area in the north Sinai.

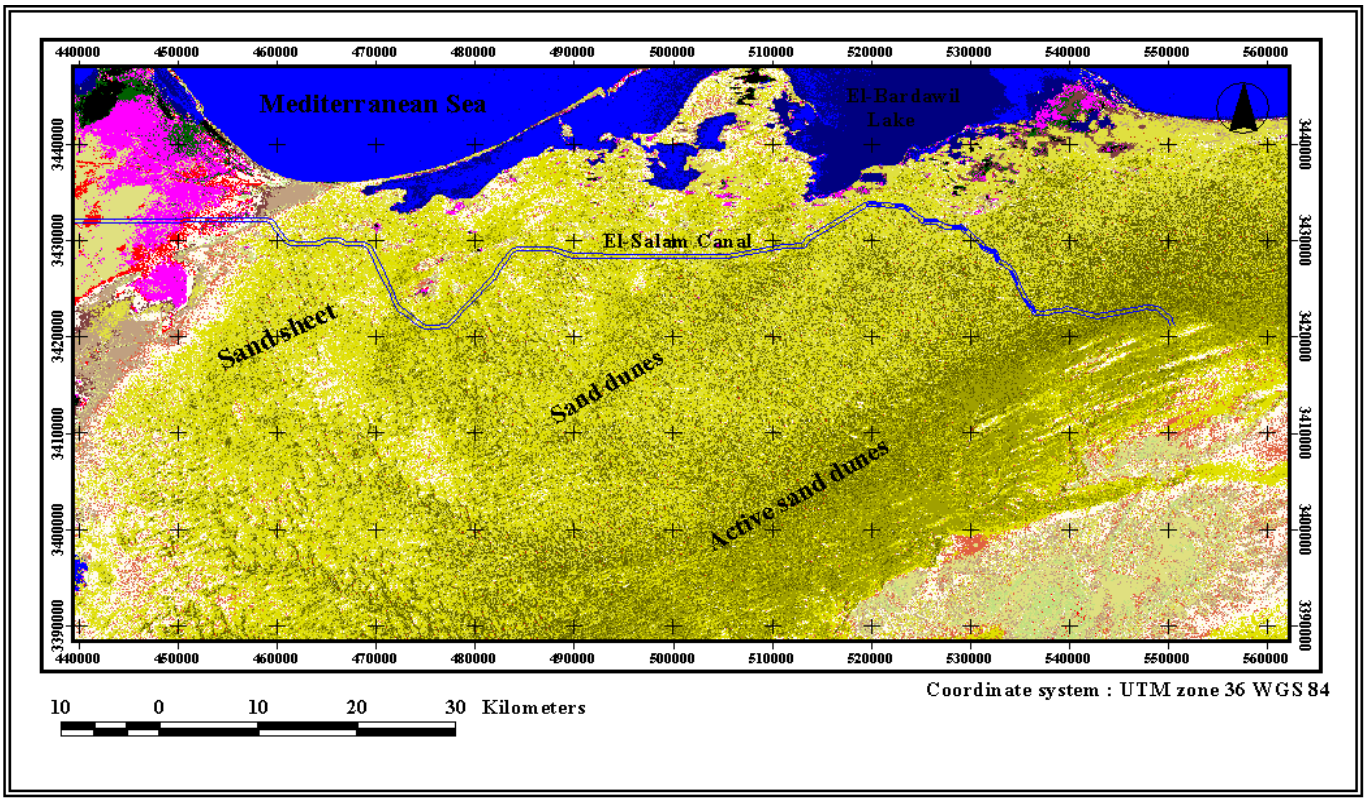

Fig. (4-13) Morphological image map of the sand dunes, active sand dunes and sand sheet in the northern part of the Sinai peninsula.

Fig. 4-14: Cultivation area partially covered by active sand dunes near to the Rabaa and Qatia area.

Fig. 4-15: Mobile sand dunes covered some of the palm trees, while some palms grows within active dunes.

Fig. 4-16: Mobile active sand dune covers partially the road in the western part of the north Sinai.

Fig. 4-17: Small canal of irrigation from the El-Salam Canal partially covered by active sand dunes in the northwest of the South El-Kantara Shark area.

The active sand dunes in the northern part of the Sinai completely flooded wide area of vegetation (natural vegetation or special farms) and covered big parts of the road connected between the Bair El-Abd and El-Arish and the road between the Ismailia to El-Tasa. In addition, the active sand dunes covered partially the small buildings in the east of the El-Nigila village and south of the El-Telol village in the studied area.

4.1.3 Morphology of the Wadi El-Arish soils

The Wadi El-Arish was described morphologically into upper, middle and lower terraces, in addition to the present channel and flood plain. According to their elevation are 35, 22, 12 and

2 meters respectively. The lowest elevation has the youngest deposit and the highest elevation has the oldest deposit.

The slope gradient of the wadi varies from the northern to the southern parts. This slope gradient variation is due to the structural role and the geomorphic feature. The average slope ranges between 1.5 to 4.5 m km^{-1}, with a length of about 250 km. The main stream runs through several conspicuous steps facing the north and parallel the present shoreline which has an E-W direction in Wadi El-Arish area. There are few numbers of small tributaries as drainage lines that find their way into the Wadi El-Arish basin particularly in the Aneiza area. These tributaries are important as contributors to the water supply of the Wadi El-Arish area.

The coastal plain area to the west of El-Arish is characterized by the coastal dunes and the beach-ridges. These two features were only identified from the satellite image. Figure (4-18) shows the image map of general view of the Wadi El-Arish stream and some of the morphological features (sand dunes, minor of tributary lines, city or villages and Gabal Libina).

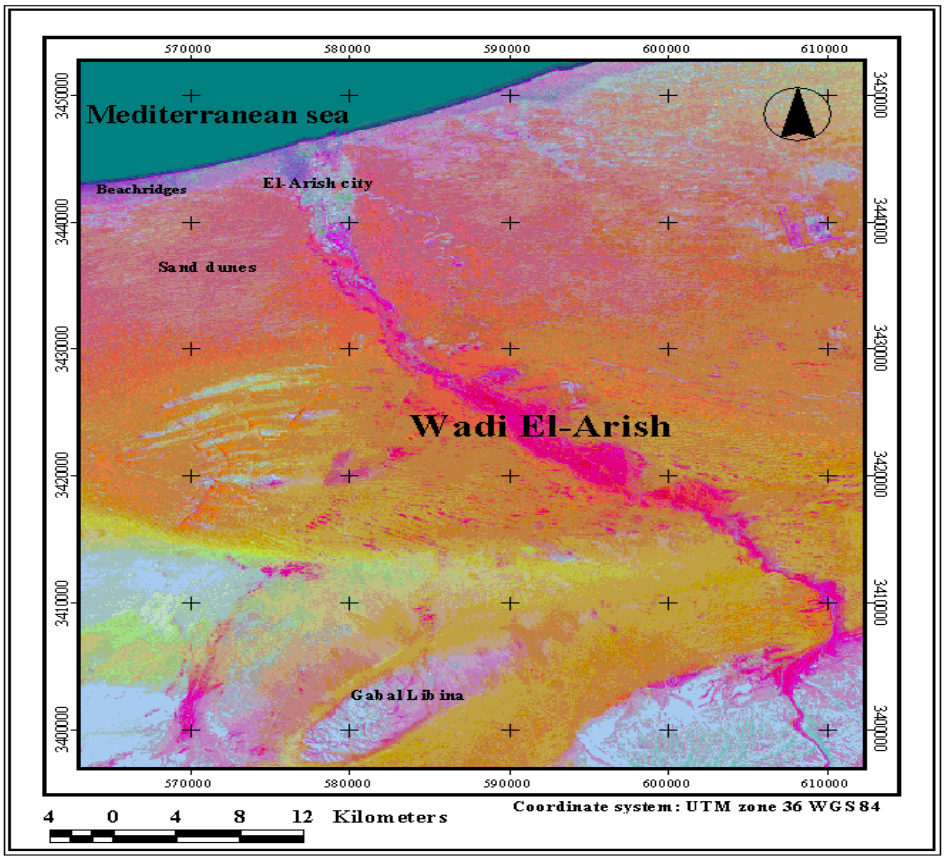

Fig. 4-18: Morphological image map of the Wadi El-Arish area from the Landsat TM image bands (1, 3 and 2).

The coastal dune belt considered as the western extend toward northeast of the Palestinian coast. They are active seif sand dunes trending obliquely to the coastline in southeast direction. They are arranged parallel to each other and are devoid of vegetation cover.

The field sampling was difficult because the landscape is often covered by sand dunes and gravels in some study areas. Topographic map (1:50.000 scale) and the Landsat TM images were very helpful in checking the field study.

Figures (4-19a and b) shows the gravel surface soils near the Gabal Libina south of the Wadi El-Arish and fine surface soils in the basin of the Wadi El-Arish area.

Fig. 4-19a: Gravel surface soils area and few shrubs in the south of the Wadi El-Arish (Gabal Libina area).

Fig. 4-19b: Fine surface soils area and many palm trees in the Wadi El-Arish area.

4.2 Soil characteristics in the study area

The morphological description of soil profiles of the study area are presented in appendix (I), with photos of some representative soil profiles. The main morphological characteristics of the studied soil profiles could be generally described as follows:

4.2.1 El-Tina Plain soil profiles

The parent material of the El-Tina Plain area is a mixture of alluvium deposits, originating from old Nile branches and lacustrine sand deposits, sometimes inter-mixed with aeolian sand deposits. The landscape is flat to almost flat and barren of plant cover (natural vegetation), with some patches are covered with some species of Halophytes. The water table in some cases is very shallow. The drainage is poor to imperfect drained. The category of soil classification is *Typic Salorthids.*

The soils varied from sand to clay texture, extremely saline and the surface is covered by a salt crust on profile (No.1) (figure 4-2) in the El-Tina Plain study area, soil color ranges from light gray to brown (dry) and grayish brown to gray (moist), soil structure is fine to medium single grains and strong or moderate, coarse to medium angular to sub-angular blocky massive. The pedological features identified within profiles depth are accumulation of gypsum crystals, common salt crystal, few lime concretions and few shells. Morphologically the studied soil profiles in this area are characterized by the salic diagnostic horizons.

4.2.2 South El-Kantara Shark, the Rabaa and the Bair El-Abd soil profiles

The landscape ranges between almost flat, undulation to sloping (hilly). The soil parent material is sandy deposits transported by winds. The natural vegetations are few to common density of distribution. Some areas are covered with patches of many palm trees and small special farms. The drainage is moderately to well drained. The category of soil classification is *Typic Torripsamments.*

The soils texture is coarse to fine sand and loamy sand texture, non saline and low calcium carbonate content. Soil color ranges from very pale brown (dry) to dark yellowish brown

(moist). Soil structure is single grains, structure less massive and massive. The pedological features identified within profiles depth are hard pans of calci-pan in profile (2) South El-Kantara Shark, few lime concretions, few fine and medium clear mottling within soil profile (2 and 3) in Bair El-Abd study area and coarse, medium and fine rood within the different layers in the studied profiles. Morphologically the studied soil profiles in these areas are characterized by a lack of diagnostic horizons.

4.2.3 Wadi El-Arish soil profiles

The landscape is flat to mainly almost flat and some parts are undulating to rolling. Soil parent material is calcareous deposits and sometimes sand deposits. The natural vegetation is few to common density of distribution and some patches are covered by the palm trees and special farms. The drainage is well drained. The categories of soil classification are *Typic Torripsamments* and *Typic Calciorthids*.

The soil texture varies widely from loam, sandy loam, loamy sand, and sand and in some area slightly gravelly sand is found on the surface samples. Soil color ranges from very pale brown (dry) to light yellowish brown or brown (moist). Soil structure is strong fine to medium massive and structure less massive. The calcium carbonate indicator ranges from strong to weak effervescence with HCl test in the field description, that index to high and moderate content of $CaCO_3$ in the study soils of the Wadi El-Arish. The soils profiles are non saline detected on studied soil surfaces and characterized by a lack the diagnostic horizons.

4.3 Chemical and physical soil property maps generated from remote sensing data

The soil properties in the northern part of the Sinai along the El-Salam Canal project reveal that the soil chemical and physical characteristics distribution are closely related to the landform and soil classification. The chemical and physical properties are reflected on soil formation, characteristics and distribution of studied soil areas. The chemical properties are organic matter (OM), calcium carbonate ($CaCO_3$), Gypsum, soil reaction (pH), electrical conductivity (EC), cation exchange capacity (CEC), exchangeable cation, soluble cations and anions in the soil extract. The nitrogen, phosphorus and potassium content were determined in the studied soil profiles and surface samples. The micronutrients (Zinc, Iron, Manganese and Copper) were

determined in profile and surface samples in the north Sinai along the El-Salam Canal project study area. The physical properties analyzed are particle size distribution and bulk density. In addition in some sites hydraulic characteristics (e.g. field capacity, saturation, hydraulic conductivity and available water) were calculated by using particle size fractions (sand and clay).

4.3.1 Soil properties and maps of the El-Tina Plain area

The results of the chemical and physical soil characteristics of the El-Tina plain study area are similar within the profile and surface samples can be described collectively rather than individually. Tables (4-1) show some results of chemical properties total calcium carbonate, organic matter, organic carbon, gypsum content and pH values in the El-Tina plain soils. These chemical properties were studied in the surface and profile samples collected from different location in the El-Tina plain area along the El-Salam Canal project in the north Sinai.

The calcium carbonate content in the El-Tina Plain soils range between 0.1 to 7.19% in profile and surface samples. Figure (4-20) shows the contour lines map covering the surface study area of the El-Tina Plain and the distribution of $CaCO_3$ content by using the Landsat TM image data. This contour lines map was preformed by using the Arc View 3.2a GIS program and final result layers from ERDAS image analysis processing.

The results of organic matter content in table (4-1) ranged between 0.08-1.24 % in studied soil profile and surface samples of the El-Tina Plain area. The organic carbon ranges between 0.03 to 0.83 %. The organic carbon was estimated from the organic matter and calcium carbonate content.

Table 4-1: $CaCO_3$, OM, Organic carbon, Gypsum and pH in the studied soils.

Sample No.	Type of sample	Location	Depth cm	CaCO3 %	OM %	C %	Gypsum %	pH ($CaCl_2$)	pH (H2O)
1	SS1-1	(Z1) South El-Kantara Shark	0-60	0.69	0.08	0.00	0.00	8.3	9.5
2	SS1-2	(Z1) South El-Kantara Shark	0-55	0.54	0.14	0.08	0.00	8.2	9.3
3	SS1.3	(Z1) South El-Kantara Shark	0-50	0.46	0.11	0.05	0.32	8.3	9.1
4	SS1-4	(Z1) South El-Kantara Shark	0-70	0.47	0.06	0.01	0.00	8.3	9.4
5	SS1-5	(Z1) South El-Kantara Shark	0-40	0.25	0.03	0.00	0.00	8.2	9.0
6	SS1-6	(Z1) South El-Kantara Shark	0-60	0.5	0.10	0.04	0.00	8.3	9.4
7	SS1-7	(Z1) South El-Kantara Shark	0-65	1.34	0.55	0.39	1.68	8.1	8.1
8	P1-1-1	(Z1) South El-Kantara Shark	0-42	0.29	0.04	0.00	0.16	8.2	8.7
9	P1-1-2	(Z1) South El-Kantara Shark	42-50	1.05	0.21	0.08	0.24	8.3	8.7
10	P1-1-3	(Z1) South El-Kantara Shark	50-125	0.34	0.05	0.01	0.00	8.3	9.3
11	P1-1-4	(Z1) South El-Kantara Shark	125-160	0.17	0.05	0.03	0.00	8.2	9.0
12	P1-2-1	(Z1) South El-Kantara Shark	0-20	3.39	0.53	0.12	0.00	8.2	9.1
13	P1-2-2	(Z1) South El-Kantara Shark	20-130	0.04	0.02	0.01	1.04	8.2	8.8
14	P1-2-3	(Z1) South El-Kantara Shark	130-164	0.34	0.08	0.04	0.56	8.3	9.5
15	P1-2-4	(Z1) South El-Kantara Shark	164-168	4.19	0.95	0.44	1.12	8.4	8.9
16	P1-2-5	(Z1) South El-Kantara Shark	168-210	0.46	0.10	0.05	0.56	8.5	9.6
17	SS2-1	(Z2) Tina Plain area	0-70	2.43	0.74	0.45	11.84	8.4	8.6
18	SS2-2	(Z2) Tina Plain area	0-60	4.39	1.24	0.83	16.96	8.2	8.4
19	SS2-3	(Z2) Tina Plain area	0-40	0.42	0.53	0.48	23.84	8.0	8.0
20	SS2-4	(Z2) Tina Plain area	0-30	0.08	0.43	0.42	24.16	7.5	7.7
21	SS2-5	(Z2) Tina Plain area	0-60	0.34	0.08	0.04	12.96	8.3	8.4
22	SS2-6	(Z2) Tina Plain area	0-50	0.19	0.06	0.06	15.92	8.6	8.9
23	SS2-7	(Z2) Tina Plain area	0-60	0.63	0.16	0.09	7.12	8.5	8.7
24	P2-1-1	(Z2) Tina Plain area	9-20	0.5	0.21	0.15	16.40	8.7	8.8
25	P2-1-2	(Z2) Tina Plain area	20-110	7.19	1.19	0.69	24.08	8.2	8.4
26	P2-2-1	(Z2) Tina Plain area	0-17	0.25	0.16	0.13	23.76	8.2	9.0
27	P2-2-2	(Z2) Tina Plain area	17-70	0.5	0.12	0.06	1.52	8.9	9.0
28	P2-2-3	(Z2) Tina Plain area	70-140	0.67	0.11	0.03	4.24	8.8	8.7

SS= Surface Sample PS= Profile Sample Z= Zone area of study $CaCo_3$ = Calcium carbonate OM= Organic Matter

Cont. table 4-1: $CaCO_3$, OM, Organic carbon, Gypsum and pH in the studied soils

Sample No.	Type of sample	Location	Depth cm	CaCO3 %	OM %	C %	Gypsum %	pH ($CaCl_2$)	pH (H2O)
29	SS3-1	(Z3) Qatia Village area	0-50	0.38	0.07	0.03	0.00	8.5	8.5
30	SS3-2	(Z3) Qatia Village area	0-55	0.48	0.22	0.16	0.00	8.4	9.5
31	SS3-3	(Z3) Rabaa Village area	0-50	0.25	0.04	0.01	0.00	8.5	8.9
32	SS3-4	(Z3) Rabaa Village area	0-45	0.29	0.04	0.00	0.00	8.4	8.8
33	SS3-5	(Z3) El-Ahrar Village area	0-60	0.07	0.02	0.01	0.00	8.3	9.5
34	SS3-6	(Z3) Rummana Village area	0-45	0.21	0.04	0.01	0.00	8.2	9.4
35	SS3-7	(Z3) El-Ganien Village area	0-55	0.38	0.06	0.01	0.00	8.4	8.9
36	SS3-8	(Z3) Rabaa Village area	0-50	0.48	0.16	0.10	0.00	8.5	9.2
37	SS3-9	(Z3) El-Nigila Village area	0-60	0.42	0.10	0.05	0.00	8.0	9.3
38	P3-1-1	(Z3) El-Ahrar Village area	0-25	0.21	0.05	0.03	14.16	8.3	8.5
39	P3-1-2	(Z3) El-Ahrar Village area	25-40	0.42	0.10	0.05	9.68	8.3	8.4
40	P3-1-3	(Z3) El-Ahrar Village area	40-75	0.21	0.07	0.04	1.76	8.5	8.8
41	P3-2-1	(Z3) Rabaa Village area	0-30	0.25	0.04	0.01	0.00	8.5	9.3
42	P3-2-2	(Z3) Rabaa Village area	30-150	0.21	0.08	0.05	0.00	8.5	9.4
43	SS4-1	(Z4) El-Kherba Village area	0-50	0.46	0.11	0.06	0.00	8.3	9.3
44	SS4-2	(Z4) El-Sadat Village area	0-45	0.5	0.09	0.03	0.16	8.5	9.2
45	SS4-3	(Z4) El-Sadat Village area	0-50	0.21	0.06	0.04	0.00	8.3	8.4
46	SS4-4	(Z4) El-Arawa Village area	0-40	0.17	0.04	0.02	0.00	8.3	9.4
47	SS4-5	(Z4) El-Telol Village area	0-40	0.16	0.05	0.03	0.00	8.3	9.2
48	SS4-6	(Z4) El-Telol Village area	0-40	1.11	0.20	0.06	7.92	8.2	8.3
49	P4-1-1	(Z4) El-Kherba Village area	0-30	0.91	0.18	0.07	0.00	8.3	9.3
50	P4-1-2	(Z4) El-Kherba Village area	30-83	0.62	0.11	0.03	0.00	8.4	9.4
51	P4-1-3	(Z4) El-Kherba Village area	83-145	0.58	0.11	0.04	0.00	8.3	9.5
52	P4-2-1	(Z4) Biar El-Abd area	0-19	1.52	0.27	0.09	0.00	8.2	9.2
53	P4-2-2	(Z4) Biar El-Abd area	19-75	0.21	0.05	0.02	2.88	8.2	9.2
54	P4-2-3	(Z4) Biar El-Abd area	75-165	0.04	0.01	0.00	0.00	8.2	9.4
55	P4-2-4	(Z4) Biar El-Abd area	165-200	0.08	0.02	0.01	0.00	8.1	9.0
56	P4-3-1	(Z4) Biar El-Abd area	0-20	0.32	0.04	0.00	0.32	8.2	9.2
57	P4-3-2	(Z4) Biar El-Abd area	20-130	0.29	0.04	0.00	0.00	8.2	9.2

SS= Surface Sample PS= Profile Sample Z= Zone area of study $CaCo_3$ = Calcium carbonate OM= Organic Matter

Cont. table 4-1: $CaCO_3$, OM, Organic carbon, Gypsum and pH in the studied soils

Samples No.	Type of sample	Location	Depth cm	CaCO3 %	OM %	C %	Gypsum %	pH ($CaCl_2$)	pH (H2O)
58	P4-3-3	(Z4) Biar El-Abd area	130-170	0.21	0.03	0.00	0.00	8.2	9.4
59	SS5-1	(Z5) Biar Lehfen area	0-45	28.8	4.61	1.15	1.36	8.1	8.3
60	SS5-2	(Z5) Abou Awaigila area	0-60	9.87	1.59	0.41	0.16	8.3	8.8
61	SS5-3	(Z5) El-Garkada Village area	0-60	7.73	1.10	0.17	0.00	8.4	9.7
62	SS5-4	(Z5) Gabal Lubna area	0-40	15.3	2.90	1.06	0.72	8.2	8.7
63	SS5-5	(Z5) Bagdad Village area	0-45	8.56	1.54	0.52	0.08	8.2	9.5
64	SS5-6	(Z5) El-Arish area	0-60	11.19	1.96	0.62	0.16	8.3	8.9
65	SS5-7	(Z5) Basin of W. El-Arish	0-60	8.23	1.32	0.33	0.24	8.4	8.7
66	P5-1-1	(Z5) El-Ressan area	0-68	26.49	4.24	1.06	1.04	8.3	9.2
67	P5-1-2	(Z5) El-Ressan area	68-140	12.34	1.63	0.15	0.96	8.3	9.0
68	P5-1-3	(Z5) El-Ressan area	140-220	5.9	0.73	0.02	0.24	8.3	9.4
69	P5-2-1	(Z5) Basin of W. El-Arish	0-40	5.12	0.62	0.01	0.00	8.3	9.4
70	P5-2-2	(Z5) Basin of W. El-Arish	40-140	3.11	0.40	0.03	0.00	8.4	10.0
71	P5-2-3	(Z5) Basin of W. El-Arish	140-200	1.22	0.15	0.00	0.00	8.4	9.9

SS= Surface Sample PS= Profile Sample Z= Zone area of study $CaCo_3$ = Calcium carbonate OM= Organic Matter

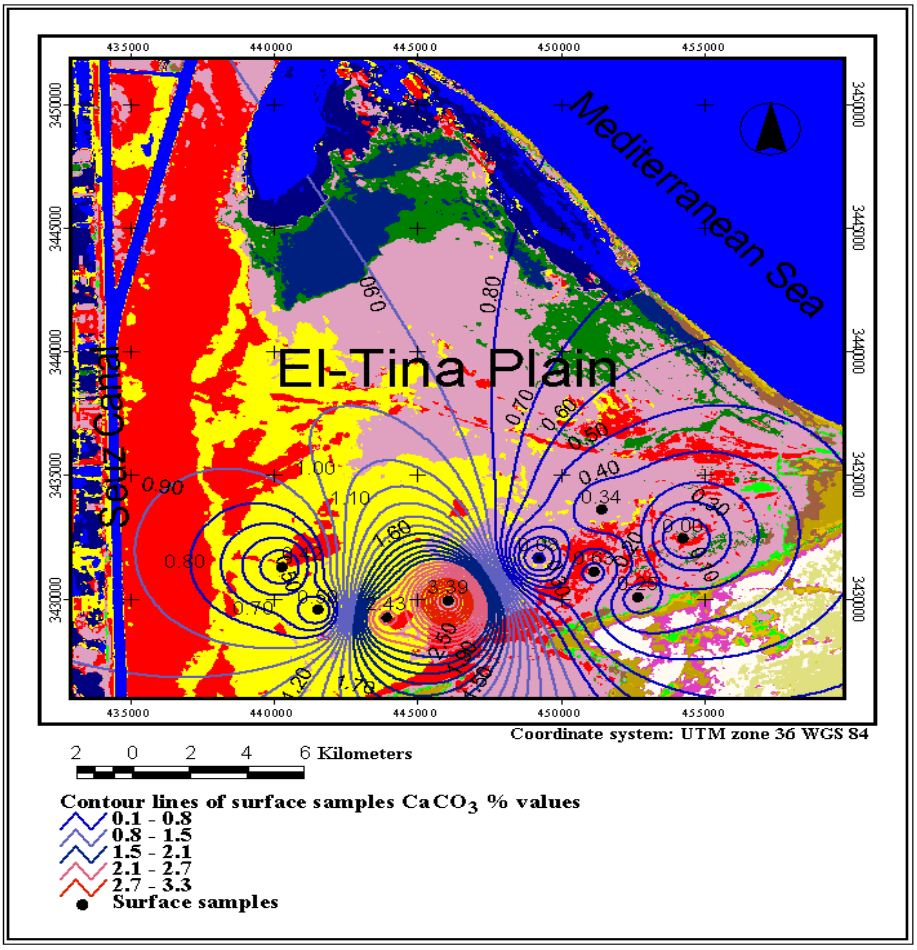

Fig. 4-20: Contour line image map of calcium carbonate content in surface samples of the El-Tina Plain area.

Figure (4-21) shows that the contour lines map covering the surface study area in the El-Tina Plain area was achieved due to the distribution of the organic matter content using GIS software and remote sensing technique by the Landsat TM image data covered the total northern part of the Sinai peninsula.

The chemical analysis data presented in table (4-1) reveal very wide variation in percent of gypsum content among the studied soil profile and surface samples in the El-Tina plain studied soil area. The gypsum content in these soils area of study are ranges between 1.5 to 24.2%. Figure (4-22) represents the contour lines map covering the El-Tina Plain area and illustrates the distribution of the percent values of gypsum content in the surface samples of study area by analysis the Landsat TM image and GIs data.

Data of the pH values in table (4-1) denote that the soil reaction in the surface and profile samples from the El-Tina Plain soils ranges between 7.5 to 8.9, that most of the studied soil samples indicating slightly to strong alkaline soil reaction. The contour lines image map of the soil reaction (pH) was achieved by using analysis of the Landsat TM image data and planning by ArcView GIS program. Figure (4-23) shows the distribution pattern of pH values in the studied surface soil samples in the El-Tina Plain area.

Table (4-2) show the results of the Electrical Conductivity (EC) by ds m^{-1}, soluble cations and anions from soil extract, Exchangeable Cations by meq $100g^{-1}$soil, Cation Exchange Capacity (CEC) by meq $100g^{-1}$soil and Exchangeable Sodium Percentage (ESP) for all surface and profile study soil samples were collected from the El-Salam Canal project along the northern part of the Sinai peninsula.

Data presented in table (4-2) show that the soils of the El-Tina Plain varied considerably in their salinity level from one profile to another and even from layer to layer in the same profile and in the surface samples. The Electrical Conductivity (EC) values range between 85 to 290 ds m^{-1}, with the relatively highest salt content in the surface layer. The salinity contour lines image map in figure (4-24) was achieved by using the satellite image and GIs data, this lines reveal the pattern of (EC) values in the El-Tina Plain surface samples.

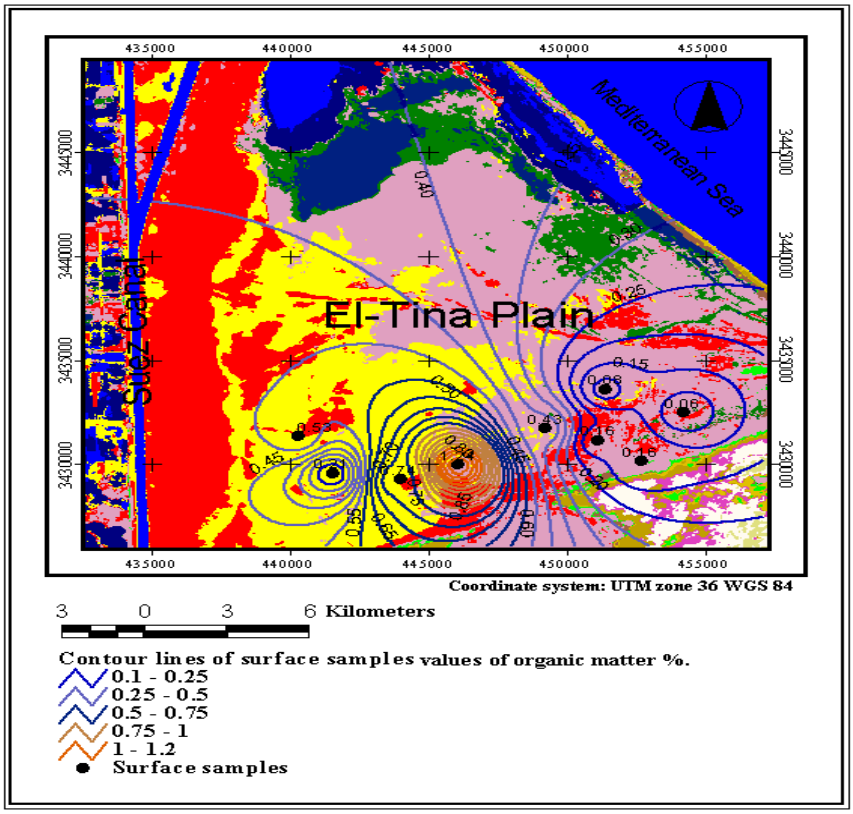

Fig. 4-21: Contour line image map of the organic matter content in surface samples of the El-Tina Plain area.

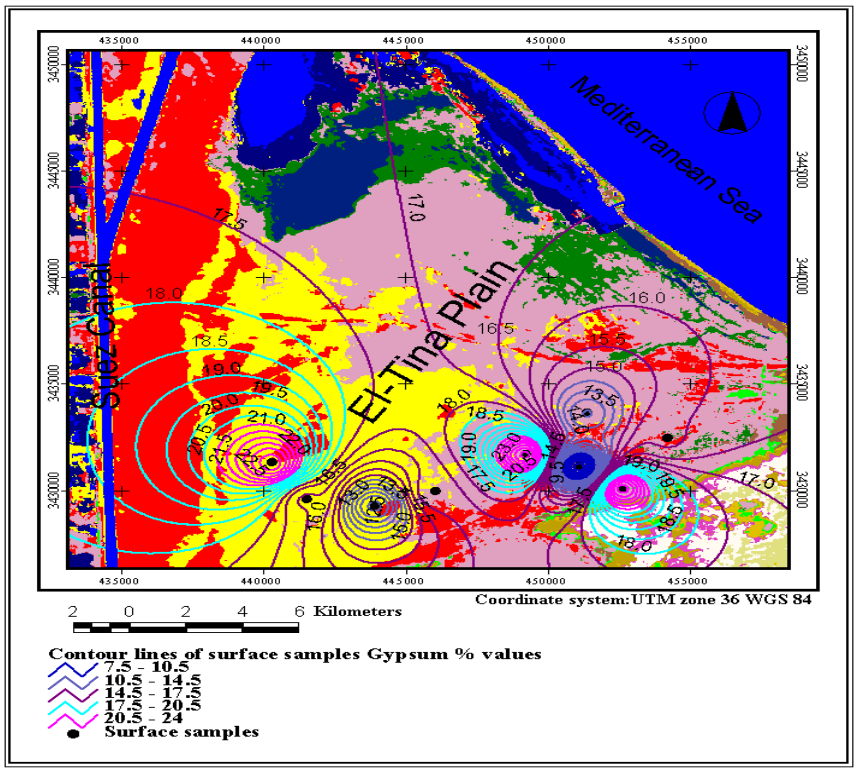

Fig. 4-22: Contour line image map of the gypsum content in surface samples of the El-Tina Plain area.

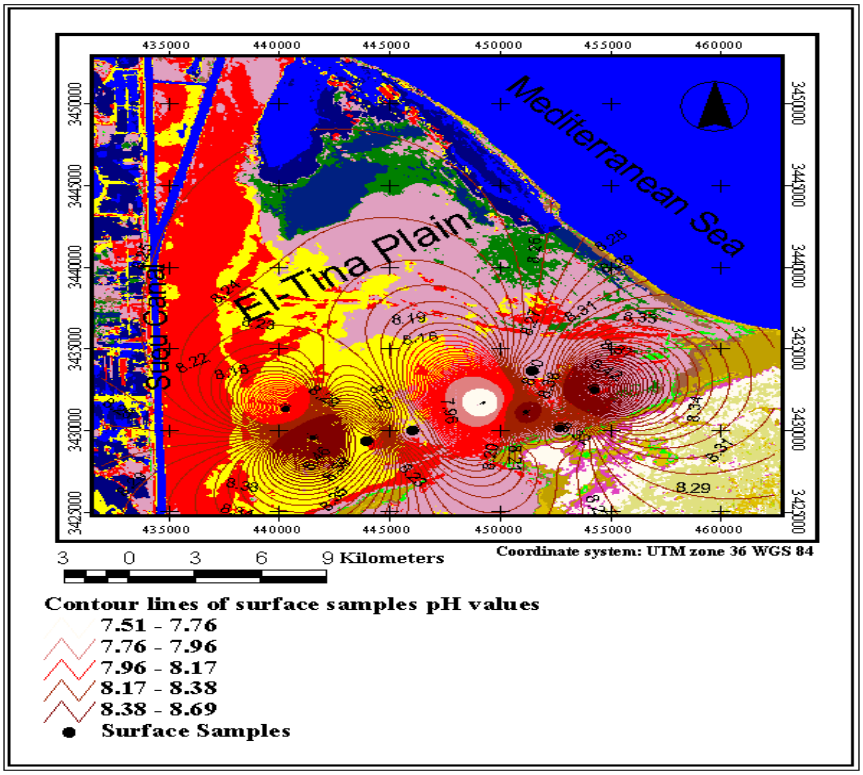

Fig. 4-23: Contour line image map of the soil reaction (pH) value in surface samples of the El-Tina Plain area.

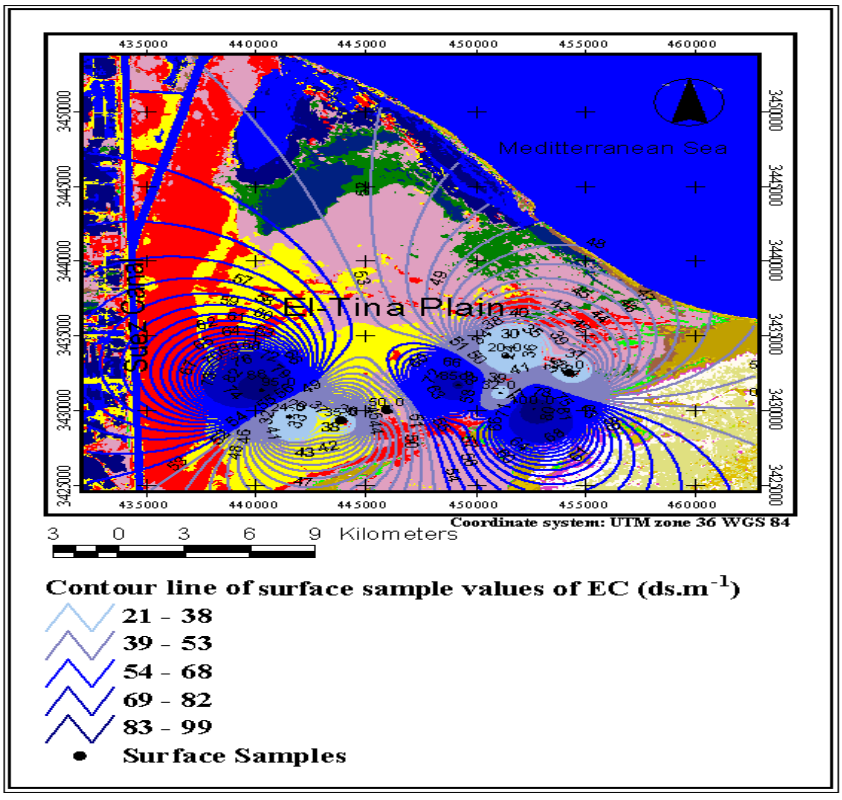

Fig. 4-24: Contour line image map of the EC (ds m^{-1}) content in surface samples of the El-Tina plain area.

Table 4-2: Chemical characteristics of soils from soil profile and surface samples.

Sample No.	Type of sample	Location	Depth cm	EC ds m^{-1}	Cations and Anions meq L^{-1}							Exchangeable Cations meq $100g^{-1}$soil					CEC	ESP
					Ca^{++}	Mg^{++}	Na^{+}	k^{+}	Cl^{-}	$SO4^{--}$	HCO_3^{-}	Na^{+}	K^{+}	Ca^{++}	Mg^{++}	Ba^{++}		
1	SS1-1	(Z1) SKS	0-60	0.4	98.9	9.9	52.2	17.8	1.7	0.3	1.9	0.5	0.3	1.5	0.7	1.6	3.9	15.2
2	SS1-2	(Z1) SKS	0-55	0.4	80.4	8.2	20.9	12.0	1.3	0.2	1.7	0.3	0.2	1.9	0.6	2.0	6.5	8.2
3	SS1.3	(Z1) SKS	0-50	0.8	95.4	8.8	81.3	7.5	1.2	1.3	1.2	1.3	0.2	1.5	0.8	1.2	5.6	15.0
4	SS1-4	(Z1) SKS	0-70	0.5	78.9	9.5	57.0	13.0	1.2	0.7	1.6	0.6	0.2	1.6	0.6	1.7	23.1	13.2
5	SS1-5	(Z1) SKS	0-40	0.4	34.9	4.7	12.6	3.0	1.5	0.3	0.9	0.3	0.1	1.0	0.4	0.8	21.1	6.1
6	SS1-6	(Z1) SKS	0-60	0.4	129.3	12.0	27.4	19.3	0.5	0.2	2.2	0.4	0.3	2.3	0.8	1.9	18.1	9.0
7	SS1-7	(Z1) SKS	0-65	16.0	300.6	108.2	162.6	6.9	161.6	19.6	4.0	21.8	0.8	1.0	15.8	4.2	26.1	20.0
8	P1-1-1	(Z1) SKS	0-42	0.4	46.4	4.8	17.8	3.0	1.1	1.2	0.5	0.3	0.1	15.5	0.2	0.4	18.0	7.0
9	P1-1-2	(Z1) SKS	42-50	0.6	138.3	12.1	50.4	14.3	2.4	1.6	2.3	0.5	0.2	2.2	0.8	1.8	20.1	15.0
10	P1-1-3	(Z1) SKS	50-125	0.4	98.4	8.4	24.4	6.5	0.6	0.3	1.6	0.3	0.2	1.9	0.5	1.6	18.0	8.6
11	P1-1-4	(Z1) SKS	125-160	0.4	39.9	5.2	11.7	2.8	1.3	0.2	0.6	0.2	0.1	0.9	0.3	0.8	21.0	4.0
12	P1-2-1	(Z1) SKS	0-20	1.0	172.7	18.5	183.9	15.3	6.5	0.8	1.9	1.9	0.2	3.6	1.5	4.0	20.5	22.2
13	P1-2-2	(Z1) SKS	20-130	1.7	77.9	18.9	295.2	6.3	4.2	6.6	1.6	2.9	0.1	1.9	1.7	2.1	25.8	23.6
14	P1-2-3	(Z1) SKS	130-164	1.5	98.9	17.7	351.3	5.8	5.7	1.7	1.8	3.4	0.1	1.6	1.6	3.8	24.9	24.0
15	P1-2-4	(Z1) SKS	164-168	0.9	170.2	10.5	128.3	5.5	2.3	2.6	2.1	1.4	0.2	2.8	0.7	2.3	12.5	17.9
16	P1-2-5	(Z1) SKS	168-210	1.0	162.8	11.0	199.1	3.5	5.1	1.6	2.0	2.0	0.1	2.0	0.7	2.1	15.1	23.0
17	SS2-1	(Z2) TP	0-70	135.0	198.2	116.9	738.4	33.0	475.2	14.5	6.1	84.7	2.1	3.1	33.1	11.0	37.5	49.9
18	SS2-2	(Z2) TP	0-60	150.0	334.0	54.8	1857.5	63.1	742.1	37.1	7.0	106.5	3.2	4.6	15.4	6.2	34.1	85.0
19	SS2-3	(Z2) TP	0-40	195.0	577.1	220.2	1860.9	85.9	1201.0	83.5	5.7	195.4	4.8	12.0	5.7	0.2	64.6	88.1
20	SS2-4	(Z2) TP	0-30	85.0	888.2	254.4	1956.8	93.4	403.5	33.2	8.1	252.0	5.5	12.2	78.4	0.2	66.5	88.0
21	SS2-5	(Z2) TP	0-60	220.0	475.8	59.4	473.5	14.3	248.7	13.4	5.5	58.0	1.3	7.7	1.9	0.1	28.4	36.3
22	SS2-6	(Z2) TP	0-50	133.0	103.3	9.9	386.9	17.5	393.5	33.1	4.0	38.7	0.3	1.3	1.4	0.0	19.1	33.3
23	SS2-7	(Z2) TP	0-60	132.0	414.9	44.7	903.3	11.0	281.4	7.9	7.9	55.8	1.3	6.9	1.5	0.1	37.5	60.6
24	P2-1-1	(Z2) TP	9--20	124.0	859.2	121.4	437.6	17.1	151.6	33.8	6.0	43.2	1.6	6.3	1.0	0.2	20.1	34.6
25	P2-1-2	(Z2) TP	20-110	275.0	254.6	90.2	1985.2	85.9	1595.8	66.4	4.6	201.8	4.7	5.4	2.6	9.7	36.1	90.1

SS= Surface Sample PS= Profile Sample Z= Zone area of study SKS= South El-Kantara Shark TP = Tina Plain

Cont. table 4-2: Chemical characteristics of soils from soil profile and surface samples.

Sample No.	Type Of sample	Location	Depth cm	EC ds m^{-1}	Cations and Anions meq L^{-1}							Exchangeable Cations meq $100g^{-1}$soil					CEC	ESP
					Ca^{++}	Mg^{++}	Na^{+}	k^{+}	Cl^{-}	$SO4^{--}$	HCO_3^{-}	Na^{+}	K^{+}	Ca^{++}	Mg^{++}	Ba^{++}		
26	P2-2-1	(Z2) TP	0-17	290.0	873	68	1799	138	999	48.8	5.1	259	1.2	14.5	1.5	0.2	23.8	82.8
27	P2-2-2	(Z2) TP	17-70	110.5	99	26	186	19	117	1.8	4.0	20.9	1.5	1.4	0.2	2.4	9.8	22.3
28	P2-2-3	(Z2) TP	70-140	98.0	118	60	275	5	213	6.0	3.9	32.7	1.6	1.4	7.5	1.7	7.5	23.6
29	SS3-1	(Z3) QV	0-50	1.3	95	16	92	6	5	2.9	3.5	1.0	0.2	1.6	0.9	0.1	10.5	17.5
30	SS3-2	(Z3) QV	0-55	4.0	313	14	151	90	88	0.0	3.8	15.0	1.4	7.4	0.7	0.7	9.2	18.8
31	SS3-3	(Z3) RV	0-50	0.4	48	8	2	18	0	0.1	2.6	0.3	0.3	1.3	0.4	1.4	10.0	1.0
32	SS3-4	(Z3) RV	0-45	0.5	57	8	12	8	1	1.0	2.2	0.3	0.2	1.4	0.3	1.0	11.3	4.1
33	SS3-5	(Z3) AV	0-60	0.4	32	8	8	4	0	0.1	1.9	0.3	0.2	0.9	0.4	1.2	13.8	2.6
34	SS3-6	(Z3) RV	0-45	0.4	34	8	13	8	0	0.1	1.1	0.2	0.2	0.9	0.4	1.2	12.9	4.3
35	SS3-7	(Z3) GV	0-55	0.7	63	10	61	18	6	0.3	2.6	0.8	0.3	1.5	0.6	1.4	10.4	14.0
36	SS3-8	(Z3) RV	0-50	0.5	95	14	13	15	1	0.2	3.4	0.3	0.3	1.8	0.6	1.5	9.4	4.4
37	SS3-9	(Z3) NV	0-60	0.4	68	9	11	9	1	0.1	2.7	0.2	0.2	1.6	0.5	1.4	30.1	3.5
38	P3-1-1	(Z3) AV	0-25	5.1	146	18	54	1	22	24.9	3.9	6.6	0.7	1.0	1.7	0.1	43.4	15.9
39	P3-1-2	(Z3) AV	25-40	6.5	656	20	67	2	25	19.7	4.3	7.4	0.8	4.0	2.3	0.1	25.6	14.9
40	P3-1-3	(Z3) AV	40-75	2.0	72	16	278	17	3	2.7	2.5	3.0	0.3	1.6	0.9	1.2	27.0	23.4
41	P3-2-1	(Z3) RV	0-30	0.4	65	8	2	11	0	0.1	2.5	0.2	0.2	1.5	0.4	1.3	30.4	1.0
42	P3-2-2	(Z3) RV	30-150	0.4	62	8	18	10	1	0.1	2.4	0.3	0.2	1.6	0.4	1.3	29.4	5.7
43	SS4-1	(Z4) KhV	0-50	0.4	113	10	9	10	0	0.1	3.9	0.2	0.2	2.3	0.5	1.8	29.6	2.9
44	SS4-2	(Z4) SV	0-45	1.4	104	13	199	13	16	0.7	3.9	2.5	0.2	1.5	0.9	1.2	27.1	23.0
45	SS4-3	(Z4) SV	0-50	2.2	554	4	27	8	1	0.0	4.0	0.4	0.2	3.1	0.2	0.1	28.3	9.0
46	SS4-4	(Z4) ArV	0-40	0.4	54	9	3	2	0	0.1	2.3	0.2	0.1	1.0	0.5	1.1	31.8	1.2
47	SS4-5	(Z4) TV	0-40	3.5	45	6	32	4	2	0.3	1.2	0.5	0.2	1.6	0.3	1.2	29.1	6.1
48	SS4-6	(Z4) TV	0-40	10.0	121	14	91	41	59	19.3	3.0	13.1	1.3	8.3	4.4	0.2	31.3	17.0
49	P4-1-1	(Z4) KhV	0-30	0.4	140	9	9	10	0	0.1	3.2	0.2	0.2	2.2	0.4	1.9	5.1	3.2

ArV= El-Arawa Village **AV= El-Ahrar Village** **GV= El-Ganien Village**
KhV= El-kherba Village **NV= El-Nigila Village** **PS= Profile Sample**
QV= Qatia Village **RV = Rabaa Village** **RV= Rumana Village**
S= Surface Sample **SV= El-Sadat Village** **TV= El-Telol Village**
Z= Zone area of study

Cont. table 4-2: Chemical characteristics of soils from soil profile and surface samples.

Sample No.	Type of sample	Location	Depth cm	EC Ds m^{-1}	Cations and Anions meq L^{-1}							Exchangeable Cations meq $100g^{-1}$soil					CEC	ESP
					Ca^{++}	Mg^{++}	Na^{+}	K^{+}	Cl^{-}	$SO4^{--}$	HCO_3^{-}	Na^{+}	K^{+}	Ca^{++}	Mg^{++}	Ba^{++}		
50	P4-1-2	(Z4) KhV	30-83	0.4	103	10	8	6	0.2	0.1	2.9	0.2	0.1	1.6	0.4	1.5	4.9	2.4
51	P4-1-3	(Z4) KhV	83-145	0.4	81	10	1	1	0.2	0.0	1.5	0.2	0.1	1.4	0.6	1.4	5.4	0.7
52	P4-2-1	(Z4) BA	0-19	0.4	169	13	63	12	0.7	0.2	3.1	0.9	0.2	4.4	1.2	4.9	12.9	14.0
53	P4-2-2	(Z4) BA	19-75	2.1	81	15	374	5	10.6	2.5	1.2	4.2	0.1	1.6	1.4	3.5	12.6	24.6
54	P4-2-3	(Z4) BA	75-165	1.3	33	14	280	5	8.1	0.7	1.0	3.3	0.1	1.8	1.3	3.9	13.4	23.7
55	P4-2-4	(Z4) BA	165-200	2.0	59	17	345	5	12.5	0.5	2.4	3.7	0.1	2.1	1.5	3.5	12.5	23.9
56	P4-3-1	(Z4) BA	0-20	0.4	50	7	7	8	0.2	0.0	2.1	0.2	0.2	1.2	0.5	1.2	7.5	2.3
57	P4-3-2	(Z4) BA	20-130	0.4	43	8	9	8	0.3	0.1	1.8	0.2	0.2	1.4	0.6	1.3	7.6	3.5
58	P4-3-3	(Z4) BA	130-170	0.4	44	7	8	8	0.2	0.1	1.0	0.2	0.2	1.2	0.5	1.3	7.5	2.8
59	SS5-1	(Z5) BL	0-45	3.7	227	10	410	15	18.2	8.8	3.9	4.8	0.2	4.3	3.1	3.3	6.9	34.0
60	SS5-2	(Z5) AAW	0-60	0.4	175	15	20	16	0.8	0.3	2.7	0.4	0.3	6.4	1.3	3.8	5.6	6.4
61	SS5-3	(Z5) GaV	0-60	0.4	157	16	39	16	0.2	0.1	2.1	0.5	0.2	2.4	0.9	2.0	4.9	13.9
62	SS5-4	(Z5) GL	0-40	2.2	180	18	262	27	15.2	0.8	4.0	3.1	0.3	4.3	1.3	3.5	5.6	22.8
63	SS5-5	(Z5) BV	0-45	0.4	155	8	46	7	1.3	0.4	1.1	0.6	0.2	3.0	0.5	2.0	4.3	14.9
64	SS5-6	(Z5) A	0-60	0.5	172	10	57	16	2.9	0.3	2.6	0.6	0.2	3.5	1.5	3.2	8.3	16.0
65	SS5-7	(Z5) BWA	0-60	0.7	164	13	32	18	4.6	0.5	2.6	0.5	0.3	3.0	1.1	2.1	3.0	6.1
66	P5-1-1	(Z5) R	0-68	1.1	209	48	48	3	4.8	1.4	3.0	4.4	0.3	7.2	6.7	9.0	5.3	14.9
67	P5-1-2	(Z5) R	68-140	1.3	190	10	275	31	8.2	1.2	2.8	3.3	0.3	5.9	4.1	7.6	12.5	23.3
68	P5-1-3	(Z5) R	140-220	0.8	169	16	152	17	4.9	0.5	2.5	1.9	0.2	3.8	2.4	4.6	8.6	19.0
69	P5-2-1	(Z5) BWA	0-40	0.4	161	14	25	5	0.2	0.1	2.2	0.4	0.2	3.0	1.1	2.7	4.9	9.0
70	P5-2-2	(Z5) BWA	40-140	0.4	151	12	57	3	0.3	0.1	2.1	0.8	0.1	2.4	0.9	2.7	4.1	16.3
71	P5-2-3	(Z5) BWA	140-200	0.4	157	9	46	1	0.3	0.0	2.1	0.6	0.1	2.0	0.6	1.9	2.1	14.9

SS= Surface Sample **S= Profile Sample** **Z= Zone area of study** **BA= Biar El-Abd**
KhV= El-kherba Village **BL= Biar Lehfen** **AAW= Abou Awaigila** **GaV=El-Garkada**
GL= Gabal Lubna **BV= Bagdad Village** **A=El-Arish** **BWA= Basin of Wadi El-Aris**
R= El-Ressan

The results presented in table (4-2) reveal that soluble cations in the El-Tina Plain soil samples are predominated by Na^+ followed by Ca^{2+} and Mg^{2+}, while K^+ is found in minor amounts in all samples. Soluble anions are predominated by Cl^- followed by SO_4^{2-} and HCO_3^-. The Cation Exchange Capacity (CEC) values were ranged between 7.5 to 66.5 meq $100g^{-1}$soil. Results of exchangeable cations in the El-Tina Plain soil samples reveal the Na^+ is the dominant exchangeable cation followed by Mg^{2+}, Ca^{2+} and K^+, while Ba^{2+} is present in much lower quantities (meq $100g^{-1}$soil). Exchangeable sodium percentage (ESP) varies from 22.3 to 90.1 in this study area.

The nitrogen content in table (4-3) is generally very low and decreases with depth in soil samples in the El-Tina plain area. The total-N content ranges between 0.02 to 0.28% and the values of phosphorus ranges between 317 to 1124 mg kg^{-1}. Meanwhile, the values of the total-K content range between moderately to relatively higher contents (262-2001 mg kg^{-1}) in the studied soils of the El-Tina Plain area.

The macronutrient status of studied soils in the northern part of the Sinai peninsula along the El-Salam Canal project is shown in table (4-4). This table reveal the concentration of the iron, manganese, zinc and copper elements in the studied soil samples by mg kg^{-1}.

The macronutrient status of studied soils in the El-Tina Plain area in table (4-4) reveal that the range of the cationic composition are characterized by the dominance of Mn^{2+}, followed by Fe^{2+} and Zn^{2+}, while Cu^{2+} is found in minor amounts in soil samples of these area. The content of Mn^{2+} ranged from 1.26 to 5.49 (mg kg^{-1}), Fe^{2+} ranged from 1.17 to 3.93 mg kg^{-1}, Zn^{2+} varies from 0.1 to 5.2 mg kg^{-1} and Cu^{2+} values from 0.04 to 1.97 mg kg^{-1} in these studied soil. samples.

The results of the particle size distribution in the investigated soil areas are shown in table (4-5). This table illustrates the percent of sand fraction, silt fraction and clay fraction in the soil of the studied area. These fractions are reveal very evident variations in their texture classes whether among the profile and surface soil samples or along the entire depths of each profile.

Table 4-3: Nitrogen, phosphorus and potassium content in the soil samples

Sample No.	Type of sample	Location	Depth cm	N %	P mg kg^{-1}	K mg kg^{-1}
1	SS1-1	(Z1) South El-Kantara Shark	0-60	0.04	339	87
2	SS1-2	(Z1) South El-Kantara Shark	0-55	0.04	295	74
3	SS1.3	(Z1) South El-Kantara Shark	0-50	0.03	241	54
4	SS1-4	(Z1) South El-Kantara Shark	0-70	0.04	263	76
5	SS1-5	(Z1) South El-Kantara Shark	0-40	0.02	114	44
6	SS1-6	(Z1) South El-Kantara Shark	0-60	0.04	288	90
7	SS1-7	(Z1) South El-Kantara Shark	0-65	0.21	354	284
8	P1-1-1	(Z1) South El-Kantara Shark	0-42	0.17	105	46
9	P1-1-2	(Z1) South El-Kantara Shark	42-50	0.09	276	80
10	P1-1-3	(Z1) South El-Kantara Shark	50-125	0.07	215	51
11	P1-1-4	(Z1) South El-Kantara Shark	125-160	0.01	143	42
12	P1-2-1	(Z1) South El-Kantara Shark	0-20	0.04	269	73
13	P1-2-2	(Z1) South El-Kantara Shark	20-130	0.02	222	43
14	P1-2-3	(Z1) South El-Kantara Shark	130-164	0.02	301	38
15	P1-2-4	(Z1) South El-Kantara Shark	164-168	0.02	291	42
16	P1-2-5	(Z1) South El-Kantara Shark	168-210	0.01	295	402
17	SS2-1	(Z2) Tina Plain area	0-70	0.10	542	748
18	SS2-2	(Z2) Tina Plain area	0-60	0.14	690	2001
19	SS2-3	(Z2) Tina Plain area	0-40	0.26	716	1745
20	SS2-4	(Z2) Tina Plain area	0-30	0.25	586	1896
21	SS2-5	(Z2) Tina Plain area	0-60	0.07	576	405
22	SS2-6	(Z2) Tina Plain area	0-50	0.04	355	291
23	SS2-7	(Z2) Tina Plain area	0-60	0.09	868	405
24	P2-1-1	(Z2) Tina Plain area	9—20	0.28	424	451
25	P2-1-2	(Z2) Tina Plain area	20-110	0.20	1124	1668
26	P2-2-1	(Z2) Tina Plain area	0-17	0.11	611	459
27	P2-2-2	(Z2) Tina Plain area	17-70	0.03	345	262
28	P2-2-3	(Z2) Tina Plain area	70-140	0.02	317	307

SS= Surface Sample PS= Profile Sample Z= Zone area of study

Cont. table4-3: Nitrogen, phosphorus and potassium content in the soil samples

Sample No.	Type of sample	Location	Depth cm	N %	P mg kg^{-1}	K Mg kg^{-1}
29	SS3-1	(Z3) Qatia Village area	0-50	0.03	193	42
30	SS3-2	(Z3) Qatia Village area	0-55	0.05	499	296
31	SS3-3	(Z3) Rabaa Village area	0-50	0.02	319	83
32	SS3-4	(Z3) Rabaa Village area	0-45	0.02	165	54
33	SS3-5	(Z3) El-Ahrar Village area	0-60	0.01	136	64
34	SS3-6	(Z3) Rumana Village area	0-45	0.01	143	44
35	SS3-7	(Z3) El-Ganien Village area	0-55	0.03	443	78
36	SS3-8	(Z3) Rabaa Village area	0-50	0.07	364	67
37	SS3-9	(Z3) El-Nigila Village area	0-60	0.02	149	46
38	P3-1-1	(Z3) El-Ahrar Village area	0-25	0.06	184	117
39	P3-1-2	(Z3) El-Ahrar Village area	25-40	0.05	253	143
40	P3-1-3	(Z3) El-Ahrar Village area	40-75	0.02	136	78
41	P3-2-1	(Z3) Rabaa Village area	0-30	0.02	310	44
42	P3-2-2	(Z3) Rabaa Village area	30-150	0.02	345	66
43	SS4-1	(Z4) El-kherba Village area	0-50	0.04	133	47
44	SS4-2	(Z4) El-Sadat Village area	0-45	0.02	136	65
45	SS4-3	(Z4) El-Sadat Village area	0-50	0.03	92	56
46	SS4-4	(Z4) El-Arawa Village area	0-40	0.01	146	39
47	SS4-5	(Z4) El-Telol Village area	0-40	0.01	200	45
48	SS4-6	(Z4) El-Telol Village area	0-40	0.04	257	162
49	P4-1-1	(Z4) El-Kherba Village area	0-30	0.03	168	54
50	P4-1-2	(Z4) El-Kherba Village area	30-83	0.02	158	35
51	P4-1-3	(Z4) El-Kherba Village area	83-145	0.01	168	36
52	P4-2-1	(Z4) Biar El-Abd area	0-19	0.04	390	61
53	P4-2-2	(Z4) Biar El-Abd area	19-75	0.02	364	40
54	P4-2-3	(Z4) Biar El-Abd area	75-165	0.02	244	39
55	P4-2-4	(Z4) Biar El-Abd area	165-200	0.02	295	40

SS= Surface Sample PS= Profile Sample Z= Zone area of study

Cont. table 4-3: Nitrogen, phosphorus and potassium content in the soil samples

Sample No.	Type of sample	Location	Depth cm	N %	P mg kg^{-1}	K Mg kg^{-1}
56	P4-3-1	(Z4) Biar El-Abd area	0-20	0.02	143	43
57	P4-3-2	(Z4) Biar El-Abd area	20-130	0.02	152	44
58	P4-3-3	(Z4) Biar El-Abd area	130-170	0.02	155	47
59	SS5-1	(Z5) Biar Lehfen area	0-45	0.13	288	58
60	SS5-2	(Z5) Abou Awaigila area	0-60	0.06	364	71
61	SS5-3	(Z5) El-Garkada Village	0-60	0.02	253	67
62	SS5-4	(Z5) Gabal Libina area	0-40	0.05	342	85
63	SS5-5	(Z5) Bagdad Village area	0-45	0.02	228	55
64	SS5-6	(Z5) El-Arish area	0-60	0.10	580	70
65	SS5-7	(Z5) Basin of W. El-Arish	0-60	0.10	637	87
66	P5-1-1	(Z5) El-Ressan area	0-68	0.12	149	94
67	P5-1-2	(Z5) El-Ressan area	68-140	0.06	491	77
68	P5-1-3	(Z5) El-Ressan area	140-220	0.03	532	63
69	P5-2-1	(Z5) Basin of W. El-Arish	0-40	0.02	393	43
70	P5-2-2	(Z5) Basin of W. El-Arish	40-140	0.02	390	37
71	P5-2-3	(Z5) Basin of W. El-Arish	140-200	0.01	320	34

SS= Surface Sample PS= Profile Sample Z= Zone area of study W= Wadi

Table 4-4: Plant available iron, manganese, zinc and copper content in the soil samples.

Sample No.	Type of sample	Location	Depth cm	Fe mg kg^{-1}	Mn mg kg^{-1}	Zn Mg kg^{-1}	Cu mg kg^{-1}
1	SS1-1	(Z1) South El-Kantara Shark	0-60	1.20	0.73	0.07	0.08
2	SS1-2	(Z1) South El-Kantara Shark	0-55	1.03	0.84	0.08	0.06
3	SS1.3	(Z1) South El-Kantara Shark	0-50	1.13	0.75	0.07	0.05
4	SS1-4	(Z1) South El-Kantara Shark	0-70	0.91	0.53	0.07	0.04
5	SS1-5	(Z1) South El-Kantara Shark	0-40	1.17	0.47	0.05	0.01
6	SS1-6	(Z1) South El-Kantara Shark	0-60	0.82	0.95	0.12	0.06
7	SS1-7	(Z1) South El-Kantara Shark	0-65	1.21	1.17	1.25	0.43
8	P1-1-1	(Z1) South El-Kantara Shark	0-42	0.87	0.44	0.14	0.07
9	P1-1-2	(Z1) South El-Kantara Shark	42-50	1.03	0.72	0.28	0.13
10	P1-1-3	(Z1) South El-Kantara Shark	50-125	1.09	0.58	0.12	0.04
11	P1-1-4	(Z1) South El-Kantara Shark	125-160	1.11	0.49	0.12	0.04
12	P1-2-1	(Z1) South El-Kantara Shark	0-20	0.89	1.09	0.46	0.29
13	P1-2-2	(Z1) South El-Kantara Shark	20-130	0.75	0.15	0.40	0.14
14	P1-2-3	(Z1) South El-Kantara Shark	130-164	0.75	0.18	0.36	0.09
15	P1-2-4	(Z1) South El-Kantara Shark	164-168	0.97	0.60	0.24	0.10
16	P1-2-5	(Z1) South El-Kantara Shark	168-210	0.69	0.55	0.27	0.12
17	SS2-1	(Z2) Tina Plain area	0-70	3.93	1.92	0.59	1.56
18	SS2-2	(Z2) Tina Plain area	0-60	3.39	1.26	1.77	1.20
19	SS2-3	(Z2) Tina Plain area	0-40	2.88	2.09	0.75	1.90
20	SS2-4	(Z2) Tina Plain area	0-30	1.28	5.49	1.26	1.43
21	SS2-5	(Z2) Tina Plain area	0-60	1.23	2.05	0.48	0.29
22	SS2-6	(Z2) Tina Plain area	0-50	1.81	2.42	0.10	0.29
23	SS2-7	(Z2) Tina Plain area	0-60	2.34	3.60	0.45	0.51
24	P2-1-1	(Z2) Tina Plain area	9--20	3.51	2.52	0.65	0.56
25	P2-1-2	(Z2) Tina Plain area	20-110	2.16	2.50	2.21	1.97
26	P2-2-1	(Z2) Tina Plain area	0-17	3.80	5.61	5.18	2.22
27	P2-2-2	(Z2) Tina Plain area	17-70	1.43	2.00	0.09	0.13
28	P2-2-3	(Z2) Tina Plain area	70-140	1.17	1.65	0.19	0.04
29	SS3-1	(Z3) Qatia Village area	0-50	0.67	1.37	0.11	0.02
30	SS3-2	(Z3) Qatia Village area	0-55	0.80	1.37	0.79	0.29
31	SS3-3	(Z3) Rabaa Village area	0-50	1.10	0.75	0.10	0.01
32	SS3-4	(Z3) Rabaa Village area	0-45	1.03	0.86	0.08	0.02
33	SS3-5	(Z3) El-Ahrar Village area	0-60	1.10	0.75	0.09	0.02
34	SS3-6	(Z3) Rumana Village area	0-45	0.98	0.75	0.07	0.01
35	SS3-7	(Z3) El-Ganien Village area	0-55	1.05	1.51	0.21	0.19
36	SS3-8	(Z3) Rabaa Village area	0-50	0.97	1.86	0.17	0.08
37	SS3-9	(Z3) El-Nigila Village area	0-60	0.86	1.55	0.10	0.03
38	P3-1-1	(Z3) El-Ahrar Village area	0-25	1.27	1.00	0.15	0.06
39	P3-1-2	(Z3) El-Ahrar Village area	25-40	1.12	1.27	0.61	0.28
40	P3-1-3	(Z3) El-Ahrar Village area	40-75	0.82	0.98	0.10	0.01
41	P3-2-1	(Z3) Rabaa Village area	0-30	0.92	0.88	0.13	0.00
42	P3-2-2	(Z3) Rabaa Village area	30-150	1.11	0.88	0.11	0.01
43	SS4-1	(Z4) El-Kherba Village area	0-50	0.93	1.35	0.08	0.02
44	SS4-2	(Z4) El-Sadat Village area	0-45	1.01	1.60	0.10	0.04
45	SS4-3	(Z4) El-Sadat Village area	0-50	0.97	0.83	0.08	0.01
46	SS4-4	(Z4) El-Arawa Village area	0-40	0.99	0.82	0.06	0.02
47	SS4-5	(Z4) El-Telol Village area	0-40	1.08	1.06	0.08	0.02

SS= Surface Sample PS= Profile Sample Z= Zone area of study

Cont. table 4-4: Plant available iron, manganese, zinc and copper content in the soil samples.

Sample No.	Type of Sample	Location	Depth cm	Fe mg kg^{-1}	Mn mg kg^{-1}	Zn mg kg^{-1}	Cu mg kg^{-1}
48	SS4-6	(Z4) El-Telol Village area	0-40	0.95	1.48	0.09	0.01
49	P4-1-1	(Z4) El-Kherba Village area	0-30	1.03	1.13	0.12	0.27
50	P4-1-2	(Z4) El-Kherba Village area	30-83	0.81	0.82	0.05	0.02
51	P4-1-3	(Z4) El-Kherba Village area	83-145	0.80	0.74	0.02	0.04
52	P4-2-1	(Z4) Biar El-Abd area	0-19	1.97	2.72	1.54	0.87
53	P4-2-2	(Z4) Biar El-Abd area	19-75	1.29	1.17	0.43	0.30
54	P4-2-3	(Z4) Biar El-Abd area	75-165	1.19	0.57	0.28	0.25
55	P4-2-4	(Z4) Biar El-Abd area	165-200	1.50	0.86	0.25	0.22
56	P4-3-1	(Z4) Biar El-Abd area	0-20	0.94	0.57	0.03	0.02
57	P4-3-2	(Z4) Biar El-Abd area	20-130	1.31	0.82	0.07	0.05
58	P4-3-3	(Z4) Biar El-Abd area	130-170	0.98	0.75	0.05	0.08
59	SS5-1	(Z5) Biar Lehfen area	0-45	0.65	1.34	1.39	1.35
60	SS5-2	(Z5) Abou Awaigila area	0-60	1.23	1.55	0.66	0.41
61	SS5-3	(Z5) El-Garkada Village area	0-60	0.55	0.65	0.10	0.08
62	SS5-4	(Z5) Gabal Libina area	0-40	0.79	0.92	0.75	0.54
63	SS5-5	(Z5) Bagdad Village area	0-45	0.81	0.62	0.98	0.86
64	SS5-6	(Z5) El-Arish area	0-60	0.64	1.88	0.59	0.57
65	SS5-7	(Z5) Basin of W. El-Arish	0-60	0.65	1.84	0.44	0.44
66	P5-1-1	(Z5) El-Ressan area	0-68	1.66	0.81	0.37	0.43
67	P5-1-2	(Z5) El-Ressan area	68-140	1.07	0.64	0.15	0.16
68	P5-1-3	(Z5) El-Ressan area	140-220	0.70	0.56	0.38	0.29
69	P5-2-1	(Z5) Basin of W. El-Arish	0-40	0.75	1.06	0.93	0.76
70	P5-2-2	(Z5) Basin of W. El-Arish	40-140	0.74	1.19	0.46	1.37
71	P5-2-3	(Z5) Basin of W. El-Arish	140-200	0.54	0.78	0.22	0.21

SS= Surface Sample PS= Profile Sample Z= Zone area of study W= Wadi

The results of texture class in the El-Tina Plain soil samples in table (4-5) ranged between loamy sand to clay in profile No.1 and loamy sand to sand in profile No.2, while the surface samples ranged from sandy clay to clay and from loamy sand to sand.

The results of bulk density and some of the hydraulic properties in the soils of the project area are shown in the table (4-6). Bulk density in the El-Tina Plain soils range between 1.2 to 1.86 g cm^{-3}. Table (4-6) show the results of saturated hydraulic conductivity in this soils. The values of soil permeability in this area ranging between 0.14 to 17.81 cm hr^{-1}. The values of available water capacity (AWC) range from 0.1 to 0.06 cm^3 water cm^{-3} soil in the El-Tina Plain soils. The values of water saturation in these soils reflects the movement of water within soils (high or low water retention in soils), that range from 0.3 to 0.6 cm^3 water cm^{-3} soil.

4.3.2 Soil properties and maps of the South El-Kantara Shark area

Table (4-1) show the results of $CaCO_3$ content in the studied soils of the South El-Kantara Shark area. The profile and surface soil samples are ranging content between 0.04 to 4.2 % of calcium carbonate content. The Landsat TM image, GIS data and results of $CaCO_3$ analysis were used to illustrate the distribution of calcium carbonate content in surface soil samples in this area, as shown in the contour line image map of figure (4-25).

The organic matter and organic carbon content in the South El-Kantara Shark soil samples range between 0.02 to 0.95 % and 0.0 to 0.44%, respectively. The contour lines map of organic matter distribution in surface soil samples in this area is shown in figure (4-26), extracted from satellite image and GIS data.

The results of the gypsum content values in table (4-1) denotes that the soils in South El-Kantara Shark range from 0 to 1.7 %. The distribution of gypsum surface content in the South El-Kantara Shark soils was planned by contour line image map, the distribution pattern of gypsum was extracted from the analysis of the Landsat TM image and GIS data. This contour line image map was preformed by Arc View program and results of gypsum content in the surface soil samples as shown in figure (4-27).

The results presented in table (4-1) reveal the soil reaction (pH) in the South El-Kantara Shark soils. The values of pH evinced the soils in the South El-Kantara Shark study area are moderately alkaline, ranging between 8.1 to 8.5 in $CaCl_2$ extract. Figure (4-28) shows the contour lines map of the South El-Kantara Shark soils for the pH values in the surface soil samples using remote sensing data and GIS technique.

Table 4-5: Particle size distribution of the studied soil profiles and surface samples.

Sample No.	Sample Type	Location	Depth (cm)	Sand Fraction (µm)				Silt Fraction (µm)				Clay <2 µm	Texture Class
				C. Sand 2000 - 630	M. Sand 630 – 200	F. Sand 200 - 63	Total %	C. Silt 63 - 20	M. Silt 20 – 6.3	F. Silt 6.3 - 2	Total %		
1	S.S	S.K.S	0 - 60	5.4	56.7	34.5	96.6	1.1	0.1	0.4	1.7	1.7	Sand
2	S.S	S.K.S	0 - 55	13.9	46.7	35.5	96.0	1.5	0.0	0.1	1.7	2.3	Sand
3	S.S	S.K.S	0 - 50	19.5	48.8	27.6	95.8	2.0	0.1	0.1	2.2	2.0	Sand
4	S.S	S.K.S	0 - 70	4.5	51.1	42.1	97.7	0.3	0.2	0.0	0.6	1.7	Sand
5	S.S	S.K.S	0 - 40	4.1	91.5	4.4	97.9	0.1	0.5	0.5	1.1	1.0	Sand
6	S.S	S.K.S	0 - 60	5.8	59.2	31.4	96.4	0.8	0.3	0.0	1.0	2.6	Sand
7	S.S	S.K.S	0 - 65	5.8	46.8	32.9	85.5	5.8	0.7	1.4	7.9	6.7	LS
8	P.S1	S.K.S	0 - 42	82.3	15.4	0.4	98.1	0.1	0.8	0.0	1.0	0.9	Sand
9	P.S1	S.K.S	42 - 50	37.3	39.1	20.6	97.0	0.9	0.2	0.3	1.3	1.7	Sand
10	P.S1	S.K.S	50 - 125	32.1	41.2	24.1	97.5	0.7	0.2	0.0	0.9	1.6	Sand
11	P.S1	S.K.S	125 - 160	35.8	51.2	12.0	99.0	0.0	0.1	0.1	0.2	0.8	Sand
12	P.S2	S.K.S	0 - 20	21.0	40.5	30.2	91.7	1.5	0.6	0.4	2.5	5.8	Sand
13	P.S2	S.K.S	20 - 130	17.2	33.8	40.5	91.5	2.0	0.6	0.0	2.6	5.9	Sand
14	P.S2	S.K.S	130 - 164	13.7	40.4	38.7	92.7	1.9	0.8	0.3	3.0	4.2	Sand
15	P.S2	S.K.S	164 - 168	11.0	52.7	27.1	90.9	3.2	1.3	1.1	5.5	3.6	Sand
16	P.S2	S.K.S	168 - 210	6.8	56.3	31.0	94.1	2.8	0.2	0.5	3.4	2.5	Sand
17	S.S	Tina Plain	0 - 70	11.9	32.2	6.3	50.5	1.1	4.0	4.1	9.2	40.3	SC
18	S.S	Tina Plain	0 - 60	10.5	21.3	13.7	45.9	3.2	4.3	3.8	11.3	43.3	Clay
19	S.S	Tina Plain	0 - 40	0.0	0.1	1.0	1.1	6.0	14.4	14.2	34.5	64.4	Clay
20	S.S	Tina Plain	0 - 30	0.0	0.6	0.5	1.1	2.5	9.8	14.7	27.0	71.9	Clay
21	S.S	Tina Plain	0 - 60	2.4	74.7	12.8	89.8	0.8	0.9	1.5	3.2	7.1	Sand
22	S.S	Tina Plain	0 - 50	2.3	86.6	8.5	97.4	0.7	0.0	0.0	0.7	1.9	Sand
23	S.S	Tina Plain	0 - 60	3.3	73.8	9.4	86.5	2.0	0.0	1.7	3.8	9.7	LS
24	P.S1	Tina Plain	9 - 20	20.0	51.9	15.1	86.9	1.6	0.2	0.0	1.8	11.2	LS
25	P.S1	Tina Plain	20 - 110	1.8	6.5	3.9	12.2	4.4	5.4	4.6	15.4	72.4	Clay
26	P.S2	Tina Plain	0 - 17	5.6	67.4	10.3	83.3	1.5	0.8	1.1	3.4	13.3	LS
27	P.S2	Tina Plain	17 – 70	5.0	82.4	8.3	95.6	1.0	0.0	0.0	1.0	3.4	Sand
28	P.S2	Tina Plain	70 – 140	1.0	80.1	14.3	95.3	0.6	1.3	0.8	2.6	2.1	Sand
29	S.S	Qatia	0 – 50	1.1	38.2	57.9	97.2	0.4	0.0	0.4	0.9	2.0	Sand
30	S.S	Qatia	0 – 55	1.8	46.5	45.5	93.8	1.5	0.3	0.6	2.5	3.7	Sand
31	S.S	Rabaa	0 – 50	3.6	63.5	31.3	98.0	0.2	0.1	0.0	0.3	1.8	Sand
32	S.S	Rabaa	0 – 45	7.3	56.1	34.8	98.1	0.2	0.0	0.0	0.2	1.7	Sand
33	S.S	El-Ahrar	0 – 60	3.1	76.4	18.9	98.0	0.1	0.2	0.0	0.3	1.7	Sand
34	S.S	Rummana	0 – 45	0.3	65.5	32.3	97.8	0.2	0.2	0.1	0.5	1.7	Sand

SS= Surface Sample PS= Profile Sample SKS= South El-Kantara Shark S= Loamy sand SC= Sand clay

Cont. table 4-5: Particle size distribution of the studied soil profiles and surface samples.

Sample No.	Sample Type	Location	Depth (cm)	Sand Fraction (µm)				Silt Fraction (µm)				Clay <2µm	Texture Class
				C. Sand 2000 - 630	M. Sand 630 – 200	F. Sand 200 - 63	Total %	C. Silt 63 - 20	M. Silt 20 – 6.3	F. Silt 6.3 - 2	Total %		
35	S.S	El-Ganien	0 - 55	6.4	66.6	24.6	97.6	0.1	0.0	0.5	0.8	1.6	Sand
36	S.S	Rabaa	0 - 50	10.5	52.6	34.1	97.1	0.8	0.0	0.2	0.9	2.0	Sand
37	S.S	El-Nigila	0 - 60	2.5	57.8	37.1	97.4	1.0	0.3	0.0	1.3	1.4	Sand
38	P.S1	El-Ahrar	0 – 25	0.9	54.9	41.7	97.6	0.6	0.4	0.0	1.0	1.4	Sand
39	P.S1	El-Ahrar	25 – 40	1.9	52.5	39.7	94.1	3.2	0.0	0.2	3.5	2.5	Sand
40	P.S1	El-Ahrar	40 – 75	3.9	75.3	19.2	98.4	0.2	0.1	0.0	0.3	1.3	Sand
41	P.S2	Rabaa	0 – 30	4.3	57.6	35.6	97.5	1.0	0.0	0.0	1.0	1.5	Sand
42	P.S2	Rabaa	30 – 150	6.5	57.0	34.2	97.7	0.7	0.3	0.1	1.1	1.2	Sand
43	S.S	El-Kherba	0 – 50	2.6	53.9	39.5	96.0	1.8	0.4	0.0	2.2	1.9	Sand
44	S.S	El-Sadat	0 – 45	6.7	53.5	37.1	97.2	1.6	0.1	0.4	2.1	0.7	Sand
45	S.S	El-Sadat	0 – 50	9.4	57.4	30.2	97.0	1.2	0.2	0.2	1.6	1.4	Sand
46	S.S	El-Amrawa	0 – 40	1.5	67.8	29.3	98.5	0.0	0.6	0.0	0.4	1.1	Sand
47	S.S	El-Telol	0 – 40	0.8	73.4	23.4	97.6	0.4	0.3	0.5	1.2	1.2	Sand
48	S.S	El-Telol	0 – 40	2.0	50.9	41.8	94.7	0.8	0.8	0.4	2.0	3.3	Sand
49	P.S1	El-Kherba	0 – 30	8.4	40.7	46.7	95.9	1.0	0.5	0.5	2.0	2.1	Sand
50	P.S1	El-Kherba	30 – 83	5.9	49.8	40.5	96.2	0.8	0.8	0.8	2.4	1.4	Sand
51	P.S1	Biar El-Abd	83 – 145	10.8	47.5	37.6	95.9	0.8	0.9	0.9	2.6	1.5	Sand
52	P.S2	Biar El-Abd	0 – 19	1.9	34.1	54.1	90.0	2.1	1.3	1.6	4.9	5.1	Sand
53	P.S2	Biar El-Abd	19 – 75	1.0	39.1	50.6	90.6	1.1	1.1	1.4	4.7	4.7	Sand
54	P.S2	Biar El-Abd	75 – 165	1.0	40.7	51.0	92.6	1.6	1.0	0.3	2.9	4.5	Sand
55	P.S2	Biar El-Abd	165 – 200	1.8	36.0	52.4	90.2	1.6	1.5	1.5	4.6	5.2	Sand
56	P.S3	Biar El-Abd	0 – 20	5.5	54.9	34.6	93.0	1.3	1.2	1.3	3.8	1.2	Sand
57	P.S3	Biar El-Abd	20 – 130	3.5	60.4	31.8	95.7	1.2	1.3	1.0	3.5	1.3	Sand
58	P.S3	Biar El-Abd	130 – 170	3.2	60.5	30.8	94.5	1.4	1.6	1.3	4.3	1.3	Sand
59	S.S	Biar Lehfen	0 - 45	0.4	25.8	40.5	66.7	9.7	4.7	1.1	15.4	18.0	SL
60	S.S	A. Awaigila	0 - 60	0.4	35.0	50.1	85.4	3.0	1.8	2.6	7.4	7.2	LS
61	S.S	El-Garkada	0 - 60	0.7	44.8	45.5	91.0	4.1	1.6	0.2	5.9	3.1	Sand
62	S.S	G. Libina	0 - 40	4.5	51.2	31.0	84.6	2.3	1.0	1.6	4.9	10.4	LS
63	S.S	Bagdad	0 – 45	0.1	63.6	30.1	93.8	1.5	1.1	1.3	3.9	2.2	Sand
64	S.S	El-Arish	0 - 60	0.3	41.5	48.6	90.5	1.2	1.2	1.0	3.3	6.2	Sand
65	S.S	El-Arish	0 - 60	0.2	50.9	41.1	92.2	1.8	1.5	1.5	4.8	3.0	Sand
66	P.S1	El-Rissan	0 – 68	5.2	15.8	21.4	42.3	7.6	9.2	14.4	31.2	26.5	Loam
67	P.S1	El-Rissan	68 – 140	1.1	20.5	28.8	50.4	6.3	12.0	12.2	30.6	19.1	Loam
68	P.S1	El-Rissan	140 –220	0.6	25.0	35.0	60.7	8.3	10.2	7.2	25.7	13.6	SL
69	P.S2	El-Arish	0 – 40	0.3	69.4	20.6	90.3	2.0	2.3	2.0	6.3	3.5	Sand
70	P.S2	El-Arish	40 – 140	0.8	62.4	27.1	90.3	2.8	2.5	1.7	7.0	2.7	Sand
71	P.S2	El-Arish	140 – 200	0.2	71.0	18.3	89.4	2.3	3.9	2.5	8.7	1.9	Sand

SS= Surface Sample **PS= Profile Sample** **SKS= South El-Kantara Shark**
LS= Loamy sand **SL= Sandy loam** **G. = Gabal A. = Abou W.= Wadi**

Table 4-6: The hydraulic characteristics and bulk density of the studied soil samples.

Sample No.	Type Of sample	Location	Depth cm	Wilting point cm^3 water cm^{-3} soil	Field capacity cm^3 water cm^{-3} soil	Bulk density g cm^{-3}	Saturation cm^3 water cm^{-3} soil	Sat. Hydraulic conduct cm h^{-1}	Available water	
									Cm^3 water m^{-3}soil	In water/foot soil
1	S.S	S.K.S*	0 - 60	0.03	0.10	1.87	0.29	17.82	0.06	0.74
2	S.S	S.K.S	0 - 55	0.04	0.10	1.83	0.31	15.68	0.06	0.77
3	S.S	S.K.S	0 - 50	0.04	0.10	1.85	0.3	16.47	0.06	0.76
4	S.S	S.K.S	0 - 70	0.03	0.09	1.88	0.29	18.73	0.06	0.73
5	S.S	S.K.S	0 - 40	0.03	0.09	1.96	0.26	21.04	0.06	0.70
6	S.S	S.K.S	0 - 60	0.04	0.10	1.83	0.31	15.76	0.06	0.76
7	S.S	S.K.S	0 - 65	0.07	0.15	1.66	0.38	5.40	0.08	0.96
8	P.S1	S.K.S	0 - 42	0.03	0.09	1.97	0.26	21.46	0.06	0.7
9	P.S1	S.K.S	42 - 50	0.03	0.10	1.88	0.29	18.21	0.06	0.74
10	P.S1	S.K.S	50 - 125	0.03	0.09	1.89	0.29	18.9	0.06	0.73
11	P.S1	S.K.S	125 - 160	0.03	0.08	1.99	0.25	22.87	0.06	0.68
12	P.S2	S.K.S	0 - 20	0.06	0.13	1.69	0.36	7.0	0.07	0.86
13	P.S2	S.K.S	20 - 130	0.06	0.13	1.69	0.36	6.9	0.07	0.86
14	P.S2	S.K.S	130 - 164	0.05	0.12	1.74	0.34	9.78	0.07	0.84
15	P.S2	S.K.S	164 - 168	0.05	0.12	1.76	0.34	10.51	0.07	0.87
16	P.S2	S.K.S	168 - 210	0.04	0.11	1.82	0.31	14.17	0.07	0.80
17	S.S	Tina Plain	0 - 70	0.22	0.32	1.32	0.50	0.15	0.10	1.18
18	S.S	Tina Plain	0 - 60	0.24	0.34	1.31	0.51	0.14	0.10	1.24
19	S.S	Tina Plain	0 - 40	0.39	0.53	1.16	0.56	0.33	0.14	1.68
20	S.S	Tina Plain	0 - 30	0.43	0.56	1.14	0.57	0.43	0.13	1.54
21	S.S	Tina Plain	0 - 60	0.07	0.14	1.66	0.38	5.36	0.07	0.89
22	S.S	Tina Plain	0 - 50	0.04	0.10	1.86	0.30	17.81	0.06	0.74
23	S.S	Tina Plain	0 - 60	0.08	0.16	1.6	0.40	3.18	0.08	0.92
24	P.S1	Tina Plain	20-Sep	0.09	0.17	1.58	0.40	2.47	0.07	0.90
25	P.S1	Tina Plain	20 - 110	0.43	0.55	1.16	0.56	0.33	0.12	1.47
26	P.S2	Tina Plain	0 - 17	0.10	0.18	1.55	0.41	1.74	0.08	0.93
27	P.S2	Tina Plain	17 - 70	0.05	0.11	1.78	0.33	12.55	0.07	0.79
28	P.S2	Tina Plain	70 - 140	0.04	0.10	1.85	0.30	16.01	0.06	0.77
29	S.S	Qatia	0 - 50	0.04	0.10	1.86	0.30	17.47	0.06	0.74
30	S.S	Qatia	0 - 55	0.05	0.12	1.76	0.34	11.19	0.07	0.82
31	S.S	Rabaa	0 - 50	0.03	0.09	1.87	0.29	18.91	0.06	0.72
32	S.S	Rabaa	0 - 45	0.03	0.09	1.88	0.29	19.4	0.06	0.72
33	S.S	El-Ahrar	0 - 60	0.03	0.09	1.88	0.29	19.31	0.06	0.72
34	S.S	Rummana	0 - 45	0.03	0.09	1.88	0.29	18.79	0.06	0.72
35	S.S	El-Ganien	0 - 55	0.03	0.09	1.89	0.29	19.26	0.06	0.72
36	S.S	Rabaa	0 - 50	0.04	0.10	1.86	0.30	17.52	0.06	0.74
37	S.S	El-Nigila	0 - 60	0.03	0.09	1.91	0.28	19.56	0.06	0.72
38	P.S1	El-Ahrar	0 – 25	0.03	0.09	1.91	0.28	19.6	0.06	0.72

SKS* = South El-Kantara Shark S.S = Surface samples P.S = Profile samples.

Cont. table 4-6: The hydraulic characteristics and bulk density of the studied soil samples.

Sample No.	Type Of sample	Location	Depth cm	Wilting point cm^3 water cm^{-3} soil	Field capacity cm^3 water cm^{-3} soil	Bulk density g cm^{-3}	Saturation cm^3 water cm^{-3} soil	Sat. Hydraulic conduct cm h^{-1}	Available water	
									Cm^3 water /cm^3 soil	In water/foot soil
39	P.S1	El-Ahrar	25 – 40	0.04	0.11	1.82	0.31	14.21	0.07	0.80
40	P.S1	El-Ahrar	40 – 75	0.03	0.09	1.93	0.27	21.03	0.06	0.70
41	P.S2	Rabaa	0 – 30	0.03	0.09	1.90	0.28	19.41	0.06	0.72
42	P.S2	Rabaa	30 – 150	0.03	0.09	1.94	0.27	20.55	0.06	0.71
43	S.S	El-Kherba	0 – 50	0.04	0.10	1.86	0.30	17.02	0.06	0.76
44	S.S	El-Sadat	0 – 45	0.03	0.09	2.01	0.24	20.19	0.06	0.70
45	S.S	El-Sadat	0 – 50	0.03	0.09	1.91	0.28	19.14	0.06	0.73
46	S.S	El-Amrawa	0 – 40	0.03	0.09	1.95	0.26	21.69	0.06	0.69
47	S.S	El-Telol	0 – 40	0.03	0.09	1.94	0.27	20.42	0.06	0.71
48	S.S	El-Telol	0 – 40	0.05	0.11	1.78	0.33	12.34	0.07	0.80
49	P.S1	El-Kherba	0 – 30	0.04	0.10	1.84	0.30	16.18	0.06	0.76
50	P.S1	El-Kherba	30 – 83	0.03	0.09	1.91	0.28	18.41	0.06	0.74
51	P.S1	Biar El-Abd	83 – 145	0.03	0.10	1.89	0.29	17.84	0.06	0.75
52	P.S2	Biar El-Abd	0 – 19	0.06	0.13	1.71	0.26	7.82	0.07	0.89
53	P.S2	Biar El-Abd	19 – 75	0.06	0.13	1.72	0.35	8.45	0.07	0.88
54	P.S2	Biar El-Abd	75 – 165	0.05	0.12	1.73	0.35	9.28	0.07	0.84
55	P.S2	Biar El-Abd	165 – 200	0.06	0.13	1.70	0.36	7.66	0.07	0.89
56	P.S3	Biar El-Abd	0 – 20	0.03	0.10	1.92	0.27	15.68	0.07	0.80
57	P.S3	Biar El-Abd	20 – 130	0.03	0.10	1.92	0.28	18.10	0.06	0.75
58	P.S3	Biar El-Abd	130 – 170	0.03	0.10	1.91	0.28	17.02	0.06	0.70
59	S.S	Biar Lehfen	0 - 45	0.12	0.22	1.47	0.44	0.89	0.09	1.13
60	S.S	A. Awaigila	0 - 60	0.07	0.15	1.64	0.38	4.89	0.08	0.95
61	S.S	El-Garkada	0 - 60	0.05	0.12	1.78	0.33	11.49	0.07	0.86
62	S.S	G. Libina	0 - 40	0.09	0.17	1.59	0.40	2.77	0.08	0.94
63	S.S	Bagdad	0 – 45	0.04	0.11	1.83	0.31	14.64	0.07	0.80
64	S.S	El-Arish	0 - 60	0.06	0.14	1.68	0.37	6.34	0.07	0.88
65	S.S	El-Arish	0 - 60	0.04	0.12	1.79	0.33	12.14	0.07	0.84
66	P.S1	El-Rissan	0 – 68	0.15	0.28	1.37	0.48	0.44	0.13	1.51
67	P.S1	El-Rissan	68 – 140	0.12	0.24	1.43	0.46	0.87	0.12	1.43
68	P.S1	El-Rissan	140 – 220	0.10	0.21	1.50	0.43	1.62	0.11	1.30
69	P.S2	W. El-Arish	0 – 40	0.05	0.12	1.76	0.34	10.55	0.07	0.88
70	P.S2	W. El-Arish	40 – 140	0.04	0.12	1.80	0.32	11.5	0.07	0.87
71	P.S2	W. El-Arish	140 – 200	0.04	0.11	1.85	0.30	12.91	0.07	0.88

S.S = Surface samples **P.S = Profile samples** **G. = Gabal** **A. = Abou** **W.= Wadi**

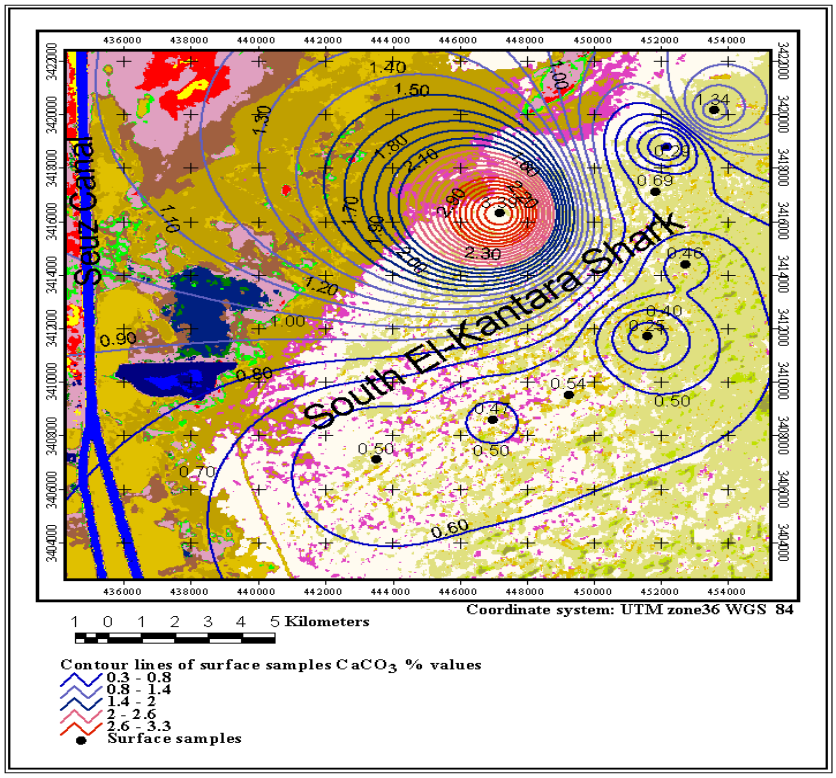

Fig. 4-25: Contour line image map of calcium carbonate content in surface samples of the South El-Kantara Shark area.

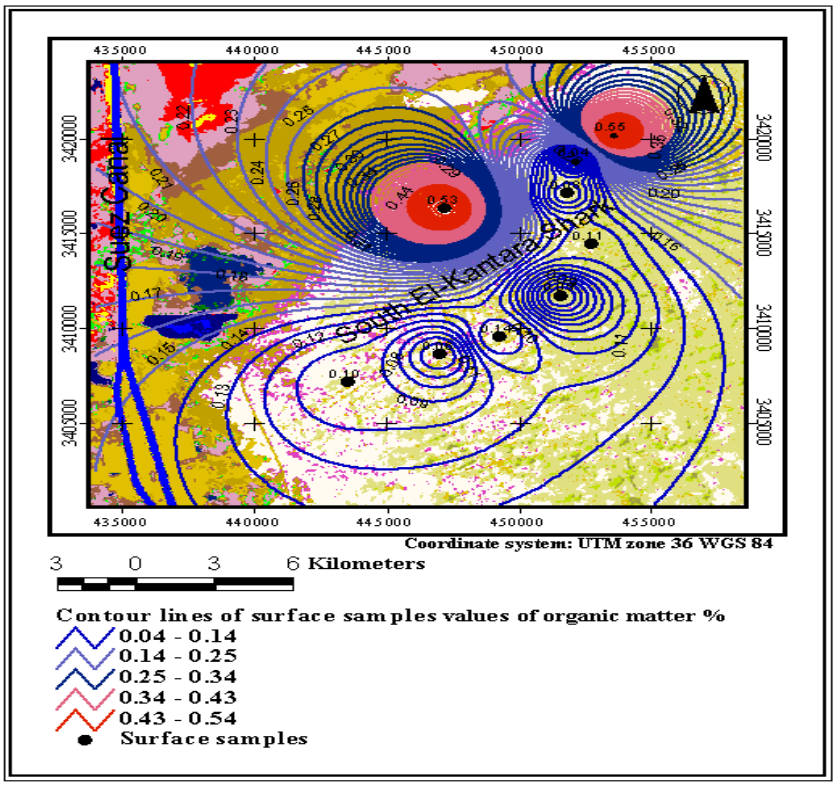

Fig. 4-26: Contour line image map of the organic matter content in surface samples of the South El-Kantara Shark area.

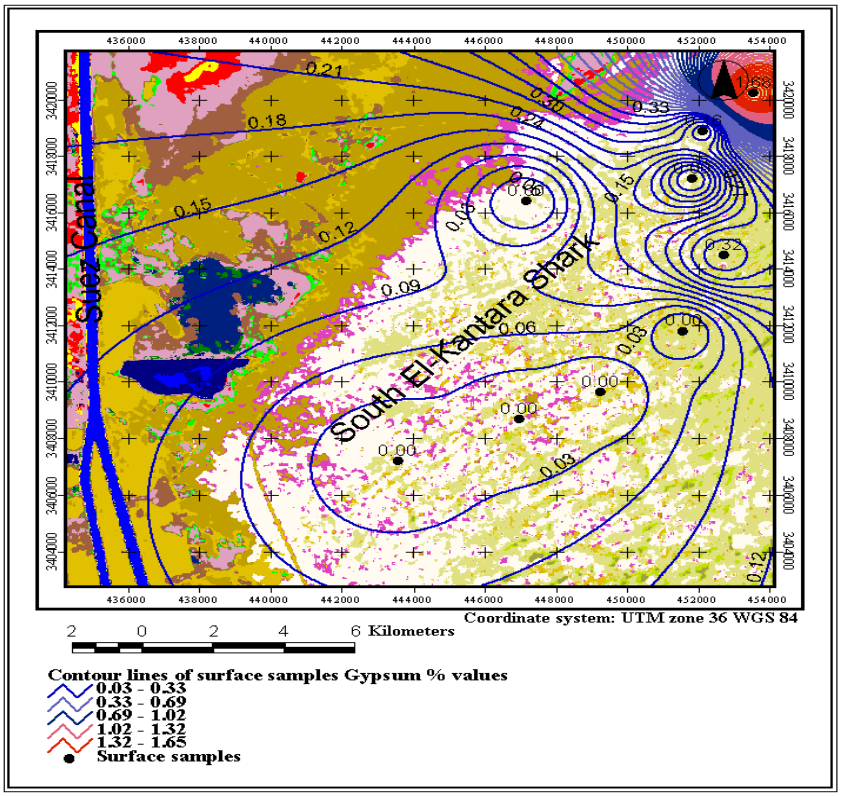

Fig. 4-27: Contour line image map of the gypsum content in surface samples of the South El-Kantara Shark area.

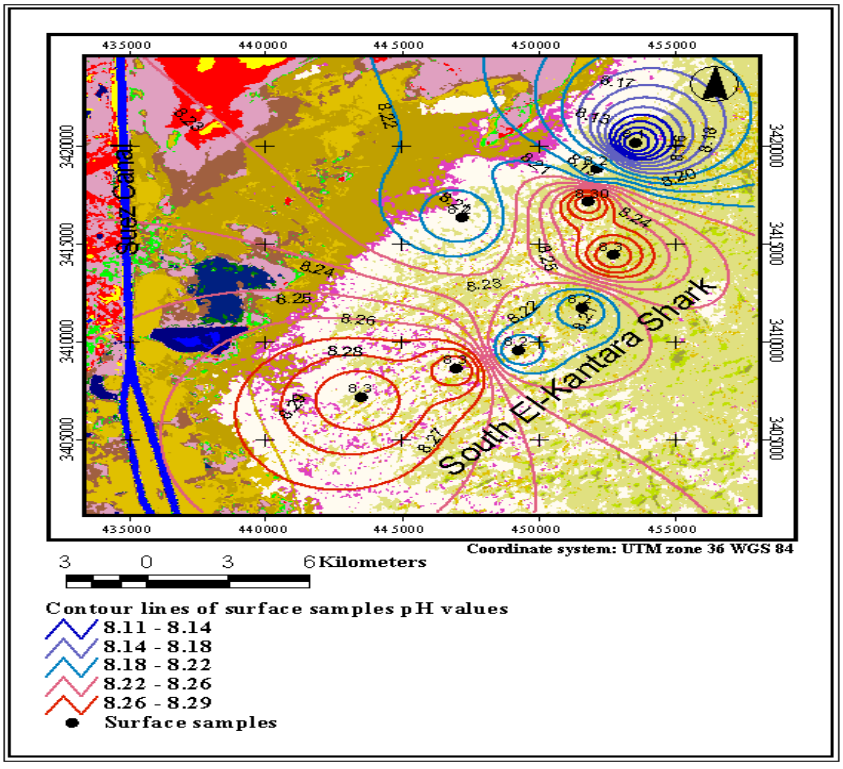

Fig. 4-28: Contour line image map of the soil reaction (pH) value in surface samples of the South El-Kantara Shark area.

The results of electrical conductivity (EC) in table (4-2) indicate that the surface and subsurface layers of the South El-Kantara Shark soils range from non-saline to slightly or moderately saline. EC value range between 0.4 to 16.0 ds m^{-1} in these studied soils. The contour lines map of EC values in surface soil samples of the South El-Kantara Shark area are shown in figure (4-29), which is extracted from satellite image, values of soil surface EC and GIS data.

Analysis of the soil extracts shows that the cationic composition is characterized by the dominance of Ca^{2+}, followed by Na^{+}, Mg^{2+} and K^{+} in surface and profile soil samples of the South El-Kantara Shark area. Soluble anions are predominated by Cl^{-} followed by $HCO_3^{-}$and SO_4^{2+}.

CEC values in table (4-2) show the soil samples in the South El-Kantara Shark area range between 3.9 to 26.1 meq $100g^{-1}$ soil.

The results of exchangeable cations in the soils of the South El-Kantara Shark reveal that calcium is the dominant cation followed by Ba^{2+}, Na^{+} and Mg^{2+}, while exchangeable K^{+} is present in minor amounts, by meq $100g^{-1}$ soil. Exchangeable Sodium Percentage (ESP) in the South El-Kantara Shark soils varies from 4 to 24 % in the profile and surface samples.

The nitrogen, phosphorus and potassium status in the soil of the South El-Kantara Shark studied area is illustrated in table (4-3). The nitrogen is generally very low and decreases with depth in profiles. The total nitrogen content in the South El-Kantara Shark soils ranges between 0.01 to 0.21 %. The values of phosphorus (P) content ranges from 105 to 354 mg kg^{-1}. The potassium (K) content ranges between 42 to 402 mg kg^{-1} in the surface and profile soil samples.

The macronutrient status of the soils in the south El-Kantara Shark studied area shown in table (4-4), reveal that the range of the cationic composition are characterized by the dominance of Fe^{2+}, followed by Mn^{2+} and Zn^{2+}, while Cu^{2+} is found in minor amounts in soil samples of this area. The content of Fe^{2+} ranged between 0.69 to 1.21 (mg kg^{-1}), Mn^{2+} ranged between 0.15 to 5.17 mg kg^{-1}, Zn^{2+} varies from 0.05 to 1.25 mg kg^{-1} and Cu2+ between values 0.01 to 0.43 mg kg^{-1} in South El-Kantara Shark area.

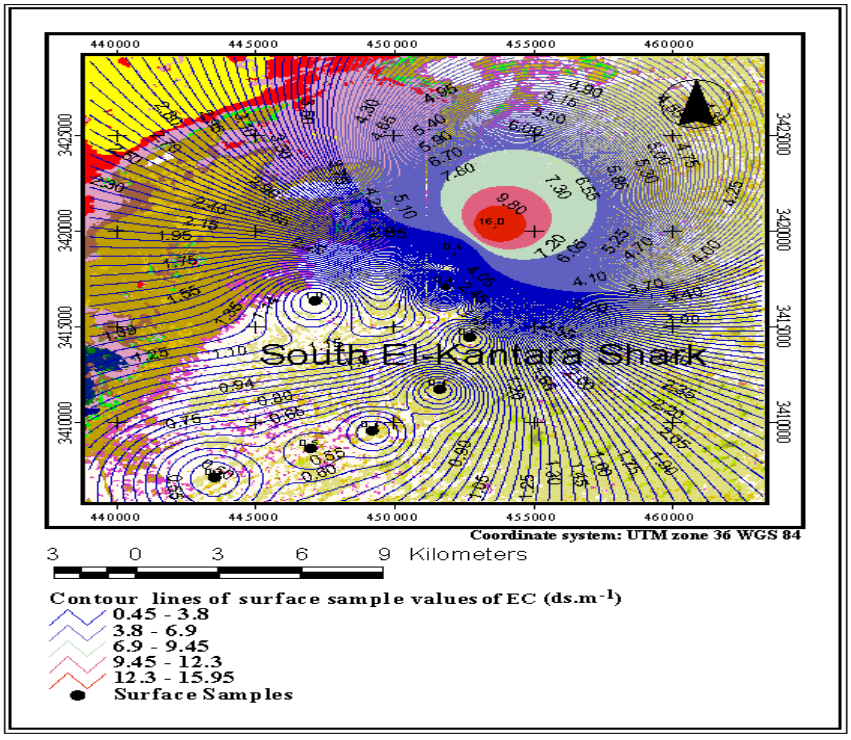

Fig. 4-29: Contour line image map of the electrical conductivity (EC) content in surface samples of the South El-Kantara Shark area.

The results of particle size distribution in the South El-Kantara Shark soils area are shown in table (4-5). They reveal that the soils texture classes in all soil samples in studied area is sand texture, except the one surface samples have a loamy sand texture class in this area.

Table (4-6) shown the physical property (bulk density) and hydraulic status in the soils of the South El-Kantara Shark area. The values of bulk density range between 1.74 to 1.99 g cm^{-3} in this soil area.

The results of hydraulic conductivity in table (4-6) reveal the soil of the South El-Kantara Shark area are characterized by high movement of water within and through there soils. The values of soil permeability range between 5.4 to 22.87 cm hr^{-1}. The values of available water in the soil of the South El-Kantara Shark indicate more available than the soils in the El-Tina Plain area. Available water values shown in table (4-6) with an average value of 0.07 cm^3 water cm^{-3}soil.

The results in table (4-6) show the range values of saturation in the South El-Kantara Shark soils, that range from 0.25 to 0.38 cm^3 water cm^{-3}soil in the surface and profile soils samples in this area.

4.3.3 Soil properties and maps of the Rabaa and the Bair El-Abd

The chemical characteristics in the Rabaa and the Bair El-Abd soil samples are listed in table (4-1). They show that the calcium carbonate content ranges between 0.07 and 0.48 % of the fine earth in the Rabaa area, while ranges between 0.04 and 1.52 % in the Bair El-Abd soils.

The data of calcium carbonate content and results of the Landsat TM image analysis with GIS data have resulted in the contour lines maps for the Rabaa and the Bair El-Abd soils area. These maps revealed the distribution of $CaCO_3$ content in the surface soil samples in those soils studied. Figures (4-30) and (4-31) show the pattern of $CaCO_3$ distribution by contour lines in the Rabaa and the Bair El-Abd soil area.

The values in table (4-1) reflect the poor of organic matter content, that are range from 0.02 to 0.22 % in the Rabaa soil samples and between 0.01 to 0.27% in the Bair El-Abd soil samples. The organic carbon values ranges between 0.01 and 0.16 % in the samples of the Rabaa area and variance from 0.0 to 0.09 % in the Bair El-Abd soil samples. The satellite image data performed plan contour line maps for organic matter content in these soil samples from the Rabaa and the Bair El-Abd areas. The wide distances between contour lines in the image maps were revealed that the poor status of organic matter content in these studied soils. Figures (4-32) and (4-33) are show the distribution of organic matter content in the surface soil samples of the Rabaa and the Bair El-Abd areas.

The data presented in table (4-1) indicate that the gypsum content is not detected in the soils of the Rabaa and the Bair El-Abd. An exception to this are the few samples (profile No.1) in the El-Ahrar profile samples, whose average value is 8.5 % and four soil samples in the Bair El-Abd area in average 2.8 %.

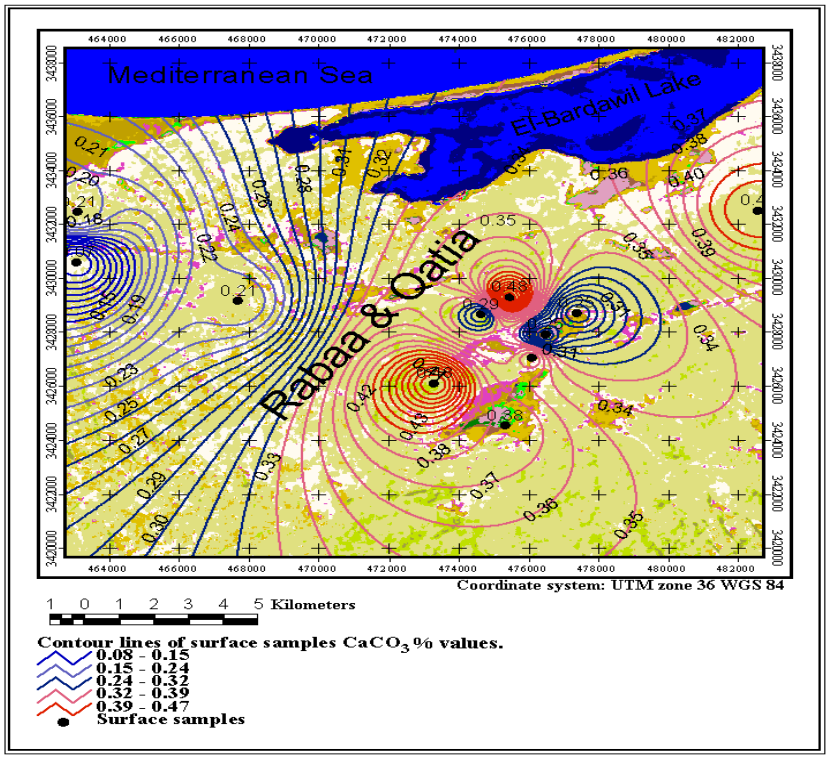

Fig. 4-30: Contour line image map of calcium carbonate content in surface samples of the Rabaa and Qatia area.

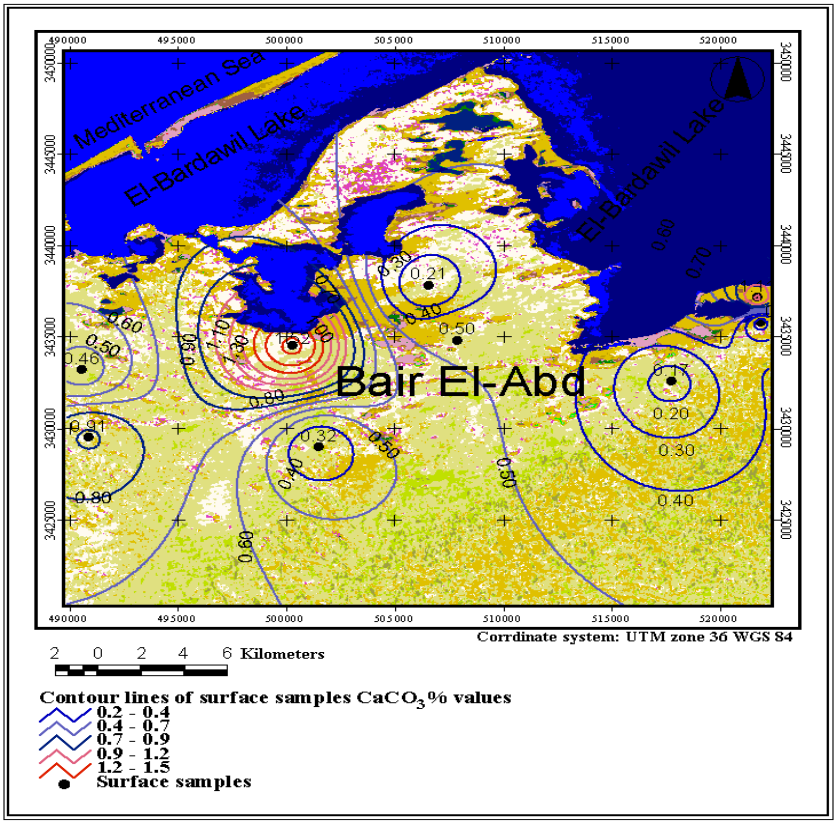

Fig. 4-31: Contour line image map of calcium carbonate content in surface samples of the Bair El-Abd area.

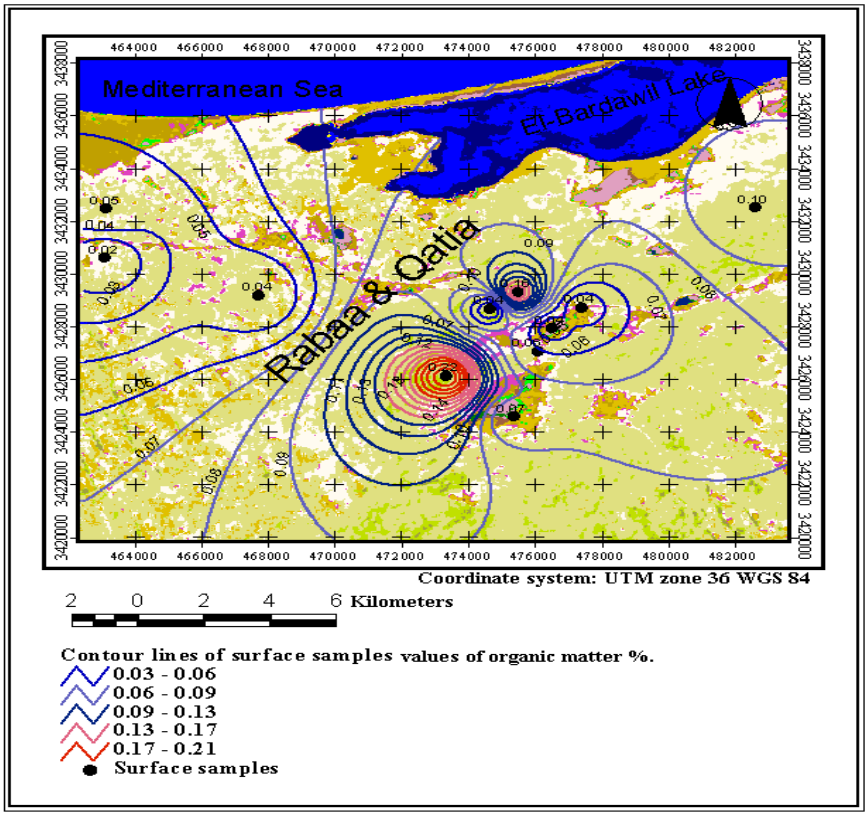

Fig. 4-32: Contour line image map of the organic matter content in surface samples of the Rabaa and Qatia area.

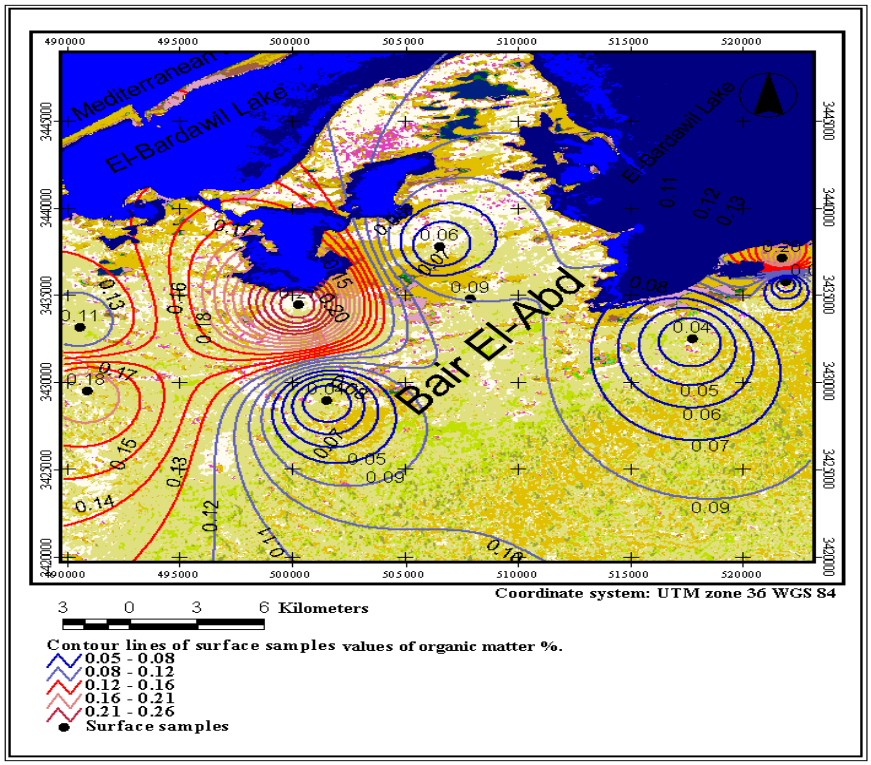

Fig. 4-33 Contour line image map of the organic matter content in surface samples of the Bair El-Abd area.

Figures (4-34) and (4-35) reveal the low distribution of gypsum content in the surface soil samples in the Rabaa and the Bair El-Abd areas.

The soil reaction (pH) values in soils of the Rabaa and the Bair El-Abd show relatively high values. These range from moderately (8.0) to strongly (8.5) alkaline in the Rabaa soil samples, while in the Bair El-Abd soils range from 8.1 to 8.5 in the soil samples. From the Landsat TM image data was achieved the distribution of contour lines maps for the Rabaa and the Bair El-Abd areas by using the results of the soil reaction (pH) values from surface soil samples in these area as shown in figures (4-36 and 4-37).

Electrical conductivity (EC) data are show in table (4-2) these values ranges from 0.4 to 6.5 ds m^{-1} in the Rabaa soil samples. The EC values in the Bair El-Abd soil samples ranging from 0.4 to 10 ds m^{-1}. The contour lines maps in figures (4-38) and (4-39) reveal the distribution of EC values of surface soil samples in the Rabaa and the Bair El-Abd area.

The chemical analysis results of soil extract in table (4-2) shows that cationic composition characterized in the Rabaa and the Bair El-Abed studied areas by the dominance of Ca^{2+} followed by Na^{+} and Mg^{2+}, while K^{+} cation is present in minor concentration in soil extract. Chloride is the predominat soluble anion in soil extract and followed by HCO_3^{-} and SO_4^{2-} in the soil extract of the surface and profile soil samples from these areas.

Cation Exchange Capacity (CEC) values in table (4-2) shows the profile and surface soil samples of the Rabaa soils are ranging from 9.2 to 43.4 meq $100g^{-1}$ soil. The values of CEC in the Bair El-Abd soil samples are less than in the Rabaa soil samples, these ranges from 4.9 to 31.8 $100g^{-1}$ soil.

Results of exchangeable cations in the soils of the Rabaa and the Bair El-Abd areas are reveal that calcium is the dominant cation followed by Na^{+}, $Ba^{2+}$and Mg^{2+}, while exchangeable K^{+} is present in minor amounts by meq $100g^{-1}$ soil. ESP values in these soil areas vary from 1 to 23.44 % and 0.72 to 24.55%, respectively.

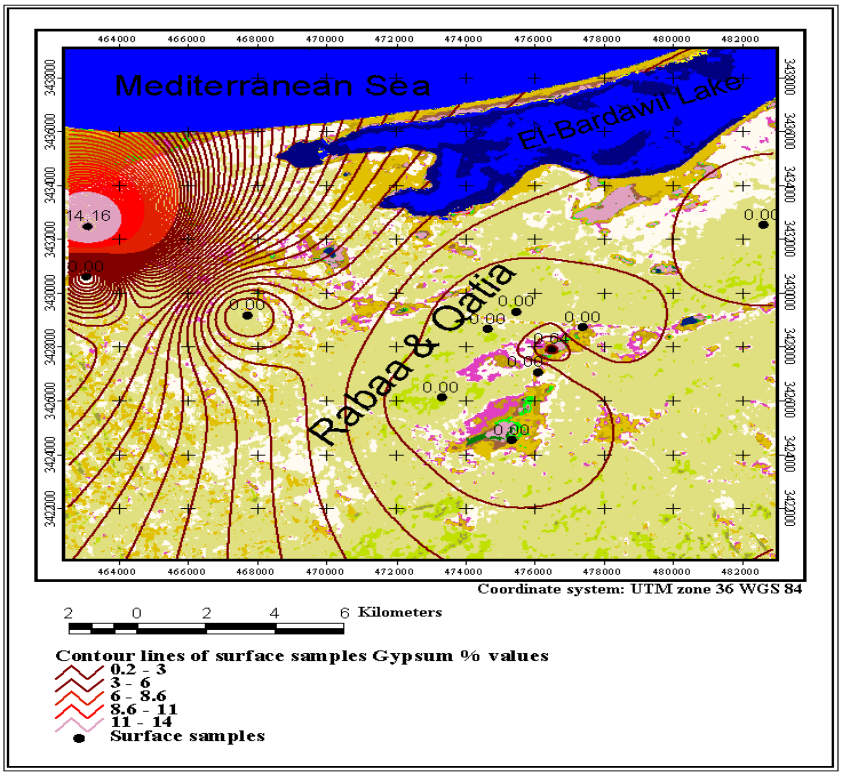

Fig. 4-34: Contour line image map of the gypsum content in surface samples of the Rabaa and Qatia area.

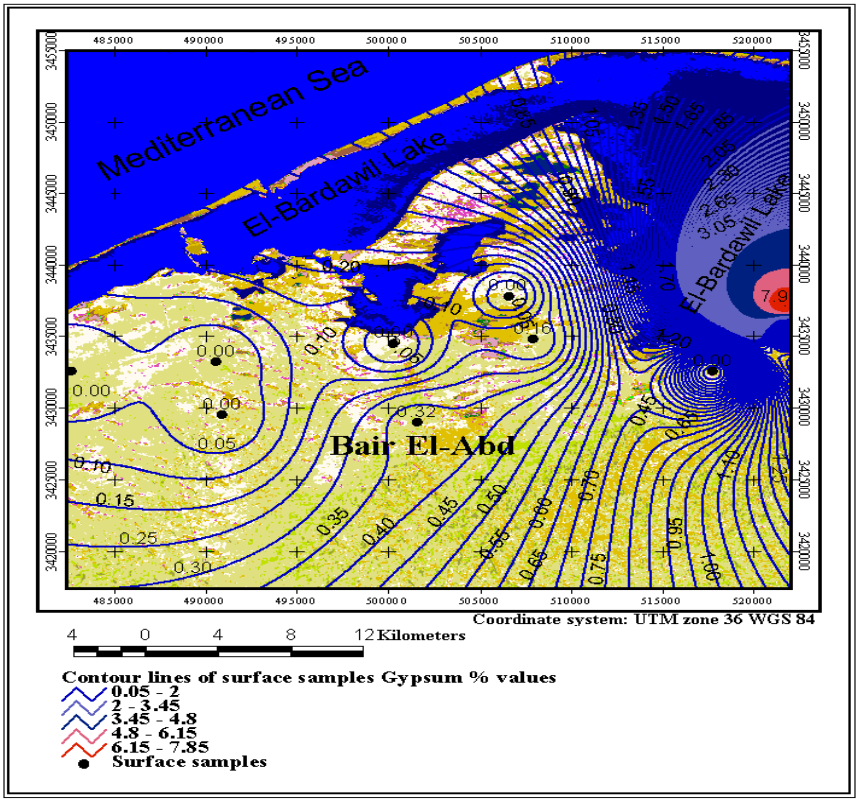

Fig. 4-35: Contour line image map of the gypsum content in surface samples of the Bair El-Abd area.

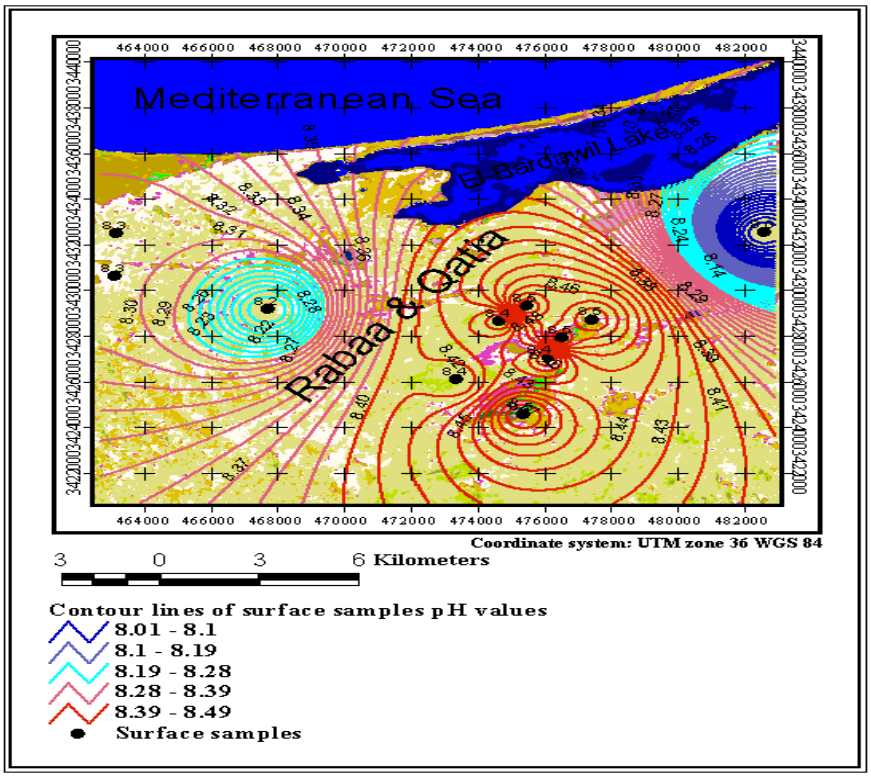

Fig. 4-36: Contour line image map of the soil reaction (pH) values in surface samples of the Rabaa and Qatia area.

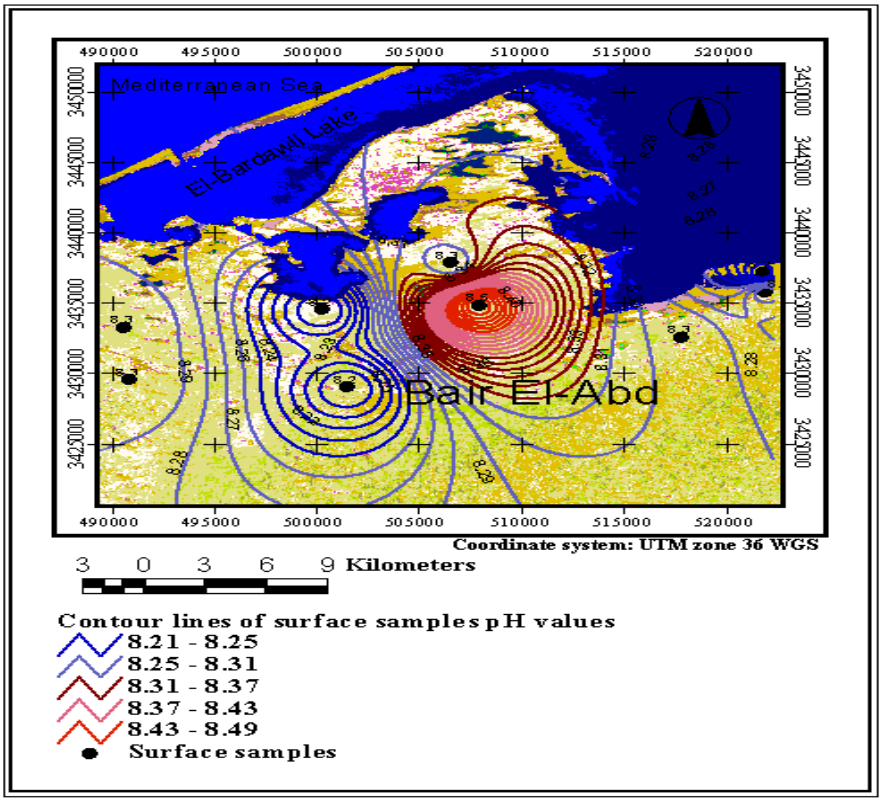

Fig. 4-37: Contour line image map of the soil reaction (pH) values in surface samples of the Bair El-Abd area.

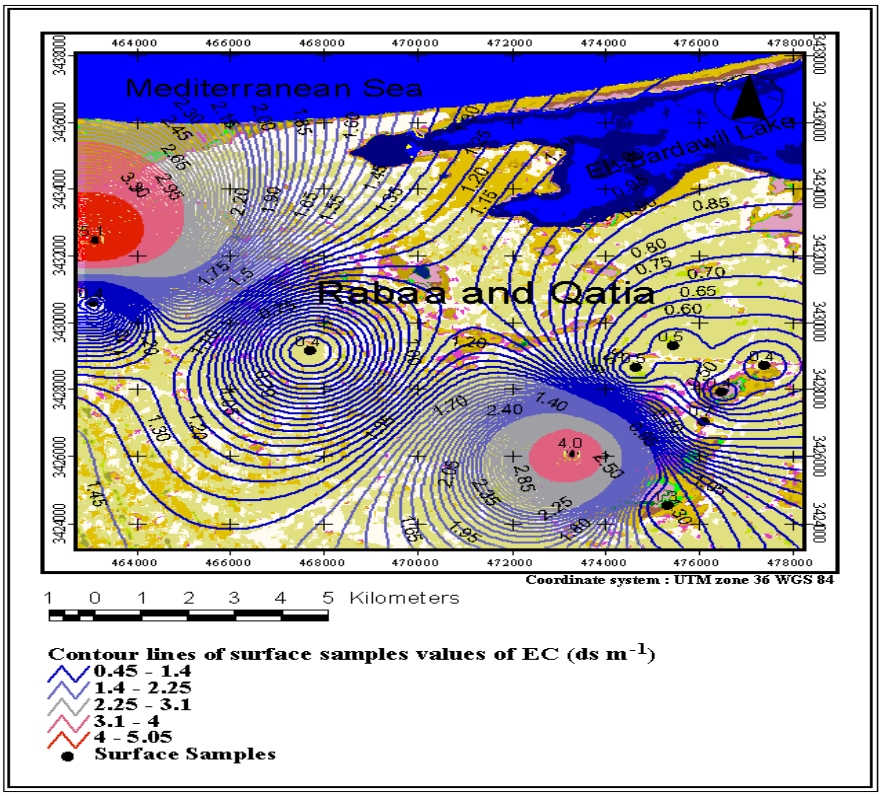

Fig. 4-38: Contour line image map of the electrical conductivity (EC) content in surface samples of the Rabaa and Qatia area.

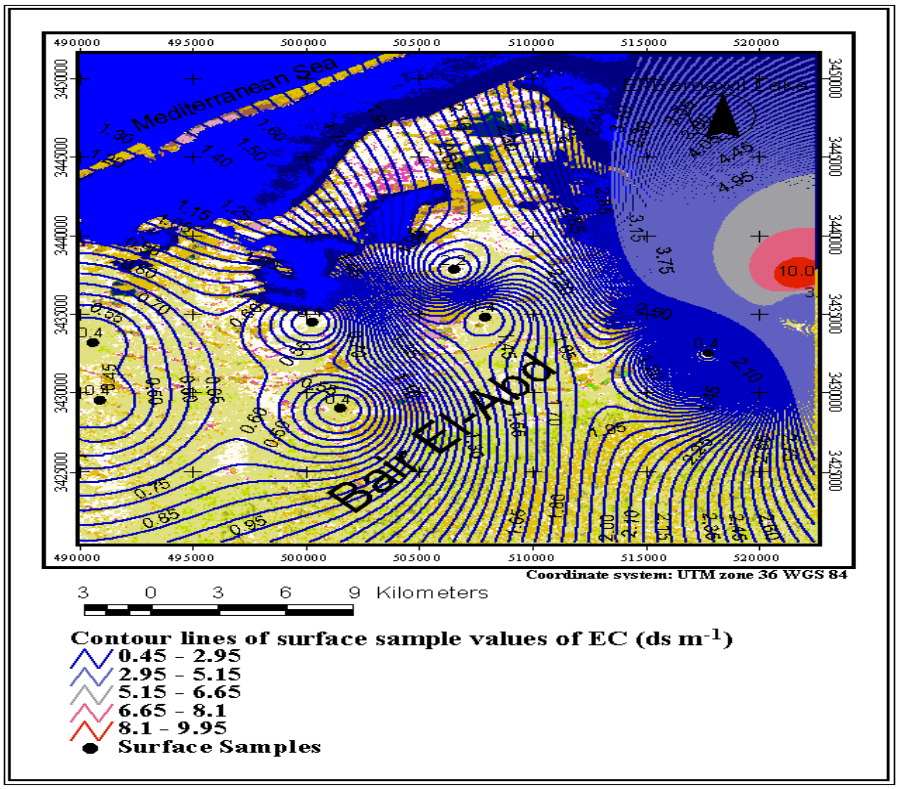

Fig. 4-39: Contour lines image map of the electrical conductivity (EC) content in surface samples of the Bair El-Abd area.

The nitrogen, phosphorus (P) and potassium (K) status in table (4-3) shows the fertility potential of the soil samples of the Rabaa and the Bair El-Abd areas. The nitrogen values are generally very low and decrease with depth in soil profiles. The total nitrogen content in these soils area ranges from 0.01 to 0.07 % and 0.01 to 0.04%, respectively. The values of phosphorus range from 136 to 499 mg kg^{-1} in the soils of the Rabaa, and from 92 to 390 mg kg^{-1} in the soil of the Bair El-Abd area. In the soils of the Rabaa potassium content values range between 42 and 296 mg kg^{-1} and range from 40 to 162 mg kg^{-1} in the Bair El-Abd soil samples.

The results in table (4-4) show the macronutrient status of the soils in the Rabaa and the Bair El-Abd areas, and reveal that the range of the cationic composition are characterized by the Mn^{2+} which is dominant cation followed by $Fe^{2+}$and Zn^{2+}, while Cu^{2+} is found in minor amounts in soil samples of the areas. The content of Mn^{2+} ranged between 0.75 and 1.86 mg kg^{-1}, Fe^{2+}ranged from 0.67 to 1.27 mg kg^{-1}, Zn^{2+} varies from 0.07 to 0.79 mg kg^{-1} and Cu^{2+} from 0.01 to 0.29 mg kg^{-1} in the Rabaa area. Meanwhile, in the soils of the Bair El-Abd area Mn^{2+} ranges from 0.57 to 2.72 mg kg^{-1}, Fe^{2+} between 0.8 and 1.97 mg kg^{-1}, Zn^{2+} from 0.02 to 1.54 mg kg^{-1} and Cu^{2+} ranges from 0.01 to 0.87 mg kg^{-1}.

The results of particle size distribution in the soil of the Rabaa and the Bair El-Abd areas are shown in table (4-5), the distribution of soils texture classes in all profile and surface soil samples revealed sand texture class in these areas.

Table (4-6) show the hydraulic characteristics and bulk density in the soils of the Rabaa and the Bair El-Abd areas. The values of bulk density range between 1.76 and 1.94 g cm^{-3} in the soil samples of the Rabaa area, while ranging from 1.7 to 2.0 g cm^{-3} in the soils of the Bair El-Abd area.

The values of soil permeability in the Rabaa soil area range from 11.19 to 21.03 cm hr^{-1} and in the Bair El-Abd range between 7.66 and 21.69 cm hr^{-1}. The average values of available water in table (4-6) show that the Rabaa and the Bair El-Abd area are 0.06 cm^3 water cm^{-3} soil. The values of saturation in the Rabaa soils range from 0.27 to 0.34 cm^3 water cm^{-3} soil and in the soils of the Bair El-Abd ranging between 0.24 and 0.36 cm^3 water cm^{-3} soil.

4.3.4 Soil properties and maps of the Wadi El-Arish

The results in table (4-1) shown that the calcium carbonate content in the soils of the Wadi El-Arish area have wide variations in $CaCO_3$ content, that are ranging from 1.22 to 26.5 % in the surface and profile samples. These values may indicate sand and calcareous deposits making up the origins of these soils area. The image contour lines map of the $CaCO_3$ distribution in the surface samples in the Wadi El-Arish area is show in figure (4-40).

The organic matter content in the soil samples of the Wadi El-Arish area rangs from 0.15 to 4.61%, while organic carbon content never exceeds 1.15%. Figure (4-41) shows the contour lines image map of distribution of organic matter content in surface soil samples in this area.

The values of gypsum content in table (4-1) show that the soils of the Wadi EL-Arish range from 0 to 1.36 %. The contour lines image map of gypsum surface content reveals the pattern of gypsum distribution in this area (figure 4-42), by using the Landsat TM image data and GIS technique.

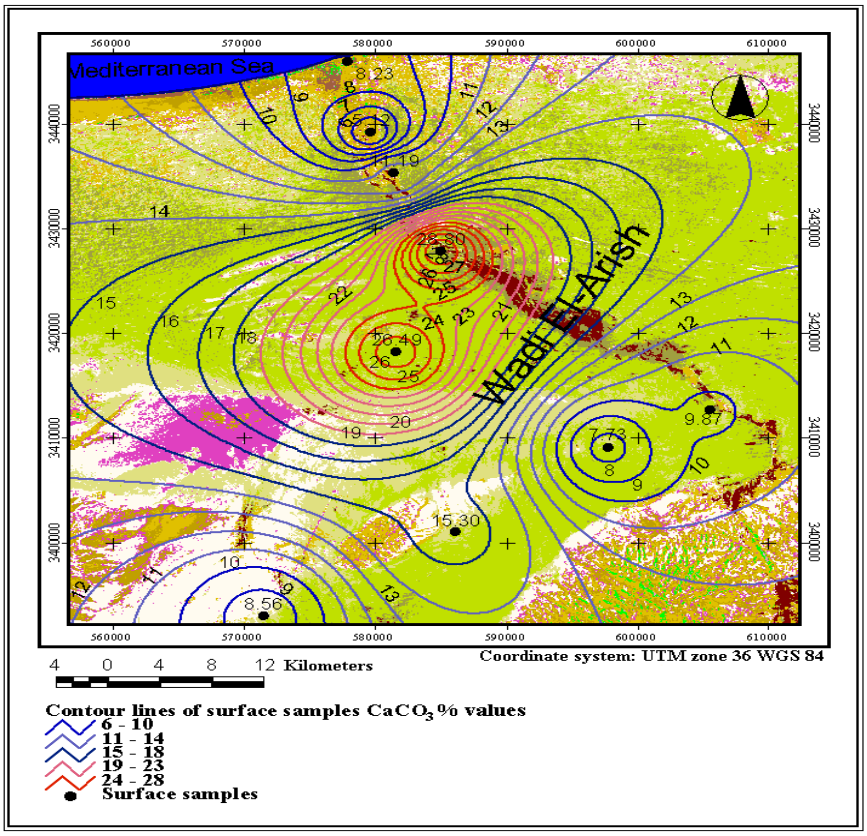

Fig. 4-40: Contour line image map of calcium carbonate content in surface samples of the Wadi El-Arish area.

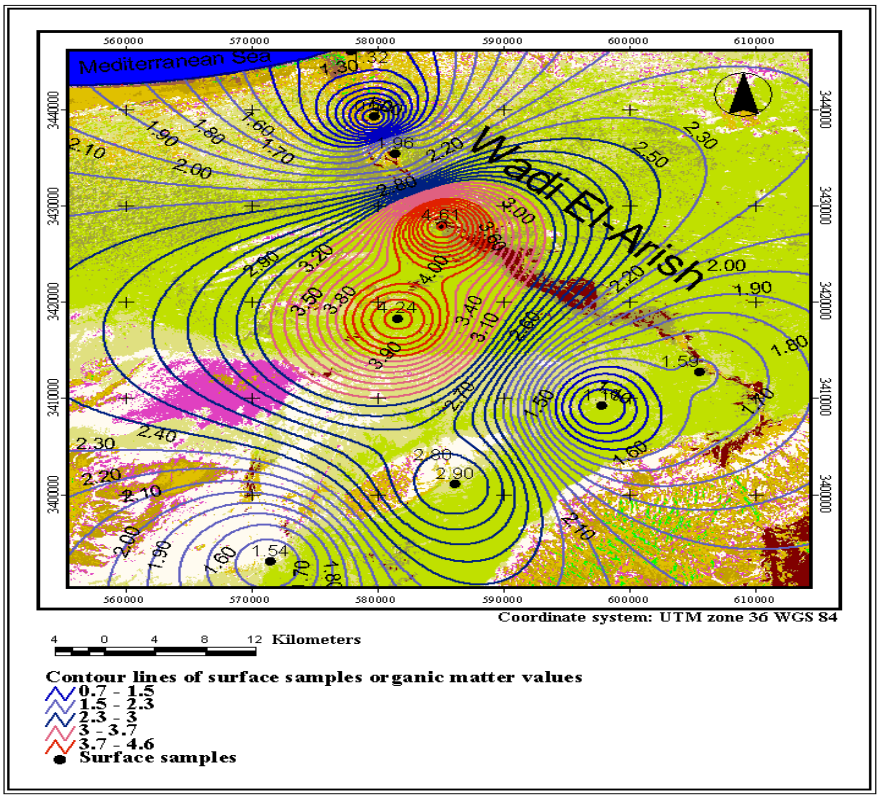

Fig. 4-41: Contour line image map of the organic matter content in surface samples of the Wadi El-Arish area.

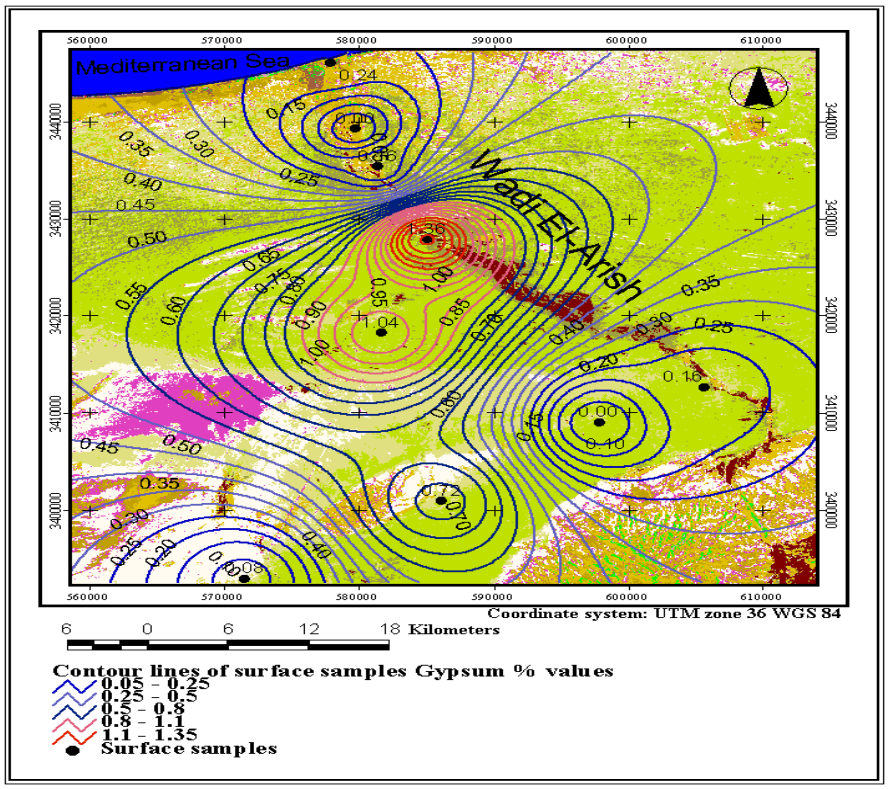

Fig. 4-42: Contour line image map of the gypsum content in surface samples of the Wadi El-Arish area.

The soil reaction (pH) values in table (4-1) reveal that the Wadi El-Arish soils are moderately alkaline, ranging from 8.1 and 8.4 in the studied soil samples. Figure (4-43) shows the contour lines map of the pH in the soil suspension at 25°C in this soils.

The representative soil samples in the Wadi El-Arish reveal that these soils are almost free of salts as indicated by the electrical conductivity (EC) values which are normally found between 0.4 to 3.7 ds m^{-1} in the surface and profile soil samples. The map in figure (4-44) is illustrated the distribution of contour lines of EC values in the surface samples in this area.

The chemical compositions of the Wadi El-Arish soil extract (table 4-2) are characterized in its cations distribution by the dominancy of Ca^{2+} followed by Na^{+}, Mg^{2+} and minor amounts of K^{+} cation whereas the anions are predominated by chloride followed by sulphate and bicarbonate. The CEC values reveal the soil samples conform with texture classes in the Wadi El-Arish soils, as their values range between 2.1 and 12.5 meq $100g^{-1}$ soil throughout the soil samples. The values of exchangeable cations in this area reveal that the calcium is the dominant cation, which may be due to the origin of this soils (Calcareous rocks). Calcium is followed by Ba^{2+}, Mg^{2+} and Na^{+}, while exchangeable K^{+} is present in minor amounts by meq $100g^{-1}$ soil in this soils. The ESP values vary from 6.11 to 33.98 % in this soils area.

The fertility potential status of nitrogen, phosphorus (P) and potassium (K) in the soils of the Wadi El-Arish area are shown in table (4-3). The values of nitrogen are in very low concentration in the surface soil samples and decreases with depth of soil profile samples. The values ranges from 0.01 to 0.12 %. The values of phosphorus varies from 149 to 580 mg kg^{-1} and total potassium ranges between 34 and 94 mg kg^{-1} in the soil samples.

The result presented in table (4-4) shows the status of macronutrients in the surface and profile soil samples of the Wadi El-Arish area. The values reveal that the cations composition are characterized by the dominance of Mn^{2+} (0.56 to 1.88 mg kg^{-1}), followed by Fe^{2+} ranging from (0.54 to 1.66 mg kg^{-1}) and Zn^{2+} ranging (0.1 to 0.98 mg kg^{-1}), while Cu^{2+} is found in minor amounts ranging between (0.08 and 086 mg kg^{-1}) in this study area.

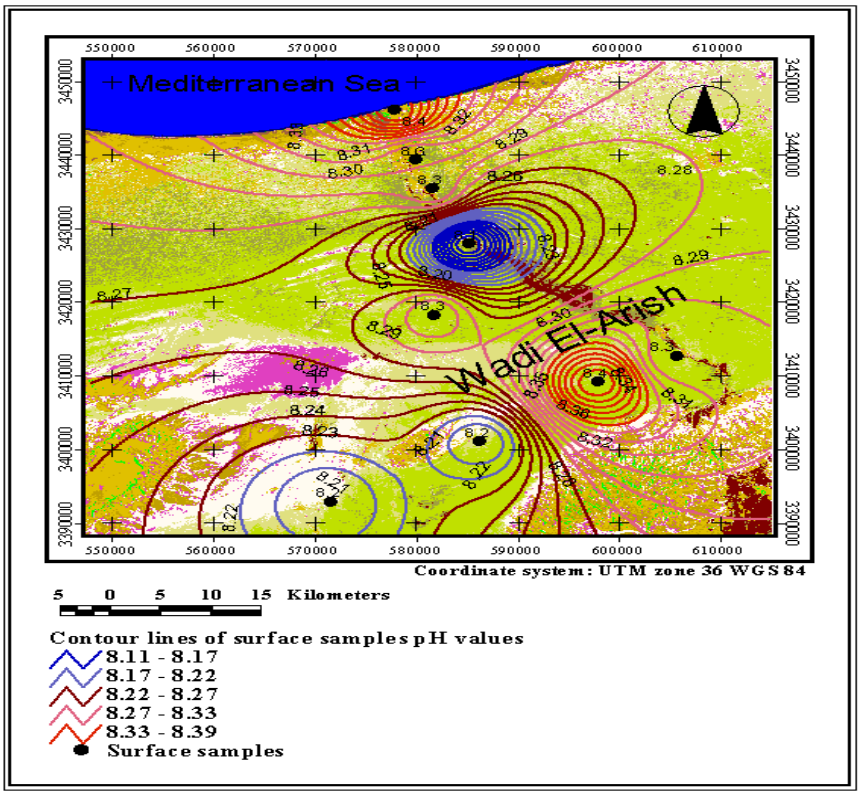

Fig. 4-43: Contour line image map of the soil reaction (pH) values in surface samples of the Wadi El-Arish area.

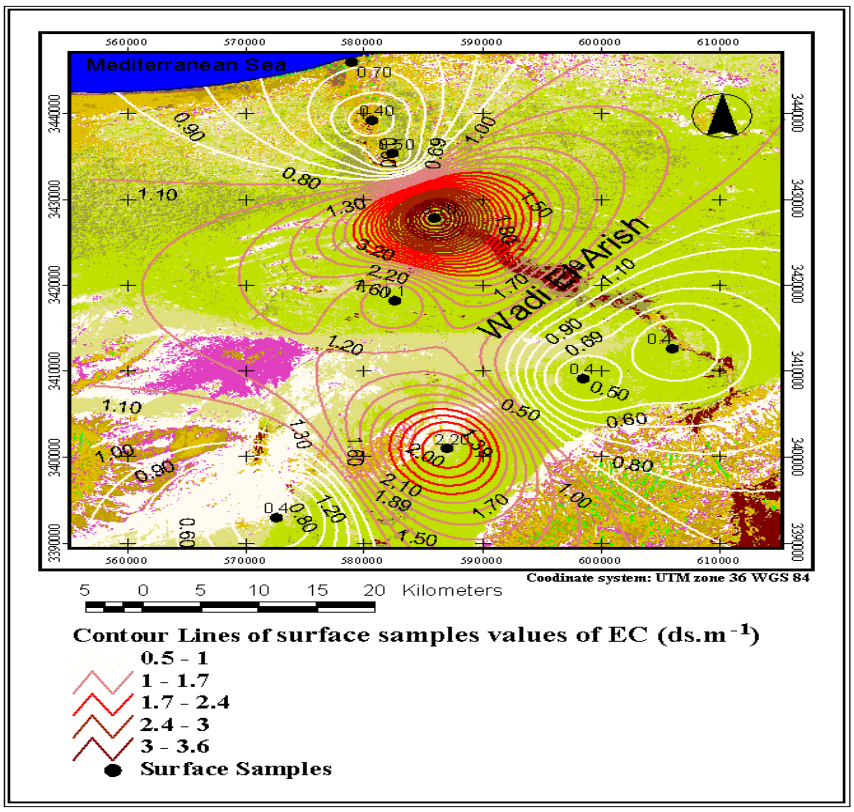

Fig. 4-44: Contour line image map of the electrical conductivity (EC) content in surface samples of the Wadi El-Arish area.

The particle size distribution in the soils of the Wadi El-Arish area are shown in table (4-5). The results reveal a very wide variation of texture classes in these soils. These classes are mainly sand, sandy loam, loam sand and loam in the soil samples of the Wadi El-Arish area.

The results of bulk density and hydraulic characteristics in the Wadi El-Arish soils are show in table (4-6). These data reveal the values of bulk density ranges from 1.37 to 1.85 g cm^{-3} in this area. The hydraulic conductivity values reveal that the soils are characterized by moderately to slowly movement of water within and through them. The values of soil permeability in this area range from 0.44 to 14.64 cm hr^{-1}. The available water values range from 0.07 to 0.13 cm^3 water cm^{-3} soil. The values of saturation in this soils range from 0.3 to 0.48 cm^3 water cm^{-3} soil. The saturation values influence the selection of suitable systems of irrigation and drainage in the Wadi El-Arish soils.

4.4 Remote sensing investigation of the study area

Remote sensing technique is one of the most important methods used for pedological (soils) studies, mapping and environmental study. In this part of the thesis, image data available and various techniques used for assessing the soil quality and survey in the study area are presented.

4.4.1 Pre-processing

Each generation of sensors shows improved data acquisition and image quality over previous generations. However, some anomalies still exist that are inherent to certain sensors and can be corrected by applying mathematical formulas derived from the distortions (LILLESAND and KIEFER 1997). In addition to this, the natural distortion that results from the curvature and rotation of the earth in relation to the sensor platform produces distortions in the image data which can also be corrected. Generally, there are three types of correction: radiometric, atmospheric and geometric corrections.

4.4.1.1 Radiometric, atmospheric and geometric corrections

Radiometric correction addresses variations in the pixel intensities that are not caused by the object or scene being scanned. These variations include differing sensitivities of the detectors,

topographic effects and atmospheric effects. While geometric correction addresses errors in the relative positions of pixels. These errors are induced by the sensor viewing geometry and terrain variations.

In the present study, the image data (the Landsat TM-5) were corrected atmospherically and geometrically. The radiometric correction is represented by atmospheric correction type. While the geometric correction is represented by terrain variation. This correction was explained in the procedure steps of correction in previous chapter of materials and methods. In addition to this, the Ground Control Points (GCP) was delivered in appendix (II). The effect of the atmosphere upon remotely sensed data are not considered as errors, since they are part of the signal received by the sensing device (BERNSTEIN 1983). However, it is often important to remove atmospheric effects, especially to change detection analysis.

In this study, the atmospheric correction was delivered with the six bands of the Landsat TM images data performed by the special program AtCProc version 2 (details by HILL 1993). The Landsat TM image after correction was showed in figure (4-45). In order to convert the digital data to 8 bit, a scaling factor was used. This range scaling factor was 283.33 for the image data covering the study area. The atmospheric correction processing of optical scanner image data steps was delivered in appendix (II).

4.4.1.2 Color composition image

The false color composition of the Landsat TM data is used for displaying the data in image files, since the data file values of an image file are related to the brightens values of false color display. The analyst can assign bands to be displayed with any of the three color guns: red, green and blue (R, G and B). the most useful color assignments are those that allow you to interpret the displayed image easily. For example, a natural color simulated image will approximate the colors that would appear to a human observer of the scene. While a color infrared simulated image shows the scene as it would appear in a color infrared film. This means that the color composite image produced from bands 3, 2 and 4 means that band 3 is assigned to red, band 2 is assigned to green and band 4 to blue. False color allows the analyst to view up to three bands of data at one times. Figure (4-46) is a color composite image

produced from bands 3, 2and 4 displayed in red, green and blue respectively for the study area in the north Sinai peninsula.

4.4.2 Image processing

4.4.2.1 Best three bands combination

The human eye employs only three primary colors at the same time, so that, the software programs used to read the images designed to read and display only three bands at the times, each band is represented by one of the primary color (red, green and blue). The TM images returns seven bands of data, so the question will be, how can we chose the most effective three-band color composite images? Trial and errors involves much effort and is times consuming because three bands can be selected from seven bands (the Landsat TM bands) in 35 ways and by knowing that any band can be assigned any color of the three primary colors, this gives a total of 210 different possible color presentation of the TM three-band images.

Using unnecessary bands can be needless or even lead to incorrect results. Extra number of bands may lead to decreasing the separability between some landcover. That happens when two land covers have different spectral signatures in some bands but are highly correlated in the other bands. This clearly appears on the classified image created by using the 7 TM bands. Using the best three-band combination instead of using all the seven TM bands can solve this problem (ABD EL-MONSEF 1996). The best three TM band combinations have the highest covariance among the 7 TM bands.

Two methods have been used in this study to select the optimum three-band combination. These methods were given by SHEFFIELD (1985) and CHAVEZ et al. (1984). Both methods revealed that TM band 2, TM band 3 and TM band 4 yield the best three band combinations in the area of study.

4.4.2.2 Principal component analysis (PCA)

The Landsat TM-5 data were transformed by principal components analysis (PCA) in order to determine their underlying dimensionality, i.e. to determine the number of PC that make up the

most informative combination giving maximum ground information. The images of PCA were displayed on high resolution monitor. The contribution of PC-transformation (PCA) in the best discrimination for soil surface was described (ABD EL-HADY 1992).

The eigenvalues in table (4-7) indicate that the TM data for the studied images along the El-Salam Canal area in the north Sinai have a two dimensional statistical structure in which almost 97% of the statistical variation are presented by the first PC. The contribution of bands in the formation of PC can be indicated by the eigenvector. The eigenvector was determined by the ERDAS program for the Landsat TM images (six bands without thermal band 6) in table (4-7). The first three PC elements are highly loaded image area by the three best combination bands. To remove any unnecessary data or noise PCA was applied to the images of the three best band combination. The image composed of the first three principal components has been subjected to unsupervised classification as shown in figure (4-47).

The image of the north Sinai district: table (4-7) shows that the first principal component (PC1) expected to be loaded with 79% of band 3, 48% of band 4 and 53% of band 5. The second principal component (PC2) is loaded with 77% of band 5, 44% of band 2 and 56% of band 1. The third principal component (PC3) is loaded with 69% of band 1, 33% of band 7 and 64% of band 5. The other principal components were expected to be loaded with a low data from different bands.

Table 4-7: Eigenvectors and eigenvalues of six bands from the Landsat TM images of the study areas.

Eigen-values						
Bands	**1**	**2**	**3**	**4**	**5**	**7**
Eigen-values	**24548**	**578**	**139**	**93**	**49**	**25**
% values	**97**	**1.2**	**1.0**	**0.3**	**0.2**	**0.17**
Eigen-vectors (matrix)						
PCs	**1**	**2**	**3**	**4**	**5**	**6**
Eigenvec. Band 1	**0.21**	**0.56**	**0.69**	**-0.43**	**-0.31**	**-0.11**
Eigenvec. Band 2	**0.35**	**0.44**	**-0.03**	**0.09**	**0.62**	**0.54**
Eigenvec. Band3	**0.79**	**-0.23**	**-0.29**	**0.23**	**0.15**	**-0.64**
Eigenvec. Band4	**0.48**	**-0.01**	**-0.23**	**0.33**	**-0.68**	**0.38**
Eigenvec. Band5	**0.53**	**0.77**	**0.64**	**0.23**	**0.18**	**-0.03**
Eigenvec. Band7	**0.41**	**0.35**	**-0.33**	**-0.69**	**0.05**	**0.07**

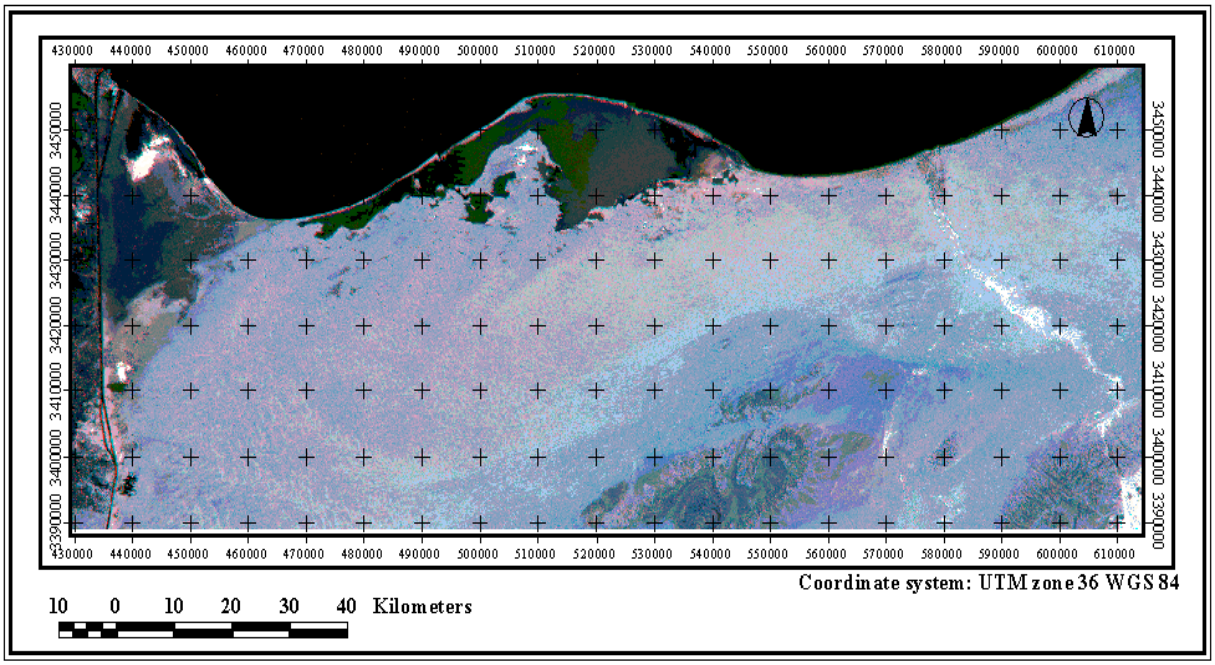

Fig. 4-45: The Landsat TM-5 image scene of the northern part of the Sinai peninsula (study area) after atmospheric correction using the AtCProc Ver.2 program.

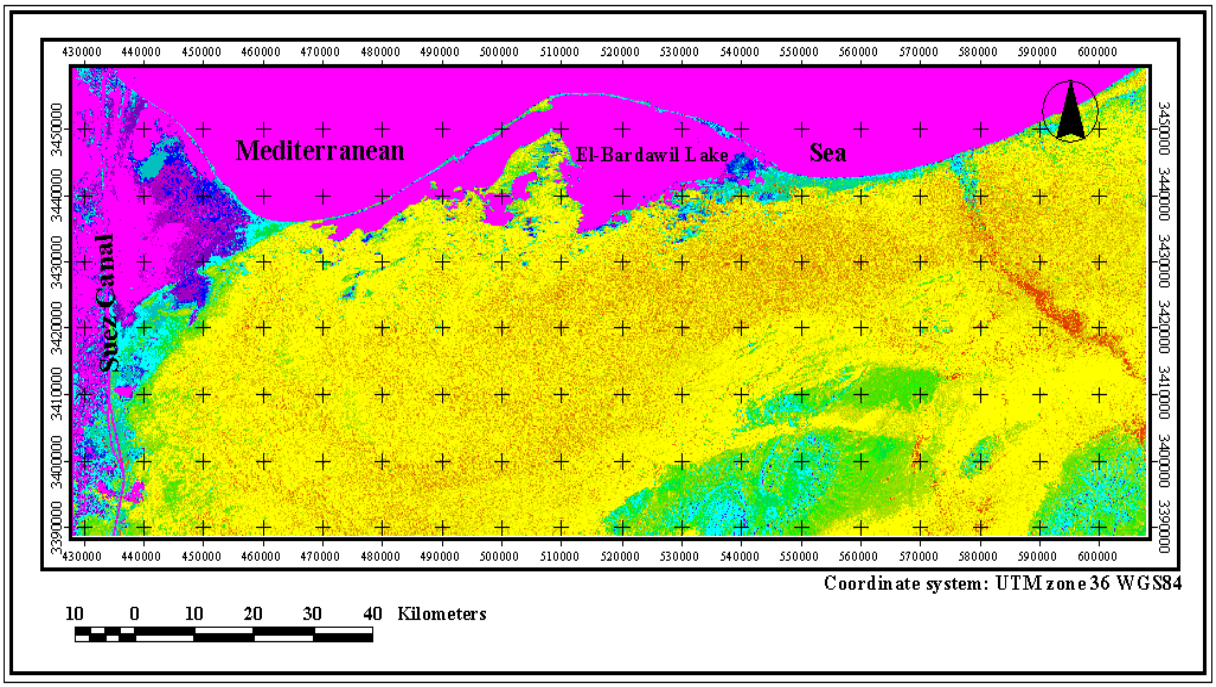

Fig. 4-46: The Landsat TM image false color covered the northern part of the Sinai peninsula.

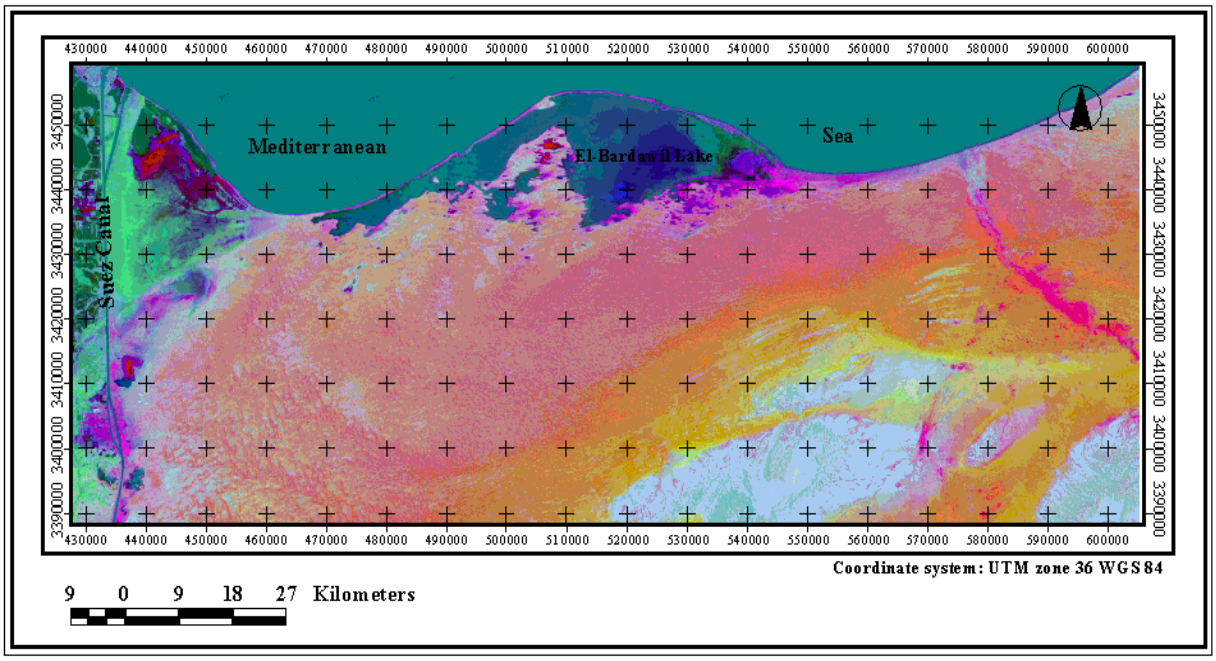

Fig. 4-47: The Landsat TM image composed of the first three principal component (PCs) of the study area.

4.4.2.3 Band ratio

Based on the spectral characteristics of the anions, cations and chemical analysis of the study soils that form the sedimentary rocks, three band ratios were chosen. The band ratios were selected: 5/7, 7/3 and 7/2 to discrimination of different soil types in the north Sinai area (figure 4-48).

Band ratio 5/7: band 7 has a strong absorption peak of CO_3^{--} (HUNT 1980), therefore reflectively of calcareous soils in the Wadi El-Arish is small. On the other hand, quartz as sand soils in the South El-Kantara Shark, the Rabaa and the Bair El-Abd has no characteristic spectral signature in this band. Calcareous soils could therefore be discriminated easily from sand soils which composed of 100 % quartz in band 7. Most of the sand soils found in the studied area have a different small percentage of clay fractions (as soils in the South El-Kantara Shark, the Rabaa and the Bair El-Abd areas), with the exception of the soils of the El-Tina Plain area. At band 5, no absorption peak of any major or minor minerals of the sedimentary rocks takes place. At band 5 the calcareous soils were more higher reflectively than clay and sand soils at band 5 (ASRAR 1989, BOWERS and HANKS 1965).

Band ratio 7/2: The high gypsum content (as soils in the El-Tina plain) has a distinct absorption peak at band 7 due to the presence of water molecules in its structure. The gypsum content is expected to be darker than any other soils units at band 7, (STONER and BAUMGRDNER 1980, MULDER and EPEMA 1986, CRIPPEN 1987). Also clay minerals and carbonate content have an absorption peak at band 7, but less stronger than that of gypsum content. Gypsum content reflects much more light than clay and carbonate content at band 2.

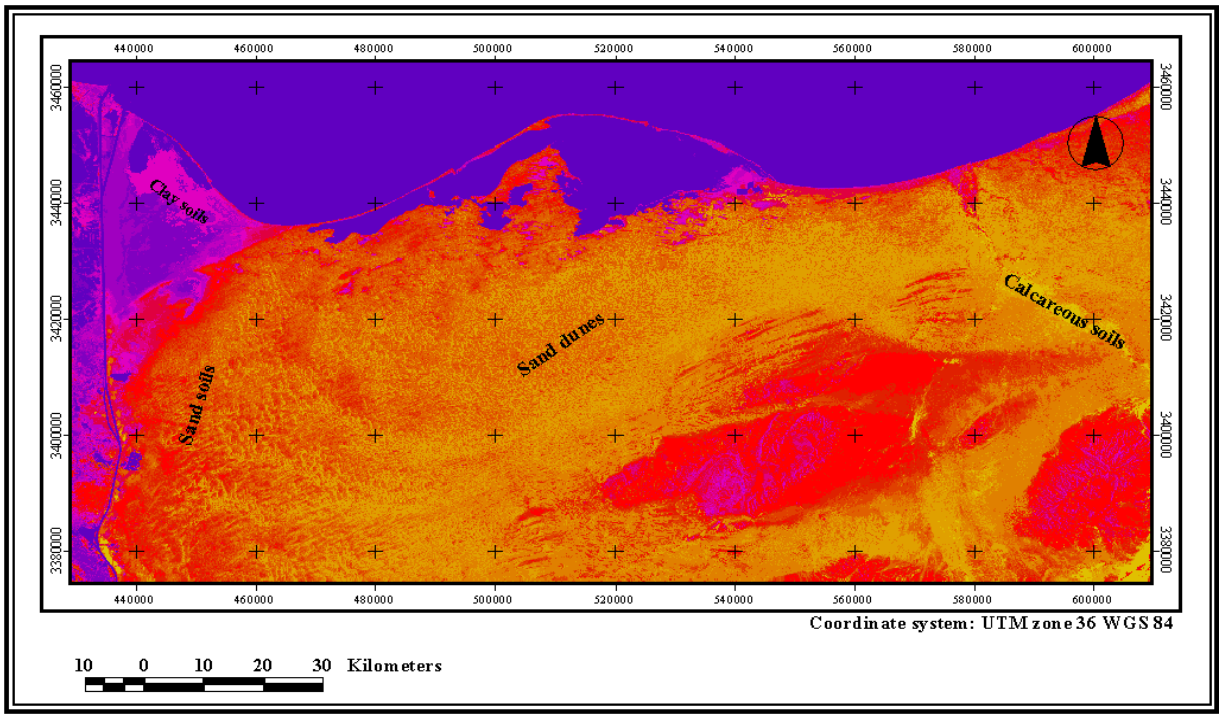

Fig. 4-48: The Landsat TM ratio band image map with PCs (5/7, 7/3 and 7/2) cover the northern part of the Sinai peninsula.

Band ratio 7/3: taking into consideration the strong absorption peak of clay minerals at 2.2 µm due to the presence of Al-OH in their structure (ASRAR 1989, NASA 1987), the ratio 7/3 is expected to be small for clay or clay deposit as the El-Tina plain soils. In this band ratio (7/3), clay soil deposits of the El-Tina plain appears to be darker than other sand soil sediments.

4.4.2.4 Supervised classification of images in the study area

Generally, the supervised classification classes of the northern part of the Sinai peninsula along the El-Salam Canal soils project are 19 classes in figure (4-49). This classes were separated and identified into different forms of landscapes ranging from deep to shallow water, salt crust to swamps, sand to clay texture, very fine sand dunes to coarse grain size and saline alkaline to

calcareous soils. The project area of the El-Salam Canal and type of canal planning were delivered in the satellite image classification by the maximum likelihood algorithm method provided by the ERDAS Imagine program version 8.3.1 and the mapping plan of the TM images by Arc View version 3.2a.

- **Supervised classification of the El-Tina Plain area**

Supervised classification image was performed by using different band combinations. Among the different tested images of the El-Tina Plain studied image, the composite image of the following band combination proved to be the best: a) Image of the 6 TM bands. b) Image of the best band combination are band 4, 5 and 7 (R, G and B). Defining the number of classes inherited within the image is the first step, and perhaps the most important step, in image classification. Depending on field work, previous studies and the enhanced images resulted during this study, 16 classes (figure 4-50) were defined for the El-Tina Plain area.

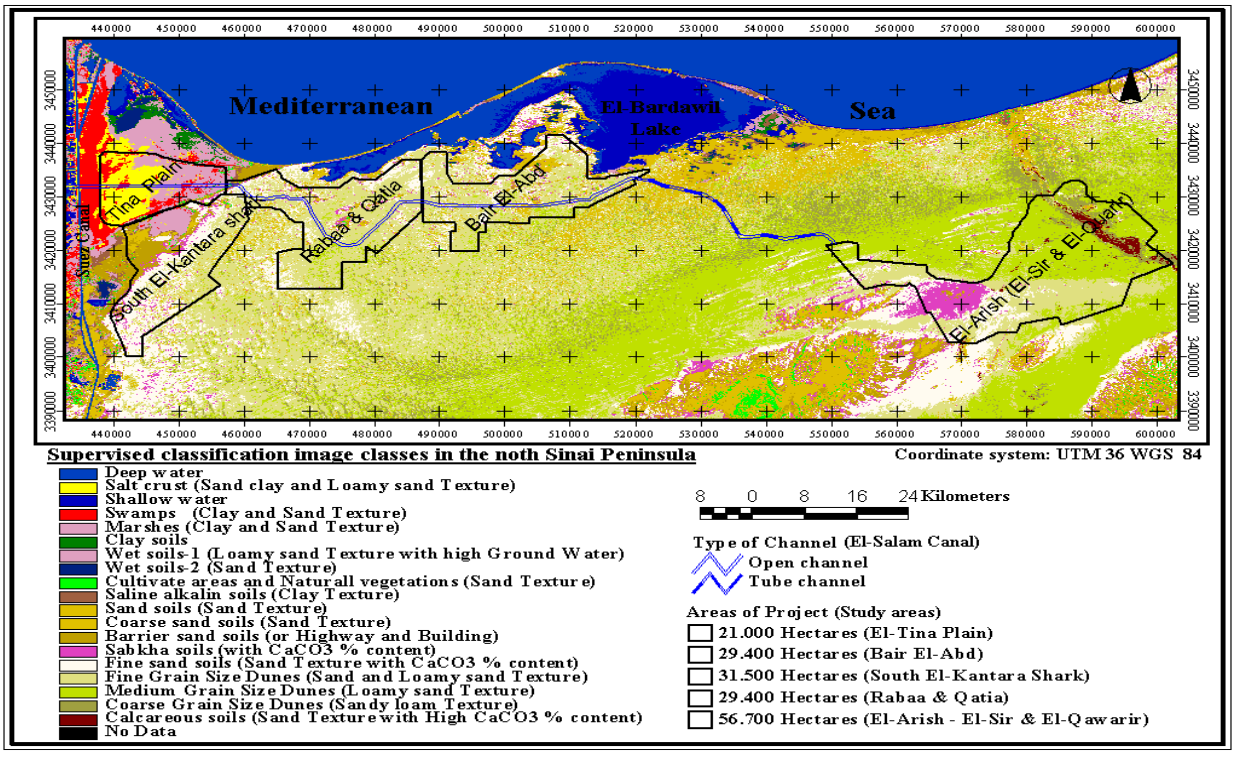

Fig. 4-49: Supervised classification of the Landsat TM image in the study area showing the classes, El-Salam Canal project areas in the north Sinai.

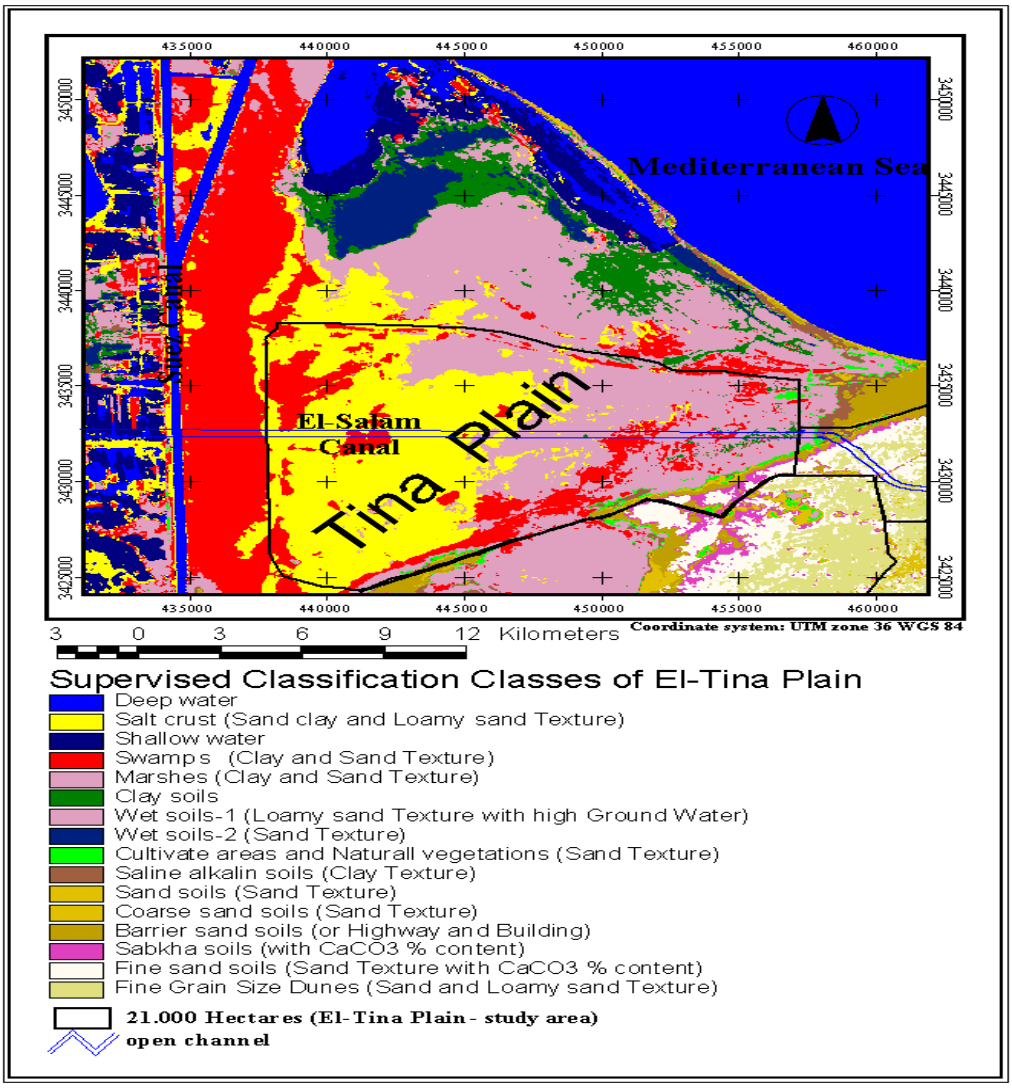

Fig. 4-50: Image of supervised classification classes in the El-Tina Plain area (bands 4, 5 and 7).

The classes are: deep water (class 1), salt crust on the surface soils and soil textures are ranges between sandy clay and loamy (class 2), shallow water, swamps and marshes (class 3 through 5) and clay soil (class 6). Classification of wet soils and cultivate areas into the three classes is mainly based on the differences in the water and vegetation content of soils. Class 10 is saline alkaline soils, these soils have a clay texture, while classes from 11 to 13 are sand soils, that differ in grain size of sand fraction. The Sabkha form with relatively high of $CaCO_3$ content is in class 14. The another two classes are sand dunes defined in class 15 and 16, that classes differences in particle size grains from mechanical analysis.

- **Supervised classification of the South El-Kantara Shark area**

Sixteen classes were recognized and identified in the South El-Kantara Shark area during field work survey and from enhanced process of the Landsat TM image in this area. These classes are:

Class 1 Deep water (Suez Canal branch)
Class 2 Salt crust (extension of salt crust of El-Tina Plain)
Class 3 Shallow water (few patches)
Class 4 Swamps (sand texture)
Class 5 Marshes (sand texture)
Class 6 Wet soil (sand texture with high ground water)
Class 7 Cultivate areas and Palm tree (sand texture)
Class 8 Saline alkaline soils (clay texture)
Class 9 Fine sand soils
Class 10 Coarse sand soils
Class 11 Barrier sand soils
Class 12 Sabkha with $CaCO_3$ content
Class 13 Fine sand soils (sand texture with $CaCO_3$ content)
Class 14 Fine sand dunes (sand texture)
Class 15 Medium sand dunes (sand texture)
Class 16 Coarse sand dunes (sand texture)

These classes are shown in figure (4-51) by using the maximum likelihood classification algorithm method. This classification was executed by using best three bands combination (4, 5 and 3 bands) of the Landsat TM-5 image bands for the South El-Kantara Shark image.

- **Supervised classification of the Rabaa and Qatia areas**

As a result of field work, previous studies and the enhanced Landsat TM images in the Rabaa and Qatia area, 15 classes were recognized and defined for these image in this studied area. These classes are: class 1 is deep water of the Mediterranean sea and the El-Bardawil lake, while class 2 represents mainly shallow water in the El-Bardawil lake. Classes 3 through 5 were marshes with a sand soil texture and wet soils with different content of water and a

relatively high ground water table. Class 6 revealed small special farms, Palm trees and natural vegetations (shrubs). Class 7 show the soils effected by high content of alkaline saline salts (saline alkaline soils), while classes 8, 9 and 10 indicated fine, coarse and barrier sand soils. Class 11 consisted mainly of a small Sabkha with relatively high $CaCO_3$ content (near to the sea beach). The classification of sand dunes into the three classes is mainly based on the differences grain size particles of the study soils (fine, medium and coarse sand dune textures) from mechanical analysis. These image classes were class 12, 13 and 14 in the Rabaa and Qatia image, respectively. These classes are shown in figure (4-52) by using the maximum likelihood classification algorithm method and three band combination (4, 5 and 3 bands) for the Rabaa and Qatia image.

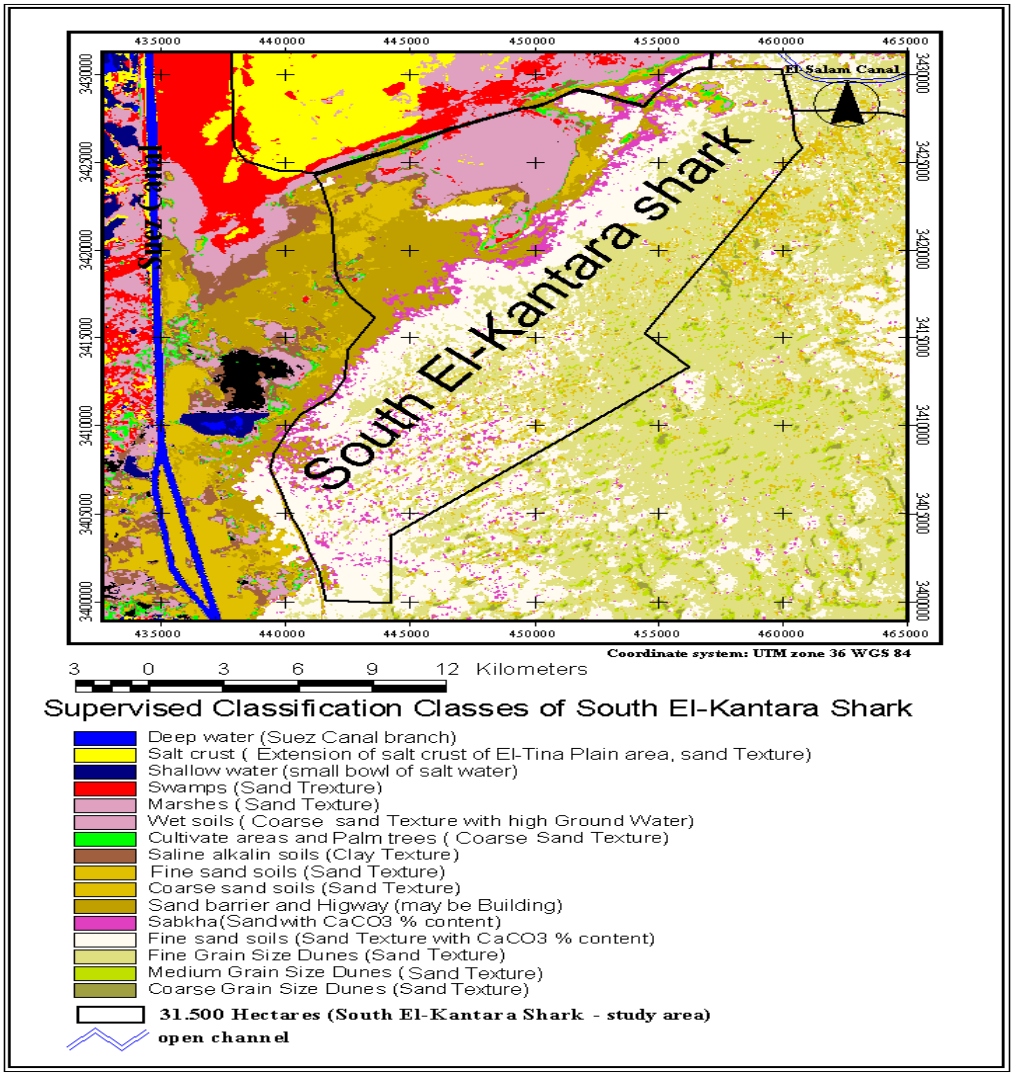

Fig. 4-51: Image of supervised classification classes in the South El-Kantara Shark area (bands 4, 5 and 3).

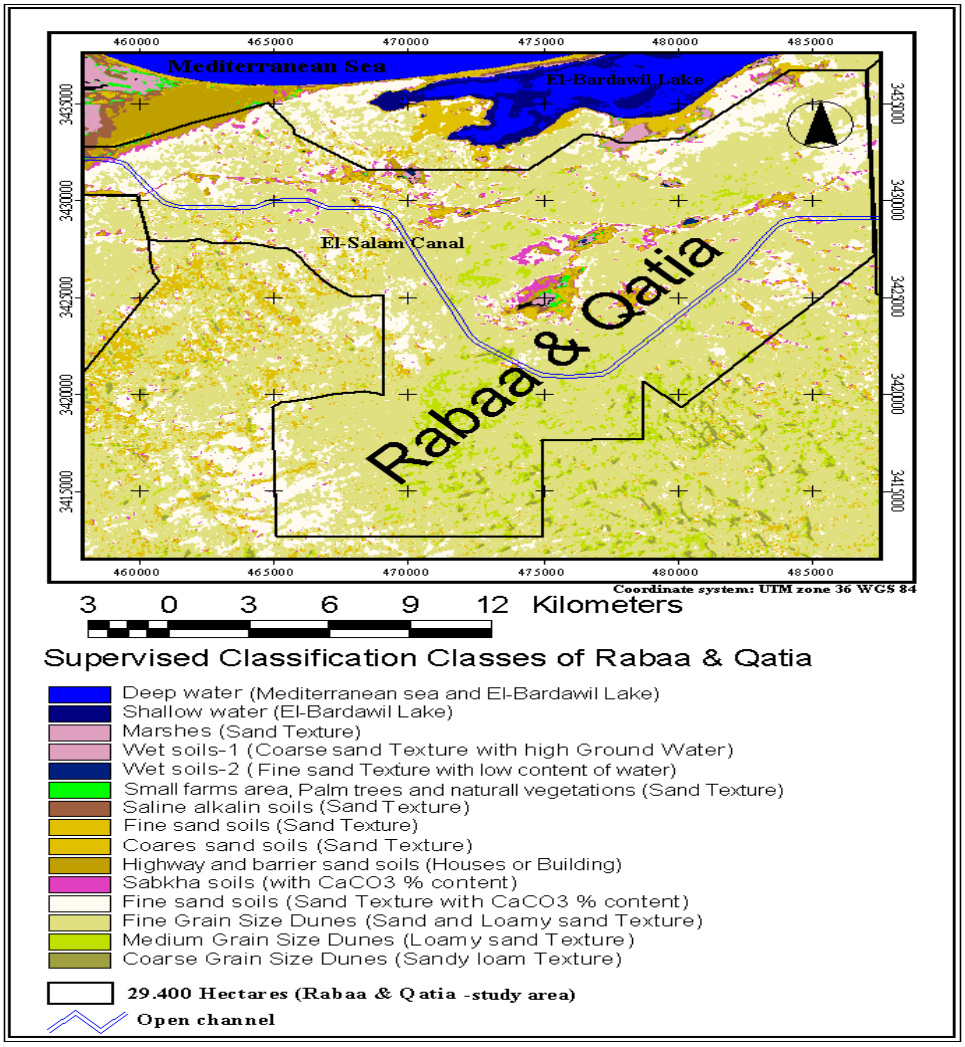

Fig. 4-52: Image of supervised classification classes in the Rabaa and Qatia areas (bands 4, 5 and 3).

- **Supervised classification of the Bair El-Abd area**

The supervised classification process, visual analysis in the Landsat TM image and field work survey with collected samples separates and identifies 15 deferent classes in the Bair El-Abd image area. These classes are:

Class 1 Deep water (the Mediterranean sea and the El-Bardawil lake)

Class 2 Shallow water (the El-Bardawil lake and small bowls)

Class 3 Marshes (sand texture)

Class 4 Wet soils-1 (sand texture with high content of water)

Class 5 Wet soils-2 (sand texture with low content of water)

Class 6 Natural vegetations and small cultivated areas (special farms)

Class 7 Saline alkaline soils (sand texture)

Class 8 Sand soils (sand texture)

Class 9 Coarse sand soils (sand texture)

Class 10 Barrier sand soils and/or highway (building)

Class 11 Flat Sabkha (with low $CaCO_3$ content)

Class 12 Fine sand soils (sand texture with low $CaCO_3$ content)

Class 13 Fine sand dunes (sand texture)

Class 14 Medium sand dunes (sand texture)

Class 15 Coarse sand dunes (sand texture)

The supervised classification classes of the Bair El-Abd image area were achieved by using the maximum likelihood classification algorithm method. This classification was executed by using three bands combination (3, 5 and 7 bands) of the Landsat TM-5 image for the Bair El-Abd area as shown in figure (4-53).

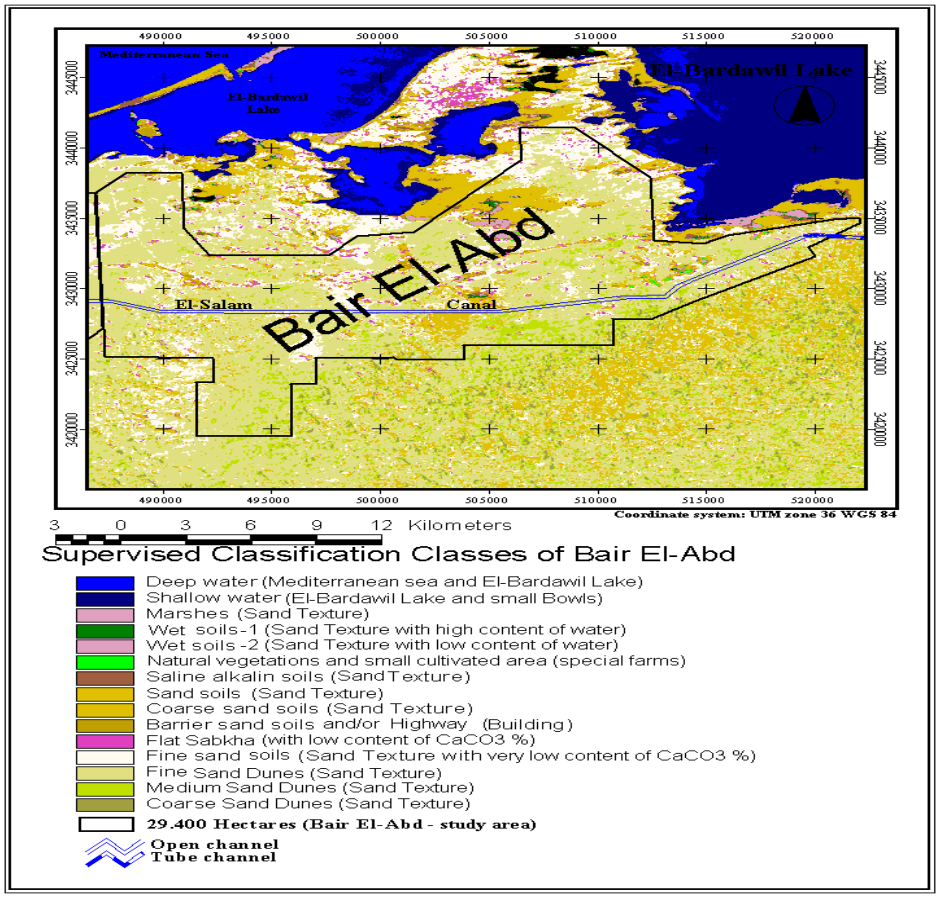

Fig. 4-53: Image of supervised classification classes in the Bair El-Abd area (bands 3, 5 and 7).

- **Supervised classification of the Wadi El-Arish area**

By using the Landsat TM image analysis, the field soil survey works and previous literatures were recognized and defined about fifteen classes from supervised classification image process in the Wadi El-Arish image area. These classes are:

Class 1 Deep water (the Mediterranean sea)
Class 2 Shallow water (coastal of the Mediterranean sea)
Class 3 Wet soils-1 (loam texture with high content of $CaCO_3$ and water)
Class 4 Wet soils-2 (sand texture with low content of $CaCO_3$ and water)
Class 5 Palm, fruit trees and natural vegetation (special farms)
Class 6 Saline soils (sandy loam texture)
Class 7 Sand soils (sand texture)
Class 8 Coarse sand soils (loamy sand texture)
Class 9 Barrier coarse sand (hill) and/or building (city of El-Arish)
Class 10 Gravely sand and highway (sand texture, high $CaCO_3$ content)
Class 11 Fine sand soils (loam texture with high content of $CaCO_3$)
Class 10 Gravely sand and highway (sand texture, high $CaCO_3$ content)
Class 11 Fine sand soils (loam texture with high content of $CaCO_3$)
Class 12 Fine sand dunes (sand texture with low content of $CaCO_3$)
Class 13 Medium sand dunes (loamy sand and sandy loam texture)
Class 14 Coarse sand dunes (sand texture)
Class 15 Calcareous soils (sandy loam texture, very high of $CaCO_3$ %)

The supervised classification classes in figure (4-54) were preformed by using different band combination of the Wadi El-Arish image bands. The composite image bands of the best combination are band 4, 5 and 7 (R, G and B). This classification was achieved by using the maximum likelihood classification algorithm method in the Imagine ERDAS 8.3.1 program.

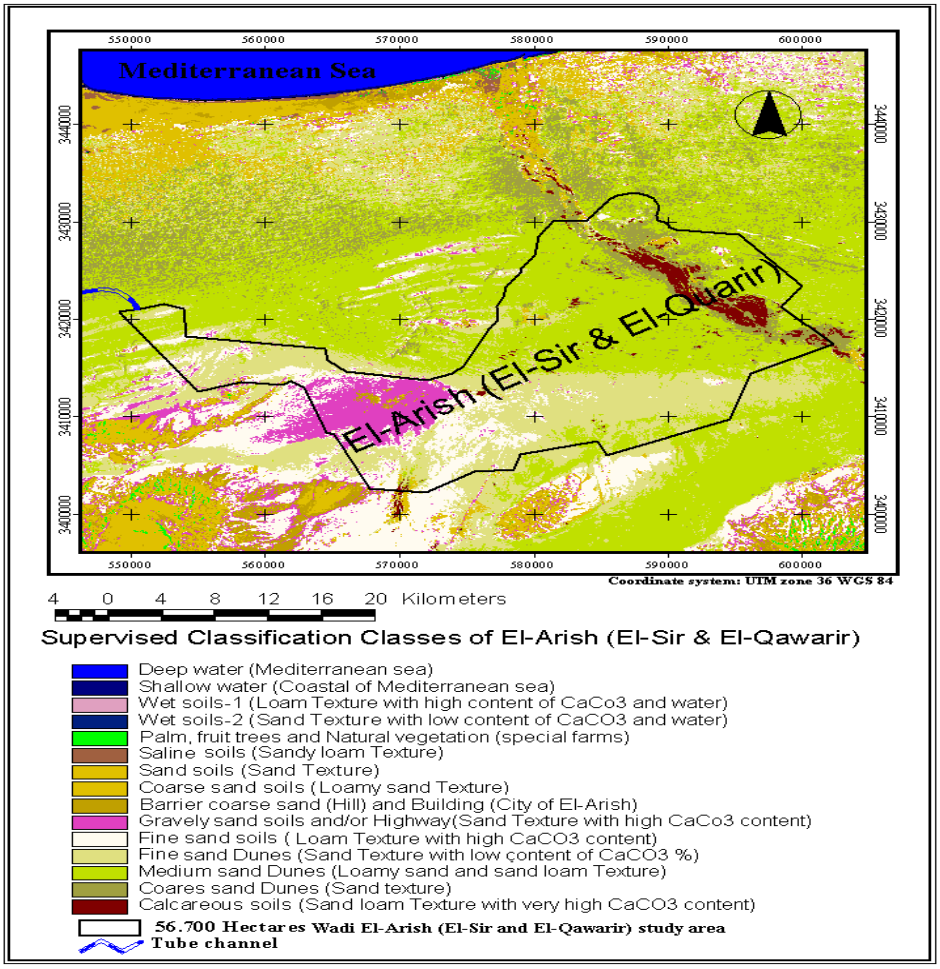

Fig. 4-54: Image of supervised classification classes in the Wadi El-Arish area (bands 4, 5 and 7).

4.4.3 Statistical correlation between TM Bands and soil characteristics

The statistical analysis was achieved by using the SPSS and SAS programs to study the correlation between the soil characteristics and the Landsat TM bands data in the soils of northern part of the Sinai peninsula along the El-Salam Canal project area.

The multivariate statistics used in differentiating between the study soil samples and the Landsat TM bands are given in tables (4-8) and (4-9), that show the data of the Landsat TM bands have correlation and regression with soil characteristics in the study soil samples. The correlation and regression statistical analysis were performed between six bands (1, 2, 3, 4, 5 and 7) of the Landsat TM bands and soil properties of EC, CEC, pH, $CaCO_3$, Gypsum, sand, silt and clay. This statistical analysis were achieved by SPSS and SAS statistical programs.

Table (4-8) shows results from a correlation analysis for selection of the combination of the TM bands for predicting selected soil variables. In general, the ability to predict each soil variable increased as additional bands were added. More correlation coefficients results are delivered in appendix (III).

The results of correlation analysis in table (4-8) reveal good correlation between the Landsat TM bands and soil characteristics. The correlation coefficient between EC, CEC, $CaCO_3$, Gypsum values and the TM bands were the key bands 3 and 4, the high accounting were 70%, 54%, 25% and 79%, respectively. While bands 1 and 5 were the key bands for organic matter values (78% and 58%). Also, bands 7 and 4 were the key bands for pH values, the high accounting was (55%). While bands 4 and 5 were the key bands for sand, silt and clay values, the high accounting were 51%, 29% and 59%, respectively.

Table (4-9) illustrated results from a stepwise regression analysis for selection of the best combination of the Landsat TM bands for predicting selected soil variables. By computing all the possible linear regression equations and considering the amount of variability explained and the biases of the resulting equation, the best subset of spectral bands was selected from the many linear regression figures. All portions of the electromagnetic spectrum of the TM data used appear to be significant in explaining variation in the soil characteristic variables. The regression statistic analysis are delivered in appendix (III).

The linear regressions between the TM bands and soil properties indicated high values and content of the EC, CEC, gypsum, silt and clay reduced reflectance intensity in appendix (III) figures (1 to 5). Meanwhile, the organic matter, $CaCO_3$, sand and pH values revealed that the low content or values of these soil properties reduced reflectance intensity in appendix (III), figures (6 to 9), respectively. The high significance of the R^2 in figure (4-55) was calculated from regression equations between the TM bands and some of the soil properties.

For electrical conductivity (EC) values the green, red, near infrared and middle infrared bands were the key bands, the high accounting for 49.3% of the variability in band 4. The spectral bands found to be most important for explaining variation in CEC concentration values were the band 2, band 3 and band 4, the best spectral accounting for 29.3% of the variability with

near infrared band. The variability in gypsum content was explained using bands from the green, near infrared and middle infrared portions of the spectrum, the high accounting in near infrared for 62.3% of the variability. The most important bands for explaining variation in silt and clay content were the green, red, near infrared and middle infrared bands of the spectrum, the highest values for 11 and 35% of the variability with near infrared band.

Table 4-8: Significant correlation coefficients between the Landsat TM bands and soil characteristics in the surveyed areas.

Band No.	EC (ds m^{-1})	CEC (meq $100g^{-1}$ soil)	pH $_{H2O}$	pH $_{CaCl2}$	$CaCO_3$ %	Gypsum %	OM %	Sand %	Silt %	Clay %
Band 1	-0.50	-0.30	0.28	0.01	0.10	-0.52	0.78	0.40	-0.28	-0.44
Band 2	-0.61	-0.44	0.40	0.02	0.20	-0.68	0.41	0.45	-0.27	-0.51
Band 3	-0.66	-0.50	0.45	0.04	0.24	-0.73	0.27	0.47	-0.26	-0.55
Band 4	-0.70	-0.54	0.49	0.02	0.25	-0.79	0.25	0.51	-0.29	-0.59
Band 5	-0.62	-0.42	0.52	0.10	0.16	-0.71	0.58	0.49	-0.28	-0.57
Band 7	-0.61	-0.44	0.55	0.11	0.23	-0.71	0.30	0.44	-0.23	-0.52

Table 4-9: Regression coefficient of (b) and beta of selected soil properties for assessing optimal of the Landsat TM bands.

b

Band No.	EC ds m^{-1}	CEC meq $100g^{-1}$ soil	$CaCO_3$ %	Gypsum %	PH $CaCl_2$	PH H_2O	Total Sand %	Total Clay %	R	R^2
Band 1	0.078	0.101	-0.065	-0.850	-11.700	-1.596	-0.338	-0.771	0.584	0.342
Band 2	0.045	0.143	0.307	-1.136	-22.187	1.603	-0.484	-1.083	0.741	0.549
Band 3	0.040	0.215	0.532	-1.315	-32.416	5.281	-0.681	-1.500	0.817	0.668
Band 4	0.071	0.133	0.404	-1.324	-30.499	4.081	-0.685	-1.464	0.875	0.766
Band 5	0.105	0.334	0.412	-1.165	-35.121	9.538	-0.778	-1.718	0.854	0.729
Band 7	0.093	0.345	0.630	-1.220	-36.353	13.594	-0.684	-1.498	0.852	0.726

Beta

Band No.	EC ds m^{-1}	CEC meq $100g^{-1}$ soil	$CaCO_3$ %	Gypsum %	PH $CaCl_2$	PH H_2O	Total Sand %	Total Clay %
Band 1	0.165	0.129	-0.035	-0.536	-0.182	-0.062	-0.653	-1.039
Band 2	0.071	0.136	0.123	-0.534	-0.256	0.046	-0.698	-1.088
Band 3	0.052	0.169	0.177	-0.511	-0.310	0.126	-0.812	-1.247
Band 4	0.104	0.118	0.152	-0.580	-0.329	0.110	-0.922	-1.374
Band 5	0.154	0.298	0.155	-0.511	-0.379	0.257	-1.047	-1.613
Band 7	0.128	0.288	0.222	-0.502	-0.368	0.344	-0.863	-1.317

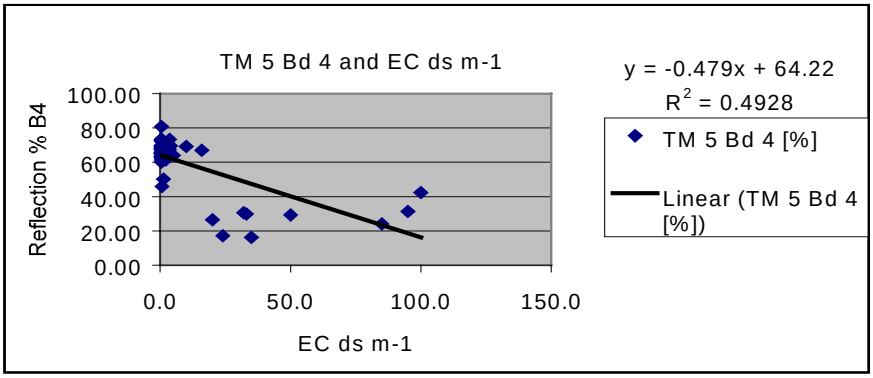

(a)

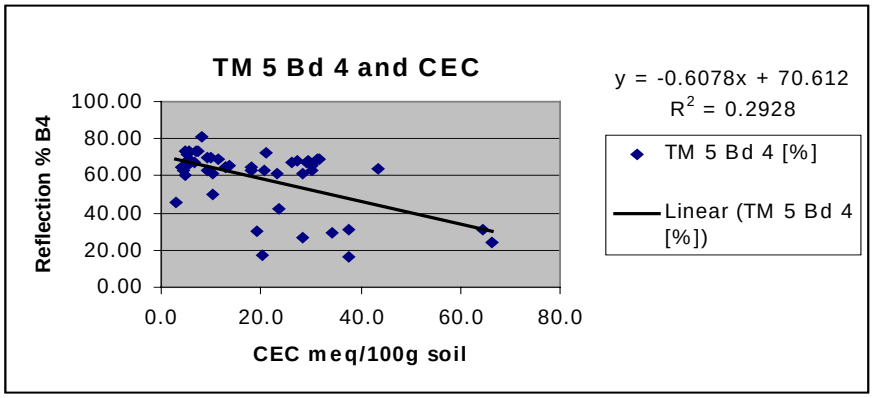

(b)

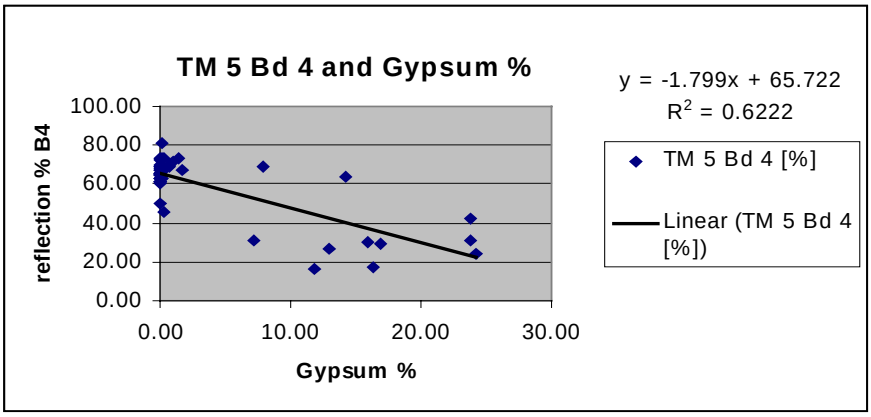

(c)

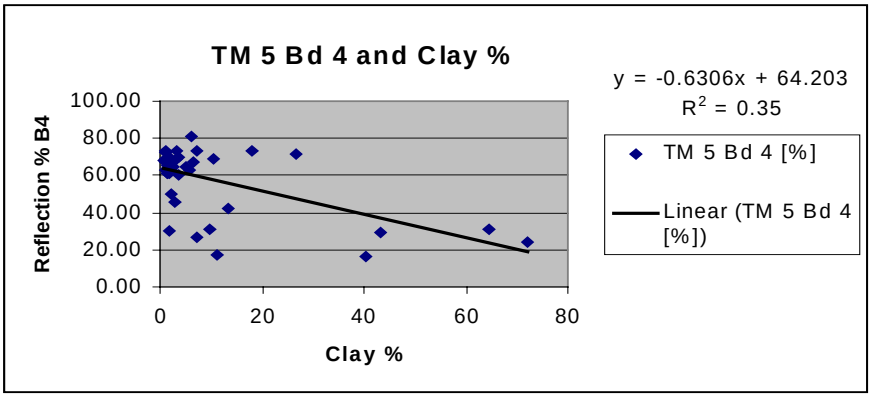

(d)

Fig. 4-55: Regression between the Landsat TM bands and some soil properties.

The variability in organic matter content was also best explained using bands from the red, near infrared and middle infrared portions of the spectrum, high accounting for 11.8% of the variability. For the $CaCO_3$ content the red, near infrared and middle infrared bands were the key bands, accounting for 6.4% of the variability. The spectral bands found to be most important for explaining variation in sand content were the red, near infrared and middle infrared, the highest accounting for 26.9% of the variability in band 4 (near infrared spectrum). The pH value was explained by bands from the red, near infrared and middle infrared portions of the spectrum, the high value for 31.6% of the variability with band 5 (middle infrared).

4.5 Evaluation of soils in the study area

From the agriculture point of view, soils of the studied areas are considered as virgin soils. Evaluating their capability is an essential stage for future practical use. In this respect many systems have been suggested to evaluate the agricultural limitations affecting land capability under the prevailing conditions. All systems aim at gaining better knowledge and understanding of the soil properties and defining limitations affecting their agricultural potentialities.

The main characteristics, which are considered limiting factors for irrigation and land use evaluation are:

A- Availability and quality of irrigation water
B- Texture class
C- Soil profile depth
D- Wetness (drainage conditions)
E- Salinity level
F- Sodicity (ESP)
G- Calcium carbonate content %
H- Gypsum content %
I- Slope % and
J- Erosion.

Land capability index was calculated (SYS, 1991) for each soil samples and consequently the land was placed in a certain capability class. The capability index (CI) would be equal to :

CI = A/100 x B/00 x C/100 x D/100 x E/100 x F/100 x G/100 x 11/100 x 1/100 x J/100 x 100

4.5.1 Soil properties evaluated

Application of the capability index for the investigated soils is presented in table (4-10). The data reveal that the studied soil samples are placed between III and VI grades, their description is as follows:

- **Grade III soils**

The soils belonging to grade III (fair soils) have the rate between 47.45 to 40.04 % in study area and which are represented by samples numbers in:

- The South El-Kantara Shark surface and profile samples No. 1, 2, 3, 4, 5, 8 and 9 (El-Amal village)
- The Rabaa and Qatia surface and profile samples No. 21, 22, 26 (Rabaa), 23 (El-Ahrar) and 27 (El-Nigila)
- The Biar El-Abd surface and profile samples No. 30, 37 (El-Kherba), 32 (El-Sadat), 33 (El-Arawa), 34 (El-Telol) and 38 (Biar El-Abd)
- The Wadi El-Arish surface and profile samples No. 40 (Abou Awaigila), 41 (El-Garkada), 42 (Gabal Libina), 45 and 47 (basin of Wadi El-Arish).

- **Grade IV soils**

The soils belonging to grade IV (poor soils) have the rate between 37.44 to 22.79 % in investigation area and which includes samples numbers in:

- The South El-Kantara Shark surface samples No. 6 and 7 (El-Amal).
- The Rabaa and Qatia surface and profile samples No. 19, 20 (Qatia), 24 (Rummana), 25 (El-Ganien), 28 (El-Ahrar) and 29 (Rabaa).
- The Biar El-Abd surface and profile samples No. 31 (El-Sadat), 35 (El-Telol) and 37 (Biar El-Abd)
- The Wadi El-Arish surface samples No. 43 (Bagdad) and 44 (El-Arish).

- **Grade V soils**

The soils belonging to grade V (very poor soils) are those having the rate between 10.04 to 18.53 % in the study area and which are represented by samples numbers in:

- The El-Tina Plain surface and profile samples numbers from 10 to 16 (El-Tina Plain)
- The Wadi El-Arish surface and profile samples numbers 39, 46 (Biar Lehfen), (El-Ressan) respectively.

- **Grade VI soils**

The soils belonging to grade VI (non agriculture soils) are those having the rate between 8 to 9.9 % in the El-Tina Plain area and which are represented by profile samples No. 17 and 18.

4.5.2 Evaluation using polygon layers of the Landsat TM image data

Using Arc/View 3.2a GIS software, the ten parameters used in Sys's equation and listed results in table (4-10) have been contoured to construct ten line Arc/View layers. This layers have been converted to polygon layers (figures 4-56 through 4-63). Calcium carbonate content and the availability and quality of irrigation parameters are not contoured due to the fact that they are equal all over the study area. Thus all the layers have been integrated into one layer. The integrated layer is used to classify or rate the soil evaluation in the study area into four categories (figure 4-64) based on the classification criteria given by STORIES (1964).

The legend of different polygon layers represent the percent of the soil characteristics values (calculate by equation) according to STORIES (1964) and MANSSOUR (1979) level of the evaluation classes, that were showed in previous table (3-5) in material and methods chapter.

All study areas were evaluated by using six bands from the Landsat TM image data except the Wadi El-Arish area. This area is such that the numbers of the collected samples were not sufficient to perform the integrated polygon layer of soil evaluation by the mentioned method, but that was evaluated by calculation equation (this soil lies in III, IV and V grades). The small number of the collected samples may be referred to the difficult topographical conditions in the Wadi El-Arish area. One of the sub-aims of this work was to use the least numbers of the soil samples to carry out the image classification, land evaluation and reduction of times and filed work in the soil survey project. This target was achieved for all studied area except that of the Wadi El-Arish due to its very large scale area (57.700 ha).

Table 4-10: Capability Index for rating of the studied soil samples in the northern part of Sinai Peninsula.

Location	Surface sample No	Profile sample No.	AWI (A)	Texture (B)	Soil Profile depth (C)	Gypsum % (D)	Slope % (E)	Drainage Condition (F)	EC dsm^{-1} (G)	ESP (H)	$CaCO_3$ % (I)	E (J)	CI (IC)	Grade	Describe of Grade
S.K.S*	1		90	65.5	100	95	100	100	100	84.7	100	100	47.5	III	FS
S.K.S	2		90	51.4	100	95	92.5	100	100	100	100	100	40.6	III	FS
S.K.S	3		90	57.0	100	95	100	100	100	85	100	100	41.4	III	FS
S.K.S	4		90	65.5	100	95	100	100	100	94.8	100	100	53.1	III	FS
S.K.S	5		90	60.9	85	95	87.5	100	100	100	100	100	41.2	III	FS
S.K.S	6		90	66.2	100	95	100	100	100	100	100	100	32.1	IV	PS
S.K.S	7		90	82.0	95	95	100	95	45	80	100	100	22.8	IV	PS
S.K.S		8	90	48.3	100	95	100	100	100	100	100	100	41.3	III	FS
S.K.S		9	90	61.0	100	95	92.5	100	100	83	100	100	40.0	III	FS
TP	10		90	88.3	100	95	100	100	43.1	54.9	100	100	17.9	V	VPS
TP	11		90	95.5	100	75	100	95	41.6	51.5	100	100	13.1	V	VPS
TP	12		90	92.3	95	75	100	95	37.1	51.2	100	100	10.7	V	VPS
TP	13		90	90.8	95	75	100	100	38.1	51.2	100	95	10.8	V	VPS
TP	14		90	67.5	100	95	95	75	44.6	63.9	100	100	11.7	V	VPS
TP	15		90	67.0	95	75	100	85	43.3	63	100	100	10.0	V	VPS
TP	16		90	82.5	100	100	100	95	43.4	53.9	100	95	15.7	V	VPS
TP		17	90	81.0	95	75	100	75	44	61	100	95	9.9	VI	NAS
TP		18	90	81.0	100	75	100	85	36.6	51.7	100	100	8.8	VI	NAS
Qatia	19		90	56.5	100	95	92.5	100	100	82.2	100	95	34.9	IV	PS
Qatia	20		90	54.9	100	95	100	95	95	81.1	100	100	34.4	IV	PS
Rabaa	21		90	59.0	100	95	100	100	100	100	100	100	50.5	III	FS
Rabaa	22		90	62.3	95	95	92.5	100	100	100	100	100	46.8	III	FS
El-Ahrar	23		90	58.7	100	95	92.5	95	100	100	100	95	41.9	III	FS
Rumana	24		90	60.3	95	95	100	100	65	100	100	100	31.8	IV	PS
El-Ganien	25		90	58.2	100	95	87.5	100	100	94.9	100	95	39.3	IV	PS
Rabaa	26		90	59.9	100	95	100	100	100	100	100	100	51.2	III	FS
El-Nigila	27		90	60.1	100	95	87.5	100	100	100	100	100	44.9	III	FS
El-Ahrar		28	90	59.0	85	95	87.5	85	93	91	100	100	26.9	IV	PS
Rabaa		29	90	54.9	100	95	77.5	100	100	100	100	95	34.5	IV	PS

S.K.S*= South El-Kantara Shark **TP= El-Tina Plian** **FS= Fair soils** **PS= Poor soils**
VPS= Very poor soils **NAS= Non agriculture** **AWI= Availability water irrigation**
CI= Capability Index **E= Erosion**

Con. table 4-10: Capability Index for rating of the studied soil samples in the northern part of Sinai Peninsula.

Location	Surface sample No	Profile sample No.	AWI (A)	Texture (B)	Soil Profile depth (C)	Gypsum % (D)	Slope % (E)	Drainage Condition (F)	EC Dsm^{-1} (G)	ESP (H)	$CaCO_3$ % (I)	E (J)	CI (IC)	Grade	Describe of Grade
El-Kherba	30		90	60.3	100	95	95	100	100	100	100	95	46.5	III	FS
El-Sadat	31		90	59.5	100	95	87.5	100	100	80.5	100	95	34.0	IV	PS
El-Sadat	32		90	57.8	100	95	100	100	100	100	100	95	46.9	III	FS
El-Arawa	33		90	52.9	95	95	100	100	100	100	100	100	43.0	III	FS
El-Telol	34		90	52.8	95	95	95	100	100	100	100	100	40.7	III	FS
El-Telol	35		90	64.6	100	100	95	100	70	85	100	100	32.8	IV	PS
El-Kherba		36	90	64.8	100	95	77.5	100	100	100	100	95	40.8	III	FS
BA		37	90	66.1	100	95	77.5	100	100	85.5	100	100	37.4	IV	PS
BA		38	90	62.2	100	95	92.5	100	100	100	100	95	46.8	III	FS
BL	39		90	85.3	95	95	87.5	100	95	60.5	37.3	100	13.0	V	VPS
A.awaigila	40		90	84.5	100	95	92.5	100	100	100	90.7	95	57.6	III	FS
G	41		90	54.3	100	95	100	100	100	94.5	93.8	100	41.2	III	FS
G. Libina	42		90	84.3	95	95	92.5	100	100	80	82.5	100	41.8	III	FS
Bagdad	43		90	54.2	95	95	85	100	100	85	91.8	100	29.2	IV	PS
El-Arish	44		90	56.3	100	95	87.5	100	100	82.8	88.8	100	30.9	IV	PS
WA	45		90	54.9	100	95	92.5	100	100	100	93.5	100	40.6	III	FS
El-Ressan		46	90	65.7	100	95	100	100	100	85	43.1	95	18.5	V	VPS
WA		47	90	56.9	100	95	87.5	100	100	100	95.0	100	40.5	III	FS

BA= Bair El-Abd **BL= Bair Lehfen** **WA= Wadi El-Arish** **G= El-Garkada**
FS= Fair soils **PS= Poor soils** **VPS= Very poor soils** **NAS= Non agriculture**
AWI= Availability water irrigation **CI= Capability Index** **E= Erosion**

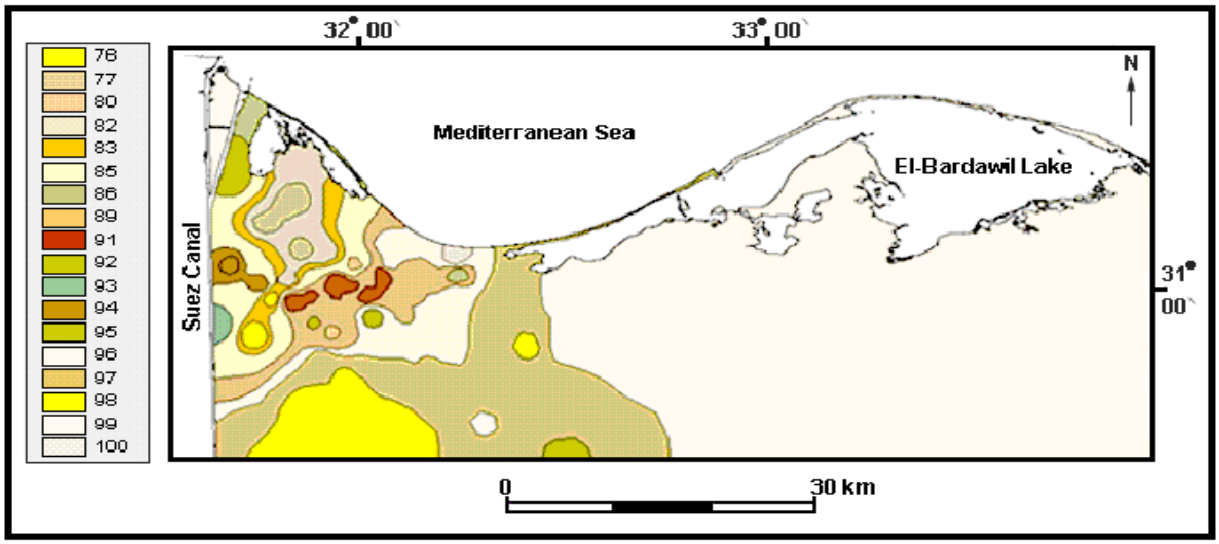

Fig. 4-56: Polygon layer representing the wetness of the study area.

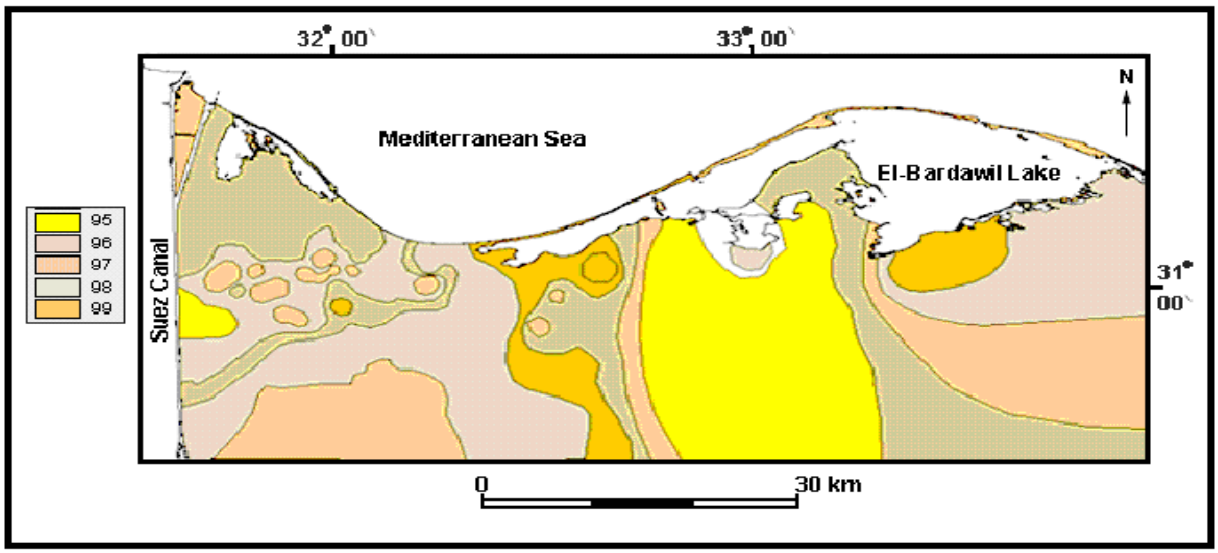

Fig. 4-57: Polygon layer representing erosion in the study area.

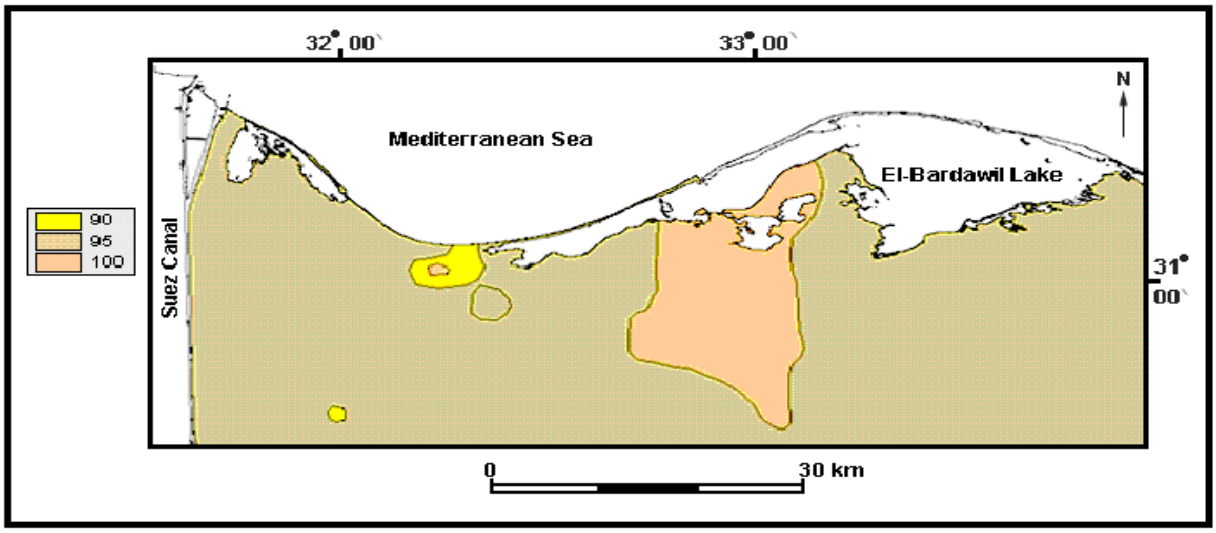

Fig. 4-58: Polygon layer representing soil profile depth (cm) in the study area.

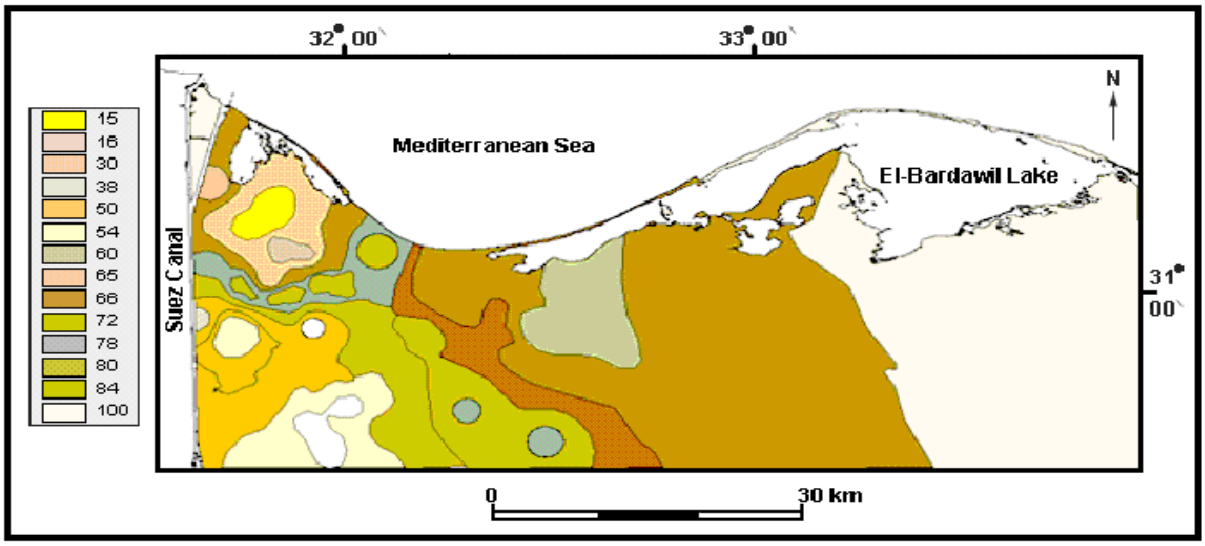

Fig. 4-59: Polygon layer representing texture classes in the study area.

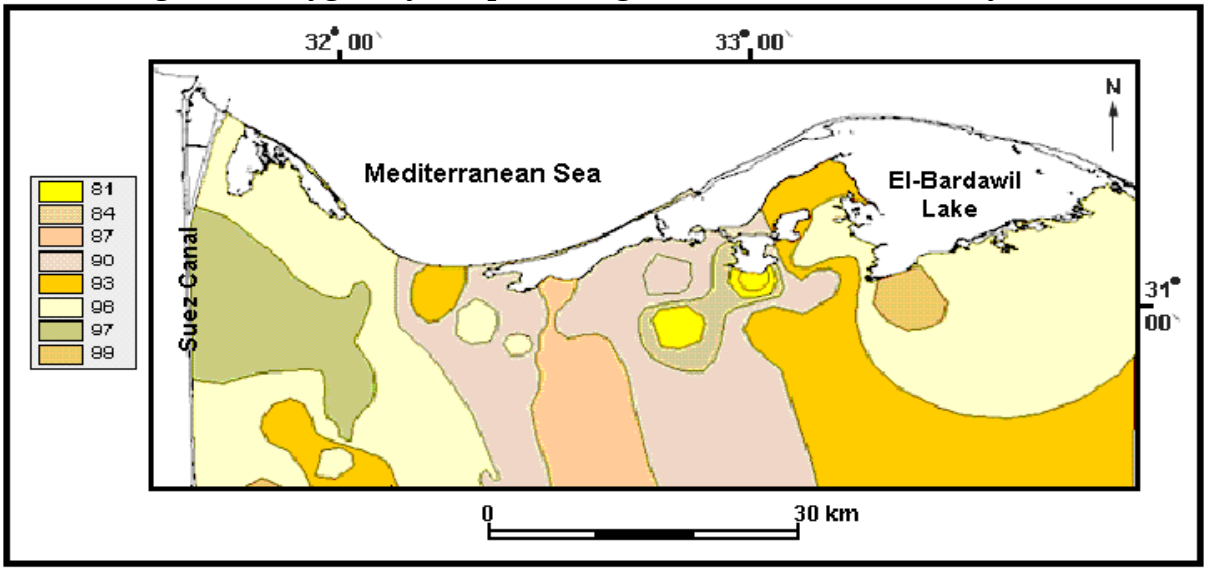

Fig. 4-60: Polygon layer representing slope of the study area.

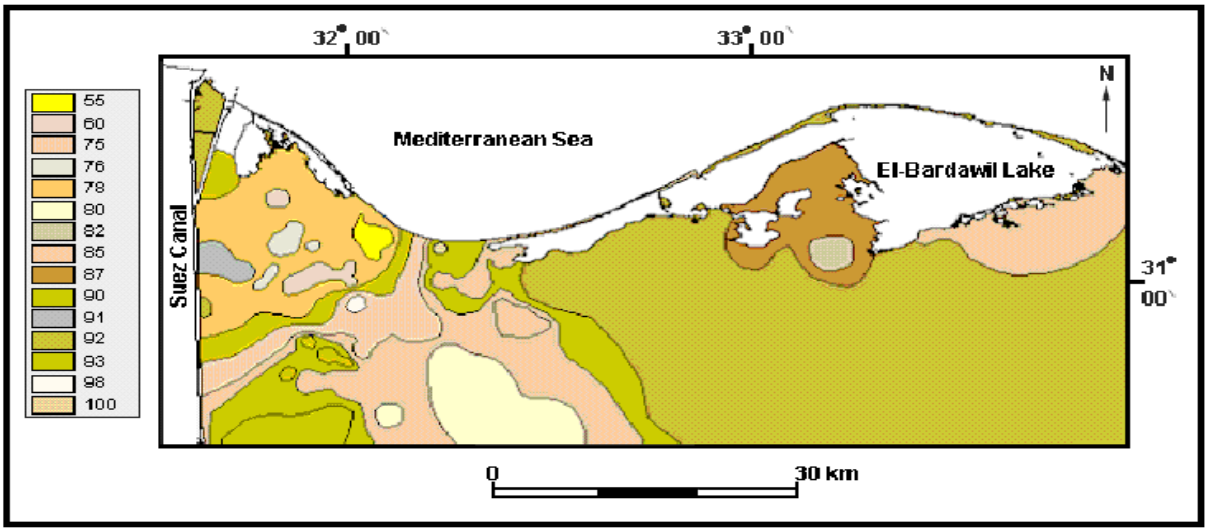

Fig. 4-61: Polygon layer representing sodicity (ESP) in the study area.

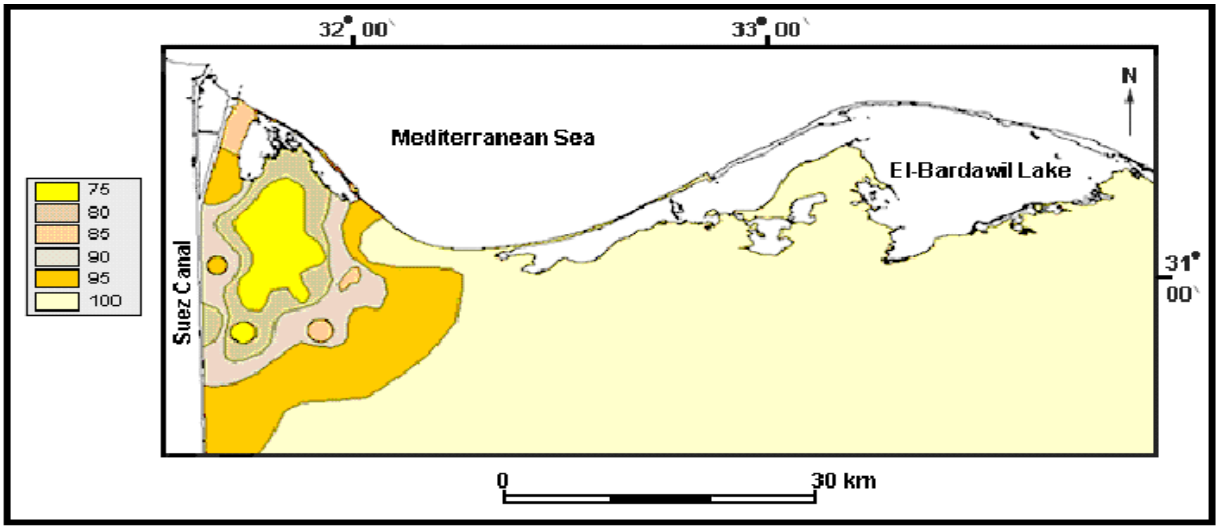

Fig. 4-62: Polygon layer representing the gypsum contents in the study area.

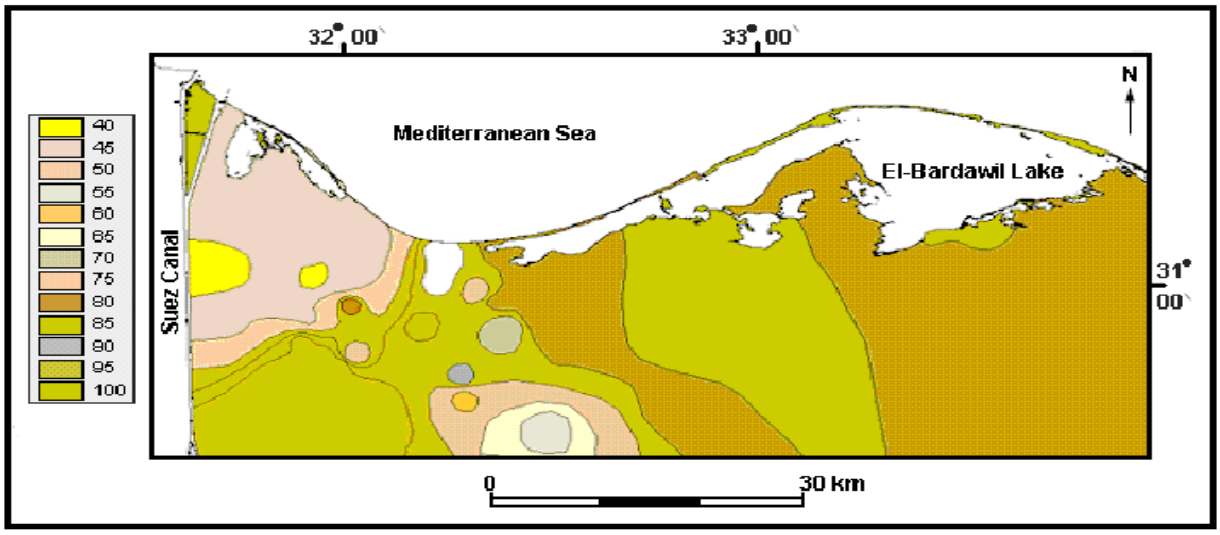

Fig. 4-63: Polygon layer representing salinity levels in the study area.

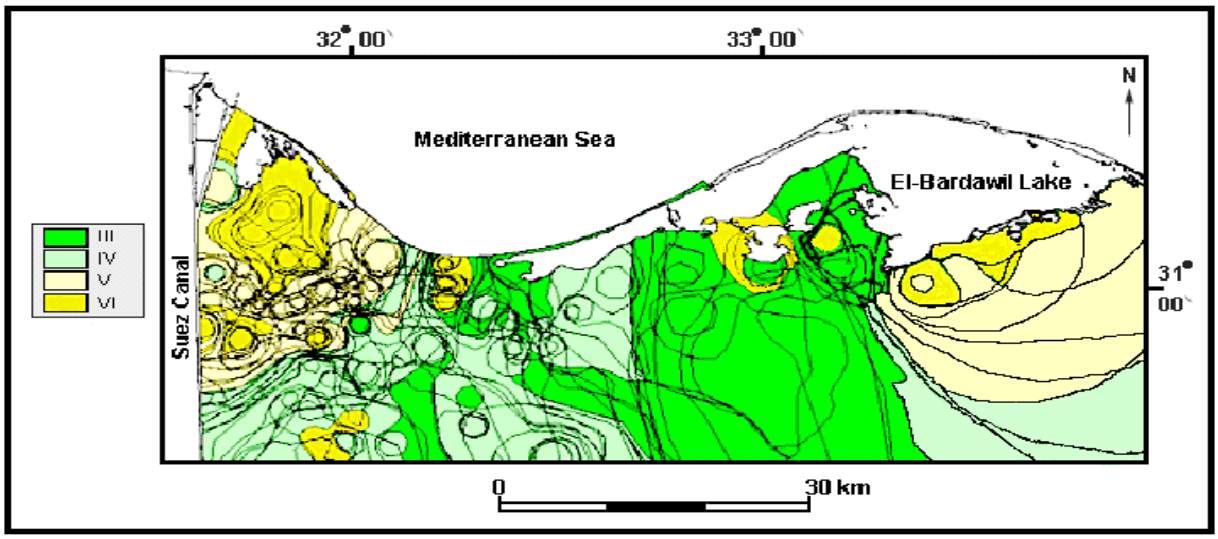

Fig. 4-64: Map of the soil ratings (evaluation classes) in the study area.

5 Discussion

5.1 Suitability of morphological units for soils in the El-Salam Canal soil area

The soils of the El-Salam Canal project area in the northern part of the Sinai peninsula are greatly affected by the type of associated landforms and morphological features. Therefore, it is necessary to give description about these through the visual analysis of the Landsat TM-5 images, previous works, field work description and soil samples collection. The morphological characteristic, landforms and soils classification in the northern part of the Sinai study area are discussed here as following:

5.1.1 Area of the El-Tina Plan and South El-Kantara Shark

The morphological features of the El-Tina Plan and South El-Kantara Shark areas in the north Sinai, from the field as described by the work survey and visual analysis of the Landsat TM images, are illustrated by the old deltiaic mud plain derived from an old branch of the River Nile inter-mixed with aeolin sand deposits and extensive dry and/or wet flat Sabkhas in the El-Tina Plain. Meanwhile, the sand sheet, sand dunes and small scattered salt Marches or Sabkha are the mainly morphological features in the South EL-Kantara Shark. These morphological results conform with description by results from ATKINS and WATER (1989) and STANLEY (1988), they reported the El-Tina Plain is an integral part of the northeastern margin of the Nile delta. During a reconnaissance field survey carried out by KHALAF et al. (1997), they reported the occurrence of an old sand dune ridge that extends in the northern part of the Sinai from NE-SW direction in the eastern part of the deltaic mud flat close to Balouza. This dune ridge is extensively deflated and some of its remnants occur as yardangs. The latter may reach up to 2 m in height. The deflation surfaces of these old dunes expose well developed aeolian primary structures. Some of the deflated old dunes are covered with recent active aeolian sands. Although the El-Tina mud plain is sharply bounded by the Pelusium fault, where a clear-cut contact with the southeasterly sandy terrain is obvious, a zone of wetland fringes the southern edge of the El-Tina Plain and extends southward of the South El-Kantar Shark. This zone is mostly formed of small scattered salt marches surrounded by extensive dry flat Sabkha. The Sabkha is covered by halite crust that may reach up to 3 cm in thickness.

EL-SHAZLY and ABD EL-GHAPHOUR (1990) and ABD EL-MALIK (1999) reported that clay soils dominate in the northwestern Sinai, namely El-Tina Plain, and also in a few individual Sabhkas. Salt efflorescence is common in the form of thin crust and rather thick pans (~ 5 cm). Beneath the salt crust is a sand zone rich in diagenetic saccaroidal gypsum crystals. Thin hard bands of gypsum may also occur at different levels close to the surface.

5.1.2 Area of the El-Bardawil, Bair El-Abd and Rabaa

The results of the morphological features in these studied area are illustrated by the individual Sabkhas, Marshes and Swamps. The meaning words of the morphological units are defined and described as following, the word Sabkhas is an arabic name (TILL, 1978). Sabkhas area (individual Sabkhas) are known in north America as “Playa” and termed in Middle East “inland Sabkhas” (COLLINSON, 1978). Marshes and Swamps are poorly drained areas with a permanent high water table and distinct assemblages of plants. Marshes are characterized by grass vegetation, water-saturated conditions and biologic productivity, but Swamps are characterized by tree vegetation growing under water-saturated conditions (WORCESTER 1969).

The description of the sand sheet and sand dunes in the Bair El-Abd and Rabaa studied area from the field work survey and visual analysis of the Landsat TM images conformed with the field studies of BAYOUMY (1998). He revealed that the sandy terrain Rummana and south El-Bardawil at the western side is subdivided into level terrain, undulating terrain and active sand dunes. The greater part of the area are covered with undulating sand terrain of aeolian origin. Gently undulating sandy terrain cover the areas of the Rabaa and Qatia, while the rolling sand terrain covers the area north of Balouza. Many Sabhkas are found in these area especially near the Rummana, the Rabaa and Qatia.

5.1.3 Area of the Wadi El-Arish area

The morphological features of the Wadi El-Arish area were recognized and observed from the field study and visual interpretation analysis for the Landsat TM-5 image classified, the main morphological features can be conclude into four units. These units are mainly present channel

(calcareous deposits), three terraces (upper, middle and lower), flood plain (sand sheet) and coastal plain (coastal sand dunes and sand beach-ridges). These morphology units in this studied area are conform with those of SHATA (1959), ABDALLAH and ABOU-KHADRAH (1977), SAID (1990) and JAPAN INTERNATIONAL COOPERATION AGENCY (JICA) (1996). They considered the Wadi El-Arish within the foreshore plain and the topographical elevation slope are comparatively steep from north to south. The land elevation is gradually high to the south along the road of the El-Arish-Lehfen to El-Hassana. The area of the Wadi El-Arish has irregular shape with contour elevation 110m running around it. The land elevation at the El-Sir and El-Quarir area (one of the big part of the El-Salam Canal project area) is <+90m above sea level (a.s.l.) at about 50% of the area, and 90-110m a.s.l. for the other landforms occur in this study area, which are flat, gently sloping, undulating and hilly.

5.2 Soil characteristics and parent material in the study area

The soils of the El-Salam Canal area differ in their chemical and physical properties according to the mode of soil formation, parent material and geographic position. Most of the studied soils in the north Sinai are fluvial, aeolian, fluviomarine and lacustrine origin deposits and parent material. Fluviomarine and lacustrine soils deposits cover the greatest part of the area of the El-Tina Plain area. Aeolian sandy soils deposits constitute most of the northern part of the Sinai (the South El-Kantara Shark, the Rabaa and the Bair El-Abd area). The soils deposits of the Wide El-Arish are highly calcareous as these soils were formed from calcareous deposits. The studied soils are characterized by conspicuous chemical and physical properties which are entirely different from one location to another.

RABIE et al. (1993) and NASR (1988) indicated that the soil of the north Sinai are quite different in their morphological features, chemical properties, salinity, water table level, structure environmental conditions. The soils of the north Sinai show very evident variations in their particle size distribution whether among the soil profiles or along the entire depth of each profile, as the textural class ranged between clay and sand. ABDEL-GAPHOU et al. (1990) reported that the soil classification recognized in the northern part of the Sinai were *Typic* subgroups of *Torripsamments, Psammaquent, Torriorthents, Hydraquents, Salorthids* and *Calciorthids*.

5.2.1 Soil properties of the El-Tina Plain area

The results of chemical and physical analysis in the El-Tina Plain soils of the studied area revealed close relation to the landform and parent material deposits. The parent materials of this area are a mixture of alluvium, fluviomarine and lacustrine origin deposits and the soil category is *Typic Salorthids*. The soil profiles in this area revealed that these soils are stratified without development and this area are characterized by the salic diagnostic horizons. The sand and clay are the main textures in these soil. This soil area was described by the JICA (1989) and KHALAF et al. (1995). This study showed that in the flat low-lying El-Tina Plain, *Typic salorthids* which are so-called salt accumulated soils having a salic horizon and consists of fluvio-lacustrine deposits. The soil textures are loamy or clay textured and poorly drained having a shallow saline groundwater table. The halophyte *Nitraria retusa* plant usually prefer to grow in areas where the Sabkha ground water in the coastal wetlands is recharged with fresh water seepage from the alluvial fans. This reduces the salinity to the level suitable for the growth of this plant in the northern part of the Sinai.

The values of calcium carbonate content in the El-Tina Plain area reveal very wide variations in total calcium carbonate content among the studied soil profile and surface samples. The geogenic nature of this soils could be the reason for the detected variations in the calcium carbonate content beside the arid climatic conditions prevailing in the studied area and the parent material (fluvialmarine and lacustrine), that include many fractions of shells present in the soils deposits. The data shows that the studied soil samples are very poor in the organic matter and organic carbon content. The low organic matter and organic carbon content in this soils may arise from the residue of marine organisms such as shells, along with the fact that these soils are formed under arid condition and are virgin soils.

The gypsum content in the El-Tina Plain soil samples revealed that the relatively higher values of gypsum content may be formed through the precipitation from the enriched underground water table of sulphate ions through capillary action and evaporation process. The alkaline pH in this soils reveal that they have a high concentration of the alkaline cations (Na^+) and anions (Cl^-) in soil solution, in addition to which the soils were effected by arid climate condition.

The relatively high salt content values in the soil samples of the El-Tina Plain area may be due to the seepage of sea water from the Suez Canal to the adjacent area through ground water fluctuations. The fluctuations and shallow water table facilitate the formation of these salt affected soils. These soils may also be due to the formation of salt crusts on the soil surface resulting from the arid climatic conditions prevailing in the studied area with high evaporation rate. This result conforms with those obtained by YOUNES et al. (1977), NADIM (1986) and NASR (1988). According to LAND MASTER PLAN (LMP) (1986) and RABIE et al. (1993), they reported that the salinity content (EC) in the El-Tina Plain soils varies from apparently salt-free to strongly salt-affected within ranges of 80-208 ds m^{-1}. MANSOUR (1997) reported that the El-Tina Plain soils area are extremely saline, ranges between 102 to 314 ds m^{-1}. BAYOUMY (1998) showed that this area hasclay soils texture with extremely high salts and thin to thick salt crust on the surface. Saline water table is very shallow 40 cm below the soil surface.

The presence of high contents of soluble Na^{+}, most probably in the forms of chlorides and sulphates, may suggest lacustrine lagoonal or even marine contribution to such sediments in the El-Tina Plain area. The moderately high Mg^{2+} content in the soil samples may indicate its origin is affected by marine deposits. The higher values of soluble cations and anions in these soils may be due to fine texture (clay texture) and the seepage of sea water from the Suez Canal. FARAG (1999) and BAYOUMY et al.(1992) indicated that the texture of the El-Tina Plain soils are clay and silty loam. The high amounts of Mg^{2+} in the soils indicates the high influence of marine deposits. The water table is present at 75-96 cm. The high values of the CEC, EC and ESP in the soil samples of this area are mainly affected by the high percent of clay content throughout the layers of soil profiles and surface samples. These are mainly attributed to the seepage of sea water from Suez Canal in this area through ground water fluctuations.

To throw light on the fertility potential of the nitrogen, phosphorus (P) and potassium (K) status in the north Sinai along El-Salam Canal areas, analysis were carried out for the uppermost layers of the studied soil samples area. The nitrogen takes the first position in the frequency of use as a fertilizer element. The phosphorus supply can be even more critical than

the nitrogen supply in some natural environments. Certain microbes can make atmospheric nitrogen available to plant, P and K supply must come from the parent material of the soils.

The nitrogen content is generally very low and it decreases with depth in the El-Tina plain surface and profile soil samples. The relatively high values of phosphorus content may be due to their fine texture in this soils (clay soil texture). BLACK (1957) mentioned that the phosphorus percentage of the soil as a whole usually increase as the texture becomes finer if the other conditions are similar. The moderately to relatively high values of total-K contents in the El-Tina Plain soils may be due to the majority of occurring silicate soil material and development from highly saline fine textured sediments. The results of potassium content in this soils can lead to the conclusion that the distribution of total-K contents in these studied areas are dependent mainly on parent material, clay content, type of clay and state of weathering. Therefore, the release of K^+ through weathering and transformation of clay and silt size minerals are responsible for major portions of total-K content in these soils. The potassium content expressed as K_2O is an essential element for plant growth and reproduction. The distribution of potassium in soils is related more to the conditions of weathering of the potash feldspars and micas than to the composition of parent rocks themselves. MANSOUR (1997) reported the total-N content was lower and ranged from 0.03 to 0.24%, total-P content was higher and ranged from 370 to 1200 mg kg^{-1} and total-K content was higher and ranged from 750 to 4400 mg kg^{-1} in the El-Tina Plain soils. The macronutrient status in the El-Tina Plain soils reveal that the moderately high Mn^{2+} content, that may be indicate to lacustrine or marine origin deposits in these soils.

The particle size distribution results may relate to the genesis and mode of formation of these soils in the studied areas. The wide variations of texture classes in the El-Tina Plain area may indicate various modes of soil formation in this area and may be attributed to the interference between the alluvial and aeolian deposits. NOMAN et al. (1987) indicated that the soil parent material in the soil of the El-Tina Plain constitutes a mixture of the Nile alluvium and lacustrine deposits, sometimes mixed with aeolian sand sediments in this area. MANSOUR (1997) reported that the sorting of these soils range between well sorted (indicating a homogeneous parent material and deposition by wind action) to poorly sorted (indicating that the soils were deposited by water action). This could be taken as a confirmation that the area

was affected by the Nile water at times when the old branches of the Nile passed across to this area and conformation these soils.

The values of bulk density in the El-Tina Plain soils may relate to status of pores, drainage and particle size class in these soils. Bulk density influences plant growth and engineering applications. Within a family particle size class, bulk density is an indicator of how well plant roots are able to extend into the soil. Table (5-1) shows the root restriction initiation and root limiting bulk densities in different soil textures (SOIL SURVEY MANUAL 1993)

Table 5-1: Particle size classes and bulk density (g cm^{-3}) with limiting root according to (SOIL SURVEY MANUAL 1993).

Particle size classes	Bulk density (g cm^{-3})	
	Restriction initiation	Root limiting
- Sandy	1.69	>1.85
- Loamy		
Coarse loamy	1.63	>1.80
Fine loamy	1.60	>1.78
Coarse silty	1.60	>1.79
Fine silty	1.54	>1.65
- Clayey		
35-45% clay	1.49	>1.58
>45 clay	1.39	>1.47

Saturated hydraulic conductivity (soil permeability) is used in soil interpretations, such as suitability for irrigation and drainage systems, absorption fields and other conservation practices. The values of saturated hydraulic conductivity in the El-Tina Plain soils have wide variation between values from rapid to moderately slow movement of water within these soils, that may indicate a wide variation of the particle size classes (clay to sand textures) in these studied area. Available water capacity (AWC) is an important soil property in designing and operating irrigation systems, designing drainage systems and protecting water sources. The values of AWC in the El-Tina Plain soils reveal that the flood irrigation system with a good deep drainage system to enhance properties in these soils are recommended. The values of saturation of water in the El-Tina Plain soils may indicate different types of texture (sand and Clay) in these area.

5.2.2 Soil properties of the South El-Kantara Shark area

The South El-Kantara Shark soils are characterized by different modes of chemical and physical properties according to soil formation and parent material. These properties though listed similar in the soils of the El-Tina plain studied area, the South El-Kantara Shark soils have a completely different mode of soil formation than the El-Tina plain soils.

The parent material of the South El-Kantara Shark soils is aeoline sand deposits. This type of parent material may be the reason for the variation of $CaCO_3$ content in these studied soil area. The soil profiles in these soils are stratified without any development horizons. The soil classification in this area is *Typic Torripsamment.* The organic matter and organic carbon values reflect the virgin and deficient status of organic matter and organic carbon content in these soils and in their parent material. In addition to this, these soils are affected by arid regional climate. The low content of gypsum in these soils may be due to their derivation from natural formation of parent material (sand deposits). The pH values shown in these study area are moderately alkaline, and may be due to concentrations of the alkaline cations. The low values of salinity (EC) in the South El-Kantara Shark soils indicates that these soils are built up of coarse sand quartz, and the slightly or moderately saline area may be due to the shallow water table in fine sand texture in this studied area. Generally, the low concentration values of cationic composition in the soils of the South El-Kantara Shark may relate to aeolian sand origin deposits in this soil.

EL-SHAZLY and ABD EL-GAPHOUR (1990) showed that the soils of the South El-Kantara Shark are generally built up of successive layers of quartzite sand and have variant degrees of salinity. In a few cases, fine textured deposits interfere with sandy deposits particularly in some dry Sabkhas. MANSOUR (1997) showed that the soils of South El-Kantara Shark range between almost flat to hilly. Soil parent material is sandy deposits transported by winds. Soil salinity ranged from non-saline to moderately saline, except Sabkas soils which are highly saline. The relatively low values of CEC, exchangeable cations and ESP in these soils are mainly affected by particle size of texture (coarse sand texture) and low content of fine fractions (silt and clay fractions) in this soils. Slightly high values of CEC may be due to fine fractions in these studied soils.

The relatively low values of phosphorus in the South El-Kantara Shark soils may be due to their fine texture, while the low potassium content may be due to status of weathering of potash feldspars in parent material, and the transformation of the fine particle size are responsible for the low content of the potassium (K) in this studied area. The slightly high content of Fe^{2+} in the soil samples of the South El-Kantara Shark soil area may relate to the origin of the sand deposits (parent material) in this area.

The particle size distribution results may indicate the demarcate genesis and mode of soil formation of the soils occupying the area under consideration in the South El-Kantara Shark. The values of bulk density in these soils may be derived from coarse size of particle classes and texture (sand texture) in this studied area. The expectancy of density root limiting is more than 1.85 g cm^{-3} in these soils in this area according to (SOIL SURVEY MANUAL 1993).

The values of soil permeability ranges, according to soil survey manual, are described by very rapid and rapid movement of water from soils. From these results it could be concluded that the South El-Kantara Shark soils are coarse to fine sand soil texture and the suitable system of irrigation in these soils is drip irrigation without any drainage system. The values of available water in the soil of these area mainly indicate the soil texture is coarse to fine sand texture in the studied soils area. The saturation values in these soils influence the selection of suitable systems of irrigation and drainage (drip irrigation without any drainage system) in these soils.

5.2.3 Soils properties of the Rabaa and Bair El-Abd area

The soil properties of the Rabaa and the Bair El-Abd area have small differences between them in the chemical and physical characteristics. These soils make up two parts of the El-Salam Canal soils project in the northern part of the Sinai peninsula. The soils have been derived from aeolian sand deposits with almost deep profiles (> 150 cm) and stratified without any development; i.e. they lack any diagnostic horizons. The category of classification soil in this area is *Typic Torripsamments*. The distribution of natural vegetation and surface condition range from few to moderate with palm trees and very small vegetables farms. The topographic surface ranges between flat or almost flat and hilly slope in this surface area.

Total calcium carbonate content in the Rabaa and the Bair El-Abd soils is very low. Moreover, it is mostly of secondary origin, mainly attributed to the weathering of parent material which compose these soils. Organic matter content in the Rabaa and the Bair El-Abd area is very low. The organic matter content values in these soils indicated that these soils are virgin with few natural vegetation cover, with these soils also affected by arid conditions. The gypsum values in these soils reflect the parent material having little concentration of gypsum (sand deposits). The pH value is above 7.9 in the soil samples of the Rabaa and the Bair El-Abd soils and may have an inadequate availability of iron, manganese, copper, zinc and especially of phosphorus and boron. These results conform with those of LAND MASTER PLAN (1987), JICA (1989) and MANSOUR (1997).

The EC values in the Rabaa soils range from non-saline to slightly saline, while the soil salinity in the Bair El-Abd soils are classified between non-saline and moderately saline in the surface and profile samples. The salinization are chlorides and sulphates-types in these soil solutions. The low values of electrical conductivity (salinity status) may be due to derivation from sand deposit parent materials in these soils. The low concentration of cations and anions in the soil extract from the Rabaa and the Bair El-Abd soils may be reflected by status of the parent material (sand deposits) transported by wind action. The relatively low values of CEC in these soils are mainly affected by particle size of texture (coarse and fine sand texture) in these soils and low content of clay. Slightly high values of CEC may be due to fine sand texture in the Rabaa and the Bair El-Abd studied soils. The low values of exchangeable cations and ESP in these soils may be due to soil texture (sand texture), while the relatively high values of exchangeable cations and ESP in these soils are mainly affected by local of the samples near the Sabkhas soils in these studied soil area. These results and explanations conform with studies from FARAG (1999), NASR (1988), and JICA (1997).

SOIL SURVEY STAFF (1993) reports that the soils have a low CEC (such as South El-Kantara Shark, Rabaa and Bair El-Abd soils), hold fewer cations and may require more frequent applications of fertilizer and amendments than soils having a high cation exchange capacity (such as, El-Tina Plain soils).

The nitrogen content values in the Rabaa and the Bair El-Abd soils is generally very low and decreases with depth in the profiles of these soils. The relatively high values of phosphorus in the soils of the Rabaa may be due to their fine texture. Meanwhile, the moderate values of phosphorus in the soils of the Bair El-Abd may be due to coarse sand texture derived from sand deposit parent materials. MANSOUR (1997) reported that the highest values of total-P in the soils of Rabaa and Bair El-Abd were those of the heavy texture soils, while the lowest values are those of the light texture soils. The total potassium content values in these soils may be due to the status of weathering of the potash feldspars in parent material and the transformation of fine particle size are responsible for content of potassium in this studied area. The slightly high content of Mn^{2+} in the studied soil samples in these area may be due to original sand deposits forming these soils. The higher values of pH in these soils may have an inadequate availability of these cations (Mn^{2+}, Fe^{2+}, Zn^{2+} and Cu^{2+}). These results conformed with the SOIL SURVEY STAFF (1993).

The particle size distribution results in the Rabaa and the Bair El-Abd soils may indicate the demarcation of the genesis and mode of formation of these soils occupying the area under consideration. The particle size distribution values in these soils reveal the soil texture classes in all samples are sand texture in this studied area. MANSOUR (1997) and FARAG (1999) reported that the texture and sorting coefficient values in the Rabaa and the Bair El-Abd soils are sand texture and well sorted materials, which may be indication of the deposition process by wind action in these areas.

The values of bulk density in the Rabaa and the Bair El-Abd soils may be derived from the coarse size of particle classes and texture (sand texture) in these soils. The expectancy of density root limiting is more than 1.85 g cm^{-3} in these soils according to the (SOIL SURVEY MANUAL 1993). The hydraulic conductivity values in the Rabaa and the Bair El-Abd soils reveal that these soils are characterized by high movement of water within and through these soils. These ranges, according to Soil Survey Manual, were considered to be very rapid and rapid movement of water from these soils. From these results it could be concluded that the soils in the Rabaa and Bair El-Abd area are range from coarse to fine sand soil texture and the suitable system of irrigation in these soils is drip irrigation without any drainage system. The available water values from the soil samples in the Rabaa and the Bair El-Abd area indicate

more available water, than the soils in the El-Tina Plain area. This may mainly indicate that the soil texture is coarse to fine sand texture in these soils. The saturation values in the Rabaa and the Bair El-Abd soils are influence the selection of suitable systems of irrigation (drip irrigation) and drainage (without any drainage system) in these areas.

5.2.4 Soil properties of the Wadi El-Arish area

The differences of soils properties in the Wadi El-Arish studied area are based on the physical and chemical characteristics in the surface and profile soil samples and parent material deposits. These properties are mostly inherited from calcareous parent rock material. The effect of soil forming factors on these soils are considered to mainly relate to the chemical processes (water action) rather than the physical (wind action), this is due to the water action and movement. Therefore the soil formations are pedogenetic rather than geogenetic. The soil parent material are calcareous deposits and sometimes of sand deposit origin. The part of the El-Salam Canal soils project in the Wadi El-Arish is El-Ser and El-Qawarir area, which is located south of the El-Arish, lay a distance of about 20 km from the coastal line. It lies between latitude 30°45`E and 34° 05`E. This area is a alluvial plain, having about 30 km from north and 55 km from east to west. The category of soil classification in this study area is *Typic Calciorthids* and *Typic Torripsamments*. The topographic surface conditions range from almost flat to rolling slope.

The different values of $CaCO_3$ content in the Wadi El-Arish soils are reveal the original deposit (sand and calcareous deposits) formations in these studied area. These results conform with the final report of DAMES and MOORE (1983) in the soils of the wadi El-Arish, which characterizes ranges of $CaCO_3$ from 3 to 32 %. This may be due to derivation from calcareous parent rocks. MANSOUR (1997) reported that the $CaCO_3$ in the soils of the Wadi El-Arish distribution in different soil fractions has irregular pattern. The calcium carbonate was distributed in coarse sand, fine, silt and clay fractions. Generally calcium carbonate distribution is dominated in coarse sand and silt fractions in all the studied soil samples of the El-Ser and El-Qawarir area.

The organic matter and organic carbon values reflect the wide variations in organic matter content in the soil of the Wadi El-Arish area. The high values of organic matter content may be due to residues of plant root from natural vegetation or crops, while low values may be due to virgin soils and climate effect (arid conditions). The low content of gypsum in these soils may be due to derivations from natural formations of parent material (sand deposits). The calcareous deposits are responsible for high gypsum content values in these area. The moderately alkaline pH values in the Wadi El-Arish soils may be due to relatively high concentration of alkaline cations. The EC values reveal that the profile and surface soil samples in the Wadi El-Arish area are classified into non-saline and slightly saline range according to the classes of soil salinity in SOIL SURVEY MANUAL (1993). The low values of EC in the Wadi El-Arish soils may be due to sand soil texture and low concentration of soluble salts in this soil solution. These results are in line with DAMES and MORE (1981) who reported that the electrical conductivity (EC) of the aeolian sand soils in the Wadi El-Arish area ranged from 0.2 to 2.0 ds m^{-1} and soil reaction is alkaline, as revealed by the pH values in these soils. The higher content of soluble Ca^{2+} in the Wadi El-Arish soils may be an indicator to their derivation from calcareous parent rocks. The results of the chemical compositions of the Wadi El-Arish soils conform with those of NOMAN et al (1982), RABIE et al. (1983), DAMES and MOORE (1981) and MANSOUR (1997), who found that the soils of the Wadi El-Arish were almost free of salts and medium saline. This was indicated by its electrical conductivity values which never exceeded 2.8 ds m^{-1}, except that the saline soil is extremely saline as indicated by the EC values in these soils. The slightly high value of CEC in the Wadi El-Arish soils may be due to fine texture (loam and sandy loam) in the El-Ressan and the Bair Lehfen soil samples. In addition to this, the low concentration from soluble salts and exchangeable cations in soil solution may indicate the low content of cation exchange capacity in the Wadi El-Arish studied soils. The slightly high values of (ESP) in the Wadi El-Arish soils may be due to relatively high concentration of sodium cations in the soil solution and slightly high percentage of fine particle (silt and clay) in these soils.

The low values of nitrogen and moderately high levels of phosphorus in the Wadi El-Arish soils may be due to their origin of deposits and fine texture. The values of total potassium in the Wadi El-Arish soils may relate to the status of less weathering of potash feldspars in parent rocks and less transformation of fine particle fractions. These results reveal that these soils

mostly lack diagnostic horizons and are undeveloped and immature. The concentration of micronutriant values (Mn^{2+}, Fe^{2+}, Zn^{2+} and Cu^{2+}) in the Wadi El-Arish soils are in agreerment with SILLANPÄÄ (1982). This conclusion and explanation for the Wadi El-Arish soils area conform with those of NOMAN et al (1982) and RABIE et al. (1983). They reported that the soils in the Wadi El-Arish have no visible diagnostic horizons that could be recognized in any of the studied soil profiles and these soils are derived from more than one parent material of different origin namely, i.e. aeolian, alluvial and beach origin. Accordingly they could be classified as related to the order: Entisols, suborder *Psamments* and great group *Torripsamment*.

The texture classes in the Wadi El-Arish soils show variations of texture classes, indicating that water and wind actions are the main factors responsible for the formation of these soils in the Wadi El-Arish area. MANSOUR (1997) reported the same results in his study in the Wadi El-Arish soils and he revealed the sorting value of the particle size distribution ranges between well and poorly sorted in these soils.

The values of bulk denisty in the Wadi El-Arish soils may relate to the status of pores in these soils which are responsible for the drainage system (ranges from well to poor drainage). The values of bulk density in these soils may reflect the characteristics of particle size texture (sand to loam) classes. The expectancy of density root limiting ranges between >1.47 and >1.85 g cm^{-3}, in these soils, according to the SOIL SURVEY MANUAL (1993). The ranges of values of hydraulic conductivity in the Wadi El-Arish soils, according to Soil Survey Manual, are considered moderately slow and rapid movement of water. From these results it can be concluded that these soils have medium to very fine particle size soil texture. The available water values in these soils reveal that they have less available water than the soils in the Rabaa and the Bair El-Abd area. This mainly relates to the very wide variation of soil texture range from medium to very fine particle size texture classes in the Wadi El-Arish studied soils area. The saturation values in these soils influences the selection of suitable systems of irrigation and drainage in these soils. The suitable irrigation in these soils are flood or/and drip irrigation systems with deep drainage system.

5.2.5 Contour line image maps of soil characteristics in the study area

The capabilities inherent in the digital analysis of the Landsat TM image data allow for the accurate differentiation of soil chemical and physical characteristics, which can be correlated with soil series being mapped in a given locale. The image analysis and the information derived from the TM image data can be useful in numerous aspects and is the interpretation of the soil survey (KIRSCHNER et al. 1978). The soil maps generated by computer analysis of the Landsat TM data can help in the preparation of the soil association map and the single feature map, such as drainage pattern and organic matter content (WEISMILLER and KAMINSKY 1978).

In this work, the contour line image maps were achieved from the Landsat TM-5 image analysis and the net results of the soil properties analysis, such as EC, CEC, OM, $CaCO_3$, Gypsum and pH values, in the studied area in the north Sinai along the El-Salam Canal project. These maps were achieved by a few number of surface and profile samples, but these soil samples covered the maim morphological feature in the different location of this studied area. The contour line maps showed two types of distribution patterns for soil properties. The first one is localized around the near soil surface samples area with high accuracy line values of the soil characteristics. The second pattern is a diffused line in the far area from the field soil samples with low accuracy of the soil characteristic values in the field. These soil properties map can help to achieved a good soil surveying study and in addition to that can help in the preparation of individual soil property maps such as for EC, CEC, OM, Gypsum and calcium carbonate content in the surface soils. The type of this maps may be reduce the times and number of soil samples in the soil survey studies on the small scales (areas) with high accuracy. These contour line maps in the north Sinai soil area can be help in the speed of development of this studied area along the El-Salam Canal project.

5.3 Analysis of satellite image data

5.3.1 Principal component analysis

Principal component analysis (PCA) is an important data transformation technique used in remote sensing work with multi-spectral data (RICHARDS 1984). The principal components

transformation is a redundancy reduction technique which leads to describing multidimensional data in which the variables are non-correlated with the first component containing most variance and the succeeding component which normally contain decreasing proportion of data scattering (JENSON and WALTZ 1979, RICHARDS 1984).

The success of principal component analysis in the differentiation between the different soils units in the studied area in the northern part of the Sinai peninsula depends mostly on the selection of the appropriate principal components (PCs). It is important to study the eigenvector used as a weighing factor in determination of different principal component. Studying the eigenvector values are a helpful tool in choosing the best principal components, which are highly loaded with most of the original bands. The results of PCA analysis from the Landsat TM-5 image data in the studied area show the TM1, TM3 and TM5 with TM7 as haveing the highest eigenvectors. This means that those TM bands have the strongest contribution in the studied images formation of the first three principal components PC1, PC2 and PC3 (about 98% of the total variance information in the studied image). Consequently, the most informative three band combination will consist of band 1, band 3 (visible portion) and band 5 or band 7 (near-middle IR). These results conform with the Optimum Factors Index (OFI) ABD EL-HADY (1988). The strong contrast is due to the fact of the distance of the pixels project on PC1 maximum (RIVEREAU et al. 1978). The first principal component (PC1) usually have all the four bands differences between the infrared bands and the visible bands (SINGH and HARRISON 1985). The PC1 and PC2 account for about 98 to 99% of the total variance information data and can be compressed into two-dimensional, without significant loss of information (MULDERS 1987). It is important to produce more than 3 PCs. Then, using eigenvectors, the three PCs highly loaded by the seven bands are chosen. The other PCs only contain the small remaining variance and noise (JIAJU, 1988).

5.3.2 Band ratios

The using of band ratio 5/7 of the calcareous soils (as soils in the Wadi El-Arish) will be higher than that of sand soils (as soils in the South El-Kantara Shark, Rabaa and Bair El-Abd area) in spite of the clay content of the sand soils. Also, the ratio 5/7 for clay soils (as soils in the El-Tina Plain area) will be higher than that of sand soils. Therefore, the band ratio 5/7 is a good

ratio for the separation of calcareous soils from sand soils in spite of their clay mineral fractions content. It is also useful in the separation of sand soils with different small clay content (as soils in the Rabaa and Bair El-Abd area). ABD EL-MONSIF (1996) reported that from laboratory measurements, the band ratio 5/7 is a best ratio for distinguishing limestone, sand and clay soils. Slightly better inter-channels (bands) correlation, determined from the pattern of training samples are used instead of the gray levels of all pixels. In addition to this, the TM 1, TM 5 and TM 7 bands provide the maximum information about the sand soils (ABD EL-HADY et al. 1992). The presence of Al-OH group in clay minerals make sand soils behave like calcareous soils (as soils in the Wadi El-Arish area) in band 7, because the Al-OH group has a strong absorption peak at 2.2 µm. This problem could be overcome by dividing band 5 by band 7. MULDERS and EPEMA (1986) reported that the band 5/7 ratio produced high contrast between clay soils in a Playa and other bare soil surfaces in the area. The ratio 7/3 has been mentioned by many geologists and pedologists as an excellent clay soils discriminator (GUPTA, 1991). By using the band ratio 7/2, the gypsum content will appear darker than any other soil units on the image (MULDERS 1985). Consequently, band 7/2 can be used due to the high content of the gypsum in soil deposits discriminator (as in the El-Tina Plain soils).

Three ratios are selected from the ratio bands analysis of the Landsat TM studied image in the north Sinai along the El-Salam Canal area. The selection was based on the soils chemical composition minerals of these soil units exposed on the surface samples of this soils along the El-Salam Canal area. These ratios bands (5/7, 7/3 and 7/2) with PCs (PC1, PC2 and PC3) are more clear than the ratios of the original bands only. ABD EL-MALIK (1999) reported that the same ratios combined between the bands and the principal components (PCs) were used in order to obtain a more interpretable image. These ratio-bands with PCs are more clear than the original bands only. A flow chart was designed on the spatial module of ERDAS Imagine 8.3.1 software (figure 5-1) to apply rationing to the image of these area.

5.3.3 Main classes of supervised classification

The geologic and topographic maps are available for the northern part of the Sinai peninsula. Therefore, supervised classification is recommended to be used in the studied area in the north Sinai along the El-Salam Canal project.

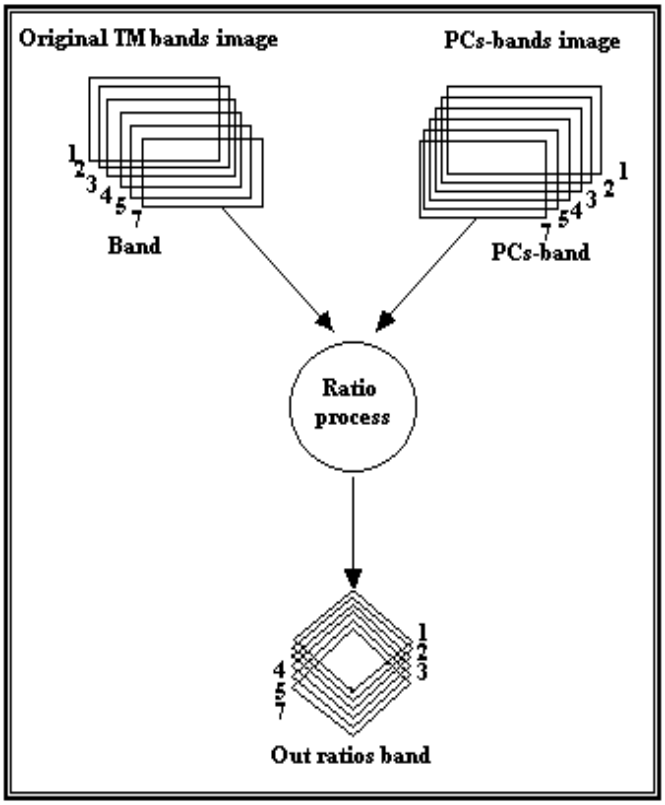

Fig. 5-1: The graphical modal of the ratio process.

Classification is usually applied to an area with a large number of classes or soil units and wherever the same soil unit or class is distributed in different places. In an area with a small number of units (classes) or when each class is restricted to one location and easily distinguished by image enhancement from the surrounding or adjacent soil units, manual tracing of the boundaries between these soil units is recommended over automatic classification. In this study, the maximum likelihood algorithm method was used to perform the supervised classification for the studied image area in the north Sinai. In remote sensing, the development of multi-spectral scanning technology to produce layered multi-spectral digital images of land areas from spacecraft, provided the opportunity to use the maximum likelihood criterion in producing thematic classification maps of large areas for such purposes as land use or land cover determination and natural cultivated land inventory (REEVES et al. 1975).

- **El-Tina plain classes**

Representative training sites of the El-Tina Plain studied area image were selected to be few enough to give accurate estimates of the classes. The classifier using training sites to produce the signature of each class. Usually evaluation of the separability of the signatures is the next step in the classification process. In fact, choosing the training sites is based on detailed study in the field. Each training site was studied carefully to be certain that it accurately represented its class. Therefore, evaluation of the separability between signatures could be considered as a measurement of the separability between the classes themselves.

Studying the maximum likelihood algorithm was chosen as a classification decision rule. The maximum likelihood classification method is the most accurate of the classification decision rule in ERDAS Imagine 8.3.1 software because it takes the most variables into consideration. Also, it takes the variability of classes into account by using the covariance matrix. This is very important in pedological applications because it is rare to find a certain layer continued on the surface without local interruption. By using this method of supervised classification was discriminated about 15 classes in the El-Tina Plain image area. These supervised classes are produced from best three band combination 4, 5 and 7 (R, G and B).

- **South El-Kantara Shark and Rabaa classes**

The supervised classification was done by using the maximum likelihood classification algorithm for the South El-Kantara Shark and Rabaa images. The supervised classes in the South El-Kantara Shark image are 16 classes, while in the Rabaa image are 15 classes. The supervised classification was executed by using the 6 bands for two images from the Landsat TM image data. The best three band combination are bands 4, 5 and 3 (R, G and B) in both images. Using the filtered composite image of the best band combination was performed to reveal the differentiate between the classes in the South El-Kantara Shark and the Rabaa images.

The main problem at the South El-Kantara Shark and the Rabaa images are the similarity of the soil composition (sand soils texture) of most soil units, and the small area extent of these units.

To overcome these problems the images of these area were enhanced before classification. The images were filtered by using a median frequency convolution kernel to enhance the texture of the images. Enhancing the texture of the images helps in the differentiation between those soil units with similar spectral characteristics. The enhanced images were classified by using the maximum likelihood classification algorithm (the histograms of the bands of data have normal distributions in both images).

- **Bair El-Abd classes**

The Bair El-Abd image have the same problem at the South El-Kantara Shark image (similarity of soil composition units with large scale area). As above, the image of study area was filtered by using a median frequency convolution kernel to resolve this problem. By this way can recognized and discriminated about 15 supervised classes in the Landsat TM image for the Bair El-Abd area. The maximum likelihood algorithm was chosen as a classification decision rule. The maximum likelihood classification method is the most accurate of the classification by using the best three bands combination (3, 5 and 7 bands) for the Bair El-Abd TM image.

- **Wadi El-Arish classes**

The supervised classification was done by using the maximum likelihood classification algorithm for the Wadi El-Arish studied image. The supervised classes in these image are 15 classes. The supervised classification was executed by using the 6 band for the image from the Landsat TM image data and the best three band combination are bands 4, 5 and 7 (R, G and B) in the studied image.

Where the accuracy of the classified image depends on the amount of information present in each training site, the stacked images were prepared in order to obtain the maximum information for the classification. Each stacked image contains eleven layers, which are:

- The 6 layers (bands) of the Landsat TM image
- a layer of chemical composition of the training site soil samples
- a layer of physical properties of the training site soil samples

- a layer of hydraulic characteristics of the training site samples
- a layer of the El-Salam Canal project area
- a layer of PCA bands of the training sites

The training sites were chosen on the this basis of stacked images and then the supervised classification process was carried out.

5.3.4 Recommendations for using the Landsat TM images in the study areas

From the visual analysis and image processing results of the Landsat TM image and field work survey, in the northern part of the Sinai peninsula along the El-Salam Canal soil project, were recommended using the raw Landsat TM image data to classification of this area. In addition to this, that can be help in extract more information about the soil morphology, soil properties and environmental conditions in this studied area from the Landsat TM images. The following conclusion were reached when classifying the TM images for morphological features in this area, soil characteristics and soil mapping in this study:

- It is recommended to use the image of the three best band combination in the classification process. These are the bands of the highest covariance matrix among the seven or six TM bands.
- Using an extra number of the TM bands may decrease the separability between different soils or units classes.
- In the areas of rugged terrain or the areas of soil units of similar spectral characteristic but different texture, it is recommended to use ancillary data (such as elevation, aspect, slope... etc.).
- If the TM image data has a normal distribution of the data file value, it is recommended to use the maximum likelihood classification algorithm (same as these TM image data under studied).
- In case of abnormal distribution of the histogram of the bands of data it is recommended to use the parallelepiped or minimum distance decision rules or by performing a first pass parallelepiped classification (another method of classification in the ERDAS program).
- Image enhancement and corrections (atmospheric or/and geometric) may be useful when ancillary data are not available or expected to do no improvement on the

classification process. Enhancing the image before classification must be done carefully. Some enhancement techniques such as rationing may enhance some features at the expense of others. High frequency filtering may complicate the image with noise, although low frequency filters may delete some important features on the image.

- Ground work has been performed in the Sinai peninsula which has yielded a good geological and pedological data. In this case, unsupervised classification is recommended.

5.4 Soil properties and bands correlation

The correlation and regression statistical discriminate analyses were used in analyzing the data results in the northern part of the Sinai peninsula along the El-Salam Canal project area. High correlation was found among the spectral data and the soil variables studied. The soil types were sufficiently differentiated based on either the spectral properties or the physical and chemical properties of the study soils area. The results indicate that selection bands of the electromagnetic spectrum are important in the development of models that will significantly predict soil properties from spectral data. A set of important spectral bands was identified in the regression equations developed for the prediction of the soil properties. The spectral band was found to be significant in contributing to the separability of the soil types which were pedogenically and characteristically related, hence significant in the prediction of the soil characteristics.

The discrimination of soil properties based on spectral characteristics depends upon select bands portions of the electromagnetic spectrum. In differentiating among the soil samples with respect to their chemical and physical soil properties, all of the spectral bands except band 6 (10.40-12.50 µm) were found to be significant as independent variables. Highly significant relationships between spectral properties and study soil properties EC, CEC, gypsum, sand, silt, clay, organic matter and pH were found from these results of the study area in the northern part of the Sinai along the El-Salam Canal soils project. Prediction of the soil properties from spectral data (the Landsat TM image data) was highly significant as shown by using the statistical analysis methods dependent upon the R^2 values. The visible portion green band 2,

red band 3, near infrared band 4, and middle infrared band 7 were the key bands in predicting EC, CEC, $CaCO_3$, gypsum and organic matter content in these studied soils. The probabilities of correct classification of soil organic matter content using the Landsat TM bands are obtained by (0.64-0.65) band 4, HENDERSON et al. (1989). While sand, silt and clay content were predicted by bands near and middle infrared bands 4 and 7 in these soils. The pH characteristic was the best predictor by using the red and near infrared bands 3 and 4. The correlation coefficients between soil properties and TM bands are show a good correlation and, also the correlation between the first three TM bands is high, while band 5 and 7 show a good correlation (MULDERS 1987).

The results of the studied area reveal two correlations between soil properties and reflection of the Landsat TM bands. These correlation are:

- The first is inversely proportional between EC, CEC, gypsum, silt and clay soil properties and the Landsat TM bands reflections (refer to the figures in appendix III).
- The second is directly proportional between $CaCO_3$, orgainc matter, total sand content and pH values of soil properties and the Landsat TM bands reflections (refer to the figures in appendix III).

Figure (5-2) and table (5-2) illustrate the comparison between soil type characteristic signatures and the Landsat TM bands reflection. The Landsat TM bands reflection has detected a very small variation reflection spectrum between sand soils and sand dunes signatures, which may be due to the same chemical and physical characteristics for two signatures. The bands reflections revealed relatively small differences between Marshes and Swamps, which may be due to the different content of water in these soils or features in the studied soil area. The bands 4, 5 and 7 spectrum reflection recorded high differential spectrum between sand and calcareous soils signatures, and between sand and clay soils that may be due to color of these soils, chemical composition and particle size of fractions in these studied soils.

These results conform with those of HOFFER (1979), BAUMGARDNER et al. (1985). Both reported that the reflectance differences which can be accounted for by differences in moisture

content, particle size and soil structure, size and shape of aggregates appear to influence the soil reflectance in varying manners. The scattergram analysis permitted the section of bands 4, 5 and 7 for image classification. Also, it reveals the importance of bands 4 and 7 for mapping the soil surface in arid regions (ABD EL-HADY et al. 1991).

Table 5-2: Comparison between soil type signatures and the Landsat TM bands.

Bands	Sand soils	Clay soils	Calcareous soils	Sand Dunes	Marshes	Swamps
B1	177.5	138.4	182.4	172.4	200.9	192.3
B2	118.6	79.47	108.7	111.6	129.2	121.4
B3	167.8	117.3	148.4	161.1	210.9	196.7
B4	144.5	100.1	123.6	139.5	166.3	156.4
B5	221.4	129.4	162.9	220.9	249.8	237.3
B7	143.6	78.3	93.8	138.5	169.4	158.5

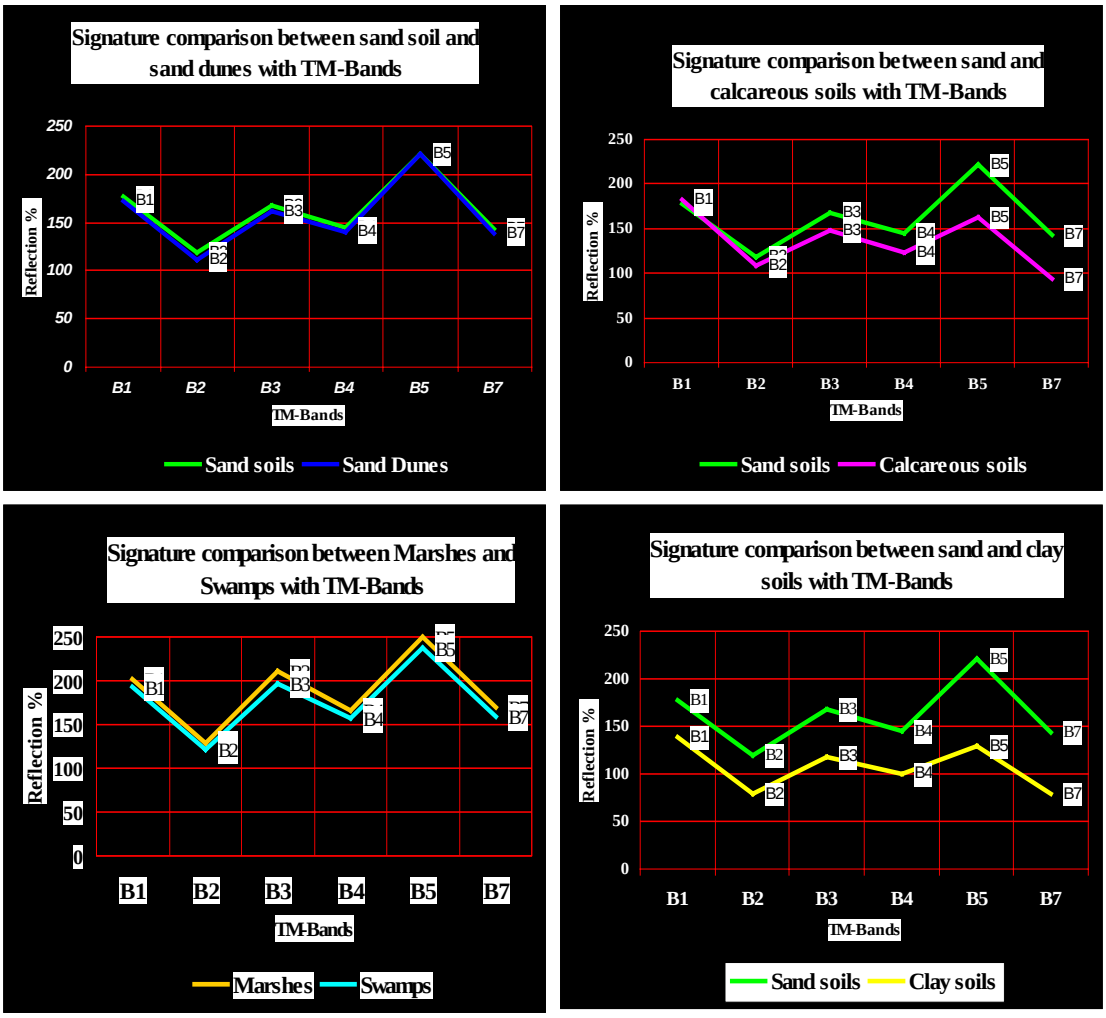

Fig. 5-2: Comparison signatures soil types, marshes and swamps with the Landsat TM bands reflections.

The results of this study are in line with the investigation of COLEMAN et al. (1991) who concluded that soil properties can be predicted from spectral data. The blue band 1, green band 2, red band 3, and middle infrared band 7 were the key bands in predicting silt content. The green, near infrared, middle infrared and thermal infrared bands 2, 5, 7 and 8 were found to be best for predicting clay content in these soils. Organic matter content was best predicted using the green band 2, middle infrared bands 6 and 7, and the thermal infrared band 8. MONTGOMERY et al. (1972) concluded that although all of the constituents of the surface of the soil assume some role in bestowing spectral character to soil, five soil parameters were found to be highly correlated with spectral reflectance. The parameters studied, CEC, silt, organic matter, iron (Fe_2O_3), and clay content were found to be the most significant for Midwestern soils. PAGE (1974) emphasized that although regression relationships for reflectance and organic matter have been established only for coastal plain soils, the procedure could be used in other areas where color changes in soils are due primarily to differences in organic matter. However, for each region it is essential to establish a regression equation which defines the relationship between reflectance and organic matter content. ABD El-Hady (1992) reported on the discrimination of the gypsiferous, calcareous and sand soil surfaces by using the PCA from the TM data. This study showed that the PC1 is composed of bands summation with a strong contribution of the TM bands 3, 5 and 7. The PC2 is expressed by the difference between the values of visible bands (1, 2 and 3) and the summation of near and far-infrared bands 5 and 7. KRISHNAN et al. (1980) found that the visible wavelength region provided better information than the infrared wavelength region for determining the organic matter content. The maximum correlation coefficient obtained for the given models in the infrared region was 0.87 and 0.98 µm for the visible wavelength region. The optimal wavelengths for organic matter were found to be 0.62 and 0.56 µm.

5.5 Evaluation of the soils along the El-Salam Canal area

Land evaluation is may be defined as: “The process of assessment of land performance when used for specified purposes” (FAO 1985) and/or “All methods to explain or predict the use potential of land” (Van Diepen et al. 1991). The potential of land resources for agricultural development in the El-Salam extension area is considered marginal to high. Even land with good potential for agricultural development has problems such as poor drainage, submergence

and salinity to the flat clayey lowland, together with erosion problems and poor retention for water and nutrients in sandy terrain.

The results of land evaluation for studied soils in the northern part of the Sinai peninsula along the El-Salam Canal soil project revealed that these soils classified in four grades (III, IV, V and VI soil grades).

The study soils of the grade (III) were affected by moderate limitations in the studied soil samples. Texture is the main limiting factor (in the South El-Kantara Shark and the Rabaa soils), also depth of soil profile (in the Bair El-Abd soils), slope (in the Wadi El-Arish soils) and wind erosion (in the South El-Kantara Shark and the Wadi El-Arish soils).

The study soils of the grade (IV) are affected by moderate to severe limitations. The texture, soil profile depth and relatively higher salinity (in the South El-Kantara Shark and Qatia soils) are the limiting factors for sample No. 7, 24 and 35, while texture and calcium carbonate content (in the Wadi El-Arish and Bair El-Abd soils) are the limiting factors for samples No. 37, 43 and 44.

The study soils of' the grade (V) have severe limitation, as they are extremely saline. Moreover, texture and drainage (in the El-Tina Plain soils) are the limiting factors of samples No. 14 and 15. Through removal of the soluble salts in the soils of the El-Tina Plain these soils could be belong to grade IV or III.

The study soils of' the grade (VI) are affect by severe limitations. Extreme salinity, texture and soil profile depth are the limiting factors for the profile sample No. 17 in the soils of the El-Tina Plain. Meanwhile, texture, strong salinity, gypsum and carbonate content are the limiting factors in the profile soil sample No. 18 in the El-Tina plain soil profile.

- **Soil evaluation of the El-Tina Plain area**

A review of the results of the study area reveals that, the El-Tina Plain soils are severely affected by many limiting factors i.e., extreme salinity with thick salt crust on the surface,

flooding and shallow saline ground water. For reclamation of these soils, lowering of the ground water level and protection against flooding are essentially required. Extremely high salt contents will require repeated leaching before the first crop can be planted. According to the LMP(1986), It is generally not economically feasible to include all of the El-Tina Plain soils in an irrigation project.

In the northern part of the El-Tina Plain area, however, a thick salt crust covers the surface, drainage by pumps will be necessary due to its low elevation and considerable cost will be necessary for salt leaching. Therefore, those areas are classified as class VI by JICA (1989) and excluded from the land reclamation. Fishery development is proposed in this area. ABD EL-GAPHOUR et al. (1990) showed that potentiality of the El-Tina Plain area is influenced by many constraints, i.e. non adequate natural drainage, excessive salt content and shallow saline water table, therefore they classified the lands as limited arable (IV). BAYOUMY (1998) and FARAG (1999) in their studies showed that soils of the El-Tina Plain have severe limitations such as extremely high content of salts thin to thick salt crust on the surface and saline water table is very shallow at 40 cm below the soil surface. The leaching of these soils under any condition will be time consuming and a costly process. From the agricultural point of view, they considered this mud flat currently not suitable for irrigation. They added that with removing the soluble salts, these soils could be classified as fair to poor soils. MANSOUR (1997) showed that the soils of the El-Tina Plain belong to grades V and VI. The limitations are mainly extremely saline as the soils were developed on Sabkhas soils.

- **Soil evaluation in the South El-Kantare Shark, the Rabaa and the Bair El-Abd area**

The level and undulating sandy terrain as well as sand dunes are largely predominant in the South El-Kantara Shark and east El-Tina Plain towards El-Arish. These soils are affected by many constraints related to soil topography and climate. Considering soil constraints, soil texture has its bearing on the low fertility and water holding capacity. Considering topography, a considerable part, including mobile elevated dunes should be excluded from any agricultural development. Also, the high wind erosivity necessitates a proper cropping system. In conclusion, a considerable portion of these lands is suitable for irrigation development but marginal, JICA (1989). On the other hand, land reclamation will be conducted as far as

possible in these areas of the sandy terrain taken into consideration the popularity of drip irrigation method, ABD EL-GAPHOUR et al. (1990). In another studied by ABD EL-HADY and YOUNES (1995) classified these soils (South El-Kantara Shark and the Bair El-Abd) into grade III. The limitations are coarse texture, slope, shallow soil depth and wind erosion. Mobile sand dunes are excluded from the land reclamation area. LAND MASTER PLAN (1986) added that for the dominant sandy soils low moisture availability is the main limitation. Relief will also be a limiting factor because of the presence of dunes. In the land management classification system, the soils of the South El-Kantara Shark, the Rabaa and the Bair El-Abd are classified as class IV.

- **Soil evaluation of the Wadi El-Arish (El-Sir and El-Quarir) area**

According to GARPAD (1994) the land management of the selected 65.000 hectares falls within class III and IV. The category III included lands with flat to undulating topography in various desert land forms. The soil texture is predominantly silty with various of gravel. The category IV includes sandy soils which are situated in undulating topography including low and medium-high dunes. The categories III and IV are rated as “moderately good arable” in the capability system for irrigated land use of the US Bureau of Reclamation (USBR). Therefore, all the land of this area is capable of agricultural utilization. In another studied by MANSOUR (1997), it is mentioned that these soils have many limitations such as, coarse texture, shallow soil depth, high calcium carbonate and gravel content. Therefore, the soils are belonging to grads III, IV and V.

The evaluation soil results for soil quality along the El-Salam Canal project area are give in table (5-3). These results were used to classify the soils under study according to their potentialities and limitations for the sustained production. The soils of the El-Tina Plain are belonging to grads V and VI, the limitations are mainly extremely saline as the soils were developed on Sabkhas. The soils of the South El-Kantara Shark, the Rabaa and the Bair El-Abd are belonging to grades III and IV, the limitations are coarse texture, shallow soil depth, slope and wind erosion. The soils of the Wadi El-Arish are belonging to III, IV, and V, the limitations are coarse texture, slope, high calcium carbonate content and wind erosion. From these results has been found also that the most important soil parameters that influence the

suitability classification in the studied area are soil texture, depth of the soil profiles, salinity, calcium carbonate content, slope and wind erosion.

Table 5-3: Evaluation soil results for soil quality along the El-Salam Canal project area.

Evaluation class	Suitability of soil quality for agriculture	Rating	Name and percentage of the area in the evaluation class	Areas size by hectare
I	Excellent	100 – 80	No soils in this rating class	---
II	Good	79 – 60	No soils in this rating class	---
III	Fair	59 – 40	SKS (40 to 47 %) * Rabaa (51 %) - El-Ahrar (42 %) - El-Nigila (45 %) Bair El-Abd (47 %) - El-Sadat (47 %) - El-Arawa (43 %) - El-Telol (41 %) - El-Kherba (47) Wadi El-Arish (41 %) - Abou Awaigila (58 %) - El-Garkada (41 %) - Gabal Libina (42 %) - Basin El-Arish (41 %)	31.500 29.400 29.400 56.700
IV	Poor	39 – 20	SKS (32 to 23 %) * Rabaa (35 %) - Qatia (34 to 35 %) - Rumana (32 %) - El-Ganien (39 %) - El-Ahrar (27 %) Bair El-Abd (37 %) - El-Telol (33 %) - El-Sadat (34 %) Wadi El-Arish - Basin El-Arish (31 %) - Bagdad (29 %)	31.500 29.400 29.400 56.700
V	Very poor	19 – 10	El-Tina Plain (10 to 18 %) Wadi El-Arish - Bair Lehfen (13 %) - El-Ressan (19 %)	21.000 56.700
VI	Not suitable	< 10	El-Tina Plain (8 %)	21.000

SKS* = South El-Kantara Shark

5.6 Recommendations for the El-Salam Canal soil project

Concerning the field soil survey, results of samples analysis, Landsat TM image data and previous data reviewed herein, the following recommendations and observations may be deduced:

- The most promising lands are moderately and marginally suitable for agricultural development. The soils are distinctly influenced by a combination of limitations, i.e., flooding, wetness, salinity, texture and hazards of wind activity and erosion. Accordingly, different remedial measures are recommended to be practiced, i.e., removal of excessive salts, improving soil structure, fertility and drainage conditions.

- Non-arable lands including mobile sand dunes and Sabkhas are to be excluded from the land reclamation area of the El-Salam Canal project in the northern part of the Sinai peninsula.

- Soils and water are the most important factors for agricultural development of any place. Therefore, the highest priority project is that a detailed soil survey be undertaken to delineate the different types of soils and would assign priorities to the area to be reclaimed. Detailed soil survey is also useful in locating experimental and extension farms for adducing farmers on planting, tillage and fertilizer practices for each soil type. Therefore, it is proposed here to carry out intensive detailed soil survey for promising areas before the final allocation of the El-Salam Canal water.

- The extension of the El-Salam Canal to the El-Sir and El-Quarir (El-Arish area) may be a high risk because of the topographic nature of the area, which is located at high elevation (60-110 m above sea level). These high altitudes indicate how high the water would need to be lifted for irrigation purposes and the associated demands for energy which would be associated with this. ABD ALLAH and ABOU-KHADRAH (1977), SAID (1990), JICA (1996), conform with these results and the field description in this studied area.

- Wind erosion in sand sheet areas and desert sand dunes can be expected. Conservation methods of wind erosion control include planting of ground cover vegetation, placement of windbreaks between the crop fields crop management and to spray hard cultivated areas through fixed chemical materials. (Bitumen).

- Unofficial water use along Hadous drain will result in water shortage in irrigation water further downstream of the El-Salam Canal, DRAINAGE RESEARCH INSTITUTE (DRI) (1993).

- Salinity levels after mixing of Damietta branch water with the drainage water from the Hadous and the El-Serw drains are predicted to be around 900-1100 mg kg^{-1}. The water is regarded as relatively high salinity water, and requires adequate drainage and special management when used for crop irrigation. Crop selection will need to take the salinity to lance of the plants into account. In addition to this, sodium levels in the irrigation water are high and this may affect the soil structure and permeability of the soils. Gypsum may be added if not present in the soil naturally in sufficient amounts. Some crops such as citrus fruits are sensitive to high sodium levels, MOUBARAK (1999) and DRI (1993).

- The impacts expected from the El-Salam Canal soil project activities on the present groundwater conditions include rising groundwater tables due to percolation losses and changes in the quality of the groundwater in the project areas.

- More water quality data are needed to assess the effects of pollutants such as heavy metals, pesticides on crops and on the groundwater (water of the El-Salam Canal is mixed water).

- Several attempts were made to stabilize the shifting dunes that encroach on the El-Arish road and those that migrate on the agricultural lands in the Wadi El-Arish and soils along the El-Salam Canal project area. It can be concluded that if shifting sand dunes will not be monitored (by remote sensing techniques) and controlled (by conservation methods), sand will completley cover some sectors of the El-Salam Canal project. MISAK and DRAZ (1997) and ABD ELMALIK (1999) have concluded that attempts to minimize sand encroachment and erodibility problems in the Wadi El-Arish have been sporadic and mostly ineffectual. During the last 20 years these attempts were centralized on the plantation of Acacia Ricinus and Casuarina trees. Then the sand dunes should be completely destroyed by leveling and then stabilized by vegetation covering the dunes with rock debris and/or mud were also recommended.

6 Summary

The northern part of the Sinai peninsula is one of the most strategic projects for agriculture extension in Egypt. This project (the El-Salam Canal) supplies about 168.000 hectares soils with mixed water from the Nile and agricultural drainage water to reclaim and cultivate these soils.

The principle goals of this study are the environmental study and soil survey of the coastal zone soils along the El-Salam Canal project to assess the development activities in this area and evaluate the soils of project. To achieve this aims, image data analysis of remote sensing data (the Landsat TM) was performed. In addition to this, field soil survey were done through field work trips, meteorological, hydrological, physical and chemical soil analysis.

This work of study reports on how remote sensing data together with a land evaluation system can be used to assess the quality of the soils in this area for agricultural use. The results show that remote sensing data is a very efficient way to evaluate large areas quickly and with sufficient accuracy. In addition to fieldwork, using of satellite images is necessary to construct a soil map for the north Sinai.

The results of such as evaluation process will help developing countries like Egypt, specially in the northern part of the Sinai peninsula area, to put their scarce resources on the most rewarding land in order to speed up the process of improving the welfare of the country and especially the rural population.

Eleven representative soil profiles and thirty six surface samples (seventy one soil samples) were collected from the study areas. These profiles and surface samples are representative of the all land cover units identified by remote sensing and field check as soils.

Four morphological units and landforms in the studied areas were identified from the Landsat TM image and field work:

- Coastal plain sand sheet and sand dunes (active and passive).
- Individual sabakha, Marsh and Swamp areas.

- Foreshore sand terrain, ridges and hummocks.
- Wadi El-Arish.

The parent materials which constitute of the study area are recognized into four groups. They are:

- Nile alluvium and lacustrine deposits (El-Tina Plain area).
- Lacustrine sand deposits (Bair El-Abd and El-Telol area).
- Aeolian sand deposits (South El-Kantara Shark, Rabaa and Qatia area).
- Calcareous and sand deposits (Wadi El-Arish area).

The soil classification has identified in two orders and three suborders in the study areas. The orders are Aridisols and Entisols, suborders are *Typic Torripsamments*, *Calciorthids* and *Typic Salorthids*.

The El-Tina Plain soils are very wide variations in $CaCO_3$. The gypsum is relatively high. The CEC, EC and ESP are relatively higher. The nitrogen and the organic matter are very low and decreases with depth, also phosphorus and total-K are relatively high, while pH is alkaline reaction in these soils.

The South El-Kantara Shark soils are sand deposits. The organic matter, $CaCO_3$ and gypsum content are low, while pH is moderately alkaline. The EC CEC, phosphorus and potassium values are relatively low in these soils.

Total calcium carbonate content, Organic matter content and gypsum in the Rabaa and the Bair El-Abd soils are very low. The EC values are non-saline to slightly saline in these soils, with relatively low values of CEC. The nitrogen and phosphorus content in these soils are very low and decrease with depth.

The Wadi El-Arish soils have high values of $CaCO_3$ content and wide variations in the content of organic matter with low content of gypsum. The pH is moderately alkaline with low values of EC and slightly higher values of CEC. The nitrogen is low, while phosphorus is moderately high in these soils.

The supervised classes (by the maximum likelihood algorithm method) in the studied areas were discriminated from the Landsat TM images as follows:

- In the north Sinai total area 19 classes were recognized and identified.
- In the El-Tina Plain area 16 classes were recognized and identified.
- In the South El-Kantara Shark 16 classes were recognized and identified.
- In the Rabaa and Qatia 15 classes were recognized and identified.
- In the Bair El-Abd 15 classes were recognized and identified.
- In the Wadi El-Arish 15 classes were recognized and identified.

Each of these classes were described and illustrated in the studied areas.

The correlation and regression statistical analysis were preformed between the Landsat TM bands (6 bands) and soil properties. The correlation coefficient relationships among spectral properties bands and soil properties are as follows:

- Band 4 (near infrared 0.76-0.9 μm) was more correlated with EC, CEC, CaCO3, Gypsum and soil texture (sand, silt and clay).
- Band 3 (red 0.63-0.69 μm) was more correlated with EC, CEC and Gypsum.
- Band 5 (mid infrared 1.55-1.75) was more correlated with organic matter, sand fraction and clay fraction.
- Band 7 (mid infrared 2.08-2.35 μm) was more correlated with pH values.
- Band 1 (blue 0.45-0.52 μm) was more correlated with organic matter.

The statistical analysis results of the studied area revealed two correlation between soil properties and the TM bands reflection. These correlation are inversely proportional between EC, CEC, gypsum, silt and clay and the TM band. The second correlation is directly proportional between $CaCO_3$, organic matter, total sand content and pH values and the TM bands reflections.

The contour line image maps were achieved from the Landsat TM-5 image and the results of the soil properties, such as EC, CEC, OM, $CaCO_3$, Gypsum and pH values in the studied area. These contour line maps can be help in the speed of development of the north Sinai along the El-Salam Canal study project.

The results of land evaluation for studied soils in the northern part of the Sinai peninsula along the El-Salam Canal soil project were revealed that these soils can be classified in four grades (III, IV, V and VI soil grades). The soils in grade (III) are limited by texture, soil profile depth (in the South El-Kantara Shark, Rabaa and Bair El-Abd soils), and by slope, wind erosion (in the Wadi El-Arish soils). The study soils in grade (IV) are restricted by texture, soil profile depth and relatively higher salinity (in the South El-Kantara Shark and Qatia soils), as well as texture and calcium carbonate (in the Wadi El-Arish and Bair El-Abd soils). The study soils in grades (V) and (VI) are affected by extremely saline, texture soil profile depth, gypsum, carbonate content and drainage (in the El-Tina Plain soils).

This work reports some observations around the soil classification and evaluation for urban soils by using the Landsat TM-5 images. In addition to this, presented some recommendations and suggestion around the El-Salam Canal project and the problems face development the northern part of the Sinai peninsula.

Zusammenfassung

Bodenkundliche Studien im nördlichen Küstenbereich der Sinai-Halbinsel (Ägypten) mit Hilfe von Fernerkundung

Das starke Bevölkerungswachstum in Ägypten führt zu der Notwendigkeit, neue Flächen für die landwirtschaftliche Produktion zu gewinnen, um ausreichend Lebensmittel produzieren zu können. Der nördliche Bereich der Sinai-Halbinsel ist eine der bedeutendsten Regionen für die Neulandgewinnung in Ägypten.
Durch das *El-Salam* Kanal Projekt sollen 168000 Hektar Land mit einer Mischung aus Nil- und Drainage-Wasser versorgt werden, um die dortigen Böden zu kultivieren.

Das Ziel dieser Studie war eine Bewertung der Böden entlang des *El-Salam* Kanals hinsichtlich ihrer natürlichen Eigenschaften und ihrer Nutzbarkeit für eine landwirtschaftliche Bearbeitung.

Zu diesem Zweck wurden im Untersuchungsgebiet Bodenproben gezogen und bodenphysikalisch und chemisch analysiert. Satellitenbilddaten (Landsat TM) wurden

klassifiziert und mit den Bodendaten in Beziehung gesetzt. Des weiteren wurden meteorologische und hydrologische Daten analysiert. Abschließend wurde die Eignung der Böden für die landwirtschaftlich Nutzung evaluiert.

Die Ergebnisse zeigen, daß mit Hilfe von Fernerkundungsdaten sehr effizient größere Regionen mit einer ausreichender Genauigkeit bewertet werden können. Zudem wurde eine Bodenkarte für das nördliche Sinai hergestellt.

Die Ergebnisse einer solchen Bodenbewertung helfen Entwicklungsländern wie Ägypten, ihre knappen Ressourcen auf erfolgversprechende Flächen zu konzentrieren, um die Lebensbedingungen, insbesondere die der ländlichen Bevölkerung, nachhaltig zu verbessern.

Elf repräsentative Bodenprofile und 36 Oberboden Proben (insgesamt 71 Bodenproben) wurden in der Testregion erhoben. Die Proben repräsentieren die Oberflächeneinheiten, die zuvor durch die Fernerkundungsdaten ausgewiesen wurden.

Insgesamt wurden durch die Bildauswertung 4 morphologische Einheiten und Landschaftsformen ausgewiesen:
Küstenebene mit Sandflächen und Dünen (aktiv und passiv)
Einzele Tonebenen, Marsch- und Sumpfflächen
Küstennahe Sandflächen, Rücken und Hügel
Wadi *El-Arish*

Das Ausgangsmaterial des Untersuchungsgebietes gliedert sich in 4 Untergruppen:
Nil-Alluvium und limnische Ablagerungen (*El-Tina* Ebene)
limnische Sandablagerungen (*Bair El-Abd und El-Telol*)
Aeolische Sandablagerungen (südliches *El-Kantara Shark*, *Rabaa* und *Qatia*)
Kalk und Sandablagerungen (Wadi *El-Arish*)

Das Untersuchungsgebiet gliedert sich nach der Bodenklassifikation (USA) in zwei Hauptgruppen (Aridisole und Entisole) und drei Untereinheiten (Typic Torripsamments, Calciorthids und Typic Salorthids).

Die Böden der *El-Tina* Ebene weisen eine hohe Variation bei $CaCO_3$ mit hohen Gipsgehalten auf. Die Kationen-Austausch-Kapazität (KAK), die elektrische Leitfähigkeit (EC) und der Gehalt an austauschbarem Natrium (ESP) sind in der Region relativ hoch. Die Gehalte an Stickstoff und organischer Substanz sind sehr gering und nehmen mit der Tiefe ab. Die pflanzenverfügbaren Phosphor- und Kaliumgehalte waren relativ hoch. Die Böden wiesen allesamt einen alkalischen pH-Wert auf.

Die Region des *südlichen El-Kantara Shark* ist geprägt von sandigen Böden. Die Gehalte an organischer Substanz, $CaCO_3$ und Gips sind gering, der pH-Wert leicht alkalisch. Die Leitfähigkeit und KAK, Phosphor und Kalium Werte sind relativ gering in diesen Böden.

Die Gehalte von Kalziumcarbonat, Gips und die organische Substanz sind in den Böden von *Rabaa* und *Bair El-Abd* sehr gering. Die elektrische Leitfähigkeit weist auf schwach saline Verhältnisse mit relativ geringen KAK Werten hin. Die Stickstoff- und Phosphorgehalte der Böden sind sehr gering und nehmen mit der Tiefe ab.

Das Gebiet des Wadi *El-Arish* weist hohe $CaCO_3$ Gehalte und starke Variationen bei der organischen Substanz auf. Zudem sind die Gipsgehalt niedrig. Die pH-Werte sind leicht alkalisch, die elektrische Leitfähigkeit ist gering und die KAK weist leicht höhere Werte auf. Die Stickstoffwerte sind gering, die Phosphorgehalte jedoch leicht erhöht in diesen Böden.

Eine überwachte Maximum Likelihood Klassifikation der Satellitenbilder führte zu folgenden Klassen:

Für den gesamten nördlichen Sinai konnten 19 Klassen ausgewiesen werden, 16 Klassen in der *El-Tina* Ebene, 16 Klassen im südlichen *El-Kantara Shark*, 15 Klassen in *Rabaa* und *Qatia*, 15 Klassen in *Bair El-Abd* und ebenfalls 15 Klassen in der Region des Wadi *El-Arish*.

Es wurde eine Korrelations- und Regressionsanalyse zwischen den einzelnen reflektiven Spektralbändern (6 Bänder) des Satelliten und den Bodeneigenschaften durchgeführt. Die Beziehungen zwischen den Spektralbändern und den Bodeneigenschaften waren im Einzelnen:

Band 1: (sichtbares Blau, 0.45-0.52 µm) Korrelation mit der organischen Substanz

Band 3: (sichtbares Rot, 0.63-0.69 µm) Korrelation mit elektrischer Leitfähigkeit, KAK und Gips

Band 4: (nahes Infrarot, 0.76-0.90 µm) Korrelation mit elektrischer Leitfähigkeit, KAK, Kalziumcarbonat, Gips und der Bodentextur (Sand, Schluff, Ton)

Band 5: (mittleres Infrarot, 1.55-1.75 µm) Korrelation mit organischer Substanz, Sand- und Tonfraktion

Band 7: (mittleres Infrarot, 2.08-2.35 µm) Korrelation mit pH-Wert

Die Ergebnisse der statistischen Untersuchungen ergaben Korrelationen zwischen den Bodenparametern und den Spektralbändern. Der Zusammenhang zwischen den Spektralbändern ist umgekehrt proportional zur elektrischen Leitfähigkeit, KAK, Gips, Schluff und Tongehalt. Des weiteren gibt es einen direkten proportionalen Zusammenhang zwischen $CaCO_3$, organischer Substanz, Sandgehalt und pH-Wert und den Spektralbändern.

Es wurden Isolinienkarten für die elektrische Leitfähigkeit, die Kationen-Austausch-Kapazität, organische Substanz, CaCO3, Gips und pH-Wert auf Basis der Satellitenbilder und der Bodendaten erstellt. Diese Karten können bei der Entwicklung der Region entlang des *El-Salam* Kanals hilfreich sein.

Als Ergebnis der Untersuchung lassen sich die Böden im Untersuchungsgebiet in 4 Einheiten (III, IV, V, VI) unterteilen. Einheit III beinhaltet Böden, die durch ihre Textur und die Profiltiefe (südliches *El-Kantara Shark, Rabaa* und *Bair El-Abd*) und durch Hangneigung und Winderosion (Wadi *El-Arish*) limitiert sind. Böden der Einheit IV sind ebenfalls durch Textur und Profiltiefe aber auch durch höhere Salinität (südliches *El-Kantara Shark*, *Qatia*) und $CaCO_3$ begrenzt. Die Böden der Einheiten V und VI zeichnen sich durch extreme Salinität aus, zudem werden die Bodeneigenschaften durch die Textur, Profiltiefe, Gips , $CaCO_3$ und Drainage beeinflußt (*El-Tina* Ebene).

Diese Arbeit befaßt sich mit Bodenklassifikationen und Bewertung auf der Basis von Landsat TM-5 Daten. Zusätzlich werden einige Empfehlungen zum *El-Salam* Kanal Projekt und Problemen bei der Entwicklung des nördlichen Sinai gegeben.

REFERENCES

Abd Allah, A. M. and Abou-Khadrah A. M. (1977): Remarks on the geomorphology of the Sinai peninsula and its associated rocks. Colloquium on the Geology of Aegean region Athens, IV: 509-516.

Abd El-Fattah, M. A. (1993): A multipurpose land information system (MPLIS) in the context of Egypt, The Canadian Conference on GIS, Ottawa, 1:830-841.

Abd El-Hady, A. M. (1988): Rapport d'activite au ministere francaise des relations exterieurs, pp. 106.

Abd El-Hady, A. M. (1992): Discrimination of the gypsiferous, calcareous and sand soil surfaces using the principal component (PC) transformation of Thematic Mapper. Egypt. J. Soil Sci., 32, No. 1, pp.71-80.

Abd El-Hady, A. M., Escadafel, R. and Rognon, P. (1992): Mapping of source zone of wind-deposited soils by the Landsat TM-5 data. Egypt. J. Soil Sci. 37, No. 1, pp. 57-70.

Abd El-Hady, A. M., Escadafel, R., Pouget, M. and Rognon, P. (1991): contribution of the Landsat data (MSS) to soil survey: application to the soil of southwestern Sinai (Egypt). INT. J. Remote Sensing, Vol. 12, No. 5, pp. 1053-1061.

Abd El-Hady, M. A. and Younes, H. A. (1995): Land capability classification of the Sinai peninsula. National Authority for Remote Sensing and space sciences. Ministry of Scientific Research, Cairo Univ., Egypt.

Abd El-Malik, K. W. M. (1999): Integrated geoenvironmental assessment of development activities in north western Sinai, Egypt. Ph. D. Thesis, Fac. Sci. Geology Department, Ain Shams University, Cairo, Egypt.

Abd El-Monsif, H. (1996): Development of appropriate image processing methods for geologic mapping of sedimentary rocks in the northern Sinai, Egypt. Ph. D.thesis (Unpublished), Fac. Sci., Suez Canal Univ.

Abdel-Gaphou, E. S. A., El-Shazly, M. M. and El-Dosouky (1990): Land capability and rational utilization of soils Egypt J. Soil Sci., 30 (1-2):73-89.

Abdel-Rahman, S. I., Younes, H. A. and Onsi, H. (1995): Utilization of remote sensing data and land information systems for landuse planning in central Sinai, Egypt, GIS/LIS, pp. 858- 868.

Anonymous (1982): EC-12 Carbon determination Modell 752-100 instruction manual 200-214.

Asrar, G. (1989): Theory and Application of Optical Remote Sensing. Chap. 3, Soil Reflectance. pp. 88-92, John Wiley & Sons, Inc.

Atkins Land and Water Management (ALWM) (1989): El-Tina Plain development project. Feasibility Study.

Attia, Y. D. (1994): Rainfed agriculture in the northern coast of the Sinai. Workshop of Sustainable Development of the Rainfed Areas in Egypt, Academy of Scientific Research and Technology, Cairo, Egypt.

Balba, A. M. (1997): Soil and water resources and development in the north Sinai , Egypt. Sahara research and Review, 9: 1-14 .

Baret, F. (1994): Imaging spectrometry in agriculture, comparison of modellistic approaches and experimental data. In: J. Hill & J. Megier Eds., Imaging Spectrometry a Tool for Environmental Observations. Dordrecht, Kluwer Academic, 20 pp.

Barrett, E. C. and Curtis, L. F. (1992): Introduction to environmental remote sensing. 3rd ed., Chapman & Hall, New York.

Baumgardner M. F., Silva L. F., Biehl L. L. and Stoner E. R. (1985): Reflectance properties of soils. In : N. C. Brady Ed., Advances in Agronomy 38. Academic Press Inc. Orlando, Florida, pp.1-44.

Baumgardner, M. F., Kristof, S. J., Johannsen, C. J. and Zachary, A. L. (1970): Effects of organic matter on the multispectral properties of soils. Proc. Indiana Academy of Science, Vol. 79, pp.413-422.

Bayoumy, M. R. (1998): Soil resources and their agricultural potentiality in Sinai. In project of development of Sinai: nitrogen fixing leucaena trees, Cairo Univ. Publications ISBN.

Bayoumy, N. A., Gobran, O. A. and Shehata, R. B. (1992): Mineralogical study of soils belonging to different physiographic units in the eastern side of Egypt. Egypt. J. Soil Sci., Vol. 23, No.3, pp. 437-453.

Bernstein, R. (1983): Image geometry and rectification: In Colwell, R. N. (Ed.) Manual of Remote Sensing (2^{nd} end). American Society of Photogrammetry, Falls Church, Virginia, pp. 873-922.

Black, C. A. (1957): Soil plant relationship. New York, John Wiley Sons, Inc.

Black, C. A., Evans, D. D., Nhite, J. I., Ensminger, L. E. and CLARK, F. E. (1982): Methods of soil analysis. Amer. Sco. Agron. Inc. Madison, Wisconsin U.S.A.

Blanchard, L. E. and Weinstein, O. (1980): Design challenges of the thematic mapper. IEEE Trans. On Geoscience and Remote Sens. GE-18, pp. 146-160.

Blume, H. P. (1966): Bodenkundliches praktikum. Paul-Parey, Stuttgart.

Bowers, S. A. and Hanks, R. J. (1965): Reflection of radiant energy from soil. Soil Science, 100: pp. 130-138.

Cahoon, G. A. (1974): Handbook of reference methods for soil testing. The Council of Soil Testing and Plant Analysis. 101 P. Athens, Georgia.

Canas, A. A. and Barnet, M. (1985): The generation and interpretation of false color principal component image. Intern. J. remote sensing, Vol. 6, pp. 867-881.

Chavez, P. S., Berlin, G. L. and Sowers, L. B. (1984): Statistical method For selecting Landsat MSS ratios. Journal Of Applied Photographic Engineering, Vol. 8, pp. 23-30.

Cipra, J. E., Baumgardner, M. F., Stoner, E. R. and Mac-Donald, R. B. (1971): Measuring radiance characteristics of soil with a field spectroradiometer. Soil Sci. Soc. Am. Proc. J. 35: 1014-1017.

Cohen, W. B. (1991): Temporal versus spatial variation in leaf reflectance under changing water stress condition. International Journal of Remote Sensing, Vol. 12, pp.1865-1876.

Coleman, T. L., Agbu, P. A., Montgomery, O.L., Gao, T. and Prasad, S. (1991): Spectral band selection for quantifying selected properties in highly weathered soils. Soil Sci. Vol. 151, No. 5, pp. 355-361.

Collinson, J. D. (1978) Lakes and deserts in: Sedimentary environments and faces (Ed. By Reading, H. G.) Elsevier, New York, pp. 61-96.

Coulson, K. L. and Reynolds, D. W. (1971): The Spectral reflectance of natural surface. J. Appl. Meteorol. 10: 1285-1295.

Crippen, R. E. (1987): The regression intersection method of adjusting image data for band rationing. Intern. J. Remote Sensing, Vol. 8, No. 2, pp. 137-155.

Curran, P. J. (1980a): Multispectral photographic remote sensing of vegetation amount. Progress in Physical Geography, 4: 315-341.

Curran, P. J. (1986): Principals of remote sensing. Essex CM20 2JE, Longman Group Limited, England.

Curran, P. J. (1985): Principles of remote sensing. London, New York: Longman.

Dames and Moore (1981): Agricultural and water investigation of the Sinai. Desert Institute, Mataria, Cairo, A.R.E.

Dames and Moore (1983): Sinai development study, final report.

De Leenheer, L., Van Ruymbeke, M. und Maes, L.(1954): Die kettenaräometer methode für die mechanische bodenanalyse. Z. Pflanzenernähr. Bodenk. 68 : 10-19.

Drainage Research Institute (DRI) (1993): Drainage water, Volume 111. Drainage Water Reuse Project.

Elachi, C. (1987): Introduction to the physics and techniques of remote sensing. Chap. 3 Use of Spectral and Radiometric Signatures in Surface Studies. John Wiley &Sons, Inc.

El-Shazly, E. M., Abdel Hady, M. A., El-Gawaby, M. A.; El-Kassas, I. A. and El-Shazly, M.M. (1974): Geology of Sinai peninsula from ERTS-1 satellite images. Remote Sensing Research Project, RESC., Acad. Sci. Res. And Tech., Cairo.

El-Shazly, M. M. and Abdel-Gaphour, E. S. A. (1990): Genesis, formation and classification of soils of the coastal plain of the Sinai peninsula. Egypt. J. Soil Sc. 30:(1-2) 59-72.

Elvidge, C. D. (1990): Visible and near-infrared reflectance characteristics of dry plant materials. International Journal of Remote Sensing, Vol.11, pp. 1775-1795.

ERDAS (1997): Erdas field guide. Atlanta Georgia, USA, ERDAS, Inc.

ESA (1991): Report from agricultural statistics department. Egyptian Survey Authority, Cairo, (In arabic).

Eurimage (2000): DESCW software version 4.15 from ESA-ESRIN, www.eurimage.com.

FAO (1985): Guidelines: land evaluation for irrigated agriculture. Soils Bulletin 55, Rome, Italy: FAO 231 pp.

FAO (1970): Guidelines to soil description. FAO, Publication, Rome.

Farag, F. M. (1999): Soils of the El-Salam Canal basin and their agricultural suitability. Annal of Agric. Sc. Moshtohor, 37 (2):1435-1453.

Faust, N. L. (1989): Image enhancement. Vol. 20, Supplement 5 of Encyclopedia of computer science and technology, Edited by Allen K. and James G., New York, Marcel D., Inc.

Freney, J. R. (1958): Determination of water-soluble sulfate in soils. Soil Sci. 86 : 241-244.

General Authority for Rehabilitation Projects and Agricultural Development (GARPAD) (1994): Preliminary feasibility study, An area of 135.000 feddans in El-Sir and El-Quarir Region of El-Arish Valley.

Goel, N. S. (1989): Inversion of canopy reflectance models for estimation of biophysical parameters from reflectance data. In :G. Asrar Ed., Theory and Applications of Optical Remote sensing. Wiley , New York, pp. 205-251.

Greenbaum, D. (1987): Lithological discrimination in central Snowdonia using airborne multispectral scanner imagery. INT. J. Remote Sensing, Vol. 8, No. 6, pp. 799.

Gupta, R. P. (1991): Remote sensing geology. Springer Verlag Berlin Heidelberg Germany, Vol. 10, pp.25-35.

Guyot G., Baret, F. and Jacquemoud, S. (1992): Imageing spectroscopy for vegetation studies. IN: F. Toselli & J. Bodechtel, Imaging Spectroscopy: Fundamentals and Prospective Applications . Kluwer Academic , Dordrecht, pp.145-165.

Henderson, T. L., Szilagyi, A., Baumgardner, M. F., Thomas Chen, Ch. and Landgrebe, D. A. (1989): Spectral band selection for classification organic matter content. Soil Sci. Soc. Am. J., Vol. 53, pp. 1778-1784.

Hill, J. (1993): High precision land cover mapping and inventory with multi-temporal earth observation satellite data. Office for official Publications of the European Communities, Brussels, Luxembourg.

Hoffer, R. M. (1976): Spectral reflectance characteristics of earth surface feautures. In "Fundamentals of Remote Sensing" Minicourse Series, Purdue University, West Lafayette, Ind.

Hoffer, R. M. (1978): Biological and physical considerations in applying computer-aided analysis techniques to remote sensor data. In P. H. Swain and S. M. Davis, Eds., Remote Sensing: The Quantitative Approach, N. Y., McGraw-Hill.

Hoffer, R. M. (1979): Computer aided analysis techniques for mapping earth surface features. Technical Report 020179, Laboratory for Applications of Remote sensing, Purdue University, West Lafayette, Indiana.

Hoffer, R. M. and Johannsen, C. J. (1969): Ecological potentials in spectral signature analysis. In Johnson, P. L. (Ed.). Remote Sensing in Ecology. University of Georgia Press, Athens, Ga.

Hord, R. M. (1982): Digital image processing of remote sensed data. New York, Academic Press, Inc.

Huete, A. R. and Jackson, R. D. (1987): The suitability of spectral indices for evaluating vegetation characteristics on arid range lands. Remote Sensing of Environment 23, pp.213-232.

Hunt, G. R. (1980): Electromagnetic radiation: The Communication Link in Remote Sensing . In: Siegal, B. S. and Gillespie, A. R. Remote Sensing in Geology , pp.5-46.

Hunt, G. R., Salisburg, J. W. and Lenhoff, C. J. (1970): Visible and near infrared spectra of minerals and rocks. I. Silicates. Minerals Mod. Geol. 1: 283-300.

Hunt, G. R., Salisburg, J. W. and Lenhoff, C. J. (1971): Visible and near infrared spectra of minerals and rocks. II. Carbonates Mod. Geol. 2: 23-30.

Hunt, G. R., Salisburg, J. W. and Lenhoff, C. J. (1973): Visible and near infrared spectra of minerals and rocks. VI. Additional silicates. Mod. Geol. 4: 85-106.

Irons, J. R., Weismiller, R. A. and Petersen, G. W. (1989): Soil reflectance. In : G.Asrar Ed., Theory and Applications of Optical Remote Sensing. Wiley, New York, pp.66-106.

Jackson, M. L. (1973): Soil chemical analysis. Prentic-Hall. Inc. Engl. Wood, Cliffs. U.S.D.

Japan International Cooperation Agency (JICA) (1989): North Sinai integrated rural development. The Master plain (August 1989).

Japan International Cooperation Agency (JICA) (1996): The feasibility study on the north Sinai integrated rural development project, Phase II, Interim Report.

Jensen, J. R. (1986): Introduction to digital image processing. Prentice-Hall, Englewood cliffs, New Jersy, USA.

Jensen, J. R. (1996): Introductory digital image processing. A Remote Sensing Perspective. Englewood Cliffs, New Jersey Prentice.

Jenson, S. K. and Waltz, F. A. (1979): Principal components analysis and canonical analysis in remote sensing. Proc. Am. Soc. Photogra. 45th Tnn. Meeting : 337.

Jiaju, Lu. (1988): Development of principal components analysis applied to multitemporal Landsat TM Data. International Journal of Remote Sensing. Vol. 9, No. 12, 1895-1907.

Khalaf, F. I., Zaghloul, E., Gad, A., Mahmoud, A. M. and Khidr, A. H. (1997): Preliminary assessment of the impacts of the drifting sands on the development activities in north-western Sinai, Egypt. Nat. Auth. Rem. Sens. and Space Sci., 120 p.

Kirschner, F. R., Kaminsky, R. A., Weismiller, H. R., Sinclairm, H. R. and Hinzel, E. J. (1978): Map unit composition assessment using drainage classes defined by Landsat data. Soil Sci. Soc. Am. J., Vol. 42, pp. 768-771.

Kontoes, C. and Stakenborg, J. (1990): Availability of cloud-free Landsat image for operational projects. The Analysis of Cloud-cover Figures over the Countries of the European Community; Int.J. Remote Sensing, Vol. 11, 1599-1608 pp.

Krishnan, P., Alexander, J. D., Butter, B. J. and Hummel, J. w. (1980): Reflectance techniques for predicting soil organic matter. Soil Sci. Soc. Am. J. 44 : 1282-1285.

Land Master Plan (LMP) (1986): LMP project regional report. Sinai, RPDA, Egypt.

Latz, K., Weismiller, R. A., Van Scoyoc, G. E. and Baumgardner, M. F. (1984): Characteristic variations in spectral reflectance of selected eroded Alfisols. Soil Sci. Soc. Am. J. 48: 1130-1134.

Legg, C. (1994): Remote sensing and geographic information systems: Geological mapping, mineral exploration and Mining. John Wiley & Sons, Inc., 605 Third Avenue, New York, USA.

Lillsand, T. M. and Kieffer, R.W. (1994): Remote sensing and image interpretation. 2rd ed., Wiley New York.

Lillsand, T. M. and Kieffer, R.W. (1997): Remote sensing and image interpretation. 3rd ed., Wiley New York.

Lindsay, W. L. and Norvell, W. A. (1978): Development of a DTPA soil test for Zinc, Iron, Manganese and Copper. Soil Sci. Soc. Amer. Pro. 42 : 421-428.

Malthus, T. J., Andrieu B., Mark Danson, F., Jaggard, K. W. and Steven, M. D. (1993): Candidate high spectral resolution infrared indices for crop cover. Remote sensing of Environment 46, pp. 204-212.

Mansour, A. A. M. (1997): Studies on soil types along El-Salam Canal territory in North Sinai .M. Sc. Thesis, Fac. Agric. Cairo Univ .

Mansour, M. A (1979): An approach to land evaluation for rural purpose of some alluvial soils of Egypt. Msc. Thesis, Fac. Agric. Cairo. Univ.

Matthews, H. L. (1972): Application of multispectral remote sensing and spectral reflectance patterns to soil survey research. Ph.D. Dissertation, Pennsylvania State University, College Station, Pa.

Mehlich, A. (1938): Use of triethanolamine acetate-barium hydroxide buffer for the determination of some base exchange properties and lime requirement of soil. Soil Sci. Soc. Am. Proc. 29:374-378.

Mikihiro, I. and Masato, K. (1986): performance of the Landsat TM-5 data in land cover classification. INT. J. Remote Sensing, Vol. 7, No. 12, pp. 1715.

Ministry of Public Works and Water Resources (MPWWR) (1994): Plans of horizontal extension. Report (in Arabic).

Misak, R. and Draz, M. Y. (1997): Sand drift control of selected coastal and desert dunes in Egypt case study. J. Arid Envi., Vol. 35, pp. 17-28.

Montgomery, O. L. (1976): An investigation of the relationship between spectral reflectance and the chemical, physical and genetic characteristic of soil. Ph.D. Dissertation, Department of Agronomy, Purdue University, West Lafayette, Ind.

Montgomery, O. L., Baumgardner, M. F. and Weismiller, W. A. (1972): Relationship between spectral reflectance and the chemical, physical and genetic characteristics of soils. LARS Information Note 082776, West Lafayette, Ind.

Moubarak, Kh. S. (1999): Studies on the reclamation of soils irrigated from El-Salam Canal. M.Sc. Thesis, Fac. Agric. Suez Canal University, Egypt.

Mulders, M. A. (1987): Remote sensing in soil science. Developments in soil science 15. Elsevier, Amsterdam, 379 pp.

Mulders, M. A. (1985): Remots sensing in soil science. Elsevier Science Publishing Company INC. 52, Vanderbilt Avenue, New York, NY 10017, USA.

Mulders, M. A. and Epema, G. F (1986): The Thematic Mapper (TM). A New tool for soil for mapping in arid Areas. 4th ISSS Symposium of Working Group remote Sensing for Soil Survey (1985). ITC Journal, Enschede, The Netherlands.

Nadim, M. A. (1986): Pedological studies on some soils in the northern Sinai. M.SC. Thesis, Fac. Agric., Ain Shams University, Egypt.

NASA (1987): Ada style guide. Version 1.1, SEL-87-002. Greenbelt, Maryland: NASA, Goddard Space Flight Center.

Nasr, Y. A. (1988): Soil qualities with special reference to mineralogy and fertility status as related to environments of some areas in Sinai, Egypt. Ph.D. Thesis, Fac. Agric., Cairo Univ. Egypt.

National Aeronautics and Space Administration (NASA) (1998): The Landsat program summary. http://geo.arc.nasa.gov/sge/lansat/lpsum.html. date 12/12/1999.

Noaman, K. I., El-Demerdashe, S. E. and Ali. O. M. (1987): Clay mineralogy in relation to lithology, topography and depositional environment of the soils of north and North-western Sinai Peninsula, A.R.E. annals of Agric. Sc., Moshtohor 25 (4) : 2425-2442.

Noman, K. I., El-Demerdashe, S., Farage, F. and Ali, O. M. (1982): Pedological study of some soils sediment in the north Sinai. Ain Shams Uni., Fac. Agr., Research Bull. No.: 2023, Cairo, Egypt.

Nowers, R. J. and Schreuder, D. R. (1981): Broadening the environmental vision of agricultural students through training: A case study of sustainable agricultural training at the Elsenburg College of agriculture, South Africa. http://www.wcape.agric.za/economics/Results/Publikasies/Riaan/Broadening%20environ20. date1/2/02.

Page, N. R. (1974): Estimation of organic matter in atlantic coastal plain soil with a Color difference meter. Agronomy Journal, Vol. 66, pp. 652-653.

Rabie, F. I., Sheta, A. and Nadim, M. (1993): Pedological and mineralogical characteristics of some soils in the northern Sinai. 2nd African Soil Sci. Sco. Conf.

Rabie, F. H., Elwan, A. A. and Sallam, A. Sh. (1983): Genesis formation and development of the north Wadi El-Arish siols. Desert Inst. Bull., A.R.E., 33, No. 1and 2, pp.217-230.

Reeves, R. G. (1975): Manual of remote sensing. American Society of Photogrammetry, Falls Church, VA, Vol. 2, pp. 2144.

Richards, J. A. (1984): Thematic mapping from multitemporal image data using the principal components transformation. Remote Sensing of Environment, 16, pp. 35-46.

Richards, J. A. (1994): Remote sensing digital image analysis an introduction. Springer-Velag Berlin Heidelberg, Germany.

Rivereau, F. C., Lallmand, C. and Thomas, G. (1978): Interet de l'analyse en composantes principals pour l'interpretation geologique des images Landsat. Photo. Interpretation, No. 5, Fascicule 6, Paeis.

Sabins, F. F. (1987): Remote sensing: Principal and interpretation. Freeman and Company, New York, 449 pp.

Said, R. (1990): The geology of Egypt. Balkema, Rotterdam, Molom, 734 p.

Saxton, K. E., Rawls, W. J., Romberger J. S. and Papendick, R. I. (1986): Estimating generalized soil-water characteristics from texture. Soil Sci. Soc. Am. J. 50 : 1031-1036.

Sayegh, A. H., Khan, N. A., Khan, P. and Ryan, J. (1978): Factors affecting gypsum and cation exchange capacity determinations in gypsiferous soils. Soil Science 125 : 294-300.

Schüller, H. (1969): Die CAL-Methode, eine neue methode zur bestimmung des pflanzenverfügbaren phosphates in Böden. Z. Pflanzenernähr. Bodenk. 123 : 48-63.

Shata, A. A. (1959): Structure development of the Sinai peninsula, Egypt. The Desert Inst. Bull. Tome 6, No. 2.

Shata, A. A. (1998): Potential water resources of the Sinai peninsula, a review paper. Project of Development of Sinai Agriculture: Nitrogen Fixing Luecaene trees, Cairo Univ. Publications ISBN.

Sheffield, C. (1985): Selecting Band Combination from Multispectral Data. Photogrammetric Engineering And Remote Sensing. Vol. 51, No. 6, pp.681-687.

Sillanpää, M. (1982): Micronutrients and the nutrient status of soils: a global study. Chapter: 8, FAO soils Bulletin 48, Rome.

Sillanpää, M. (1990): Micronutrient assessment at the country level: An International Study. Pub. By Food and Agriculture Organization (FAO)of the United Nations Rome.

Singh, A. and Harrison, A. (1985): Standardized principal components. International Journal. of Remote Sensing, 6, pp. 883-896.

SIS publications, (1999): The Al-Salam Canal project http://www.sis.gov.eg/calendar/htm1/c1191196.htm/, pp.1-7 data 11/7/1999.

SIS publications, (2000): The National Project for the Development of the Sinai (1994-2017). http://www.sis.gov.eg/public/sinai/html/text00.htm. chaps.1&2. Date 10/5/2000.

Soil Survey Manual (1993): Soil survey manual. Handbook Superintendent of Documents U.S. Government Printing Office, Pittsgurg, PA, U:S.A. (Online: http://bookstore.gpo.gov. date 25/11/1993).

Soil Survey Manual (1951): Soil survey manual. U.S.D.A. Handb. No. 18 U.S. Government Printing Office, Washington, D. C.

Soil Taxonomy (1975): Soil Taxonomy: A basic system of soil classification for marking and interpreting soil surveys. Agric. Handb. No. 436 SCS-USDA U:S. Government Printing Office, Washington, D.C.

Stanley, D. (1988): Subsidence in the north-eastern Nile delta. Rapid Rates, Possible Causes, and Consequences. Science, Vol. 240, pp. 497-500.

Stoner, E. R. and Baumgardner, M. F. (1980): Physicochemical, site, and bi-directional reflectance factor characteristics of uniformly moist soils. LARS Tech. Rep. 111679. Purdue University, West Lafayette, Indiana.

Stoner, E. R. and Baumgardner, M. F. (1981): Characteristic variations in reflectance of surface soils. Soil Sci. Soc. Am. J. 45 : 1161-1165.

Storie, R. E. (1964): Handbook of soil evaluation. Associated students bookstorie, University of California, Berkeley, California.

Sys, C. (1991): Land Evaluation. part I and II, Lecture Notes, Ghent Univ., Ghent, Belgium.

Till, R. (1978): Arid shorelines and evaporates in : sedimentary environments and faces. (Ed. By Reading, H. G.) pp. 178-206.

US Geological Survey (1982): Landsat data Notes, Issue No.23 (July, 1982). Eros Data Center, Sioux Falls, S. Dakota : pp. 1-12.

USDA Soil Survey Staff (1975): Soil survey manual. Handbook no. 18, U.S. Depaetment of Agriculture, Washington, D.C.

Van Diepen, C. A., Van Keulen H., Wolf J. and Berkhout, J. A. A. (1991): Land evaluation from intuition to quantification, in Advances in Soil Science, Stewart, B.A. Editor, New York, Springer. P.139-204.

Way, D. (1978): Terrain analysis, a guide to site selection using aerial photographic Interpretation. 2nd ed., Dowden, Hutchinson and Ross, Stroudsburg, PA, 1978.

Weismiller, R. A. and Kaminsky, S. A. (1978): Application of remote sensing technology to soil survey research. J. Soil Water Conservation. No. 33 (6), pp. 287-289.

Weismiller, R. A., Van Scoyoc G. E., Pazar S. E., Latz K. and Baumgardner M.F. (1985): Use of soil spectral properties for monitoring soil erosion. In :S.A. El-Swaify Ed., Proc. Conf. Soil Erosion and Conservation, Jan.16-22, Hawaii, pp.119-127.

Wessman, C. A. (1994): Estimating canopy biochemistry through imaging spectrometry. In : J. Hill & J. Megier Eds., Imaging Spectrometry a Tool for Environmental Observations. Dordrecht, Kluwer Academic, . 14 pp.

Worcester, Ph. G. (1969): A text book of geomorphology. Affiliated east-west Press PVT. LTD New Delhi.

Younes, H. A., Abdel-Samie. A. G., Mohamed, S. A. and Afifi, M. Y. (1977): Pedological studies on the soils of fluvio-marine origin in the Port Said Region Desert Inst. Bull., A.R.E, 21 (1) 251-266.

APPENDIX I

Morphological description of the studied soil profiles in the northern part of the Sinai peninsula along the El-Salam Canal project.

First area of study El-Tina Plain

Profile No.: 1
Location: El-Tina Plain (about 1 km South El-Salam canal)
Slope: Flat to almost flat
Vegetation: Non natural vegetation
Drainage: Poorly drained
Parent material: Alluvium deposits
Remark: The upper layer 9 cm salt crust
Classification: Typic Salorthids

Depth (cm)	Description
0-9	Salt crust (white color; hard; continuous; abrupt smooth boundary.
9-20	Light gray (10 YR 7/2, dry) to brown (10 YR 5/3, moist); sandy; weak, medium single grains; non sticky, non plastic, loose, loose; few gypsum crystals; weak effervescence with HCl; non roots; some of medium shells; clear smooth boundary.
20-110	Gray (10 YR 5/1, dry) to dark gray (10 YR 4/1, moist); clay; strong, fine, massive; very sticky, very plastic, firm, very hard; few gypsum crystals; moderate effervescence with HCl; non roots; some of few shells.

Profile No.: 2
Location: El-Tina Plain
Slope: Flat to almost flat
Vegetation: Non natural vegetation
Drainage: Imperfectly drained
Parent material: Sandy deposits
Remark: ~ 1 cm salt mixed with particle soils.
Classification: Typic Salorthids

Depth (cm)	Description
0-17	Grayish brown (10 YR 5/2, moist); sandy clay; moderate, fine, massive; sticky, plastic, friable; many salt crystals and few fine gypsum crystals; weak effervescence with HCl; non roots; few shells; clear smooth boundary.
17-70	Brown (10YR 5/3, moist); sandy; weak, medium, single grains; non sticky, non plastic, loose; few salt crystals, non effervescence with HCl; non roots; gradual smooth boundary.
70-140	Grayish brown (10 YR 5/2, moist); sandy; weak, medium, single grains; non sticky, non plastic, loose; non effervescence with HCl; non roots.

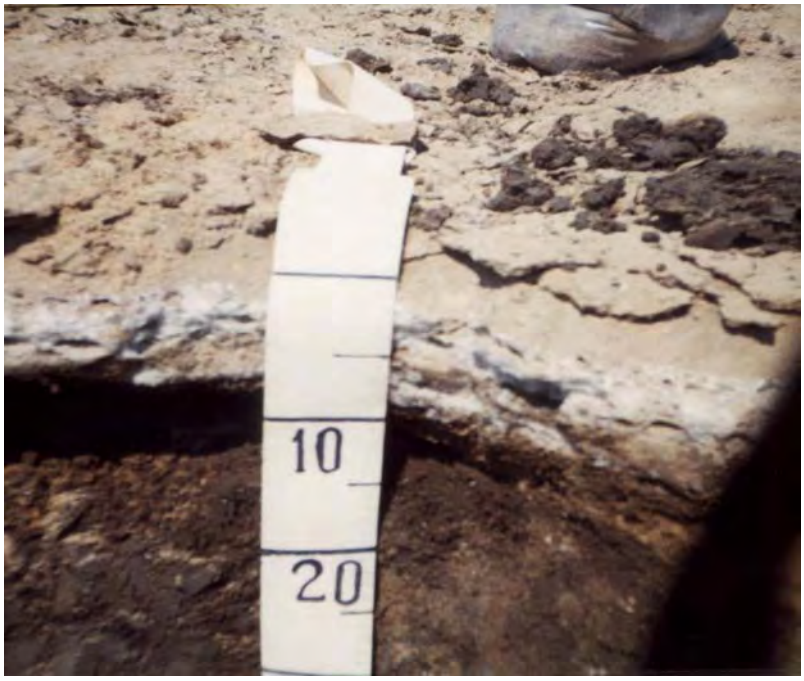

Fig. A1-1: Profile No. (1) in the El-Tina Plain area.

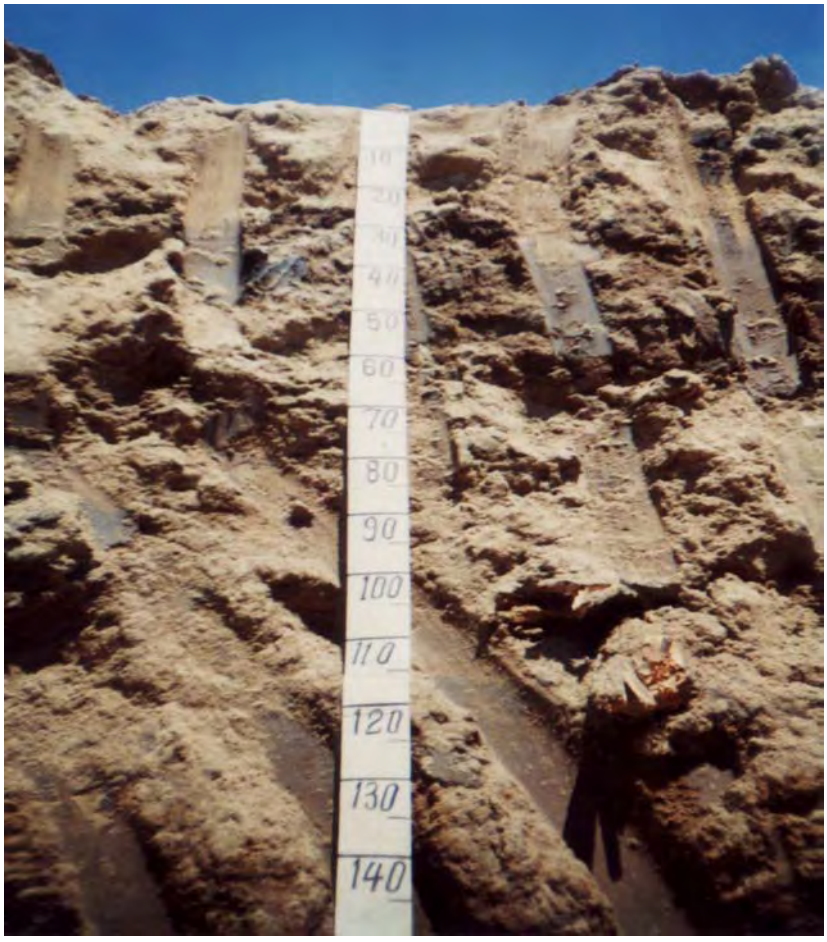

Fig. A1-2: Profile No. (2) in the El-Tina Plain area.

Second area of study South El-Kantara Shark

Profile No.: **1**

Location: **El-Amal village**
Slope: **Almost flat**
Vegetation: **Few natural vegetation**
Drainage: **Well drained**
Parent material: **Sandy deposits**
Classification: **Typic Torripsamments**

Depth (cm)	Description
0-42	Yellow (10 YR 8/6, dry) to brownish yellowish (10 YR 6/6 moist); coarse sand; single grains; non sticky, non plastic, loose, loose; non effervescence with HCl; few fine roots; clear smooth boundary.
42-50	Yellow (10 YR 8/6, dry) to yellowish brown (10 YR 5/6, moist); sandy; massive; non sticky, non plastic, loose, slightly hard; non effervescence with HCl; many fine and few medium roots; clear smooth boundary.
50-125	Yellow (10 YR 8/6, dry) to yellowish brown (10 YR 5/6, moist); coarse sand; single grains; non sticky, non plastic, loose, loose; non effervescence with HCl; diffuse smooth boundary.
125-160	Yellow (10 YR 8/6, dry) to brownish yellowish (10 YR 6/6, moist); fine sand; single grains; non sticky, non plastic, loose, soft; non effervescence with HCl.

Profile No.: **2**

Location: **El-Amal village**
Slope: **Undulation**
Vegetation: **Few natural vegetation**
Drainage: **Well drained**
Parent material: **Sandy deposits**
Classification: **Typic Torripsamments**

Depth (cm)	Description
0-20	**Very pale brown (10 YR 7/3, dry) to pale brown (10YR 6/3, moist); loamy sand; massive; slightly sticky, slightly plastic, soft, very friable; weak effervescence with HCl; few medium roots; clear smooth boundary.**
20-130	**Very pale brown (10 YR 8/3, dry) to pale brown (10 YR 6/3, moist); sandy loam; massive; slightly sticky, slightly plastic, slightly hard, friable; medium effervescence with HCl; few fine roots; few, fine and medium mottling; clear wavy boundary.**
130-164	**Light yellowish brown (10 YR 6/4, dry) to grayish brown (10 YR 5/2, moist); loamy sand; massive; slightly sticky, slightly plastic, slightly hard, very friable; medium effervescence with HCl; non roots; many, fine and medium mottling; clear wavy boundary.**
164-168	**Hard pans (very pale brown 10 YR 8/3, dry) to light yellowish brown (10 YR 6/4, moist); very hard; continuous; calcipan; strong effervescence with HCl; clear wavy boundary.**
168-210	**Yellow (10 YR 8/6, dry) to brownish yellow (10 YR 6/6, moist); loamy sand; massive; slightly sticky, slightly plastic, soft; very friable; weak effervescence with HCl; non roots.**

Fig. A1-3: Profile No. (1) in the South El-Kantara Shark area.

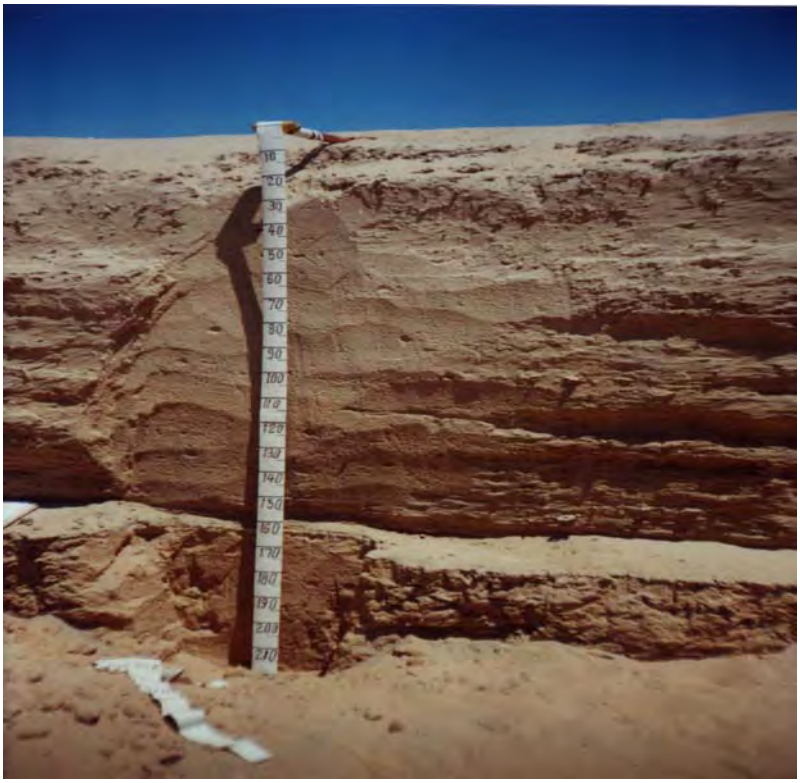

Fig. A1-4: Profile No. (2) in the South El-Kantara Shark area.

Three area of study Rabaa and Qatia

Profile No.: **1**
Location: **El-Ahrar village (4km from road El-Arish El-Kantara)**
Slope: **Sloping (Hilly)**
Vegetation: **Common natural vegetation**
Drainage: **Moderately well drained**
Parent material: **Sandy deposits**
Classification: **Typic Torripsamments**

Depth (cm)	Description
0-25	Yellow (10 YR 7/6, dry) to yellowish brown (10 YR 5/6, moist); fine sandy; weak, fine, single grains; non sticky, non plastic, loose, loose; many fine and medium roots; non effervescence with HCl; clear smooth boundary.
25-40	Very pale brown (10 YR 8/4, dry) to light yellowish brown (10 YR 6/4, moist); sandy; weak, medium, single grains; non sticky, non plastic, loose, loose; few fine and medium roots, non effervescence with HCl; gradual smooth boundary.
40-75	Light yellowish brown (10 YR 6/4, moist); coarse sand; single grains; non sticky, non plastic, loose; non effervescence with HCl.
75	Water table

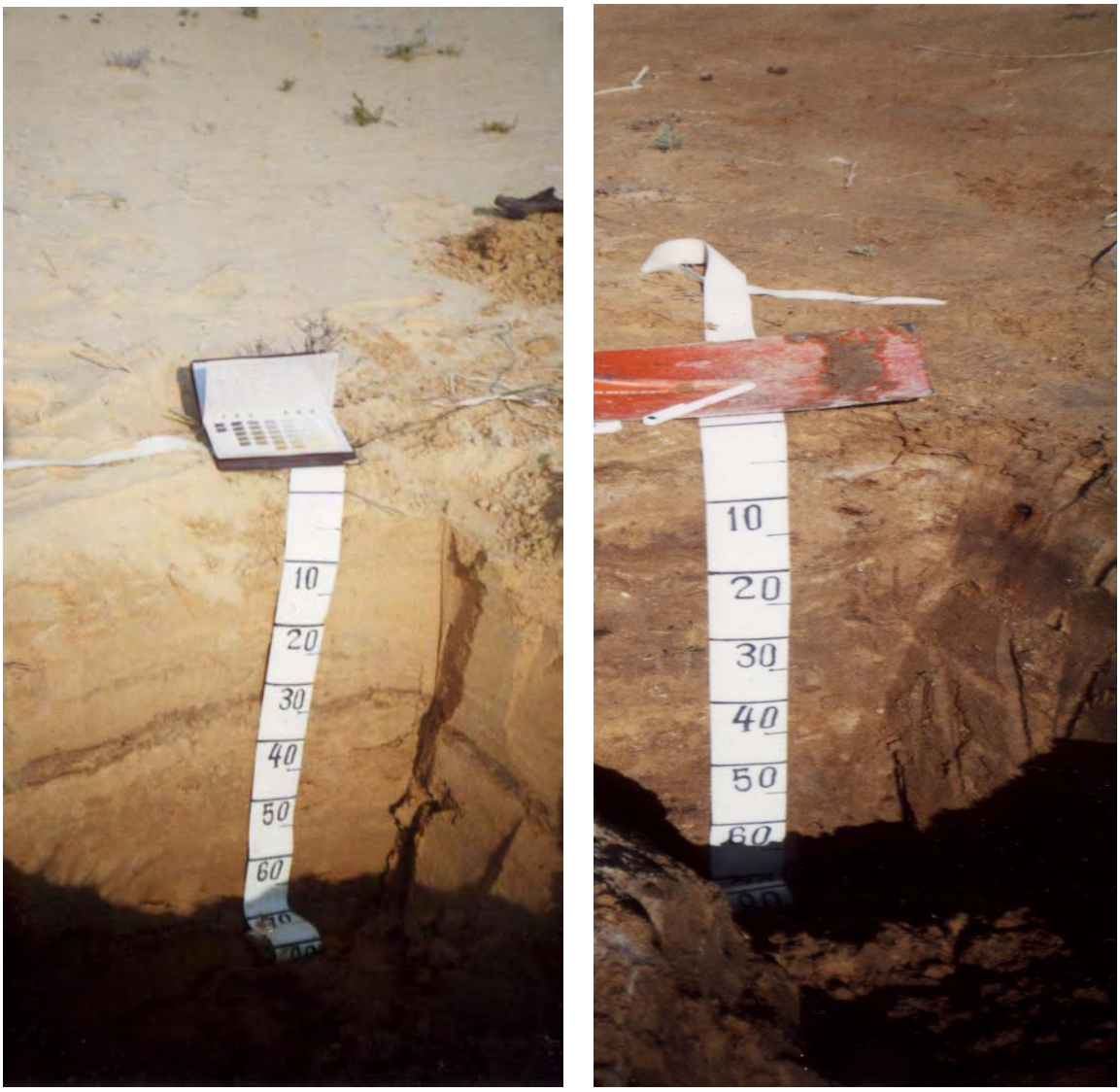

(a) **(b)**

Fig. A1-5: Profile No. 1(a and b) in the Rabaa and Qatia area.

Profile No.: **2**
Location: **Rabaa village (near to climate station ~ 6 km road of El-Arish)**
Slope: **Sloping (Hilly)**
Vegetation: **Common natural vegetation**
Drainage: **Well drained**
Parent material: **Sandy deposits**
Classification: **Typic Torripsamments**

Depth (cm)	Description
0-30	**Yellow (10 YR 7/6, dry) to very pale brown (10 YR 7/4, moist); fine sand; weak, fine, less massive; non sticky, non plastic, loose, soft; common fine roots, many medium and few coarse roots; non effervescence with HCl; clear smooth boundary.**
30-150	**Brownish yellow (10 YR 6/6, dry) to light yellowish brown (10 YR 6/4, moist); sandy; moderate, medium, weak massive; non sticky, non plastic, very friable, slightly hard; weak effervescence with HCl; few fine and medium roots.**

Four area of study Bair El-Abd

Profile No.: 1
Location: El-Kherba village
Slope: Sloping (Hilly)
Vegetation: Common palm tree and small farm
Drainage: Well drained
Parent material: Sandy deposits
Classification: Typic Torripsamments

Depth (cm)	Description
0-30	Light yellowish brown (10 YR 6/4, dry) to yellowish brown (10 YR 5/4, moist); fine sand; moderate, fine, massive; non sticky, non plastic, very friable, soft; non roots; non effervescence with HCl; clear smooth boundary.
30-83	Very pale brown (10 YR 7/3, dry) to yellowish brown (10 YR 5/6, moist); sand; structure less massive; non sticky, non plastic, loose, loose; few fine roots, non effervescence with HCl; clear smooth boundary.
83-145	Very pale brown (10 YR 7/4, dry) to yellowish brown (10 YR 5/4, moist); coarse sand; structure less massive; non sticky, non plastic, loose, loose; non roots; weak effervescence with HCl.

Profile No.: **2**
Location: **Bair El-Abd (~ 4 km road of El-Arish to El-Kant.)**
Slope: **Sloping (Hilly)**
Vegetation: **Medium natural vegetation**
Drainage: **Well drained**
Parent material: **Sandy deposits**
Classification: **Typic Torripsamments**

Depth (cm)	Description
0-19	**Light yellowish brown (10 YR 6/4, dry) to brown (10 YR 5/3, moist); sand; weak, medium, massive; non sticky, non plastic, loose, loose; few, medium, distinct, clear mottling; non roots; weak effervescence with HCl; clear, smooth boundary.**
19-75	**Light yellowish brown (10 YR6/4, dry) to brown (10 YR 5/3, moist); loamy sand; moderate, fine massive; slightly sticky, slightly plastic, friable, slightly hard; common, medium, distinct, clear mottling; non roots, weak effervescence with HCl; clear, smooth, boundary.**
75-165	**Very pale brown (10 YR 8/3, dry) to yellowish brown (10 YR 5/3, moist); loamy sand; weak, fine, massive; slightly sticky, slightly plastic, friable, soft; few, fine, faint, diffuse mottling; few, fine roots; weak effervescence with HCl; clear smooth boundary.**
165-200	**Yellow (10 YR 7/6, dry) to dark yellowish brown (10 YR 5/4, moist); loamy sand; weak, fine, massive; slightly sticky, slightly plastic, friable, soft; few, fine, distinct, clear mottling; few, fine roots; non effervescence with HCl.**

Fig. A1-6: Profile No. (1) in the Bair El-Abd area.

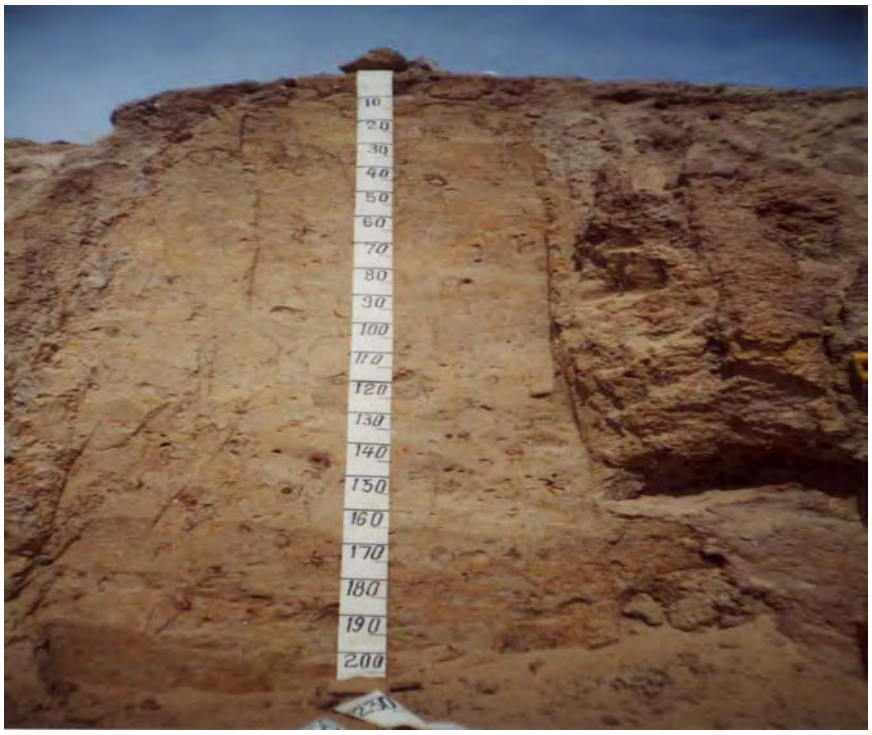

Fig. A1-7: Profile No. (2) in the Bair El-Abd area.

Profile No.: **3**
Location: **Bair El-Abd (~ 3 km from road of El-Arish direction of south)**
Slope: **Undulating**
Vegetation: **Few natural vegetation**
Drainage: **Well drained**
Parent material: **Sandy deposits**
Classification: **Typic Torripsamments**

Depth (cm)	Description
0-20	**Very pale brown (10 YR 7/4, dry) to yellowish brown (10 YR 5/4, moist); fine sand; loose; non sticky, non plastic, loose, loose; few, fine roots; non effervescence with HCl; gradual, wavy boundary.**
20-130	**Yellow (10 YR 7/6, dry) to light yellowish brown (10 YR 6/4, moist); sand; structure less, massive; non sticky, non plastic, loose, loose; few, fine, faint, diffuse mottling; non roots; non effervescence with HCl; clear, smooth boundary.**
130-170	**Yellow (10 YR 7/6, dry) to yellowish brown (10 YR 5/6, moist); coarse sand; structure less, massive; non sticky, non plastic, loose, loose; non roots; non effervescence with HCl.**

Fig. A1-8: Profile No. (3) in the Bair El-Abd area.

Five area of study Wadi El-Arish

Profile No.: **1**
Location: **El- Risan (~ 18 km south Bair Lehfen road)**
Slope: **Flat to almost flat**
Vegetation: **Few natural vegetation**
Drainage: **Well drained**
Parent material: **Calcareous deposits**
Classification: **Typic Calciorthids**

Depth (cm)	Description
0-68	**Very pale brown (10 YR 7/4, dry) to light yellowish brown (10 YR 6/4, moist); loamy; strong, fine, massive; very sticky, very plastic, firm, hard; few, fine roots; strong effervescence with HCl; clear, smooth boundary.**
68-140	**Light yellowish brown (10 YR 6/4, dry) to brown (10 YR 5/6, moist); loamy; moderate, fine, massive; sticky, plastic, firm, slightly hard; non roots; moderate effervescence with HCl; clear, smooth boundary.**
140-220	**Brown (10 YR 5/6, dry) to light yellowish brown (10 YR 6/4, moist); sandy loam; strong, medium, massive; sticky, plastic, friable, hard; non roots; moderate effervescence with HCl.**

Profile No.: **2**
Location: **W. El-Arish (~ 4 km from El-Arish road)**
Slope: **Rolling**
Vegetation: **Common vegetation**
Drainage: **Well drained**
Parent material: **Sandy deposits**
Classification: **Typic Torripsamments**

Depth (cm)	Description
0-40	Very pale brown (10 YR 7/4, dry) to brown; sandy ; weak; fine, massive; slightly sticky, slightly plastic, friable, slightly hard; fine and medium, common roots; moderate effervescence with HCl; clear smooth boundary.
40-140	Very pale brown (10 YR 7/4, dry) to yellowish brown (10 YR 5/4, moist); sandy loam; structure less, massive; slightly sticky, slightly plastic, friable, soft; few, fine and medium roots; weak effervescence with HCl; clear smooth boundary.
140-220	Very pale brown (10 YR 8/4, dry) to light yellowish brown (10 YR 6/4, moist); loamy sand; structure less, massive; slightly sticky, slightly plastic, friable, soft; non roots; weak effervescence with HCl.

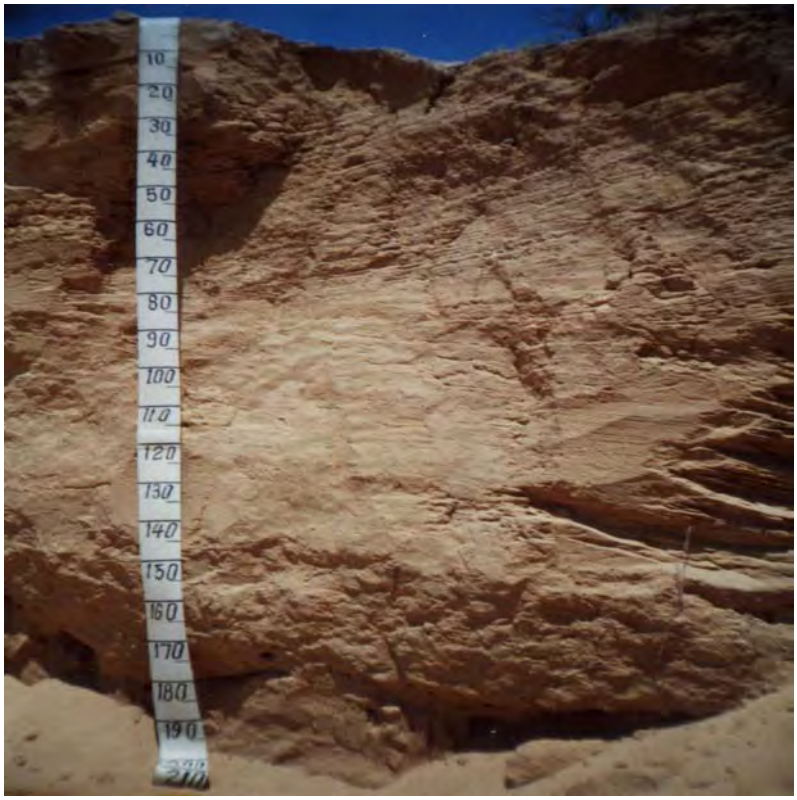

Fig. A1-9: Profile No. (1) in the El-Arish area.

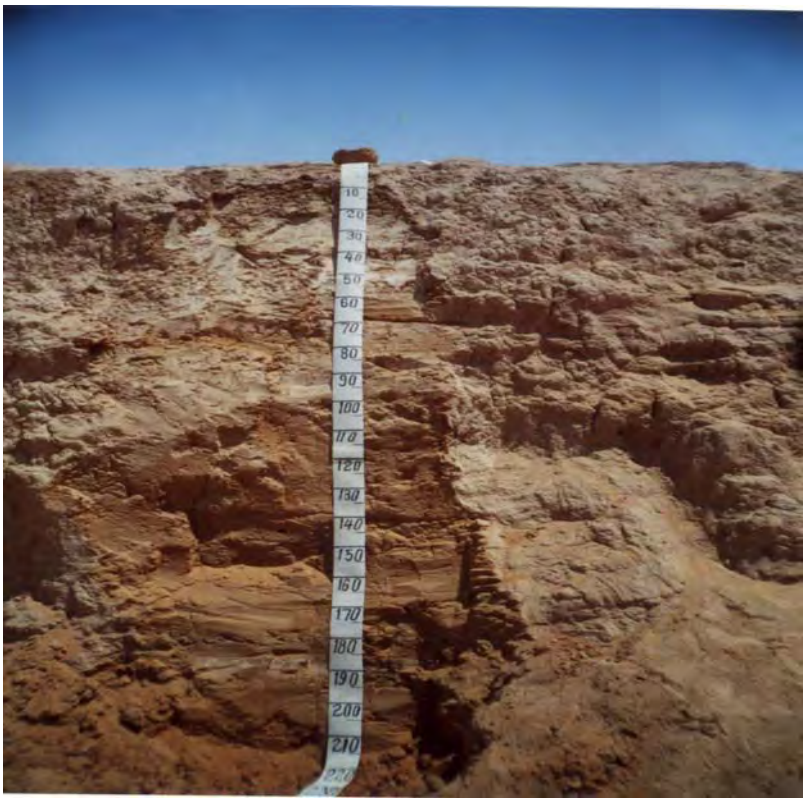

Fig. A1-10: Profile No. (2) in the El-Arish area.

APPENDIX II

ATMOSPHERIC CORRECTION PROCESSING

```
--------------------------------------------------------------------------------
AtCProc: ATMOSPHERIC CORRECTION PROCESSING OF OPTICAL SCANNER DATA

(c) feut jan01                          vers.  2.0 / delphi5
--------------------------------------------------------------------------------

AtCProc Run 15.06.01 14:29:17

                Image ID : Landsat TM Egypt, 29 July 1987
                 Sensor : TM5

           Acquisition date : 29/ 7/1987
         GMT acquisition time :        7.82
      Scene center longitude [d] :       33.14
      Scene center latitude [d] :        30.56
        Platform altitude [km] :        707.88
        Platform heading [d] :         10.12
  Sun elevation at scene centre [d] :   59.65
        Sun azimuth angle [d] :        104.73
        Sun zenith angle [d] :         30.35
                mu0 :                0.8630
  Earth-sun distance in astr. units :     1.0149
          Scan azimuth [d] :      0.00
  Backscattering angle at nadir [d] :    149.65

      Aerosol Scattering Model :   [2]  Multiple Scattering (SOBOLEV)

           Aerosol type :   [1]  Continental aerosol, clear sky

       Rayleigh phase function :     1.3086    (3/4)*(1+cos**2psi)
        Aerosol phase function :     0.1571    TTHG (g1,g2,alfa) with
                                  0.8360 0.5370 0.9680

         Gaseous Absorption :   [1]  MODTRAN MLS = c:\atmdata\atm.dat
   H2O vertical path length scaling :     1.0000

         Calibration File ID : c:\atmdata\tm5.cal

========================== Calibration Coefficients ==========================

 Band    micron        bias (a0)   gain(a1)

   1    - 0.486         -0.1520     0.0760
   2    - 0.570         -0.1840     0.1460
   3    - 0.660         -0.2050     0.1100
   4    - 0.840         -0.1942     0.0940
   5    - 1.676         -0.0359     0.0130
   6    - 2.223         -0.0153     0.0060
```

---------- Altitude Scaling Factors for Absorber and Scatterer ----------

Sensor Altitude [km] : 707.8800
Terrain Altitude [km] : 0.1000

h2o	o3	o2	co2/ch4	
0.9381	0.9996	0.9882	0.9882	down to ground
0.0000	0.0000	0.0000	0.0000	down to sensor
1.0000	1.0000	1.0000	1.0000	up to sensor

ray	mie	
0.9882	0.9311	down to ground
0.0000	0.0000	down to sensor
1.0000	1.0000	up to sensor

==========

Scene-Based Aerosol Estimate

==========

Calibration target file ID (image) : eg87.ref
Reflectance reference file ID (archive) : tmvturb.row

Target radius [km] : 0.250
Reference Target Type : Water

---------- Atmospheric Parameters (from Aerosol Estimate) ----------

	App. Reflectance		Optical Depth Rayleigh		Aerosol		
micron	ro*(tar)	ro*(bck)	downward	upward	downward	upward	Band
0.486	0.1704	0.1744	0.1619	0.1639	1.8010	1.8010 -	1
0.570	0.1521	0.1609	0.0841	0.0851	1.7617	1.7617 -	2
0.660	0.0956	0.1035	0.0462	0.0467	1.2740	1.2740 -	3
0.840	0.0394	0.0396	0.0174	0.0176	0.6058	0.6058 -	4
1.676	0.0142	0.0143	0.0012	0.0012	0.4236	0.4236 -	5
2.223	0.0060	0.0038	0.0005	0.0005	0.1080	0.1080 -	6

---------- Transmittance ----------

	downward			upward			
micron	td	ts	T	td	ts	T	Band
0.486	0.1188	0.5374	0.6561	0.1402	0.5400	0.6802 -	1
0.570	0.1356	0.5569	0.6925	0.1577	0.5556	0.7133 -	2
0.660	0.2398	0.5337	0.7734	0.2669	0.5223	0.7893 -	3
0.840	0.5098	0.3776	0.8874	0.5361	0.3596	0.8957 -	4
1.676	0.6323	0.2937	0.9260	0.6539	0.2773	0.9312 -	5
2.223	0.8895	0.0910	0.9805	0.8972	0.0847	0.9819 -	6

---------- Atm. Reflectance, Path Radiance, Solar Irradiance ----------

			Solar Irradiance			
micron	ro(atm)	L(atm)	TOA/AU	At-Sensor	Ground	Band
0.486	0.1518	7.9303	190.129	164.080	106.842 -	1

0.570	0.1137	5.5595	178.040	153.648	101.614	-	2
0.660	0.0616	2.5613	151.345	130.610	97.461	-	3
0.840	0.0200	0.5583	101.772	87.829	74.117	-	4
1.676	0.0094	0.0547	21.101	18.210	15.612	-	5
2.223	0.0040	0.0085	7.761	6.697	6.263	-	6

(Path Radiance in [mW/cm2/sr/micr], Solar Irradiance in [mW/cm**2/micr])**

---------- Solar Irradiance at Ground, Gaseous Transmittance ----------

	Global Irradiance			Gaseous Transmittance			
micron	scattered	direct	total	downward	upward		Band
0.486	87.504	19.338	106.842	0.992	0.993	-	1
0.570	81.717	19.897	101.614	0.955	0.961	-	2
0.660	67.245	30.216	97.461	0.965	0.969	-	3
0.840	31.540	42.577	74.117	0.951	0.955	-	4
1.676	4.952	10.661	15.612	0.926	0.932	-	5
2.223	0.581	5.682	6.263	0.954	0.957	-	6

---------- Estimated Angstrom Relation ----------

Angstrom relation (log. regression) : tau = 0.594 lambda-1.681**

Number of Bands : 6
Bands : 1 2 3 4 5 6
r : -0.9545
r^2 : 0.9111

Horizontal Visibility (0.55 micr) : 1.4027 kilometer

==========

Atmospheric Conditions for Radiative Transfer Calculation
(all parameters based on Angstrom relation)

==========

	Optical Depth					
	Rayleigh		Aerosol			
micron	downward	upward	downward	upward		Band
0.486	0.18763	0.16386	2.15446	1.99695	-	1
0.570	0.09741	0.08507	1.64799	1.52751	-	2
0.660	0.05350	0.04673	1.28804	1.19388	-	3
0.840	0.02018	0.01762	0.85877	0.79599	-	4
1.676	0.00141	0.00123	0.26891	0.24925	-	5
2.223	0.00052	0.00046	0.16727	0.15504	-	6

---------- Transmittance ----------

	downward			upward			
micron	td	ts	T	td	ts	T	Band
0.486	0.0961	0.5373	0.6334	0.1152	0.5431	0.6583	- 1
0.570	0.1746	0.5477	0.7223	0.1994	0.5423	0.7417	- 2
0.660	0.2614	0.5232	0.7847	0.2892	0.5107	0.7999	- 3
0.840	0.4152	0.4424	0.8576	0.4433	0.4245	0.8678	- 4
1.676	0.7631	0.1923	0.9555	0.7784	0.1803	0.9587	- 5
2.223	0.8455	0.1267	0.9722	0.8560	0.1183	0.9743	- 6

---------- Atm. Reflectance, Path Radiance, Solar Irradiance ----------

micron	ro(atm)	L(atm)	Solar Irradiance spa	ro(ws)	TOA	At-Sensor	Ground	Band
0.486	0.1667	8.7090	0.102	0.0179	190.129	164.080	103.143	- 1
0.570	0.0966	4.7221	0.122	0.0160	178.040	153.648	105.984	- 2
0.660	0.0570	2.3680	0.130	0.0141	151.345	130.610	98.875	- 3
0.840	0.0251	0.7008	0.123	0.0109	101.772	87.829	71.625	- 4
1.676	0.0071	0.0412	0.062	0.0042	21.101	18.210	16.109	- 5
2.223	0.0051	0.0109	0.042	0.0027	7.761	6.697	6.211	- 6

(Path Radiance in [mW/cm2/sr/micr], Solar Irradiance in [mW/cm**2/micr])**

DNs corresponding to modelled path radiance = theor. histogram minimum (DO)

114.440	-	1
32.159	-	2
21.323	-	3
7.261	-	4
3.135	-	5
1.802	-	6

(Path Radiance in [mW/cm2/sr/micr], Solar Irradiance in [mW/cm**2/micr])**

---------- Solar Irradiance at Ground, Gaseous Transmittance ----------

micron	Global Irradiance scattered	direct	Gaseous Transmittance total	downward	upward	Band
0.486	87.490	15.653	103.143	0.992	0.993 -	1
0.570	80.368	25.616	105.984	0.955	0.961 -	2
0.660	65.931	32.944	98.875	0.965	0.969 -	3
0.840	36.946	34.678	71.625	0.951	0.955 -	4
1.676	3.243	12.867	16.109	0.926	0.932 -	5
2.223	0.809	5.401	6.211	0.954	0.957 -	6

---------- Parameter File ID : C:\TM\eg290787.txt
Water Vapour File ID : c:\atmdata\atm.dat
Input Data File ID : c:\atmdata\eg87.ref

Output Data File ID :

Byte range scaling factor : 283.33 (ro_max = 0.90)

Table A2-1: Ground control points (GCP) on first scene covering part of the study areas.

NO. GCP	X Image Correctio	Y Image Correction	X Image Reference	Y Image Reference	X Residual	Y Residual	RMS
GCP#1	0.19568203	0.09294193	3994.01944	695115.458	-5822.02196	3270362.56	0.1722012
GCP#2	0.54294309	-0.42374821	3772.28447	688818.435	-5830.03648	3271090.93	0.33944757
GCP#3	0.46330236	-0.23703892	2161.16425	658301.166	-2329.76476	3376606.17	0.39807239
GCP#4	0.59995168	0.23804226	5938.77666	768649.874	-1418.19321	3386125.39	-0.55070673
GCP#5	0.16221358	0.13929501	664.034872	610239.175	-3712.04208	3344036.82	-0.08312729
GCP#6	0.26916411	-0.08310226	4033.84662	705138.409	-3727.14789	3329210.94	-0.25601433
GCP#7	0.0868717	-0.0773357	3175.05453	672365.159	-5743.06413	3276083.17	0.03957122
GCP#8	0.23518529	0.23211081	3560.01108	689711.299	-4217.02833	3317436.07	-0.03790372
GCP#9	0.44213709	0.24540142	3969.96352	700986.362	-4283.02442	3313836.41	0.36778166
GCP#10	0.58691457	-0.28999864	3578.8353	705663.929	-587.045735	3419659.8	0.51026414
GCP#11	0.46392415	0.40162554	1303.00927	618563.721	-5991.05654	3277083.12	-0.23221228
GCP#12	0.64636322	-0.08715601	2154.99696	643465.115	-5778.07817	3279435.25	-0.64046018
GCP#13	0.53997086	-0.47968492	569.977782	602262.404	-4960.86952	3309260.87	0.24793328
GCP#14	0.48133693	0.47129761	1152.14929	635489.278	-1011.06431	3418058.46	-0.09779468
GCP#15	0.71889058	0.66966029	1251.00813	638563.751	-944.396689	3419509.24	-0.2614551
GCP#16	0.16954399	-0.02272456	2042.07759	663989.111	-203.899248	3437010.65	0.16801416
GCP#17	0.26516537	-0.07638054	2162.84434	667438.814	-192.771418	3436810.93	0.25392653
GCP#18	0.18987277	-0.04545259	994.881057	630876.924	-1050.28015	3417635.46	0.18435219
GCP#19	0.08291336	-0.06903893	802.627056	624719.332	-1223.77877	3413561.52	-0.0459157
GCP#20	0.0388899	-0.02275964	2009.66777	648187.694	-3705.15822	3338484.21	-0.03153448
GCP#21	0.04098657	-0.03865401	1336.9613	632838.673	-2856.12385	3365282.96	-0.01362962
GCP#22	0.03292865	-0.01807834	1079.83925	625363.45	-2910.06266	3364861.04	-0.02752216
GCP#23	0.06259333	-0.03709453	1132.63723	629265.333	-2342.19919	3380636.31	-0.05041747
GCP#24	0.03728125	-0.02348478	1351.58684	638640.055	-1588.74422	3400932.5	-0.02895439
GCP#25	0.07338182	-0.05758478	1278.98392	638213.813	-1207.52183	3411984.52	-0.04548499
GCP#26	0.04957724	-0.04482834	1393.61531	642363.833	-991.401502	3417585.31	-0.02117364
GCP#27	0.1186395	-0.08772977	4135.36819	723512.282	-78.9137254	3431582.99	-0.0798675
GCP#28	0.06882864	-0.06677829	2706.30901	681962.803	-378.908456	3429236.49	-0.0166746
GCP#29	0.02378724	0.00162521	4380.7941	719714.226	-2599.54293	3359508.82	-0.02373165
GCP#30	0.02928613	-0.01900376	3988.77538	708661.289	-2600.53238	3361155.83	-0.02228304
GCP#31	0.04090889	-0.02928491	3287.02277	690638.708	-2187.77238	3375784.53	-0.02856451
GCP#32	0.05502755	-0.04049945	3032.74119	683836.735	-2101.99355	3379287.75	-0.03725354
GCP#33	0.03091719	-0.01572098	2922.1829	680838.461	-2074.57351	3380534.42	0.02662186
GCP#34	0.04338441	-0.02598718	2557.37396	670412.299	-2108.51153	3381134.93	-0.03474008
GCP#35	0.05690898	-0.02929519	2512.52729	669937.913	-1922.79241	3386559.38	-0.04878958
GCP#36	0.05872572	-0.04933245	2554.5293	672166.925	-1676.84073	3393310.98	-0.03185937
GCP#37	0.01779106	-0.01119327	4767.94599	736736.808	-1162.10589	3398359.62	-0.01382868
GCP#38	0.03057754	-0.02351506	3953.13675	714537.951	-982.175035	3406910.62	-0.01954553
GCP#39	0.07262845	-0.05213729	3705.37933	707035.591	-1104.22327	3404529.22	-0.05056278
GCP#40	0.06047508	-0.05137557	2855.7663	681989.557	-1363.33459	3400858.11	-0.03190275
GCP#41	0.01641762	-0.00053429	5110.09661	733563.328	-4176.40536	3311961.09	0.01640893
GCP#42	0.01321071	-0.00235278	5983.97581	763538.328	-2918.91773	3343661.45	0.01299952
GCP#43	0.02925736	0.00932014	5396.39297	753062.231	-1488.17801	3386486.2	-0.02773316
GCP#44	0.02942627	-0.02349727	6356.32929	785464.263	-230.096705	3417836.14	-0.01771393
GCP#45	0.00653656	0.00520084	6650.07124	792491.375	-524.605473	3408282.99	0.00395953
GCP#46	0.03245174	-0.02180303	5275.1363	751414.364	-1071.81889	3398736.72	-0.0240363
GCP#47	0.03320323	0.01323639	2211.61186	649058.899	-4839.0872	3305670.96	0.03045082
GCP#48	0.07981284	0.07399564	5771.44269	747692.457	-5237.46312	3279237.06	0.02991211
GCP#49	0.0430208	-0.03506034	5243.3998	752913.286	-508.848537	3414735.84	-0.02493114
GCP#50	0.09424942	0.05046205	6322.27996	762012.717	-5520.48194	3268910.34	0.07960235
GCP#51	0.10737222	0.07503145	6401.47279	762138.416	-6015.98441	3254609.45	0.07680543

Table A2-2: Ground control points (GCP) on second scene covering part of the study areas.

NO.GCP	X Image Correction	Y Image Correction	X Image Reference	Y Image Reference	X Residual	Y Residual	RMS
GCP #1	0.06633074	-0.0559384	3510.6345	662687.222	-2243.37459	3212453.68	-0.03564635
GCP #2	0.01815268	0.00238897	3185.28766	643511.781	-4573.67291	3148198.65	0.01799479
GCP #3	0.14576413	-0.0751559	3129.02797	641913.638	-4576.01269	3148371.66	-0.12489505
GCP #4	0.02047596	0.01843961	3280.50872	646913.778	-4406.4187	3152500.29	0.00890202
GCP #5	0.05766319	0.01189906	3163.29125	644086.322	-4295.72052	3156126.25	0.05642212
GCP #6	0.05965677	-0.0050863	3005.21713	643437.635	-3409.65968	3181774.12	0.05943955
GCP #7	0.4168372	0.10838656	3178.28066	651316.182	-2711.88022	3200697.84	0.40249919
GCP #8	0.45501685	0.23225612	2787.88914	644986.727	-1625.23411	3232998.36	0.39127666
GCP #9	0.25204093	-0.03502353	2791.86492	645935.803	-1428.47026	3238522.47	0.24959564
GCP #10	0.37318949	-0.06853387	3133.06548	660689.828	-231.835923	3270771.28	0.36684261
GCP #11	0.24853341	0.04639729	6693.27982	735463.781	-6179.78742	3087821.68	0.24416418
GCP #12	0.1064559	-0.02427067	6290.07198	724986.682	-5973.0471	3095376.26	-0.10365227
GCP #13	0.03131264	-0.03047632	5819.30065	713160.496	-5638.0448	3106848.83	0.00718858
GCP #14	0.04279203	0.01322544	5550.28141	705236.32	-5718.30114	3105746.14	-0.04069699
GCP #15	0.25036518	0.028056	3999.23508	662116.484	-5581.81597	3116274.95	-0.24878823
GCP #16	0.17666751	0.04305247	2868.55911	629661.584	-5720.74587	3117248.36	0.17134145
GCP #17	0.1782061	0.05541592	2530.37125	626038.669	-4345.39919	3157449.48	-0.16937086
GCP #18	0.48965395	-0.48552513	2699.99611	633635.84	-3686.03782	3175301.69	-0.0634534
GCP #19	0.09441247	-0.03874991	1918.10183	613815.514	-3173.97769	3193099.15	-0.08609389
GCP #20	0.05162639	-0.02029503	2990.12894	644614.664	-3036.45537	3192351.79	-0.04746995
GCP #21	0.44586811	-0.03353645	2915.77453	647061.881	-1978.47929	3222471.26	-0.44460509
GCP #22	0.21934936	-0.01372028	3419.83372	664060.074	-1328.2054	3238626.09	-0.21891983
GCP #23	0.05685117	0.00570453	3560.66507	667934.707	-1350.43023	3237400.2	0.05656424
GCP #24	0.39203743	-0.0119479	3789.70431	677560.832	-611.355795	3257224.32	-0.39185532
GCP #25	0.08473968	0.00887832	2827.24562	647937.19	-1194.75763	3244950.22	0.0842733
GCP #26	0.05886198	-0.0207594	2585.74812	635613.652	-2479.18006	3209797.52	-0.05507976
GCP #27	0.15261252	0.04150084	1683.28413	603936.721	-3933.86938	3172698.77	-0.14686137
GCP #28	0.17332135	-0.01668503	942.876204	583537.671	-3825.37516	3178948.37	-0.17251638
GCP #29	0.16364085	-0.00886333	572.017843	571334.288	-4233.60828	3169045.43	-0.16340064
GCP #30	0.2504867	-0.01191153	525.098753	562637.467	-5950.37777	3120872.98	-0.25020332
GCP #31	0.23723515	-0.01253503	1322.79736	584835.807	-6015.89164	3115600.59	0.23690376
GCP #32	0.08473857	0.0068543	3332.44074	641139.282	-6091.25851	3104801.05	-0.0844609
GCP #33	0.09455053	0.00518009	1271.97658	587909.657	-4966.68202	3145373.29	-0.09440853
GCP #34	0.09934805	0.01516245	1398.09015	593837.579	-4413.99984	3160401.85	-0.09818419
GCP #35	0.71352878	0.01935354	1479.03793	591686.188	-5446.71369	3130977.45	0.71326626
GCP #36	0.06145778	0.01475416	1305.54842	585684.499	-5705.04032	3124425.18	-0.05966048
GCP #37	0.02650953	0.00076194	1035.34385	589261.406	-3099.70971	3199000.26	-0.02649858
GCP #38	0.04026285	0.00026632	1639.42713	603361.039	-3780.02416	3177225.89	-0.04026197
GCP #39	0.03997741	-0.01352819	2247.14046	621837.221	-3465.19707	3183475.88	-0.03761889
GCP #40	0.03784883	-0.01176165	2751.64415	637161.984	-3207.08034	3188572.98	-0.03597495
GCP #41	0.03252809	-0.0045602	3207.95699	649684.007	-3285.36114	3184399.48	-0.03220685
GCP #42	0.0501508	-0.01326545	3445.91085	657014.25	-3139.75145	3187475.61	-0.04836456
GCP #43	0.0119318	-0.0031437	3332.53952	651313.71	-3723.25206	3171524.59	-0.01151021
GCP #44	0.02159453	0.00687432	3411.90686	653038.473	-3842.42655	3167824.11	-0.02047114
GCP #45	0.02762666	0.02623266	638.494784	578462.244	-3010.67456	3203221.29	0.00866488
GCP #46	0.00942451	0.00386989	797.254167	587914.98	-1851.32855	3235202.42	-0.00859333
GCP #47	0.024722	-0.02386935	841.753219	594212.495	-676.968438	3268099.91	-0.0064367
GCP #48	0.01418985	0.01029639	1480.22325	611236.545	-902.278845	3258997.76	-0.00976403
GCP #49	0.00951206	-0.00131219	1785.02447	620013.976	-858.273678	3258923.23	-0.00942111
GCP #50	0.02126613	-0.00230961	1598.97794	616463.307	-464.400268	3270823.18	-0.02114034
GCP #51	0.01589657	0.0098294	1529.51299	615184.944	-306.406408	3275574.65	-0.01249335

Con. table A2-2: Ground control points (GCP) on second scene covering part of study areas

NO. GCP	X Image Correction	Y Image Correction	X Image Reference	Y Image Reference	X Residual	Y Residual	RMS
GCP #52	0.02547261	-0.00981112	2241.39905	635514.029	-243.584216	3274275.75	0.02350735
GCP #53	0.06106337	0.01191475	2228.55803	633559.222	-614.615437	3263877.74	0.05988968
GCP #54	0.02284653	-0.021628	2343.75675	635610.61	-892.475224	3255550.51	0.00736164
GCP #55	0.00852403	-0.00328407	2339.38586	634761.156	-1061.68028	3250801.71	0.007866
GCP #56	0.01384357	0.00058847	2291.33084	632208.994	-1340.62661	3243149.41	0.01383106
GCP #57	0.02301462	0.00606169	2181.58956	628061.349	-1586.35917	3236699.04	0.022202
GCP #58	0.01697017	-0.00693126	2082.047	623411.029	-2015.85405	3225025.71	-0.01549014
GCP #59	0.01887303	0.01767111	1924.91744	617714.292	-2311.48135	3217373.78	-0.00662744
GCP #60	0.01635393	0.00144668	1590.27321	606909.808	-2631.4325	3209801.71	-0.01628981
GCP #61	0.00350339	-0.00349715	903.859277	594109.83	-1108.42651	3255675.23	-0.00020903
GCP #62	0.08006319	0.08006291	1338.01285	606063.016	-1174.26785	3251947.37	0.00021164
GCP #63	0.01355075	0.01200626	1495.78063	608812.142	-1568.77686	3240151.6	0.00628273
GCP #64	0.01840808	0.01796212	1218.16779	598836.198	-2070.11968	3227222.73	0.00402736
GCP #65	0.0072697	0.00724001	1216.71083	596411.796	-2624.90087	3211597.19	-0.00065637
GCP #66	0.02399129	0.02106635	1201.49916	594312.117	-3014.00829	3200698.79	-0.01148002
GCP #67	0.0606749	0.0310683	1170.60665	605438.664	-221.16183	3279526.09	0.05211721
GCP #68	0.0473122	0.01627975	1143.39358	604637.881	-228.965216	3279423.42	0.04442312
GCP #69	0.04002065	0.03097173	1006.9578	600014.178	-410.443315	3274897.82	0.02534569
GCP #70	0.01491661	0.01079646	1366.62967	609386.303	-587.871556	3268347.07	0.0102928
GCP #71	0.02654677	-0.01489697	4082.10901	688115.5	-72.7493417	3271150.95	0.02197297
GCP #72	0.02343594	-0.00202835	3475.91438	670962.929	-89.3932714	3273296.26	0.023348
GCP #73	0.00485713	0.00077413	4268.20494	689114.007	-1061.1617	3242497.68	-0.00479504
GCP #74	0.03088625	0.01209776	4332.80512	692361.246	-729.073322	3251577.02	0.02841838
GCP #75	0.04151782	0.02643094	2981.63412	654912.29	-583.77231	3261498.21	0.03201772
GCP #76	0.02987724	0.00653499	5271.76807	718262.16	-858.786834	3243872.81	0.02915379
GCP #77	0.39908246	0.00817565	6090.75277	741786.772	-754.27422	3243273.55	-0.39899871
GCP #78	0.00775275	-0.00141921	6730.20252	761936.765	-258.39811	3254499.34	0.00762174
GCP #79	0.001548	0.00024303	6653.5377	756711.523	-971.943999	3234724.65	0.0015288
GCP #80	0.01641223	0.01443995	5892.96546	734387.706	-1179.75899	3232148.91	-0.00780057
GCP #81	0.01008051	-0.00630755	4260.97314	688063.217	-1258.30091	3236974.14	-0.0078633
GCP #82	0.03870155	0.02879078	5810.17537	731135.143	-1393.99565	3226470.42	0.02586312
GCP #83	0.01734089	0.01287098	6585.96202	753086.327	-1372.68066	3223724.34	-0.01162086
GCP #84	0.01741281	-0.00213021	6991.86071	762663.781	-1805.59974	3209775.66	-0.01728202
GCP #85	0.01542986	-0.00424412	6626.83839	749938.711	-2373.49731	3195348.64	-0.01483469
GCP #86	0.05410098	0.01123982	5266.85302	710685.332	-2590.52492	3195100.53	0.05292053
GCP #87	0.07644411	0.0355193	4188.50711	679236.924	-2838.08014	3192776.14	0.06769107
GCP #88	0.08821251	0.01531678	4163.80839	676465.744	-3321.08822	3179273.86	0.08687256
GCP #89	0.00949502	-0.00799492	5215.4797	706585.217	-3207.86931	3177926.29	0.00512217
GCP #90	0.06635378	0.03800542	6185.64524	733536.541	-3298.11842	3171200.63	0.05439129
GCP #91	0.01272412	0.00752793	6468.29734	738987.644	-3883.0334	3153499.75	0.01025834
GCP #92	0.03847786	0.01040718	6370.04585	734912.245	-4187.32157	3145350.48	0.0370437
GCP #93	0.05339138	0.01192548	6713.11101	741763.387	-4842.77608	3125400.11	-0.05204251
GCP #94	0.02883197	0.0006183	6762.85422	740712.407	-5413.77333	3109099.27	0.02882534
GCP #95	0.01214115	-0.00198713	5957.72549	716436.443	-5783.64895	3102149.27	0.01197743
GCP #96	0.01498495	0.01375794	6002.13378	719260.857	-5417.51519	3112273.5	-0.00593866
GCP #97	0.04204658	0.03677126	5566.54724	706262.775	-5586.25681	3109398.14	0.02039092
GCP #98	0.03105959	0.03101897	5328.00704	700413.182	-5383.18397	3116148.14	-0.00158795
GCP #99	0.01966358	0.01757048	5460.88613	706161.631	-4916.52644	3128724.15	0.00882807
GCP #100	0.01032595	0.00714747	4910.17887	691386.313	-4743.56134	3135972.27	-0.00745244
GCP #101	0.05294602	0.01400611	4158.81925	670734.786	-4622.51294	3142624.92	0.05105987
GCP #102	0.0289322	0.02838212	5070.69583	697216.134	-4439.49545	3143847.77	0.00561491
GCP #103	0.03986707	0.03973942	4932.7782	694889.833	-4076.39964	3154673.17	0.0031878
GCP #104	0.2914327	-0.29143225	4889.53294	700463.373	-2492.98339	3199475.94	-0.00051017
GCP #105	0.03680261	-0.00912868	4972.63942	706636.93	-1602.81495	3224199.07	0.03565248

Table A2-3: Ground control points (GCP) on third scene covering part of the study areas.

NO. GCPs	X Image Correction	Y Image Correction	X Image Reference	Y Image Reference	X Residual	Y Residual	RMS
GCP #1	0.93946502	-0.63087176	6451.9838	664813.009	-1534.01996	3538237.17	0.69612884
GCP #2	0.61932462	-0.60925759	6197.9888	655039.543	-2104.07883	3523362.39	0.11121227
GCP #3	0.87591663	0.82925125	6301.93428	646486.813	-4591.26031	3452910.03	-0.28208564
GCP #4	0.89708988	-0.68583508	5349.96282	609810.158	-6731.09481	3397161.09	0.57827372
GCP #5	0.59716258	0.5562167	5341.01058	619563.152	-4576.09124	3457785.39	-0.21731575
GCP #6	0.70666924	0.60792766	5330.16842	621309.334	-4133.1542	3470289.21	-0.36028513
GCP #7	0.09945408	0.0560105	5781.51061	633637.246	-4205.34408	3466185.72	0.08218234
GCP #8	0.29022271	0.10567902	6218.42976	638561.89	-5793.09879	3419512.68	0.27029829
GCP #9	0.42119541	-0.28229932	6454.74408	667485.737	-974.35563	3553935.37	-0.31259026
GCP #10	0.29487128	0.21329139	6448.42777	653985.996	-3856.15691	3472912.66	-0.20360711
GCP #11	0.45886132	0.00619093	6761.45783	659989.208	-4457.05129	3454557.65	-0.45881955
GCP #12	0.46555697	0.46329787	6058.85604	618962.641	-9061.68667	3328311.62	0.04580803
GCP #13	0.38582006	-0.3817994	5908.85626	611262.909	-9810.06922	3307960.97	0.05555481
GCP #14	0.08548454	0.07514092	6181.67583	616763.801	-10279.7635	3293485.78	0.04076087
GCP #15	0.74239737	-0.591682	5298.98477	590188.921	-10661.0296	3286835.42	-0.44840414
GCP #16	0.03428327	-0.00490684	6337.74325	618564.575	-10837.1649	3277084.7	-0.0339303
GCP #17	0.03340043	-0.01307618	6540.6856	626237.011	-10410.7895	3288138.05	-0.03073438
GCP #18	0.02525757	0.00132259	6577.11625	630138.815	-9788.85738	3305461.87	-0.02522292
GCP #19	0.01793276	0.00727293	6274.2072	624140.531	-9246.84887	3322107.85	-0.01639172
GCP #20	0.02841763	0.02496166	5170.81851	592913.966	-9298.62267	3325756.41	-0.01358223
GCP #21	0.03092872	0.01516898	5278.99143	590588.503	-10457.4655	3292662.35	-0.02695344
GCP #22	0.04156849	-0.00042143	5100.89155	583887.727	-10824.4826	3283163.36	-0.04156635
GCP #23	0.02888359	-0.00673942	5889.5592	605336.655	-10975.7009	3275261.94	-0.02808633
GCP #24	0.31288691	0.00114652	5841.61497	604640.609	-10835.5485	3279435.19	0.31288481
GCP #25	0.01980371	0.00820935	6011.6081	610564.588	-10586.8254	3285635.92	0.01802203
GCP #26	0.0379067	0.00693601	5582.87031	599640.901	-10345.4879	3294407.77	0.03726674
GCP #27	0.00790719	-0.00561549	5201.1318	591517.324	-9784.18232	3311959.83	-0.00556686
GCP #28	0.03189885	0.02304039	5250.24479	599911.586	-8268.59263	3354360.29	0.02206076
GCP #29	0.03439296	0.002369	6137.5363	630412.533	-7062.25316	3384184.9	0.03431127
GCP #30	0.02541261	0.02513169	6636.05184	643813.327	-7191.8866	3378231.35	-0.00376812
GCP #31	0.00692183	-0.00450458	6111.351	631512.711	-6665.54451	3395462.68	-0.00525553
GCP #32	0.00807341	-0.00310427	6073.80131	632058.63	-6319.73929	3405362.77	0.00745275
GCP #33	0.02759416	0.01336636	6353.0864	640489.287	-6192.9656	3407636.67	0.0241408
GCP #34	0.01279709	0.01112458	6249.36473	638213.108	-6055.34975	3411986.59	0.0063253
GCP #35	0.00362152	0.00336593	6324.11595	640887.353	-5931.06279	3415136.23	-0.00133639
GCP #36	0.01122063	0.00643016	5899.33207	629338.134	-5848.9011	3419412.6	0.00919541
GCP #37	0.01866975	0.01542123	5759.67709	624413.49	-6065.59509	3413964.02	0.01052354
GCP #38	0.00280919	-0.00038596	5340.04075	611715.567	-6262.74335	3410360.2	-0.00278255
GCP #39	0.01486719	-0.00538558	6465.36243	645714.186	-5745.17943	3419711.34	0.01385745
GCP #40	0.02327999	0.01160349	6707.1973	653336.579	-5565.78645	3423638.16	0.02018209
GCP #41	0.01325181	-0.00189055	6342.09503	659764.775	-1961.12893	3526710.69	0.01311626
GCP #42	0.01563972	0.01302369	6797.39114	672437.677	-1985.76003	3523911.34	0.00865935
GCP #43	0.01194719	0.00953995	6549.04102	663941.055	-2314.60572	3515811.27	0.00719198
GCP #44	0.0420302	0.04128887	6884.57603	668067.293	-3459.34879	3482062.11	0.00785922
GCP #45	0.01017292	0.00857229	5908.30918	636363.808	-4385.28415	3460536.22	0.0054776
GCP #46	0.01210764	0.01081425	6693.66947	660284.915	-3982.28406	3468237.47	0.00544491
GCP #47	0.02270769	0.01679737	6162.75178	627886.899	-7761.07511	3364412.78	0.01528029
GCP #48	0.03383733	0.01878899	5108.32689	597414.386	-7946.95847	3364063.24	0.02814141
GCP #49	0.02612966	0.01396396	5213.6898	601687.718	-7662.92373	3371564.32	0.02208545
GCP #50	0.00999114	0.00510897	5959.95864	644336.878	-2975.87799	3499937.92	0.00858612

Table A2-4: Ground control points (GCP) on fourth scene covering part of the study areas.

NO. GCP	X Image Correction	Y Image Correction	X Image Reference	Y Image Reference	X Residual	Y Residual	RMS
GCP #1	0.40233093	0.3845746	5273.45231	449140.506	3305696.201	-0.11820555	-0.03761889
GCP #2	0.09494517	0.02298712	5555.4581	460414.163	3323319.417	0.09212045	-0.03597495
GCP #3	1.78484539	1.73814107	6404.14229	475388.378	3269567.622	-0.40563369	-0.03220685
GCP #4	0.9216076	0.82855421	5219.42581	445864.335	3295995.175	-0.4035573	-0.04836456
GCP #5	0.06822343	0.06800159	5192.42133	445865.19	3300494.027	0.00549722	-0.01151021
GCP #6	0.31649181	0.29428764	5220.14751	449591.418	3316819.268	-0.11645536	-0.02047114
GCP #7	0.8183159	-0.72577145	5767.23651	474542.169	3368343.027	0.37801681	0.00866488
GCP #8	1.88209134	-1.6658634	5359.25411	464813.764	3379993.157	0.87588066	0.01799479
GCP #9	1.20063849	-1.11690304	6686.78232	503813.805	3383645.801	0.44052286	-0.12489505
GCP #10	0.68623715	-0.37080946	5346.12451	455688.57	3330718.824	0.57742685	0.00890202
GCP #11	0.38003036	0.38002926	5638.5621	461014.808	3313193.148	0.00091411	0.05642212
GCP #12	0.59096515	0.58887977	5587.14412	459013.512	3310193.342	0.04960271	0.05943955
GCP #13	0.91869208	0.8949725	5875.45789	466338.479	3304595.017	-0.20741111	0.40249919
GCP #14	0.64210892	0.63516207	5120.67143	442689.982	3294144.467	-0.09419666	0.39127666
GCP #15	0.7021495	0.7011698	6524.35517	486814.442	3314322.888	-0.03707873	0.24959564
GCP #16	0.20024646	0.04181161	5618.42924	463115.464	3328195.492	0.19583266	0.36684261
GCP #17	0.52133353	0.51939842	5725.54168	462863.911	3309367.561	0.04487683	0.00416418
GCP #18	1.27288743	1.27201453	6699.11038	513289.909	3434400.251	-0.04713215	-0.10365227
GCP #19	0.62394207	0.61722963	6303.12119	501391.65	3431892.427	0.09127589	0.00718858
GCP #20	1.18988441	1.10644061	5900.5703	489739.809	3431643.441	0.43773747	-0.04069699
GCP #21	0.34573081	-0.34571277	6115.78938	497497.533	3440538.66	-0.00353136	-0.24878823
GCP #22	1.07065629	-0.79026223	5481.04346	477069.592	3428818.369	-0.72235069	0.17134145
GCP #23	0.86010478	-0.8388844	5386.79346	473513.633	3424144.114	-0.18987678	-0.01639172
GCP #24	0.71517153	-0.16188572	5686.2957	481439.247	3419991.788	-0.69660844	-0.01358223
GCP #25	0.35324369	0.34884279	6436.46804	503838.537	3424069.675	0.05558608	-0.02695344
GCP #26	1.28565715	1.28463608	6460.47793	505512.987	3429420.726	0.05122949	-0.04156635
GCP #27	1.25783298	1.25324713	6786.40099	514639.891	3427842.106	0.10730993	-0.02808633
GCP #28	1.05857199	1.05557935	6858.45551	517088.678	3429940.944	0.07954179	0.31288481
GCP #29	0.97193031	0.78435296	6677.95881	508112.362	3408870.431	-0.57396774	0.01802203
GCP #30	0.03814726	0.03794618	5833.98386	481888.447	3398569.615	0.00391164	0.03726674
GCP #31	3.64370568	-3.64238249	6644.18092	500290.279	3371193.18	0.09818801	-0.00556686
GCP #32	0.316569	0.31457093	6293.00522	490939.202	3374967.322	0.03551141	0.02206076
GCP #33	1.07606049	-1.0758605	6136.56812	480564.802	3342343.365	0.02074534	0.03431127
GCP #34	0.49895863	-0.4989415	6605.60603	493739.648	3340196.613	-0.00413529	-0.00376812
GCP #35	0.89407734	-0.89407724	6406.54267	484864.296	3322717.996	0.00043616	-0.00525553
GCP #36	1.55724917	-1.55724916	6563.55144	488615.336	3318441.605	0.00073451	0.00745275
GCP #37	0.66642293	-0.66642284	6361.21966	482916.048	3319093.588	-0.00034931	0.05292053
GCP #38	0.04194724	0.04192218	5946.67624	471566.241	3322444.198	-0.00144961	0.06769107
GCP #39	0.19179341	-0.19153719	6209.61684	477090.555	3310892.892	0.00991042	0.08687256
GCP #40	0.02339289	0.02332293	5921.89585	470092.862	3318196.897	-0.00180783	0.00512217
GCP #41	0.02794863	0.0222621	5256.50377	455389.878	3343468.506	0.01689747	0.05439129
GCP #42	0.13182513	0.02776719	6513.99065	511265.324	3453217.245	-0.12886756	0.01025834
GCP #43	0.03145557	0.02846659	6206.23657	471814.371	3281818.478	0.01338304	0.02662186
GCP #44	0.03617165	0.03617062	6461.58398	479490.143	3283521.59	0.00027176	-0.03474008
GCP #45	0.03558406	0.03557138	6582.6649	485165.474	3295744.558	-0.00095016	-0.04878958
GCP #46	0.04692067	0.04329391	5995.78964	468641.73	3298094.092	0.01808832	-0.03185937
GCP #47	0.03513191	0.02944968	6184.01623	474338.451	3299569.182	0.01915639	-0.01382868
GCP #48	0.03043103	0.02145861	5842.35998	470114.253	3331192.918	0.02157721	-0.01954553
GCP #49	0.01438013	0.00886584	5293.71165	457765.081	3350766.094	0.01132188	-0.05056278
GCP #50	0.94881791	-0.94881752	6275.46073	486914.363	3355442.916	0.00086357	-0.03190275

Table A2-5: Universal transverse mercator (UTM) for locations of the study areas and type of samples.

Location	Longitude	Latitude	Samples Type	Depth	UTM (X)	UTM (Y)
S.K.S	32° 29`45	30° 53`10	S.S 1	0 - 60 cm	451811.791	3417089.131
S.K.S	32° 28`09	30° 49`03	S.S 2	0 - 55 cm	449226.832	3409497.133
S.K.S	32° 30`19	30° 51`42	S.S 3	0 - 50 cm	452702.498	3414376.038
S.K.S	32° 26`44	30° 48`32	S.S 4	0 - 70 cm	446963.711	3408553.770
S.K.S	32° 29`37	30° 50`14	S.S 5	0 - 40 cm	451574.824	3411671.991
S.K.S	32° 24`35	30° 47`44	S.S 6	0 - 60 cm	443528.163	3407093.647
S.K.S	32° 30`50	30° 54`49	S.S 7	0 - 65 cm	453550.839	3420129.171
S.K.S	32° 29`57	30° 54`05	P.S (8 to 10)	0 - 42 cm	452137.994	3418780.861
S.K.S	32° 26`50	30° 52`43	P.S (12 to 16)	0 - 20 cm	447161.363	3416279.939
Tina Plain	32° 24`46	30° 59`44	S.S 17	0 - 70 cm	443937.143	3429257.329
Tina Plain	32° 26`05	31° 00`06	S.S 18	0 - 60 cm	446035.682	3429923.757
Tina Plain	32° 22`28	31° 00`49	S.S 19	0 - 40 cm	440288.599	3431278.343
Tina Plain	32° 28`04	31° 01`03	S.S 20	0 - 30 cm	449199.777	3431662.959
Tina Plain	32° 29`26	31° 02`05	S.S 21	0 - 60 cm	451382.674	3433561.473
Tina Plain	32° 31`13	31° 01`29	S.S 22	0 - 50 cm	454214.376	3432440.575
Tina Plain	32° 29`16	31° 00`45	S.S 23	0 - 60 cm	451106.234	3431099.856
Tina Plain	32° 23`15	30° 59`53	P.S(24 to 25)	9 - 20 cm	441525.324	3429547.411
Tina Plain	32° 30`14	31° 00`12	P.S(26 to 28)	0 - 17 cm	452639.594	3430076.967
Qatia	32° 44`30	30°57`14	S.S 29	0 - 50 cm	475326.036	3424520.293
Qatia	32° 43`13	30° 58`04	S.S 30	0 - 55 cm	473286.996	3426064.464
Rabaa	32° 45`13	30° 59`03	S.S 31	0 - 50 cm	476474.304	3427873.246
Rabaa	32° 44`03	30° 59`27	S.S 32	0 - 45 cm	474619.468	3428616.354
El-Ahrar	32° 36`47	31° 00`29	S.S 33	0 - 60 cm	463062.911	3430558.947
Rummana	32° 39`42	30° 59`43	S.S 34	0 - 45 cm	467698.969	3429127.706
El-Ganien	32° 44`58	30° 58`35	S.S 35	0 - 55 cm	476074.521	3427012.159
Rabaa	32° 44`34	30° 59`48	S.S 36	0 - 50 cm	475443.115	3429260.904
El-Nigila	32° 49`03	31° 01`33	S.S 37	0 - 60 cm	482582.129	3432479.220
El-Ahrar	32° 36`48	31° 01`30	P.S(38 to 40)	0 - 25 cm	463095.958	3432436.750
Rabaa	32° 45`47	30°59`29	P.S(41 to 42)	0 - 30 cm	477377.784	3428671.693
El-Kherba	32° 54`03	31° 01`55	S.S 43	0 - 50 cm	490536.104	3433146.411
El-Sadat	33° 04`56	31° 02`47	S.S 44	0 - 45 cm	507845.631	3434745.910
El-Sadat	33° 04`06	31° 04`25	S.S 45	0 - 50 cm	506518.498	3437761.947
El-Amrawa	33° 11`09	31° 01`33	S.S 46	0 - 40 cm	517736.007	3432479.747
El-Telol	33° 13`46	31° 03`18	S.S 47	0 - 40 cm	521891.603	3435719.953
El-Telol	33° 13`40	31° 04`03	S.S 48	0 - 40 cm	521729.742	3437104.958
El-Kherba	32° 54`15	30° 59`55	P.S(49 to 51)	0 - 30 cm	490851.035	3429451.951
Biar El-Abd	33° 00`10	31° 02`37	P.S(52 to 55)	0 - 19 cm	500265.063	3434435.160
Biar El-Abd	33° 00`57	30° 59`38	P.S(56 to 58)	0 - 20 cm	501511.642	3428924.777
Biar Lehfen	33° 53`37	30° 58`46	S.S 59	0 - 45 cm	584992.568	3427807.168
Abou Awaigila	34° 06`26	30° 50`24	S.S 60	0 - 60 cm	605542.118	3412536.839
El-garkada	34° 01`32	30° 48`33	S.S 61	0 - 60 cm	597764.300	3409045.400
Gabal Libina	33° 54`10	30° 44`13	S.S 62	0 - 40 cm	586084.936	3400940.752
Bagdad	33° 44`59	30° 39`56	S.S 63	0 - 45 cm	571487.108	3392921.931
El-Arish	33° 51`25	31° 02`50	S.S 64	0 - 60 cm	581433.731	3435290.807
El-Arish	33° 49`15	31° 08`38	S.S 65	0 - 60 cm	577909.021	3445977.523
El-Rissan	33° 51`28	30° 53`33	P.S(66 to 68)	0 - 68 cm	581645.293	3418145.153
El-Arish	33° 50`22	31° 04`56	P.S(69 to 71)	0 - 40 cm	579734.686	3439156.799

S.K.S: South El-Kantaea Shark **S.S: Surface Samples.** **P.S.: Profile Samples**

APPENDIX III

This appendix was had the results of regression and correlation statistical analysis between the Landsat TM-5 bands and different soil properties. The correlation and regression analysis were achieved by SPSS and SAS statistical programs. In addition to, this part was had regression figures (A3-1 to A3-9) reflect the relation between soil characteristic and the Landsat TM-5 bands.

Regression

Variables Entered/Removed[b]

Model	Variables Entered	Variables Removed	Method
1	EC [dc/m], O.M. [%], pH (CaCl2), PH (H2O), CEC [meq/100 g], Total Silt [%], Gypsum [%], Clay <2 µm, CaCO3 [%], Total Sand [%][a]	.	Enter

a. All requested variables entered.

b. Dependent Variable: TM 5 Bd 1 [%]

Model Summary

Model	R	R Square	Adjusted R Square	Std. Error of the Estimate
1	.585[a]	.342	.160	10.6160

a. Predictors: (Constant), EC [dc/m], O.M. [%], pH (CaCl2), PH (H2O), CEC [meq/100g], Total Silt [%], Gypsum [%], Clay <2 µm, CaCO3 [%], Total Sand [%]

ANOVA[b]

Model		Sum of Squares	df	Mean Square	F	Sig.
1	Regression	2111.583	10	211.158	1.874	.082[a]
	Residual	4057.157	36	112.699		
	Total	6168.740	46			

a. Predictors: (Constant), EC [dc/m], O.M. [%], pH (CaCl2), PH (H2O), CEC [meq/100g], Total Silt [%], Gypsum [%], Clay <2 µm, CaCO3 [%], Total Sand [%]

b. Dependent Variable: TM 5 Bd 1 [%]

Coefficients[a]

Model		Unstandardized Coefficients		Standardized Coefficients	t	Sig.
		B	Std. Error	Beta		
1	(Constant)	207.517	544.977		.381	.706
	Clay <2 µm	-1.079	5.528	-1.454	-.195	.846
	Total Silt [%]	-.408	5.700	-.267	-.072	.943
	Total Sand [%]	-.689	5.558	-1.331	-.124	.902
	PH (H2O)	-1.814	4.978	-.070	-.364	.718
	pH (CaCl2)	-11.520	11.264	-.179	-1.023	.313
	Gypsum [%]	-.869	.614	-.548	-1.416	.165
	O.M. [%]	-2.991	16.053	-.263	-.186	.853
	CaCO3 [%]	.433	2.656	.234	.163	.871
	CEC [meq/100g]	.101	.196	.129	.514	.610
	EC [dc/m]	8.391E-02	.190	.177	.441	.662

a. Dependent Variable: TM 5 Bd 1 [%]

Regression

Variables Entered/Removed[b]

Model	Variables Entered	Variables Removed	Method
1	EC [dc/m], O.M. [%], pH (CaCl2), PH (H2O), CEC [meq/100 g], Total Silt [%], Gypsum [%], Clay <2 µm, CaCO3 [%], Total Sand [%][a]	.	Enter

a. All requested variables entered.

b. Dependent Variable: TM 5 Bd 2 [%]

Model Summary

Model	R	R Square	Adjusted R Square	Std. Error of the Estimate
1	.742[a]	.551	.427	11.7696

a. Predictors: (Constant), EC [dc/m], O.M. [%], pH (CaCl2), PH (H2O), CEC [meq/100g], Total Silt [%], Gypsum [%], Clay <2 µm, CaCO3 [%], Total Sand [%]

ANOVA[b]

Model		Sum of Squares	df	Mean Square	F	Sig.
1	Regression	6126.180	10	612.618	4.422	.000[a]
	Residual	4986.829	36	138.523		
	Total	11113.009	46			

a. Predictors: (Constant), EC [dc/m], O.M. [%], pH (CaCl2), PH (H2O), CEC [meq/100g], Total Silt [%], Gypsum [%], Clay <2 µm, CaCO3 [%], Total Sand [%]

b. Dependent Variable: TM 5 Bd 2 [%]

Coefficients[a]

Model		Unstandardized Coefficients		Standardized Coefficients	t	Sig.
		B	Std. Error	Beta		
1	(Constant)	301.233	604.198		.499	.621
	Clay <2 µm	-1.568	6.129	-1.575	-.256	.800
	Total Silt [%]	-.305	6.319	-.148	-.048	.962
	Total Sand [%]	-.884	6.162	-1.273	-.143	.887
	PH (H2O)	2.021	5.519	.058	.366	.716
	pH (CaCl2)	-22.031	12.488	-.255	-1.764	.086
	Gypsum [%]	-1.108	.681	-.520	-1.627	.112
	O.M. [%]	6.918	17.798	.454	.389	.700
	CaCO3 [%]	-.815	2.944	-.328	-.277	.784
	CEC [meq/100g]	.151	.218	.144	.693	.493
	EC [dc/m]	3.652E-02	.211	.057	.173	.863

a. Dependent Variable: TM 5 Bd 2 [%]

Regression

Variables Entered/Removed[b]

Model	Variables Entered	Variables Removed	Method
1	EC [dc/m], O.M. [%], pH (CaCl2), PH (H2O), CEC [meq/100 g], Total Silt [%], Gypsum [%], Clay <2 µm, CaCO3 [%], Total Sand [%][a]	.	Enter

a. All requested variables entered.

b. Dependent Variable: TM 5 Bd 3 [%]

Model Summary

Model	R	R Square	Adjusted R Square	Std. Error of the Estimate
1	.821[a]	.673	.583	12.1377

a. Predictors: (Constant), EC [dc/m], O.M. [%], pH (CaCl2), PH (H2O), CEC [meq/100g], Total Silt [%], Gypsum [%], Clay <2 µm, CaCO3 [%], Total Sand [%]

ANOVA[b]

Model		Sum of Squares	df	Mean Square	F	Sig.
1	Regression	10936.133	10	1093.613	7.423	.000[a]
	Residual	5303.687	36	147.325		
	Total	16239.821	46			

a. Predictors: (Constant), EC [dc/m], O.M. [%], pH (CaCl2), PH (H2O), CEC [meq/100g], Total Silt [%], Gypsum [%], Clay <2 µm, CaCO3 [%], Total Sand [%]

b. Dependent Variable: TM 5 Bd 3 [%]

Coefficients[a]

Model		Unstandardized Coefficients		Standardized Coefficients	t	Sig.
		B	Std. Error	Beta		
1	(Constant)	362.802	623.098		.582	.564
	Clay <2 µm	-1.886	6.321	-1.567	-.298	.767
	Total Silt [%]	2.692E-02	6.517	.011	.004	.997
	Total Sand [%]	-.879	6.355	-1.047	-.138	.891
	PH (H2O)	6.168	5.692	.147	1.084	.286
	pH (CaCl2)	-32.354	12.879	-.309	-2.512	.017
	Gypsum [%]	-1.247	.702	-.484	-1.776	.084
	O.M. [%]	14.443	18.355	.783	.787	.436
	CaCO3 [%]	-1.828	3.037	-.609	-.602	.551
	CEC [meq/100g]	.227	.224	.179	1.010	.319
	EC [dc/m]	1.966E-02	.217	.026	.090	.928

a. Dependent Variable: TM 5 Bd 3 [%]

Regression

Variables Entered/Removed[b]

Model	Variables Entered	Variables Removed	Method
1	EC [dc/m], O.M. [%], pH (CaCl2), PH (H2O), CEC [meq/100 g], Total Silt [%], Gypsum [%], Clay <2 µm, CaCO3 [%], Total Sand [%][a]	.	Enter

a. All requested variables entered.

b. Dependent Variable: TM 5 Bd 4 [%]

Model Summary

Model	R	R Square	Adjusted R Square	Std. Error of the Estimate
1	.879[a]	.773	.710	8.9635

a. Predictors: (Constant), EC [dc/m], O.M. [%], pH (CaCl2), PH (H2O), CEC [meq/100g], Total Silt [%], Gypsum [%], Clay <2 µm, CaCO3 [%], Total Sand [%]

ANOVA[b]

Model		Sum of Squares	df	Mean Square	F	Sig.
1	Regression	9853.204	10	985.320	12.264	.000[a]
	Residual	2892.412	36	80.345		
	Total	12745.616	46			

a. Predictors: (Constant), EC [dc/m], O.M. [%], pH (CaCl2), PH (H2O), CEC [meq/100g], Total Silt [%], Gypsum [%], Clay <2 µm, CaCO3 [%], Total Sand [%]

b. Dependent Variable: TM 5 Bd 4 [%]

Coefficients[a]

Model		Unstandardized Coefficients		Standardized Coefficients	t	Sig.
		B	Std. Error	Beta		
1	(Constant)	383.059	460.148		.832	.411
	Clay <2 µm	-2.104	4.668	-1.974	-.451	.655
	Total Silt [%]	-.241	4.812	-.110	-.050	.960
	Total Sand [%]	-1.142	4.693	-1.535	-.243	.809
	PH (H2O)	4.967	4.203	.134	1.182	.245
	pH (CaCl2)	-30.338	9.511	-.327	-3.190	.003
	Gypsum [%]	-1.258	.519	-.552	-2.427	.020
	O.M. [%]	14.393	13.555	.881	1.062	.295
	CaCO3 [%]	-1.942	2.242	-.730	-.866	.392
	CEC [meq/100g]	.147	.166	.131	.885	.382
	EC [dc/m]	5.103E-02	.160	.075	.318	.752

a. Dependent Variable: TM 5 Bd 4 [%]

Regression

Variables Entered/Removed[b]

Model	Variables Entered	Variables Removed	Method
1	EC [dc/m], O.M. [%], pH (CaCl2), PH (H2O), CEC [meq/100 g], Total Silt [%], Gypsum [%], Clay <2 µm, CaCO3 [%], Total Sand [%][a]	.	Enter

a. All requested variables entered.

b. Dependent Variable: TM 5 Bd 5 [%]

Model Summary

Model	R	R Square	Adjusted R Square	Std. Error of the Estimate
1	.859[a]	.739	.666	9.6159

a. Predictors: (Constant), EC [dc/m], O.M. [%], pH (CaCl2), PH (H2O), CEC [meq/100g], Total Silt [%], Gypsum [%], Clay <2 µm, CaCO3 [%], Total Sand [%]

ANOVA[b]

Model		Sum of Squares	df	Mean Square	F	Sig.
1	Regression	9401.888	10	940.189	10.168	.000[a]
	Residual	3328.782	36	92.466		
	Total	12730.670	46			

a. Predictors: (Constant), EC [dc/m], O.M. [%], pH (CaCl2), PH (H2O), CEC [meq/100g], Total Silt [%], Gypsum [%], Clay <2 µm, CaCO3 [%], Total Sand [%]

b. Dependent Variable: TM 5 Bd 5 [%]

Coefficients[a]

Model		Unstandardized Coefficients		Standardized Coefficients	t	Sig.
		B	Std. Error	Beta		
1	(Constant)	333.049	493.639		.675	.504
	Clay <2 µm	-1.991	5.008	-1.869	-.398	.693
	Total Silt [%]	.203	5.163	.093	.039	.969
	Total Sand [%]	-.836	5.035	-1.125	-.166	.869
	PH (H2O)	10.523	4.509	.284	2.334	.025
	pH (CaCl2)	-35.104	10.203	-.379	-3.441	.001
	Gypsum [%]	-1.085	.556	-.476	-1.951	.059
	O.M. [%]	16.152	14.541	.990	1.111	.274
	CaCO3 [%]	-2.233	2.406	-.840	-.928	.360
	CEC [meq/100g]	.346	.178	.309	1.948	.059
	EC [dc/m]	8.151E-02	.172	.120	.473	.639

a. Dependent Variable: TM 5 Bd 5 [%]

Regression

Variables Entered/Removed[b]

Model	Variables Entered	Variables Removed	Method
1	EC [dc/m], O.M. [%], pH (CaCl2), PH (H2O), CEC [meq/100 g], Total Silt [%], Gypsum [%], Clay <2 µm, CaCO3 [%], Total Sand [%][a]	.	Enter

a. All requested variables entered.

b. Dependent Variable: TM 5 Bd 7 [%]

Model Summary

Model	R	R Square	Adjusted R Square	Std. Error of the Estimate
1	.866[a]	.750	.680	10.0434

a. Predictors: (Constant), EC [dc/m], O.M. [%], pH (CaCl2), PH (H2O), CEC [meq/100g], Total Silt [%], Gypsum [%], Clay <2 µm, CaCO3 [%], Total Sand [%]

ANOVA[b]

Model		Sum of Squares	df	Mean Square	F	Sig.
1	Regression	10875.045	10	1087.504	10.781	.000[a]
	Residual	3631.348	36	100.871		
	Total	14506.393	46			

a. Predictors: (Constant), EC [dc/m], O.M. [%], pH (CaCl2), PH (H2O), CEC [meq/100g], Total Silt [%], Gypsum [%], Clay <2 µm, CaCO3 [%], Total Sand [%]

b. Dependent Variable: TM 5 Bd 7 [%]

Coefficients[a]

Model		Unstandardized Coefficients		Standardized Coefficients	t	Sig.
		B	Std. Error	Beta		
1	(Constant)	686.528	515.586		1.332	.191
	Clay <2 µm	-6.030	5.230	-5.302	-1.153	.257
	Total Silt [%]	-3.961	5.392	-1.689	-.735	.467
	Total Sand [%]	-4.929	5.258	-6.212	-.937	.355
	PH (H2O)	15.266	4.710	.386	3.241	.003
	pH (CaCl2)	-34.799	10.657	-.352	-3.266	.002
	Gypsum [%]	-1.139	.581	-.468	-1.961	.058
	O.M. [%]	26.113	15.188	1.499	1.719	.094
	CaCO3 [%]	-3.552	2.513	-1.251	-1.414	.166
	CEC [meq/100g]	.392	.186	.328	2.113	.042
	EC [dc/m]	6.520E-02	.180	.090	.363	.719

a. Dependent Variable: TM 5 Bd 7 [%]

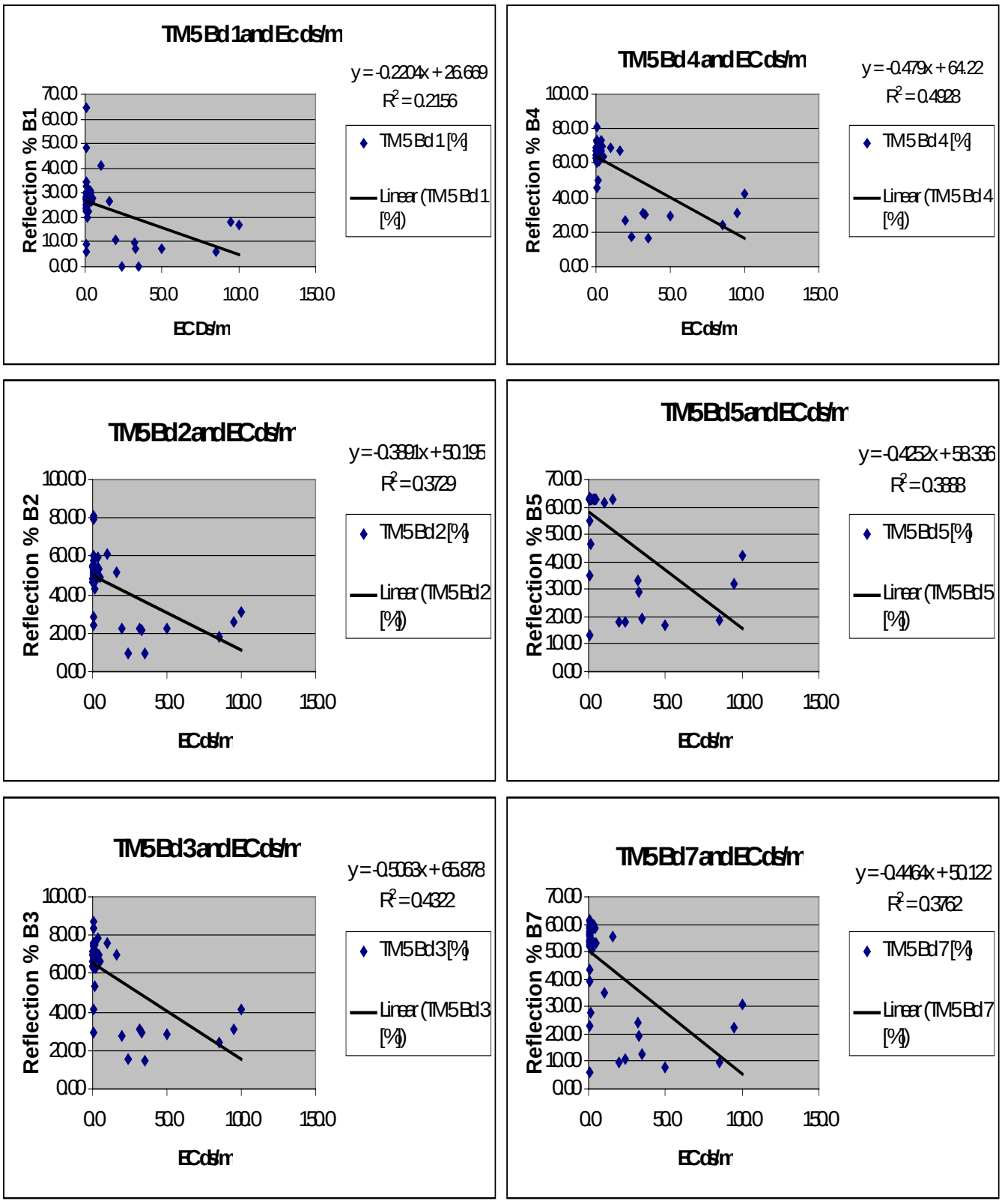

Fig. A3-1: Liner regression between the Landsat TM bands and Electrical Conductivity (EC ds m^{-1}).

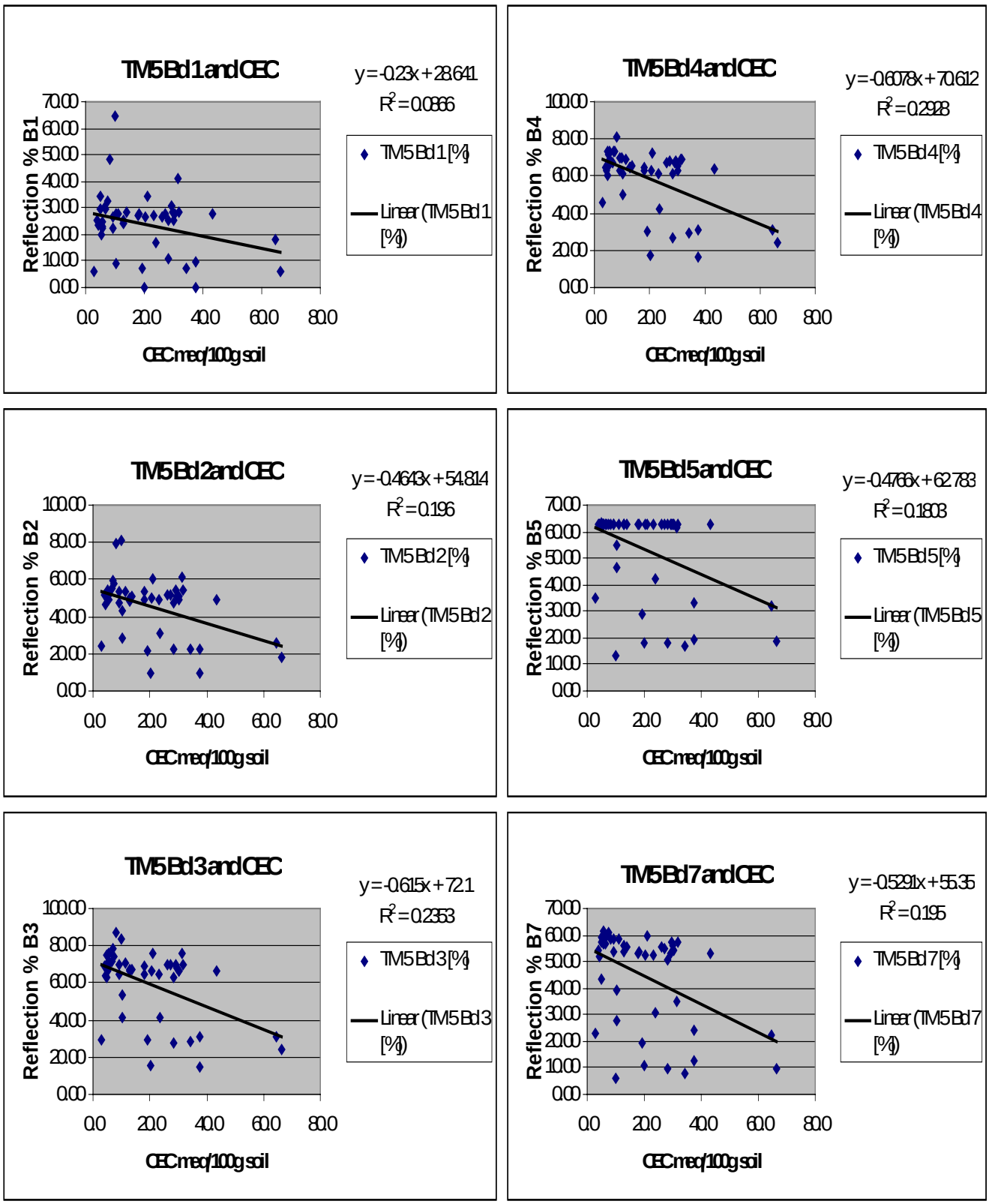

Fig. A3-2: Liner regression between the Landsat TM bands and Cation Exchange Capacity (CEC meq 100g^{-1} soil).

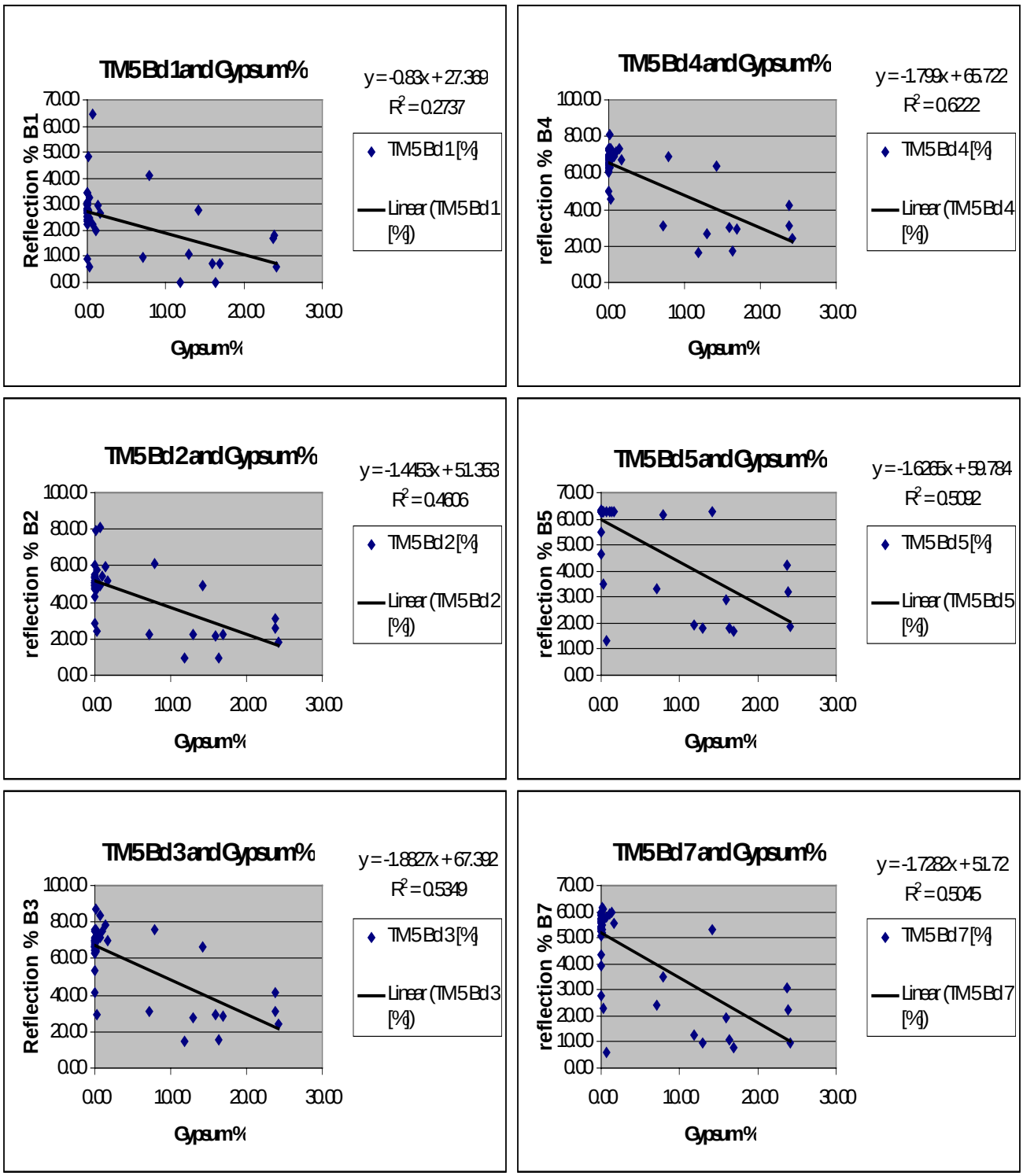

Fig. A3-3: Liner regression between the Landsat TM bands and gypsum content %.

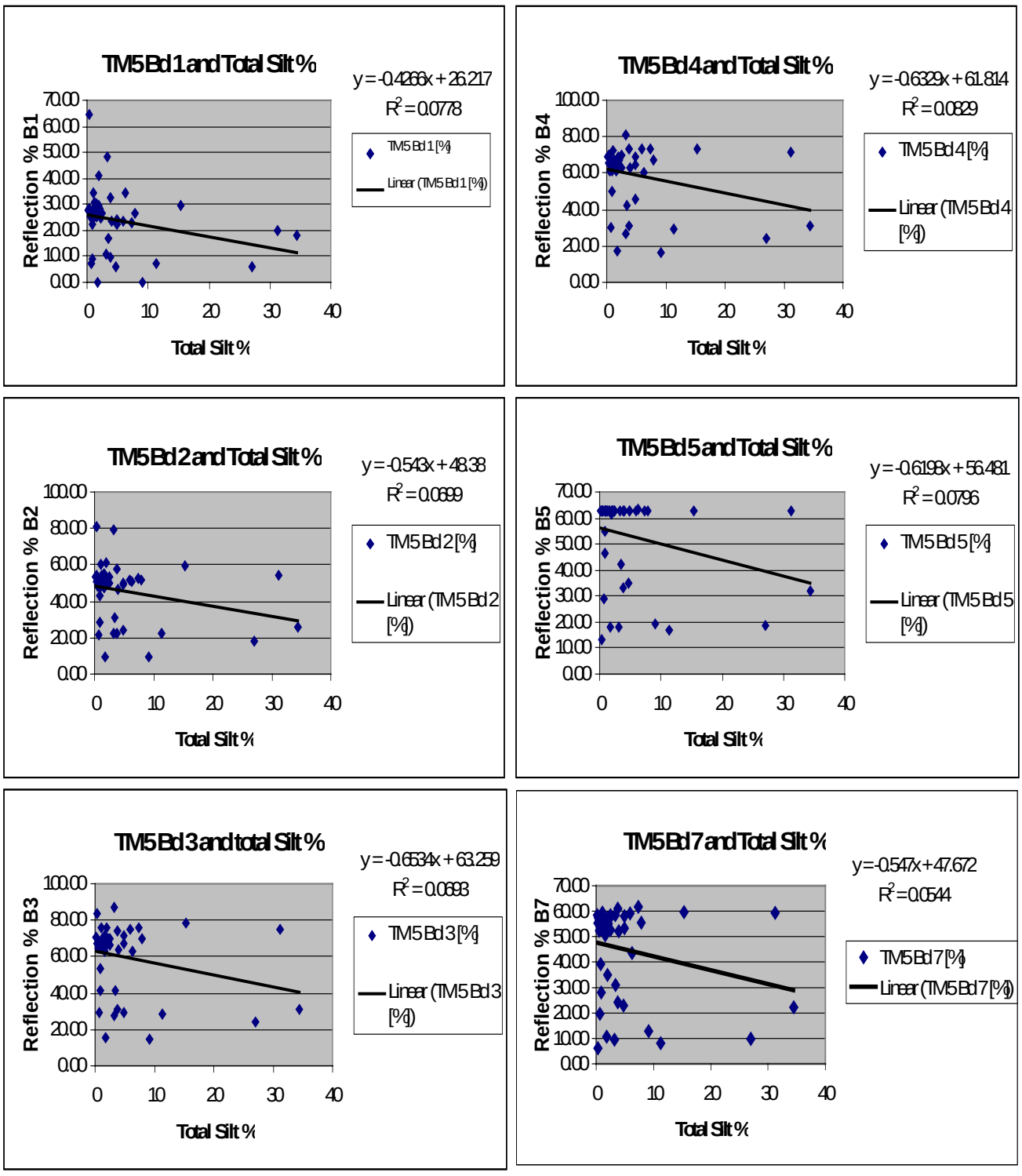

Fig. A3-4: Liner regression between the Landsat TM bands and total silt fraction %.

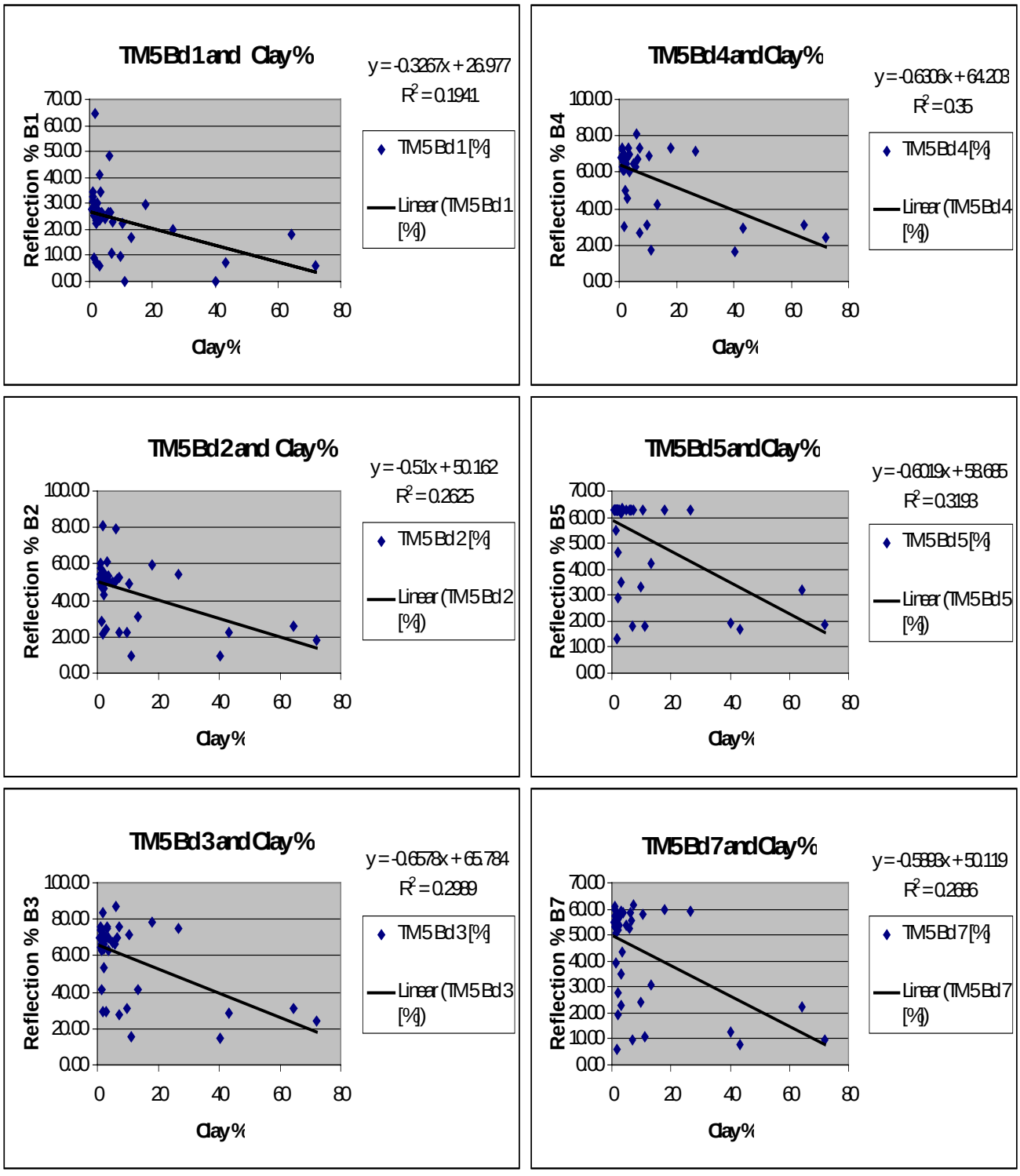

Fig. A3-5: Liner regression between the Landsat TM bands and total clay fraction %.

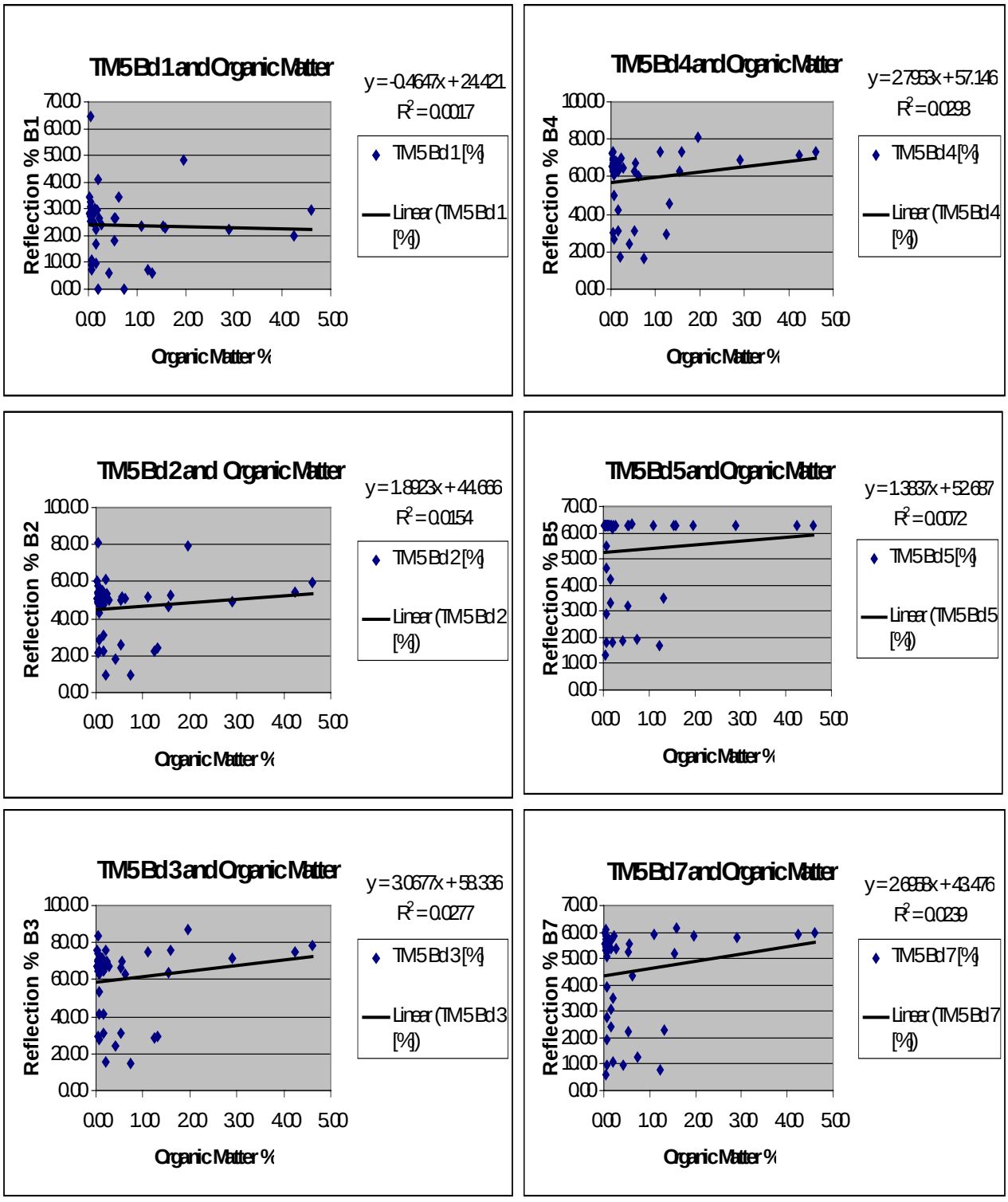

Fig. A3-6: Liner regression between the Landsat TM bands and orgainc matter %.

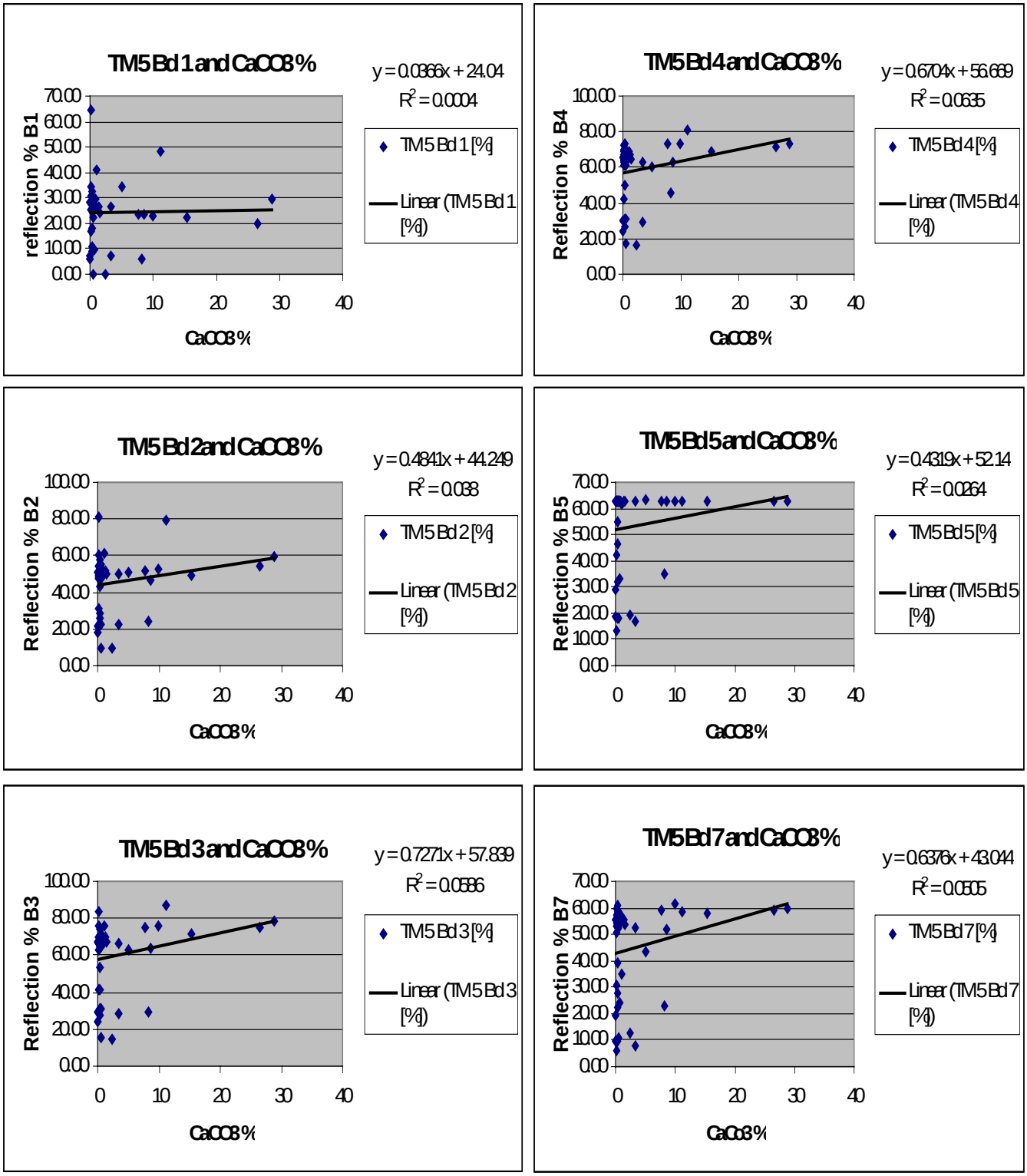

Fig. A3-1: Liner regression between the Landsat TM bands and total carbonate content ($CaCO_3$ %).

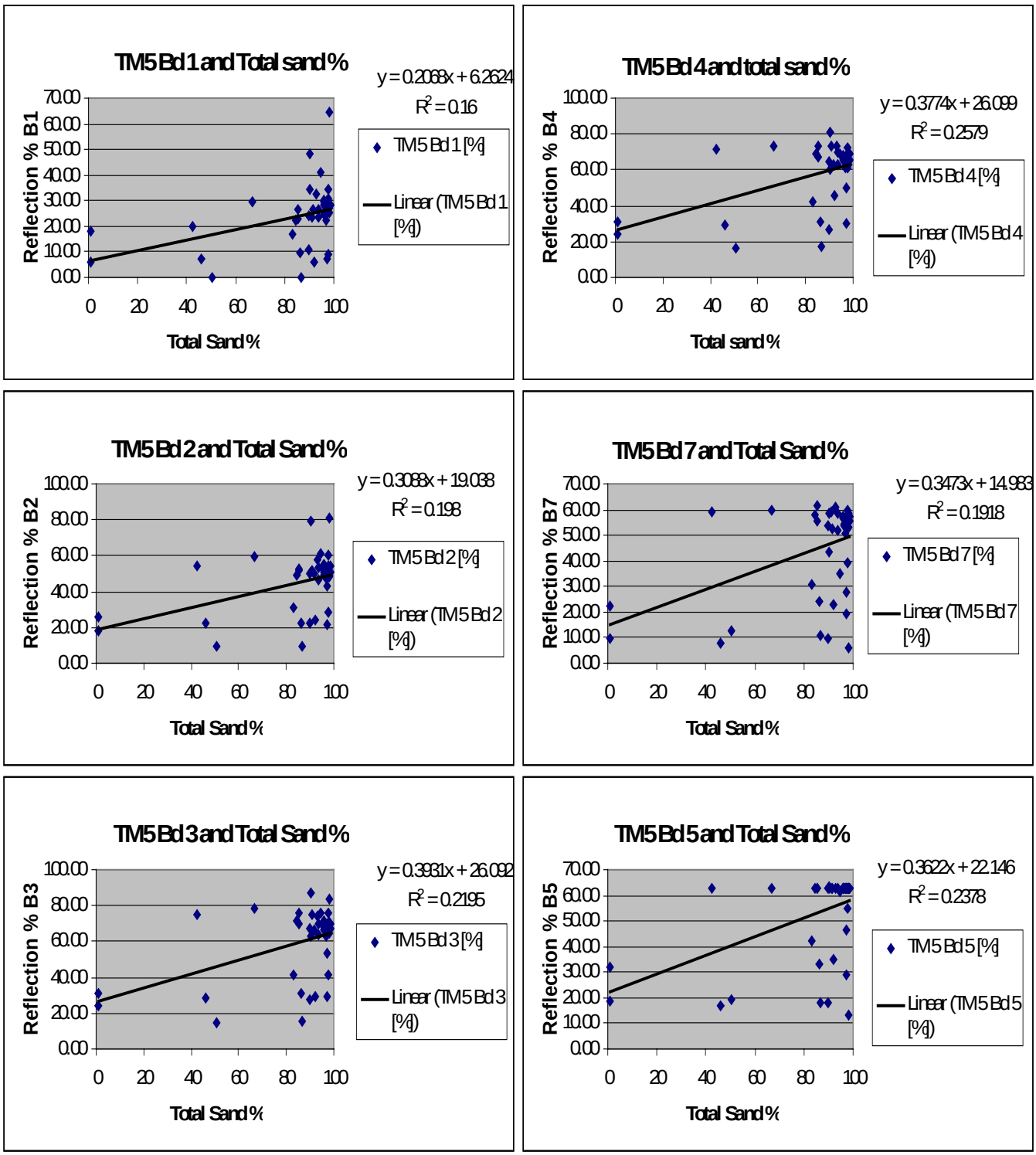

Fig. A3-8: Liner regression between the Landsat TM bands and total sand fraction %.

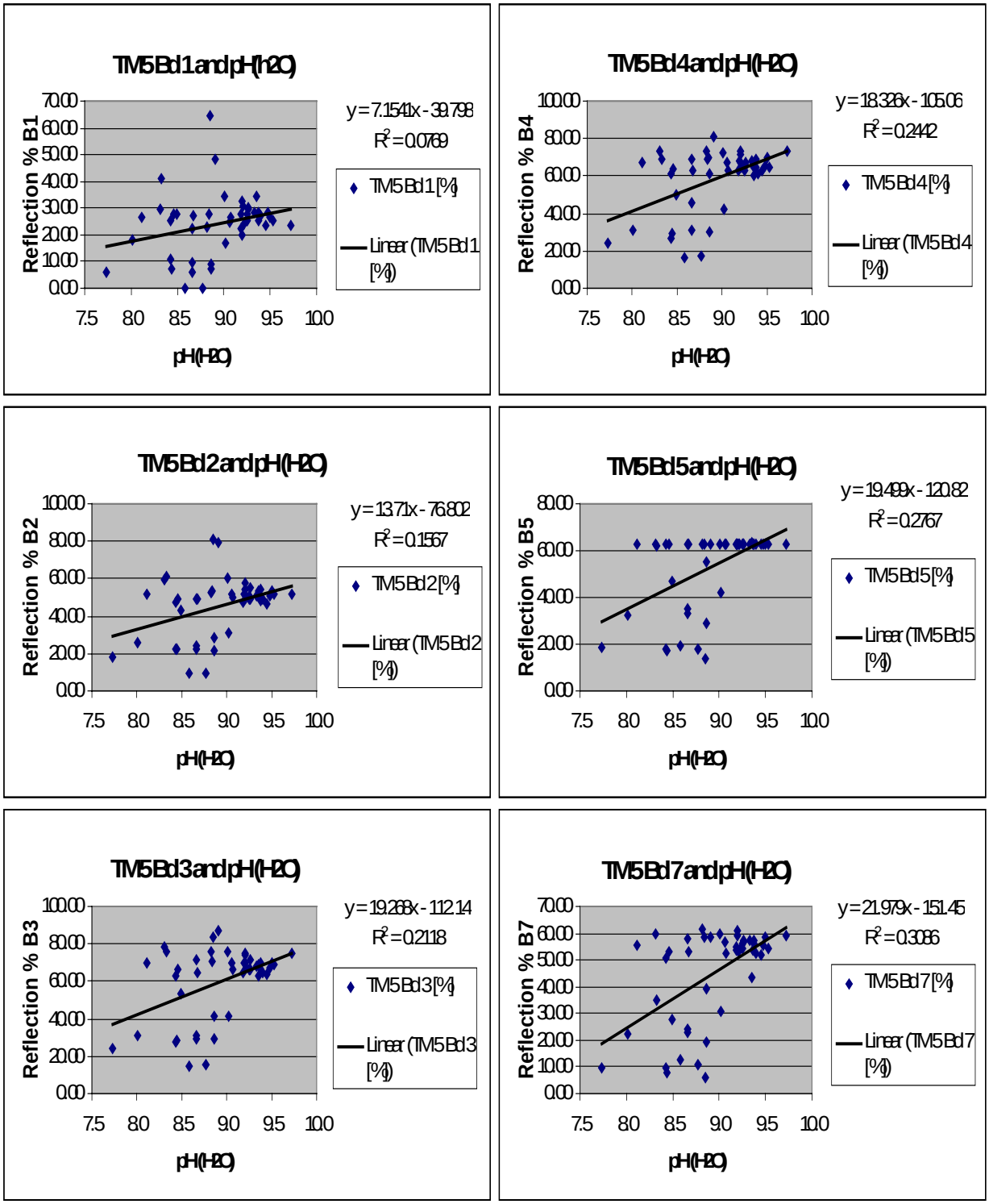

Fig. A3-9: Liner regression between the Landsat TM bands and pH values.

Lieferbare Sonderhefte / Following special issues are available:

	Jahr 2000	€
208	Ingo Hagel Differenzierung und Charakterisierung von Weizen verschiedener Anbausysteme und Sorten durch Proteinfraktionierung	7,00
210	Ursula Pultke Freilanduntersuchungen zum Schwefelhaushalt eines Agrarökosystems mittels Analyse stabiler S-Isotope	7,00
212	Franz Ellendorff und Hartmut Stützel (Herausgeber) Workshop "Nachhaltige Landwirtschaft" vom 31.05. – 02.06.1999	10,00
213	Ulrich Dämmgen (Herausgeber) Versauernde und eutrophierende Luftverschmutzung in Nordost-Brandenburg	7,00
214	Ulf Prüsse Entwicklung, Charakterisierung und Einsatz von Edelmetallkatalysatoren zur Nitratreduktion mit Wasserstoff und Ameisensäure sowie des Stahlschneideverfahrens zur Herstellung Polivinylalkohol-verkapselter Katalysatoren	10,00
215	Torsten Hemme Ein Konzept zur international vergleichenden Analyse von Politik- und Technikfolgen in der Landwirtschaft	15,00
216	Sven Dänicke und Elisabeth Oldenburg (Herausgeber) Risikofaktoren für die Fusariumtoxinbildung in Futtermitteln und Vermeidungsstrategien bei der Futtermittelerzeugung und Fütterung	7,00
218	Luit J. de Kok, Dieter Grill, Malcom J. Hawkesford, Ewald Schnug and Ineke Stulen (Editors) Plant Sulfur Research in Europe, Cost Action 829 Fundamental, Agronomical and Environmental Aspects of Sulfur Nutrition and Assimilation in Plants	7,00
219	Carsten in der Wiesche Untersuchungen zur Sanierung PAK-kontaminierter Böden mit Weißfäulepilzen	7,00
220	Ingo Hagel Auswirkungen einer Schwefeldüngung auf Ertrag und Qualität von Weizen schwefelmangel-gefährdeter Standorte des Ökologischen Landbaus	7,00
221	Franz-Josef Bockisch (Herausgeber) Beurteilung der raumklimatischen Wirkungen von Dämmstoffen aus nachwachsenden Rohstoffen	7,00
	Jahr 2001	
222	Margret Lahmann Prognose der Nachfrage nach Milch und Milcherzeugnissen in Deutschland und Frankreich bis zum Jahre 2005	12,00
223	Josef Kamphues und Gerhard Flachowsky (Herausgeber) Tierernährung – Ressourcen und neue Aufgaben	17,00
226	Jörg Hartung and Christopher M. Wathes (Editors) Livestock Farming and the Environment	7,00
229	Volker Moennig and Alex B. Thiermann (Editors) Safeguarding Animal Health in Global Trade	7,00
230	Nežika Petrič Pränatale Regulation der sexuellen Differenzierung von Luteinisierungshormon und Wachstumshormon, Genexpression und Sekretion beim Schwein	7,00
231	Bernhard Osterburg und Hiltrud Nieberg (Herausgeber) Agrarumweltprogramme – Konzepte, Entwicklungen, künftige Ausgestaltung	7,00

	Jahr 2002	€
227	Franz Ellendorff, Volker Moennig, Jan Ladewig and Lorne Babiuk (Editors) Animal Welfare and Animal Health	7,00
228	Eildert Groeneveld and Peter Glodek (Editors) Animal Breeding and Animal Genetic Resources	7,00
232	Kerstin Panten Ein Beitrag zur Fernerkundung der räumlichen Variabilität von Boden- und Bestandesmerkmalen	7,00
233	Jürgen Krahl Rapsölmethylester in dieselmotorischer Verbrennung – Emissionen, Umwelteffekte, Optimierungspotenziale -	10,00
234	Roger J. Wilkins and Christian Paul (Editors) Legume Silages for Animal Production - LEGSIL	7,00
235	Torsten Hinz, Birgit Rönnpagel and Stefan Linke (Editors) Particulate Matter in and from Agriculture	7,00
236	Mohamed A. Yaseen A Molecular Biological Study of the Preimplantation Expression of Insulin-Like Growth Factor Genes and their Receptors in *In Vitro* Produced Bovine Embryos to Improve *In Vitro* Culture Systems and Embryo Quality	8,00
237	Mohamed Ali Mahmoud Hussein Kandil The effect of fertilizers for conventional and organic farming on yield and oil quality of fennel (*Foeniculum vulgare* Mill.) in Egypt	7,00
238	Mohamed Abd El-Rehim Abd El-Aziz Hassan Environmental studies on coastal zone soils of the north Sinai peninsula (Egypt) using remote sensing techniques	7,00